Technische Universität München

TUM School of Natural Sciences

NMR based methods for the rapid determination of food thickeners

----

Investigations of metabolic pathways during infections with the obligate intracellular pathogen *Chlamydia trachomatis* using isotopologue profiling

Sandra Radziej

Vollständiger Abdruck der von der TUM School of Natural Sciences der Technischen
Universität München zur Erlangung einer

Doktorin der Naturwissenschaften (Dr. rer. nat.)

genehmigten Dissertation.

Vorsitz: Prof. Dr. Thomas Brück

Prüfer der Dissertation:

1. apl. Prof. Dr. Wolfgang Eisenreich
2. Prof. Dr. Thomas Rudel

Die Dissertation wurde am 10.03.2023 bei der Technischen Universität München eingereicht und durch die TUM School of Natural Sciences am 16.06.2023 angenommen.

The presented Ph.D work was performed in the laboratory of Dr. Julia Scherb-Forster at the Bavarian Health and Food Safety Authority in Oberschleißheim, at the Faculty of Chemistry of the Technical University of Munich at the Chair of Biochemistry as well as the Bavarian NMR center (BNMRZ) Structural Membrane Biochemistry between February 2019 and February 2023 under the supervision of apl. Prof. Dr. Wolfgang Eisenreich.

The biggest happiness lies within the smallest things in life.

(Author unknown)

Acknowledgements

The presented work would have not been possible without the support of all those people who accompanied me on this part of my way.

First and foremost, I want to thank my supervisor **Prof. Dr. Wolfgang Eisenreich** for his constant support and encouragement during my work at the Bavarian Health and Food Safety Authority in Oberschleißheim and at the TUM Garching, for giving me the opportunity of becoming a member of his group and the chance to work on various fascinating projects.

Furthermore, I want to thank **Dr. Julia Scherb-Forster** for supervising and supporting me during my work on the project 18-27 (which I am glad to have been part of) within the scope of my doctoral thesis at the Bavarian Health and Food Safety Authority in Oberschleißheim, for her encouragement, enthusiasm and motivation.

I also want to thank **Dr. Claus Schlicht** for initiating the project 18-27, for enabling the cooperation with the TUM Garching, for giving me the opportunity to work on the project within the scope of my doctoral thesis and for his support during my work at the Bavarian Health and Food Safety Authority in Oberschleißheim.

Further, I want to thank all employees of the **LH2 section** at the Bavarian Health and Food Safety Authority in Oberschleißheim for the hospitality and the pleasant working atmosphere during my work on the project 18-27; especially **Dr. Andreas Miller** for giving me the opportunity to perform my work in the laboratory, for his support and interest in my work, **Tobias Kauer**, **Patrick Scheiding** and **Renate Müller** for helping me patiently with all the little issues.

I also want to thank the whole **NMR team** for the pleasant working atmosphere and help during my work on the project 18-27; especially **Dr. Nicholas Schramek** for his support with NMR spectroscopy, for enabling access to the spectrometers and for his interest in my work.

Further, I want to thank **Dr. Maria Butzenlechner** for her support and interest in my work on the project 18-27.

I want to thank the **Bavarian Health and Food Safety Authority** and the **Bavarian State Ministry of the Environment and Consumer Protection** for the support by funding me during my work on the project 18-27 within the scope of my doctoral thesis.

Furthermore, I want to thank **Prof. Dr. Thomas Rudel** and **Dr. Adriana Moldovan** for the productive and pleasant collaboration and the continuous support during my work on the DFG-project 451958427 which I am glad to have been part of.

I also want to thank **Prof. Dr. Werner Goebel** for his constant support and interest in my work on the DFG-project 451958427.

Further, I want to thank the whole **working group** for the pleasant working atmosphere, especially **Dr. Claudia Huber** for her support and guidance and **Christian Seitz** for the good collaboration. A special thanks goes to **Dr. Thomas Steiner**, **Dr. Thomas Geisberger** and **Christine Schwarz** for the enjoyable cooperation, for helping me patiently with all the little issues (I cannot thank enough) and for the daily scrum-meetings.

I also want to thank all students during their internship under my supervision for their active support in the laboratory, especially **Lukas Hofmann** and **Jendrik Schwarz**.

I want to thank the **Deutsche Forschungsgemeinschaft** for the financial support during my work on the DFG-project 451958427.

Finally, I want to give my sincere thanks to my **family** (especially my **parents**) and **friends** for the endless encouragement, patience and support during my whole life.

Table of contents

List of abbreviations

3-PG	3-phosphoglycerate
ARB	aberrant reticulate body
ATP	adenosine triphosphate
BMDM	bone marrow-derived macrophages
CoA	coenzyme A
COSY	correlated spectroscopy
C. trachomatis	*Chlamydia trachomatis*
C. burnetii	*Coxiella burnetii*
DM	degree of methylation
DNA	deoxyribonucleic acid
DOSY	diffusion ordered spectroscopy
EB	elementary body
ELISA	enzyme-linked immunosorbent assay
FASII	Type II fatty acid synthesis
GAP	glyceraldehyde-3-phosphate
GC-MS	gas chromatography mass spectroscopy
HMBC	heteronuclear multiple bond correlation
HPLC	high performance liquid chromatography
HSQC	heteronuclear single quantum coherence
HFT	Human fallopian tube
IBP	intracellular bacterial pathogen
IFN-γ	interferon-gamma
KDO	3-deoxy-D-manno-octulosonic acid
LCV	large cell variant
LED	longitudinal eddy current delay
LFGB	Lebensmittel- und Futtermittelgesetzbuch
LPS	lipopolysaccharide
MALDI	matrix-assisted laser desorption/ionization
mDAP	*meso*-diaminopimelic acid
MFA	metabolic flux analysis
NAD	nicotinamide adenine dinucleotide
NADPH	nicotinamide adenine dinucleotide phosphate
N. meningitidis	*Neisseria meningitidis*
NMR	nuclear magnetic resonance
PC	phosphatidylcholine

LIST OF ABBREVATIONS

PCR	polymerase chain reaction
PE	phosphatidylethanolamine
PEP	phosphoenolpyruvate
PG	phosphatidylglycerol
PPP	pentose phosphate pathway
qNMR	quantitative nuclear magnetic resonance
RB	reticulate body
RNA	ribonucleic acid
STE	stimulated echo
SCV	small cell variant
TCA	tricarboxylic acid

Summary

Human health is one of the most important things in life. A balanced and varied nutrition is the basis for a healthy lifestyle because it contributes significantly to one's own well-being, can prevent diseases and promotes growth and development. In recent years, there is a growing interest in so-called "clean-labelling products", meaning food products that are promoted to be free of additives, because the consumption of such products is associated with a healthy lifestyle. However, food additives like coloring agents, sweeteners and flavour enhancers are often used in premixtures and food products due to their functional properties. This implies the risk of misleading the consumer by advertising products as "clean-labelling products" despite the usage of food additives. Consequently, there is a need to rapidly determine food additives in foodstuff. For the analysis of thickening agents in food products, the officially accepted §64 LFGB method L 00.00-13 is often applied which is based on many time-consuming preparation steps and the cleavage of thickeners into their monosaccharide units. Furthermore, procedures that are based on a similar principle are described in the literature. However, these methods seem to be only partially suitable for a screening.

Therefore, protocols which enable a fast identification of thickening agents in premixtures and food products by NMR spectroscopy without time-consuming sample preparation were developed in the present work. For this purpose, characteristic marker signals in the ^{1}H-NMR spectrum and typical diffusions coefficients in the DOSY spectrum of the thickeners gum arabic, *kappa*-carrageenan, agar-agar, locust bean gum, guar gum and pectin were determined. The assignment of the signals was done using two-dimensional spectra (^{1}H,^{1}H-COSY, ^{1}H,^{13}C-HSQC, ^{1}H,^{13}C-HMBC) and data from the literature. Consequently, a screening-method was developed which allowed the unequivocally identification of various thickening agents in different premixtures and food matrices (i.a. dairy drinks, cake glaze, pastilles) without previous sample preparation by using a combination of ^{1}H-NMR spectroscopy and DOSY. However, not all thickening agents could be determined with this method due to matrix effects and low application rates. Thus, a method for a simple and fast concentration of thickeners was developed which allowed the separation of high molecular weight thickening agents from low molecular weight substances (e.g. sucrose, glucose) in various premixtures by using centrifugal concentrators (cut-of 100 kDa). This method is characterized by a simple sample preparation in contrast to the §64 LFGB method. The application on different premixtures (i.a. bakery mix, milk powder, instant flavored drink) demonstrated that the declared thickening agents could be unequivocally identified in the ^{1}H-NMR spectrum of the filter residue after separation using centrifugal concentrators whereas a large amount of low molecular weight substances was detected in the proton spectrum of the filtrate. However, it should be noted that a successful identification is strongly influenced by the composition of the analysed sample.

Although not all labelled thickening agents could be determined due to matrix effects and low application rates, the developed protocols can be used in addition to the officially accepted §64 LFGB method as well as other well-established methods.

Beside the nutrition, the presence of bacteria (i.a. in the gut and on the skin) plays an important role for human well-being, because they beneficially contribute to a functioning digestion, protect the body from diseases and strengthen the immune system. In contrast to “harmless” bacteria, the contact with harmful bacteria (e.g. salmonellae, legionella, staphylococcus) might lead to diverse acute and chronical diseases and organ failure. The Gram-negative obligate bacterium *Chlamydia trachomatis* belongs to these pathogens, because an infection can lead to numerous diseases like conjunctivitis, cervicitis, urethritis or pneumonitis. For the successful treatment of a *chlamydial* infection, the knowledge about the bacterial metabolism is of vital importance. Nowadays, the “metabolic flux analysis” is increasingly used for the analysis of intracellular metabolic pathways. For this purpose, an isotopically enriched substance is added to the bacterial culture and the synthesized metabolites are analyzed at a specific time-point. Thereafter, activities and flows in different metabolic pathways can be discovered on the basis of the isotopologue composition. Labelling experiments with [U-$^{13}C_6$]glucose, [U-$^{13}C_4$]malate and [U-$^{13}C_5$]glutamate in various host cells (i.a. Caco-2 and HeLa-cells) as well as in axenic culture demonstrated that *Chlamydia trachomatis* is able to metabolize different substrates in a biphasic lifestyle. In order to guaranty a sufficient supply with essential nutrients and thus survival, the metabolism of the host is further manipulated. Although recent studies focused on the investigation of the intracellular metabolism of *Chlamydia trachomatis*, little is known about the metabolic adaptation of primary cells during an infection.

Therefore, metabolic fluxes of uninfected and with *Chlamydia trachomatis* infected human M1 and M2 polarized macrophages as well as human fallopian tube cells were analyzed in the present work. For this purpose, host cells were cultivated in RPMI-1640 medium for 30 hours with [U-$^{13}C_6$]glucose as “tracer” and the metabolites (protein-derived amino acids, TCA intermediates and fatty acids) as well as the supernatants were analyzed by GC-MS and NMR spectroscopy.

The ^{13}C-profiles of uninfected human fallopian tube cells demonstrated that glucose was efficiently metabolized *via* glycolysis (approx. 9.6% enrichment in alanine), whereas only small amounts were used to feed the TCA cycle and for the synthesis of fatty acids. Isotopic labelling of infected fallopian tube cells showed a similar pattern for the protein-derived amino acids as well as for the metabolites of the TCA cycle. Furthermore, the glucose amounts in the supernatants were in the same order of magnitude. The increased ^{13}C-enrichment in the arachidic acid (C20:0) and the detection of the bacterial-specific fatty acids anteiso- and iso-C15:0 in the infected host cell indicated that human fallopian tube cells seem to be suitable to serve as host cells for the replication of *Chlamydia trachomatis*.

In contrast to the fallopian tube cells, the uninfected M2 polarized macrophages contained substantially smaller ^{13}C-enrichment rates in alanine (approx. 1.5%), whereas the excess values in the metabolites of the TCA cycle and in the fatty acids were in the same order of magnitude. Isotopologue distributions of the infected M2 polarized macrophages displayed similar patterns for the protein-derived amino acids as well as for the metabolites of the TCA cycle. Again, the fatty acid C20:0 in the infected host cell contained a significant higher enrichment (approx. 15%) in contrast to the uninfected M2 macrophages (approx. 4%). Furthermore, the bacterial-specific cell wall component *meso*-diaminopimelic acid (approx. 33% enrichment) could be detected and a significant utilization of glucose in the supernatants were observed. Therefore, it has been assumed that M2 polarized macrophages seem to be suitable to serve as host cells for *Chlamydia trachomatis*.

The uninfected M1 polarized macrophages showed similar ^{13}C-enrichments in the amino acids (except alanine), TCA intermediates and fatty acids as the M2 polarized macrophages. Moreover, the labelling rates in the uninfected and infected M1 macrophages were in the same order of magnitude. Additionally, no bacterial-specific metabolites could be detected and no significant differences in the utilization of glucose in the supernatants of the infected M1 polarized macrophages were determined. Thus, it has been assumed that M1 polarized macrophages seem to be inappropriate to serve as host cells for *Chlamydia trachomatis*.

Zusammenfassung

Die Gesundheit zählt zu den höchsten Gütern des Menschen. Eine ausgewogene und abwechslungsreiche Ernährung bildet dabei den Grundstock für eine gesunde Lebensweise, da sie maßgeblich zum eigenen Wohlbefinden beiträgt, der Entstehung von Krankheiten vorbeugen kann sowie das Wachstum und die Entwicklung fördert. In den letzten Jahren ist die Nachfrage nach sogenannten „clean labelling-Produkten“, also Lebensmitteln, welche auf der Verpackung mit dem Verzicht von bestimmten Zusatzstoffen beworben werden, stark angestiegen, da der Konsum solcher Produkte mit einer gesunden Lebensweise in Verbindung gebracht wird. Dennoch werden Zusatzstoffe wie Farbstoffe, Süßungsmittel oder Geschmacksverstärker aufgrund ihrer technologischen Wirkung häufig in Vormischungen und Lebensmitteln eingesetzt. Dies birgt die Gefahr, dass Produkte trotz Verwendung von Zusatzstoffen als „clean labelling-Produkte“ beworben und Verbraucher somit getäuscht werden. Demzufolge besteht die Notwendigkeit, Zusatzstoffe schnell in Lebensmitteln nachweisen zu können. Für die Analyse von Verdickungsmittel in Lebensmitteln wird häufig die §64 LFGB Methode L 00.00-13 angewandt, welche auf zahlreichen langwierigen Aufarbeitungsschritten sowie anschließender Spaltung der Verdickungsmittel in ihre Monosaccharid-Einheiten beruht. Auch in der Literatur sind Verfahren beschrieben, welche auf einem ähnlichen Prinzip beruhen. Diese Methoden sind für ein Screening jedoch nur bedingt geeignet.

Aus diesem Grund wurden in der vorliegenden Arbeit Protokolle entwickelt, welche eine schnelle Identifizierung von Verdickungsmittel in Vormischungen und Lebensmitteln mittels NMR-Spektroskopie ohne zeitaufwendige Probenvorbereitung ermöglichen. Dazu wurden charakteristische Marker-Signale im ^{1}H-NMR-Spektrum sowie typische Diffusionskoeffizienten im DOSY-Spektrum für die Verdickungsmittel Gummi arabicum, *kappa*-Carrageen, Agar-Agar, Johannisbrotkernmehl, Guarkernmehl und Pektin bestimmt. Die Zuordnung der jeweiligen Signale erfolgte mit Hilfe von zweidimensionalen Spektren (^{1}H,^{1}H-COSY, ^{1}H,^{13}C-HSQC, ^{1}H,^{13}C-HMBC) und Daten aus der Literatur. Anschließend wurde eine Screening-Methode entwickelt, welche durch die kombinierte Anwendung von ^{1}H-NMR-Spektroskopie und DOSY eine eindeutige Identifizierung von verschiedenen Verdickungsmittel in unterschiedlichen Vormischungen und Lebensmittelmatrices (u.a. Milchgetränke, Tortengusspulver, Pastillen) ohne vorherige Probenaufarbeitung ermöglichte. Aufgrund von Matrixeffekten und geringen Einsatzmengen ließen sich mit dieser Methode jedoch nicht alle Verdickungsmittel nachweisen. Um Verdickungsmittel möglichst einfach und schnell aufzukonzentrieren, wurde daher eine Aufarbeitungsmethode entwickelt, bei der durch die Verwendung von Zentrifugen-Filtereinheiten (cut-off 100 kDa) eine Trennung der hochmolekularen Verdickungsmittel von den niedermolekularen Bestandteilen (z.B. Saccharose, Glucose) in unterschiedlichen

Vormischungen erreicht wurde. Diese Methode zeichnet sich im Gegensatz zur §64 LFGB Methode durch eine einfache Probenaufarbeitung aus. Anhand von unterschiedlichen Vormischungen (u.a. Backmischung, Milchpulver, Instant-Getränkepulver) konnte gezeigt werden, dass sich die deklarierten Verdickungsmittel nach Isolierung mittels Zentrifugen-Filtereinheiten im ^{1}H-NMR-Spektrum des Rückstandes eindeutig nachweisen ließen, während ein Großteil der niedermolekularen Substanzen im Protonenspektrum vom Filtrat detektiert wurde. Es gilt jedoch zu beachten, dass eine erfolgreiche Identifizierung stark von der Zusammensetzung der untersuchten Probe abhängig ist.

Obwohl sich aufgrund von Matrixeffekten und geringen Einsatzmengen nicht alle deklarierten Verdickungsmittel nachweisen lassen, können die erarbeiteten Protokolle dennoch als Ergänzung zur amtlich anerkannten §64 LFGB Methode sowie anderen etablierten Methoden verwendet werden.

Für das menschliche Wohlbefinden spielt neben der Ernährung auch das Vorhandensein von Bakterien (u.a. im Darm und auf der Haut) eine wichtige Rolle, da diese nicht nur zu einer funktionierenden Verdauung beitragen, sondern den Körper auch vor Krankheiten schützen und das Immunsystem stärken. Im Gegensatz zu den „gutartigen“ Bakterien kann der Kontakt mit gesundheitsschädlichen Bakterien (z.B. Salmonellen, Legionellen, Staphylokokken) zu diversen akuten und chronischen Krankheiten sowie Organversagen führen. Zu den Pathogenen zählt auch das gramnegative, obligat intrazelluläre Bakterium *Chlamydia trachomatis*, da eine Infektion zahlreiche Krankheiten wie Konjunktivitis, Zervizitis, Urethritis oder Pneumonitis hervorrufen kann. Um eine Chlamydien-Infektion erfolgreich behandeln zu können, ist das Verständnis des bakteriellen Stoffwechsels von entscheidender Bedeutung. Für die Analyse von intrazellulären Stoffwechselwegen findet die „metabolic flux analysis“ heutzutage immer häufiger Anwendung. Dazu wird eine isotopenmarkierte Substanz zur Bakterienkultur zugesetzt und die entstandenen Stoffwechselprodukte zu einem bestimmten Zeitpunkt analysiert. Anhand der Isotopenzusammensetzung können anschließend Aktivitäten und Flüsse in verschiedenen Stoffwechselwegen aufgedeckt werden. Markierungsexperimente mit [U-$^{13}C_6$]Glucose, [U-$^{13}C_4$]Malat sowie [U-$^{13}C_5$]Glutamat in verschiedenen Wirtszellen (u.a. Caco-2 und HeLa-Zellen) sowie in axenischer Kultur zeigten, dass *Chlamydia trachomatis* in der Lage ist, unterschiedliche Substrate in einer biphasischen Lebensweise zu verstoffwechseln. Um eine ausreichende Versorgung mit essentiellen Nährstoffen und somit ein Überleben zu gewährleisten, wird zudem der Stoffwechsel der Wirtszelle manipuliert. Obwohl sich bereits mehrere Studien mit Untersuchungen zum intrazellulären Stoffwechsel von *Chlamydia trachomatis* befasst haben, ist wenig über die Anpassung des Stoffwechsels von Primärzellen während einer Infektion bekannt.

Aus diesem Grund wurden in der vorliegenden Arbeit Stoffwechselflüsse von nicht-infizierten sowie mit *Chlamydia trachomatis* infizierten humanen M1- und M2-Makrophagen sowie humanen Eileiterzellen untersucht. Dazu wurden die Wirtszellen in RPMI-1640 Medium mit [U-$^{13}C_6$]Glucose als „Tracer“ 30 Stunden kultiviert und die Stoffwechselprodukte (aus Proteinen gewonnene Aminosäuren, Metabolite vom Citrat-Zyklus und Fettsäuren) sowie die Überstände anschließend mittels GC-MS und NMR-Spektroskopie analysiert.

Die ^{13}C-Profile der nicht-infizierten humanen Eileiterzellen zeigten, dass Glucose effizient über die Glykolyse (ca. 9,6% Anreicherung in Alanin) verstoffwechselt wurde, während geringere Mengen in den Citrat-Zyklus und in die Fettsäure-Synthese einflossen. Die Isotopenmarkierungen der infizierten Eileiterzellen zeigten ein ähnliches Muster für die Aminosäuren sowie Metabolite vom Citrat-Zyklus. Des Weiteren lagen die Glucose-Mengen in den Überständen in der gleichen Größenordnung. Die erhöhte ^{13}C-Anreicherung in der Arachinsäure (C20:0) sowie die Detektion der bakterien-spezifischen Fettsäuren anteiso- und iso-C15:0 in der infizierten Wirtszelle deuteten zudem darauf hin, dass Eileiterzellen als Wirtszellen für eine Replikation von *Chlamydia trachomatis* geeignet sind.

Im Gegensatz zu den Eileiterzellen wiesen die nicht-infizierten M2-Makrophagen deutlich geringere ^{13}C-Anreicherungsraten in Alanin (ca. 1,5%) auf, während die Markierungen in den Metaboliten vom Citrat-Zyklus sowie in den Fettsäuren in der gleichen Größenordnung lagen. Die Isotopenmarkierungen der infizierten M2-Makrophagen zeigten ein ähnliches Muster für die aus Proteinen gewonnenen Aminosäuren sowie für die Metabolite vom Citrat-Zyklus. Erneut wies die Fettsäure C20:0 in der infizierten Wirtszelle eine deutliche höhere Markierung (ca. 15%) auf als in der nicht-infizierten Zelle (ca. 4%). Zudem konnte die bakterien-spezifische Zellwandkomponente *meso*-Diaminopimelinsäure (ca. 33% Anreicherung) detektiert sowie ein signifikanter Glucose-Verbrauch in den Überständen festgestellt werden. Es wurde daher angenommen, dass M2-Makrophagen als Wirtszellen für *Chlamydia trachomatis* geeignet sind.

Die nicht-infizierten M1-Makrophagen wiesen ähnliche ^{13}C-Anreicherungen in den Aminosäuren (außer Alanin), Metaboliten vom Citrat-Zyklus und Fettsäuren wie die M2-Makrophagen auf. Zudem lagen die Markierungsraten in den nicht-infizierten und infizierten M1-Makrophagen in der gleichen Größenordnung. Des Weiteren konnten keine bakterien-spezifischen Metabolite sowie keine signifikanten Unterschiede im Glucose-Verbrauch in den Überständen der infizierten M1-Makrophagen festgestellt werden. Es wurde daher angenommen, dass M1-Makrophagen als Wirtszelle für *Chlamydia trachomatis* nicht geeignet sind.

1. Introduction

One of the most important things in life is the human health as it is directly correlated to the quality of life (Kaplan and Ries, 2007). It is well known that a balanced and healthy nutrition including carbohydrates, proteins, fats, vitamins and minerals plays a crucial role for the maintenance of human health (Cena and Calder, 2020). For example, the intake of dietary fiber beneficially effects the condition by reducing the risk of cardiovascular diseases, diabetes and hypertension (Anderson et al., 2009). In the food industry, the application of food additives for the production of foodstuff is difficult to avoid due to their ability of achieving specific quality attributes and ensuring food safety (Wu et al., 2022). Beside their technological functions, food additives can further positively contribute to human health while affecting the gut microbiome or helping to control body weight (Blanco-Pérez et al., 2021; Mooradian et al., 2017). However, the intake of high amounts of various additives might lead to health-related consequences like allergic reactions, autoimmune diseases, hyperactivity and neuropsychiatric reactions (Carocho et al., 2014; Csáki, 2011; Czarnecka et al., 2021; Simon, 2003).

Human health is not only influenced by the nutritional lifestyle, but might also be affected by viral and bacterial infections causing different diseases or even mortality. Bacterial infections can be spread either directly from person to person through aerosols, respiratory secretions and direct contact or indirectly from contaminated objects like food or household items (Doron and Gorbach, 2008). Depending on infection type and illness progression, different antibacterial agents are prescribed for the prevention or treatment of diseases caused by bacteria (Bush and Macielag, 2000). The mode of actions contain the inhibition of deoxyribonucleic acid (DNA) synthesis, ribonucleic acid (RNA) synthesis, cell wall synthesis or protein synthesis (Kohanski et al., 2010). Nevertheless, bacterial pathogens develop resistance to antibiotics over time leading to diseases that cannot be medicated with conventional drugs. The main causes for resistance are natural mutations in the genetic material of the bacteria, the excessive consumption of antibiotics, travelling through different countries and poor sanitary conditions (Mancuso et al., 2021; Ramay et al., 2020; Schwartz and Morris, 2018). Resistance of bacteria is based on the ability to decrease the efficiency of the antibiotic uptake, to modify cell target components so that antibiotics can no longer bind to these, to inactivate the drug by enzymatic degradation or transfer of chemical groups and to increase the capability of efflux pumps in order to release the antibiotic from the bacterial cell (Eisenreich et al., 2022; Reygaert, 2018). Therefore, the constant further development of novel antibiotics and the detection of new therapy targets are urgently needed in order to efficiently treat bacterial infections.

1.1 Food thickeners and their applications

The addition of different food additives to premixtures or food products for the enhancement of food taste, texture and other qualities is becoming an increasing trend in recent decades (Cox et al., 2021). There are more than 330 food additives that are registered for the usage in various premixtures and food in the European Union (Chazelas et al., 2020). As defined in Art. 3 (2a) of the regulation (EC) No. 1333/2008, a food additive is “any substance not normally consumed as a food in itself and not normally used as a characteristic ingredient of food, whether or not it has nutritive value, the intentional addition of which to food for a technological purpose in the manufacture, processing, preparation, treatment, packaging, transport or storage of such food results, or may be reasonably expected to result, in it or its by-products becoming directly or indirectly a component of such foods”. Although the addition and labelling of food additives are strictly regulated in the regulation (EU) No. 1333/2008, food fraud scandals including mislabelling of products occurred in the past years (Moreira et al., 2021). Food fraud is defined as an international act of “deliberate and international substitution, addition, tampering, or misrepresentation of food, food ingredients, or food packaging; or false or misleading statements made about a product, for economic gain” (Spink and Moyer, 2011). For example, Sudan I – IV dyes are not allowed to be used as colouring agent in foodstuff in the European Union due to their genotoxic and cancerogenic properties. However, these substances are regularly found in different food products like chilli spices, palm oil and meat products (Adjei et al., 2020; Fonovich, 2013; Genualdi et al., 2016). Therefore, food monitoring concerning food safety, quality and declaration is very important to discover and prevent food fraud (Pacholczyk-Sienicka et al., 2021). Due to their different chemical properties, food additives are categorised in functional classes (Partridge et al., 2019). One example for an important functional class are the thickening agents which are increasingly used in different food applications (Saha and Bhattacharya, 2010). Different raw materials like plants or microorganisms are used for the production of food-grade thickeners (Himashree et al., 2022). Thickening agents are defined in the regulation (EC) No. 1333/2008 as “substances which increase the viscosity of a foodstuff”. Additionally, the specification of these additives is regulated in the regulation (EU) No. 231/2012. Due to their ability of binding water, thickeners are able to modify the rheology by increasing the viscosity and adjusting the food texture which is important for a specific mouth feeling (Saha and Bhattacharya, 2010). Furthermore, the shelf-life of a product can be extended by using thickener based edible coatings (Rohasmizah and Azizah, 2022). For the therapeutically treatment of dysphagia, the addition of thickening agents helps people with difficulty swallowing to safely swallow liquids by increasing the viscosity of the product (Cichero, 2013). In the following the chemical structure, the application field and health benefits of some commonly used food thickeners are described in more detail.

Carrageenan (E407) and Agar-Agar (E406)

Carrageenans are extracted from the cell wall of red seaweeds (*Rhodophyceae*) and belong to the group of sulphated polygalactans with a molecular weight above 100 kDa (du Preez et al., 2020). The main structure of carrageenan contains repeating units of D-galactose and 3,6-anhydro-D-galactose with α-1,3 and ß-1,4 linkages (Chauhan and Saxena, 2016). A distinction is made between the three major types *kappa*-carrageenan, *iota*-carrageenan and *lambda*-carrageenan (Figure 1) which differ in their composition, molecular weight, number and position of sulphate groups (Liu et al., 2021).

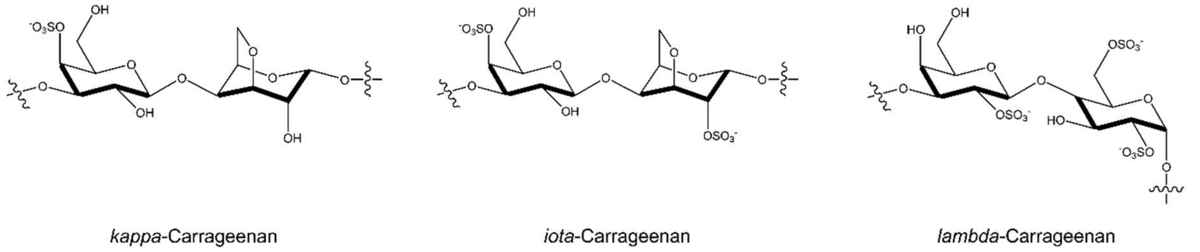

Figure 1: Representative moieties of *kappa*-carrageenan, *iota*-carrageenan and *lambda*-carrageenan.

Because of their ability to bind water and build gels, carrageenans are often used as thickening, gelling and stabilizing agents in a wide range of applications (Liao et al., 2021). The viscosity and strength of the gels depend on different factors like the number of sulphate groups, the temperature, the association with cations (sodium, calcium, kalium) and the concentration (Hilliou, 2021; Lai et al., 2000). Synergistic effects could be observed when *kappa*-carrageenan was mixed with locust bean gum leading to an improvement of mechanical properties (Martins et al., 2012). In the food industry, this combination is often used in cooked meats (Saha and Bhattacharya, 2010). Additionally, many other processed food products contain carrageenan as a stabilizer or thickening agent (McKim, 2014). In dairy products like ice cream and chocolate milks, carrageenans are used to prevent separations by interacting with milk proteins and forming networks (Langendorff et al., 2000). Furthermore, they are added to low-fat or fat-free meat and cheese products to improve the texture (Błaszak et al., 2018; Trius and Sebranek, 1996). Although food-grade carrageenans were classified to be safe for consumers by different authorities worldwide, the effect on human health is controversial discussed in the literature (Liu et al., 2021). Recent studies with mice showed that an intake of *kappa*-carrageenan for a longer period of time has an influence on the insulin sensitivity and inhibits the insulin signalling pathway (Bhattacharyya et al., 2012; Zhou et al., 2021). Furthermore, clinical trials suggested that the consumption of carrageenan might contribute to inflammatory bowel diseases by interacting with gut microbiome (Borsani et al., 2021). Nevertheless, many benefits concerning carrageenan intake are described. One example is the antiviral activity of carrageenan on different virus types like hepatitis A or SARS-CoV-2 (Frediansyah, 2021;

Girond et al., 1991; Valado et al., 2019). Moreover, an increasing number of studies demonstrated the effectiveness of carrageenans against cancer by regulating the immune response (Liu et al., 2019). However, further research is needed to get more information about the effect of carrageenan on benefits and risk factors of human health (Liu et al., 2021).

Another hydrocolloid is agar-agar – a mixture of the two polysaccharides agarose and agaropectin – which is obtained from red macroalgae by a long-term extraction procedure (Gómez Barrio et al., 2022). The main structure of agarose (Figure 2) consists of alternating (1,3)-ß-D-galactopyranose and (1,4)-3,6-anhydro-α-L-galactopyranose units, whereas agaropectin has additionally sulphate groups (Gu et al., 2017; Wang et al., 2012).

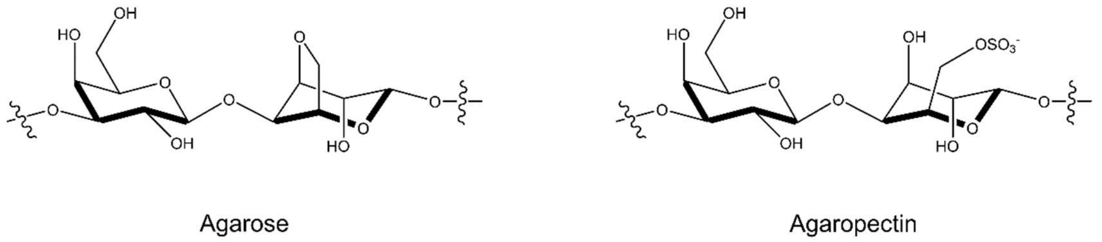

Agarose

Agaropectin

Figure 2. Representative moieties of agarose and agaropectin, the typical components of agar-agar.

Agar-Agar is mainly used as growth medium for multiple microorganisms in cell culture (Petrovski and Tillett, 2012). Furthermore, it is often applied in pharmaceuticals, cosmetics and foodstuffs due to its thickening, gelling and stabilising properties (Lee et al., 2017). Common application fields include dairy products like yoghurt and cream cheese, beverages like wine and beer as well as confectionary and desserts like jellies and donuts (Leandro et al., 2020). Agar-Agar is also known for its anti-inflammatory, anti-diabetic and antioxidant activities (Louala and Lamri-Senhadji, 2019). Furthermore, it was hypothesized that the consumption might help to reduce body weight by increasing the bulk of food and delaying the gastric emptying, to supply the prevention and treatment of obesity and to inhibit the proliferation of colon cancer cells (Clegg and Shafat, 2014; Louala and Lamri-Senhadji, 2019; Yun et al., 2021). Nevertheless, additional investigations concerning beneficial effects of agar-agar are required.

Locust bean gum (E410), guar gum (E412) and tara gum (E417)

Locust bean gum is usually obtained from seed endosperms of carob trees (*Ceratonia siliqua*), whereas guar gum is extracted from the endosperm of cluster beans (*Cyamopsis tetragonoloba*) and tara gum is produced from seed endosperms of the *Caesalpinia spinosa* tree (Barak and Mudgil, 2014; Mudgil et al., 2014; Wu et al., 2015). These three polysaccharides belong to the galactomannans and only differ in the ratio of mannose and galactose unit (Xu et al., 2022). In particular, guar gum has a mannose/galactose ratio of 2/1; tara gum shows a characteristic ratio of 3/1 and the mannose/galactose ratio in locust bean gum is 4/1 (Dionísio and Grenha, 2012). The typical structures are shown in Figure 3.

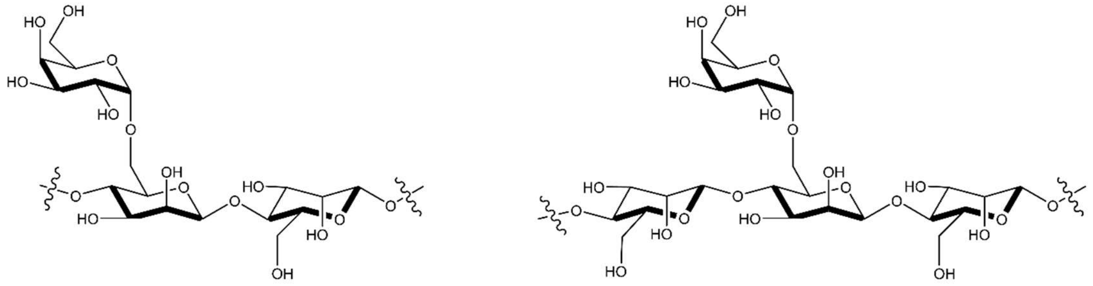

Guar gum

Tara gum

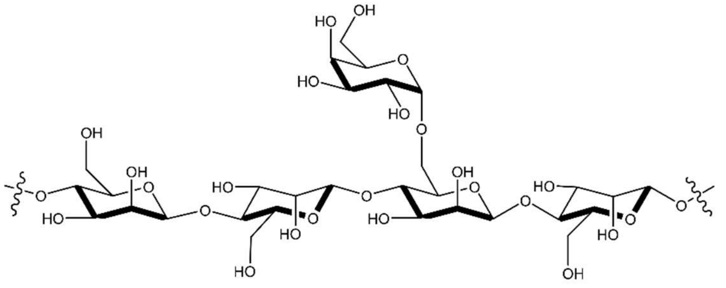

Locust bean gum

Figure 3. Representative moieties of the galactomannans guar gum, tara gum and locust bean gum.

In the food industry, galactomannans are applied in products like beverages for phase stabilization, bakery products for the increase of volume and viscosity, noodles for the enhancement of strengthening effects, ice creams for inhibition of ice crystallization and low-fat yoghurts for texture improvements (Barak and Mudgil, 2014). Furthermore, combinations of locust bean gum with guar gum, xanthan gum or *kappa*-carrageenan are often used due to synergistic effects (Martins et al., 2012; Schorsch et al., 1997). The consumption of guar gum helps to control body weight by decreasing the appetite and slowing gastric emptying, lowers the total and LDL-cholesterol and contributes to a better mineral absorption (Mudgil et al., 2014). Locust bean gum also shows beneficial effects like preventing cardiovascular diseases, reducing inflammatory bowel diseases and influencing the rate of carbohydrate degradation (Barak and Mudgil, 2014).

Gum arabic (E414)

The hydrocolloid gum arabic is exudated from *Acacia senegal* or *Acacia seyal* trees (Patel and Goyal, 2015). Although different branched structures have been proposed, the exact conformation of gum arabic depends on various factors like source, climate conditions and processing methods (Jarrar et al., 2021; Swenson et al., 1968). Hence, the molecular weight of gum arabic shows variations from 60 to 580 kDa (Duvallet et al., 1989). Arabinogalactan (Figure 4) – the main substructure of gum arabic – contains a linear backbone of (1,3)- and (1,6)-ß-D-galactopyranosyl units with linked α-L-arabinofuranoses, α-L-rhamnopyranoses, ß-D-glucuronic acids and 4-O-methyl-ß-D-glucuronic acids (Ashour et al., 2022; Churms et al., 1983).

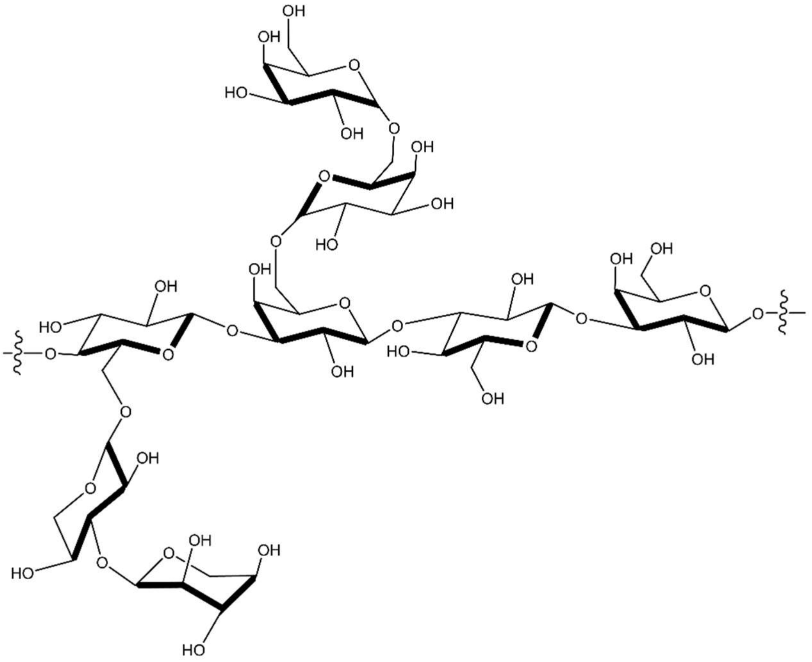

Arabinogalactan

Figure 4. Representative moiety of arabinogalactan, a typical substructure of gum arabic.

Gum arabic is able to stabilize oil-in water interfaces and is therefore often applied as an emulsifier in the food industry (Yadav et al., 2007). Due to its low viscosity formation in aqueous solutions, it is often used in high concentrations as thickening and stabilizing agent in a wide range of foodstuff like bakery products or soft beverages (Barak et al., 2020). Furthermore, the usage of gum arabic as a composite for edible coatings helps to increase the shelf-life and quality of fruits and vegetables like strawberries or tomatoes (Mahfoudhi et al., 2014; Tahir et al., 2018). A large number of studies showed that the consumption of gum arabic has biological effects on human health like increasing nitrogen extraction in patients with chronic renal failure, decreasing blood pressure and increasing plasma short-chain fatty acids (Phillips and Phillips, 2011).

Pectin (E440)

Pectin is a plant cell wall component with complex construction that is extracted from different raw materials like citrus peels, apple pomace or sugar beet pulp (Thakur et al., 1997). It is composed of the polysaccharides homogalacturonan, rhamnogalacturonan I, rhamnogalacturonan II and xylogalacturonan (Xiao and Anderson, 2013). Although all four substructures contain a linear chain of (1,4)-α-D-galacturonic acid, the exact composition depends on the source, the extraction method and the environment (Thakur et al., 1997). The residues of homogalacturonan can be methylated or acetylated, whereas the other types are even more complex and contain different other sugars like xylose, rhamnose or arabinose (Mohnen, 2008). The typical moiety of rhamnogalacturonan I is shown in Figure 5.

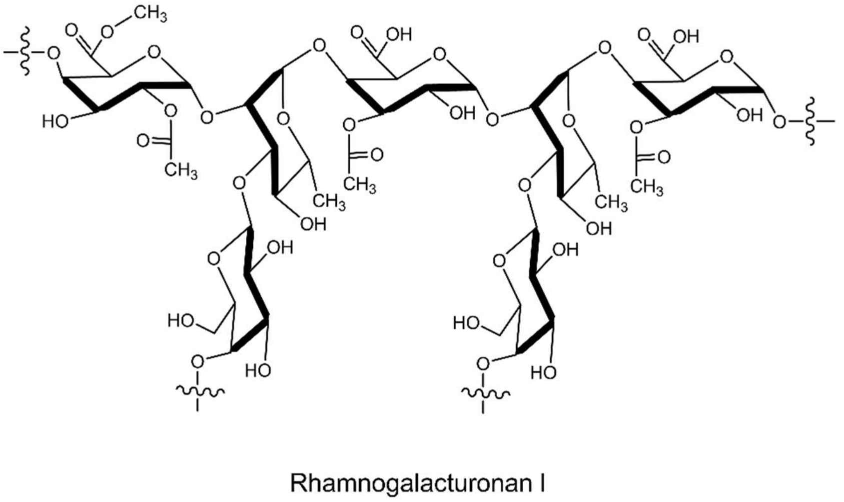

Figure 5. Representative moiety of rhamnogalacturonan I, a typical substructure of pectin.

According to its degree of methylation (DM), pectin can be divided into high methoxy pectin (more than 50% DM) and low methoxy pectin (less than 50% DM) showing different chemical features (Chan et al., 2017). Therefore, it is commonly standardized with sucrose or glucose in order to guaranty consistent attributes (Naseri et al., 2008). Furthermore, this polysaccharide is often modified (e.g. substitution, chain elongation, depolymerisation) in order to adjust specific functional properties (Chen et al., 2015). In the food industry, pectin is applied as a gelling and thickening agent in various products like jams, desserts or dairy products, but also in coatings and films to extend the shelf-life of foodstuff (Freitas et al., 2021). Although it has been proven that pectin beneficially affects human health by interacting with the gut microbiome, modulating the immune response directly or indirectly and inhibiting hypersensitivity reactions, further studies are required to elucidate the exact mechanism (Blanco-Pérez et al., 2021).

1.2 NMR spectroscopy as powerful tool for targeted and untargeted analysis

Nuclear magnetic resonance (NMR) spectroscopy is becoming more and more important in various fields (Gerothanassis et al., 2002). Developed in 1946 by Felix Bloch and Edward Purcell and optimized by Richard R. Ernst while designing a pulse fourier transform NMR spectrometer in order to increase the sensitivity, the main application of NMR spectroscopy is the structure elucidation (Ernst, 1992; Thomas, 1991). By recording one- and two-dimensional NMR spectra like correlated spectroscopy (COSY), heteronuclear single quantum coherence (HSQC) or heteronuclear multiple bond correlation (HMBC), correlations between protons and carbon atoms can support the determination of the exact structure from measured components (Kwan and Huang, 2008). Furthermore, the diffusion ordered spectroscopy (DOSY) allows the measurement of diffusion coefficients from substances with different molecular weight by using pulse sequences like the stimulated echo (STE) or longitudinal eddy current delay (LED) pulse sequence (Johnson, 1999; Thrippleton et al., 2003). For the determination of the molecular weight from linear and dispersed polymers, DOSY measurements with standards of known molecular weight can replace classical gel permeations chromatography measurements (Li et al., 2012). The DOSY technology is also applied in food science. For example, the self-diffusion of different aroma components in a food matrix of *iota*-carrageenan in low concentration could be easily observed by using DOSY experiments (Gostan et al., 2004). Additionally, the purity and the molecular weight of polysaccharides in the crude extract of various mushrooms was unequivocally determined in the DOSY spectra (Politi et al., 2006).

Nowadays, proton NMR spectroscopy is also an appropriate analytical tool for impurity analyses, degradation and quantification of various compounds in chemicals, pharmaceuticals and natural products (Jaki et al., 2021). Due to the direct proportionality of signal intensity to number of nuclei, absolute concentrations can be calculated by using an internal standard (Barding et al., 2012). Quantitative NMR (qNMR) measurement is of great interest for food analysis as it enables an easy, fast and simultaneous determination of different compounds in complex matrices (Simmler et al., 2014). For example, the fatty acid chain composition in different meat products and fish oils could be directly verified by using qNMR spectroscopy (Gottstein et al., 2019; Siciliano et al., 2013). Furthermore, food additives like sweeteners (acesulfame potassium) or preservatives (benzoic acid, sorbic acid and their salts) were quantitatively determined in processed foods by proton NMR spectroscopy after solvent extraction. The results demonstrated robustness, good linearity and high precision of the studies (Ohtsuki et al., 2015; Ohtsuki et al., 2012b; Ohtsuki et al., 2012a).

These days consumer pay more attention to food labelling because high quality food products are associated with health benefits and food safety (Petrescu et al., 2019). However, in the past various food products were fraudulently labelled concerning geographical origin due to economic reasons (Zhao et al., 2022). Therefore, targeted and untargeted NMR spectroscopy is more frequently used in combination with multivariate statistical analysis for the investigation of authenticity and geographical origin (Hong et al., 2017). For example, extra native olive oil is well known for its high beneficial effects like reducing the risk of cardiovascular diseases (Yubero-Serrano et al., 2019). However, it is often diluted with oil of lower quality for the expand of profit (Lozano-Castellón et al., 2022). In order to determine the geographical origin, NMR data of olive oils obtained from various geographical areas are frequently coupled with multivariate statistical analysis like the principal component analysis (Rongai et al., 2017). This combination is also applied for the geographical determination of other food categories like beverages (e.g. wine, coffee, fruit juices), animal origin food products (e.g. meat, fish, milk) or walnuts (Arana et al., 2015; Godelmann et al., 2013; Hassoun et al., 2020; Marchetti et al., 2019; Schmitt et al., 2020).

Taken together, one- and two-dimensional NMR spectroscopy is a powerful tool for targeted and untargeted analysis in various research areas (e.g. chemistry, biology, food science) as it enables the structure elucidation of unknown substances as well as a fast and precise identification and quantification of compounds in different matrices.

1.3 Review of analytical methods for the determination of thickeners

Many different well-established procedures for the identification and quantification of food-grade thickeners in various matrices are described in the literature. The most common methods are summarized in the following section.

Gas chromatography and high performance liquid chromatography

For the determination of food thickeners, food authorities in Germany use the officially accepted §64 Lebensmittel- und Futtermittelgesetzbuch (LFGB) method L 00.00-13 which is based on the protocol from Glück and Thier (1980). The method comprises the removal of fat, starch, proteins, sugars and salts, the precipitation of the food thickeners, the acid hydrolysis into sugar monosaccharides, the derivatization and the measurement by gas chromatography with flame ionization detection. It enables the identification and simultaneously quantification of nine different polysaccharides like locust bean gum, carrageenan and xanthan in food products. Furthermore, recovery values of 80 - 90% can be achieved in dairy products like skim milk, ice cream mixtures and pudding products. Nevertheless, it should be noted that this method lacks sensitivity. In complex matrices with two or more thickening agents, it might be difficult to assign the signals in the chromatogram to the residual monosaccharides and determine the amount of the thickeners because the acid hydrolysis can lead to similar sugar composition. For example, the thickening agents carrageenan and agar-agar cannot be distinguished from each other with this method due to their comparable structural units (Glück and Thier, 1980).

Furthermore, the concentration of the thickening agents alginate, xanthan gum and pectin in complex foodstuff like milk products can be determined by high performance liquid chromatography (HPLC) after freeze-drying and direct methanolysis. Even though high reproducibility and recovery can be achieved, the presence of other thickening agents like gum arabic may reduce the precision (Quemener et al., 2000).

Size exclusion chromatography

Food thickeners can also be separated and identified using gel permeations chromatography or gel filtration chromatography (Gaborieau and Castignolles, 2011). For example, gum arabic was qualitative and semi-quantitative analysed in wines by gas chromatography mass spectroscopy (GC-MS) after precipitation of the polysaccharides and isolation of the pure gum arabic by size-exclusion chromatography although the evolved method is based on many challenging preparation steps and lacks accuracy due to the natural variation of gum arabic (Gallina et al., 2004).

Capillary electrophoretic determination

Schneider et al. (1999) presented a capillary electrophoretic method which is based on the hydrolysis of thickening agents into their monosaccharide units, derivatization with 2-aminoanthracene and fluorescence detection. This method allowed the fast identification of food thickeners in food systems like cherry jams and lyophilized pasta sauce although the monosaccharides arabinose and mannose could not be separated (Schneider et al., 1999). In another study of Hassan et al. (2002), carrageenans were analysed in different food matrices (e.g. tart cream, salad dressing and ice cream) by potentiometric titration using the titrants protamine or poly-L-arginine and polyanion carrageenan or polycation protamine sensors. Spiking experiments demonstrated the robustness and high accuracy of the developed method (Hassan et al., 2002). More recently, a DNA biosensor for the direct determination of carrageenans was developed. The electrostatical interaction of the DNA-methylene blue solution with carrageenans led to a realise of the colouring agent resulting in a decreased electrochemical signal (Hassan et al., 2019).

Polymerase chain reactions

Meyer et al. (2001) and Urdiain et al. (2004) developed a DNA-based method for the qualitative discrimination of locust bean gum and guar gum. By using specific designed primers for the polymerase chain reaction (PCR), the two food additives could be fast and simple identified in processed food like milk products, salad dressing and meat, although this method seemed to be inappropriate for a quantification and could only be used as an indirect verification of the polysaccharides according to the specific DNA sequence of the plants (Meyer et al., 2001; Urdiain et al., 2004).

Enzyme-linked immunosorbent assays

Different enzyme-based binding protein assays can also be applied for a fast and sensitive screening and quantification of thickening agents in food products. For example, the enzyme-linked immunosorbent assay (ELISA) uses antigens or antibodies that are bound on a solid phase and are specific for the target substances. After having added a second antibody which is bound to an enzyme, the enzyme activity can be measured by a microplate reader (Aydin, 2015). By using this technique, food-grade thickeners like xanthan gum, carrageenan and gum arabic in concentrations of 0.001% – 0.01% (w/w) could be simple and rapid determined in food samples like jelly or pudding without any observed cross-reactions except for tragacanth and galactomannans in a gum arabic assay (Arakawa et al., 1991; Haines and Patel, 1997). Guar gum and locust bean gum could further be quantitatively determined using inhibition curves of reference material (Pettolino et al., 2002).

Colorimetric reactions

Soedjak (1994) showed that anionic hydrocolloids like carrageenan could also be determined using colorimetric methods. After reaction with methylene blue, the absorbance maximum of the purple complex was increased at 559 nm whereas the methylene blue solution showed decreased absorbance maxima at 610 nm and 664 nm. Although the applicability of the assay to determine carrageenan in milk solutions was demonstrated, it should be noted that various components like phosphate or milk proteins might influence the measurement by rivalling with carrageenan for the binding site of the dye (Soedjak, 1994). Additionally, a similar method using alacian blue for the complex formation enabled a simple determination of carrageenan in different food products like jellies and salad dressing even though variations depending on the carrageenan type were observed (Yabe et al., 1991). Pechanek et al. (1982) demonstrated that gelling and thickening agents could also be analysed by electrophoretic methods. After removal of fat, starch and protein components from the food product, the polysaccharides were electrophoretic separated using polyacrylamide gels, agarose gels or cellulose acetate membranes. The colour reaction with fuchsin or methylene blue enabled the unequivocally identification of low concentrated food thickeners in food products like vanilla pudding cream, ice cream or ketchup, although the galactomannans guar gum and locust bean gum showed similar migration behaviour making a differentiation impossible (Pechanek et al., 2020).

NMR spectroscopy

More recently, there has been a growing interest in the detection of food thickeners by NMR spectroscopy. For the quantification of carrageenans in blends, the polysaccharides were precipitated with ethanol, dissolved in water and measured by proton NMR spectroscopy. This protocol enabled a fast and simple determination of intact carrageenan types even if the exact composition had a significant influence on the precision of the results (Tojo and Prado, 2003). Additionally, Grün et al. (2015) established a protocol for the isolation and purification of non-starch polysaccharides in gelled foodstuff. After dissolving in hot water, enzymatic removal of fat, starch and proteins, precipitation in ethanol and centrifugation, the thickening agents in the dry final product could be unequivocally identified by non-targeted NMR spectroscopy (Grün et al., 2015). This method was further optimised and validated by Merkx et al. (2018). By fitting ^{1}H-NMR spectra of reference materials into the NMR spectrum of the isolated product, the components could be discovered according to their specific signature. Furthermore, the food thickeners were hydrolysed using the Saeman procedure and quantitatively determined according to their monomeric units by qNMR. Although a good precision and accuracy could be achieved, a degradation factor should be considered for a precise quantification of the monosaccharide content (Merkx et al., 2018).

1.4 The intracellular pathogen *Chlamydia trachomatis*

Not only the consumption of valuable food plays an important role for a beneficial lifestyle, but also the right balance of probiotic and prebiotic bacteria in the gut microbiome is essential for human health (Lenoir-Wijnkoop et al., 2007). However, infections with pathogenic bacteria (e.g. *Neisseria meningitidis*, *Staphylococcus aureus*, *Mycobacterium tuberculosis*) can also occur leading to various human diseases like meningitis, pneumonia, tuberculosis or even to multiorgan failure and death (Doron and Gorbach, 2008). According to a recent research analysis, 1.27 million deaths associated with antimicrobial resistance of bacteria were estimated for 2019 (Antimicrobial Resistance Collaborators, 2022). A prominent example for an intracellular bacterial pathogen (IBP) is *Chlamydia trachomatis* (*C. trachomatis*), a Gram-negative bacterium (Witkin et al., 2017). It is the most common cause of sexually transmitted bacterial infections worldwide with over 130 million cases each year and infects eyes, lungs, cervix, urethra and rectum leading to trachoma, inclusion conjunctivitis, cervicitis, urethritis, infant pneumonitis, spontaneous abortion and infertility (Barnes, 1989; Mishori et al., 2012; Newman et al., 2015). For the treatment of uncomplicated *chlamydial* infections, antibiotics like azithromycin, doxycycline or ofloxacin are recommended, whereas erythromycin base or amoxicillin are prescribed for pregnant women (Jones, 1991; Miller, 2006; O'Connell and Ferone, 2016).

<u>Life cycle of *C. trachomatis*</u>

The developmental cycle of *C. trachomatis* (Figure 6) is characterized by two different morphologically stages, the infectious non-replicative elementary body (EB) form and the replicative non-infectious reticulate body (RB) form (Witkin et al., 2017). It is initiated by the following steps: attachment of the EB form on host cells by forming a complex of host receptors (e.g. FGFR, PDGFR, EPHA2), *chlamydia* adhesion (e.g. CT017, Hsp70, Pmps) and heparan sulphate-like glycosaminoglycan. Once inside the host, a membrane-bound compartment – the inclusion – is formed and the EBs start to differentiate into the replicative RB form. Cells begin rapidly to divide using various nutrients like amino acids or adenosine triphosphate (ATP) from the host. During the second differentiation back into the EB form, a large number of gene expressions of proteins with unknown function can be observed. At the end of the cycle, EBs are released from the host by extrusion or cell lysis activated by cysteine proteases and new host cells can be occupied (AbdelRahman and Belland, 2005; Bastidas et al., 2013; Gitsels et al., 2019; Omsland et al., 2012). Under stress conditions like treatment with interferon-gamma (IFN-γ), azithromycin, nutrient deficiency or herpes virus infections, *C. trachomatis* is able to convert from the RB form into the persistent, non-dividing aberrant reticulate body (ARB) form (Witkin et al., 2017; Xue et al., 2017). In general, persistence is a survival strategy of bacterial cells to overcome the critical situation by reducing their metabolism to a minimum, slowing down DNA replication and stopping cell division. Furthermore, persister formation might be a main cause for chronic bacterial infections even if the clinical significance has not been elucidated so far. Upon removal of the unfavorable growth conditions, ARBs start to reconvert into the RB form and divide again in normal growth rates (AbdelRahman and Belland, 2005; Eisenreich et al., 2020; Wood et al., 2013). Recent in-vitro studies showed that the response of *C. trachomatis* depends on the specific inducement, although the exact mechanism of persistent formation is poorly understood (Panzetta et al., 2018).

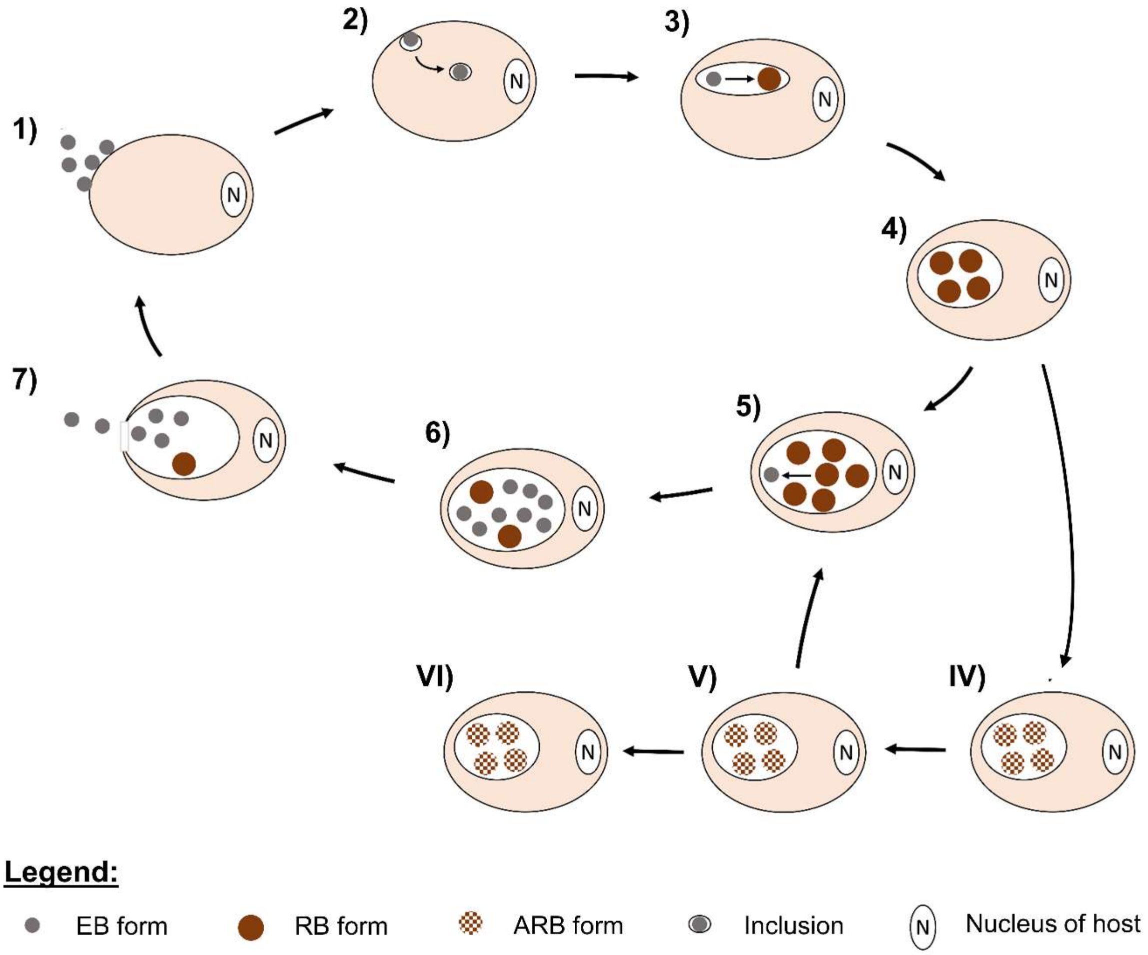

Figure 6. The life cycle of *C. trachomatis*. 1) Attachment and entry of the infectious, non-replicative EB form. 2) Building of an inclusion. 3) Differentiation of the EB form into the replicative, non-infectious RB form. 4) Replication of the RB form. 5) Differentiation of the RB form back into the EB form. 6) Continued reorganization into the EB form. 7) Release and extrusion of the EB form. IV) Under stress conditions: conversion of the RB form into the persistent ARB form. V) Reconversion of the ARB form back into the RB form. VI) Remaining in the ARB form leading to chronical infections. Based on (Corsaro and Venditti, 2004; Hammerschlag, 2004).

General metabolism of *C. trachomatis*

C. trachomatis is a strict obligate intracellular pathogen that assimilates different carbon sources from the host for an efficient replication (Nicholson et al., 2004). Its central carbon metabolism is shown in Figure 7. One major source for energy production is the Embden-Meyerhof pathway. Due to a lack of the enzyme hexokinase in *C. trachomatis*, glucose-6-phosphate produced from glucose by the host cell is directly imported *via* an UhpC transporter and further converted into glyceraldehyde-3-phosphate (GAP). The intermediate is then oxidized to pyruvate, an important precursor for the production of amino acids (e.g. alanine, glycine, serine), acetyl-coenzyme A (acetyl-CoA) as well as lactate (Ende and Derré, 2020; Iliffe-Lee and McClarty, 1999). Interestingly, the utilization of carbon sources for the biosynthesis of metabolites strongly depends on the development stage of *C. trachomatis*. In the EB form, glucose-6-phosphate is required for the protein synthesis whereas glycogen serves as energy supplier for the intracellular growth. In contrast, the RB form seems to import ATP and nicotinamide adenine dinucleotide (NAD) acquired from the host *via* the nucleotide transporter ATP/ADP translocase Npt1. ATP is then used for the biosynthesis of proteins because glucose-6-phosphate does not serve as a precursor, whereas NAD functions as universal electron carrier (Fisher et al., 2013; N'Gadjaga et al., 2022)

For the initiation of the fatty acid and lipid synthesis, the intermediate acetyl-CoA is carboxylated to malonyl-CoA *via* the acetyl-CoA carboxylase. Consequently, the enzyme malonyl-CoA-ACP transacylase converts malonyl-CoA into malonyl-ACP which is used for the elongation of the acyl-CoA chain, an important intermediate for the production of phospholipids (Yao and Rock, 2018). Furthermore, *C. trachomatis* encodes the genes for the type II fatty acid synthesis (FASII). This pathway enables the *de novo* synthesis of bacterial specific branched-chain fatty acids like iso-C15:0 and anteiso-C15:0 - two essential substrates for the efficient growth and replication - from the precursors isoleucine, leucine, valine and acetyl-CoA (provided from host or pathogen) *via* a branched-chain fatty acid synthetase (Wylie et al., 1997; Yao et al., 2014; Yao and Rock, 2018).

An essential structure element of bacterial cell walls for the maintenance of cell morphology is peptidoglycan, a macromolecule containing a linear ß-1,4-linked polysaccharide chain with N-acetylglucosamine, N-acetylmuramic acid, *meso*-diaminopimelic acid (mDAP), D-alanine and D-glutamate (Otten et al., 2018). Although it was not possible to identify peptidoglycan in *C. trachomatis* for a long time, new labelling techniques enabled the analysis of the biosynthesis, modification and degradation of peptidoglycan in this bacterium (Liechti et al., 2014). Because mammalian cells do not synthesize mDAP, the enzymes involved in the synthesis pathway have gained attention as drug targets for the treatment of bacterial infections. For the biosynthesis of mDAP, the amino acid aspartate is utilized in a condensation reaction with the precursor pyruvate *via* the enzymes *lysC, asd, dapA, dapB* and *dapF* (McCoy et al., 2006). It was further demonstrated that the enzyme *dapF* can act as an epimerase and racemase depending on the availability of the substrates mDAP or L-glutamate. Therefore, the growth of *C. trachomatis* can be influenced by supressing one of both activities (Singh et al., 2020). Although mDAP does not only serve as a precursor for the synthesis of peptidoglycan but also for the lysine biosynthesis in various bacterial strains, the *lysA* gene which is responsible for the decarboxylation of mDAP to lysine seems to be missing in *C. trachomatis* (McCoy et al., 2006).

Another main important carbon pathway is the pentose phosphate pathway (PPP) which was discovered in the 1930s. It comprised the oxidative and non-oxidative part and is mainly responsible for the production of nicotinamide adenine dinucleotide phosphate (NADPH). Similar to the Embden-Meyerhof pathway, the oxidative PPP uses glucose-6-phosphate at the beginning. After conversion to 6-phosphogluconate, this intermediate is further decarboxylated to ribulose-5-phosphate generating one reducing equivalent of NADPH. This step is also very important for the maintenance of the redox status under stress situations and for the “Warburg effect” of cancer cells. In the non-oxidative part of the PPP, different sugars are interconverted by exchanging C2 and C3 units *via* transaldolases and transketolases. Therefore, the end product of the oxidative PPP, ribulose-5-phosphate, serves as a precursor in the non-oxidative PPP for the production of ribose-5-phosphate and xylulose-5-phosphate which can further be converted to sedoheptulose-7-phosphate, erythrose-4-phosphate, xylulose-5-phosshate, fructose-6-phosphate and GAP, which in turn play a key role in the glycolytic pathway as well as for the production of energy and various metabolites (Alfarouk et al., 2020; Stincone et al., 2015). For example, the reaction of fructose-6-phosphate with ammonia from the amino acid glutamate leads to the formation of glucosamine-6-phosphate, an important intermediate for the peptidoglycan synthesis in bacteria (Barreteau et al., 2008).

The lipopolysaccharide (LPS) is a further characteristic cell wall component of Gram-negative bacteria with various functions like the protection of bacteria cells from harmful substances by forming an effective permeability barrier, contributing to the infection process by activating different signalling cascades and modulating host responses (Bertani and Ruiz, 2018; Di Lorenzo et al., 2022; Matsuura, 2013). It is composed of the hydrophobic lipid A, different polysaccharides and repeating units of O-antigens. Although the exact LPS structure depends on the specific pathogen, the biosynthetic pathway seems to be similar in all Gram-negative bacteria (Wang and Quinn, 2010). The initial step in the biosynthesis of LPS is the conversion of the PPP intermediate seduheptulose-7-phosphate into D-glycerro-D-manno-heptose-7-phosphate *via* the enzyme *GmhA* (Taylor et al., 2008). Furthermore, the PPP intermediate ribulose-5-phosphate and phosphoenolpyruvate (PEP), an important intermediate built from

GAP, serve as precursors for the synthesis of 3-deoxy-D-manno-octulosonic acid (KDO) which is then incorporated into c*hlamydial* LPS *via* the KDO transferases *KdtA* or *GseA* (Cipolla et al., 2010; Gronow and Brade, 2001). Because LPS is necessary for the regeneration of the infectious *chlamydial* EB form, there has been a growing interest in discovering the chemical structure of the lipid A moiety (Nguyen et al., 2011). The analysis of a purified LPS from *C. trachomatis* type L2 by NMR spectroscopy and matrix-assisted laser desorption/ionization (MALDI) MS revealed that the LPS of this *Chlamydia* species is a trisaccharide built of KDO and lipid A (Fadel and Eley, 2008; Kosma, 1999; Rund et al., 1999). More specifically, the lipid A moiety in this subtype seems to be composed of D-glucosamine, phosphate and various fatty acids like tetradecanoic, iso- and anteiso-tetradecanoic, hexadecanoic and 3-hydroxyeicosanoic acids (Nurminen et al., 1985). Furthermore, the results from experiments of mouse bone marrow-derived macrophages (BMDM) transfected with *chlamydial* LPS revealed minimal properties of activating canonical and noncanonical inflammatory pathways (Yang et al., 2019a). According to a study by Fadel and Eley (2008), LPS is not only a major component of the cell wall in *C. trachomatis*, but might also serve as adhesin for the attachment to receptors of human epithelial cells. However, further research is required to elucidate the role of LPS in bacterial infectivity (Fadel and Eley, 2008).

The tricarboxylic acid (TCA) cycle in *C. trachomatis* is incomplete because the enzymes citrate synthase, aconitase and isocitrate dehydrogenase are missing as shown by genome sequence analysis. Moreover, fatty acids and acetate do not serve as carbon sources since *C. trachomatis* does not encode genes for glyoxylate-bypass enzymes. However, exogenous substrates like glutamate or oxoglutarate can be scavenged to fulfil the TCA cycle (Stephens et al., 1998). The simultaneously usage of different substances (e.g. glucose, malate, glutamate) as carbon substrates during colonization of the host cells is termed “bipartite metabolism” (Eisenreich et al., 2017). Generally, this concept includes the catabolic part which is fed by C3 substrates (e.g. pyruvate, serine, glycerol) for the production of essential metabolites of the TCA cycle and the generation of energy as well as the anabolic part which is fed by important intermediates from the glycolytic pathway and PPP for the biosynthesis of cell wall components. The interaction of these two different networks depends on the state of the host cell and seems to be a common survival strategy of IBPs like *C. trachomatis* to overcome the lack of specific nutrients (Eisenreich et al., 2020; Eisenreich et al., 2017).

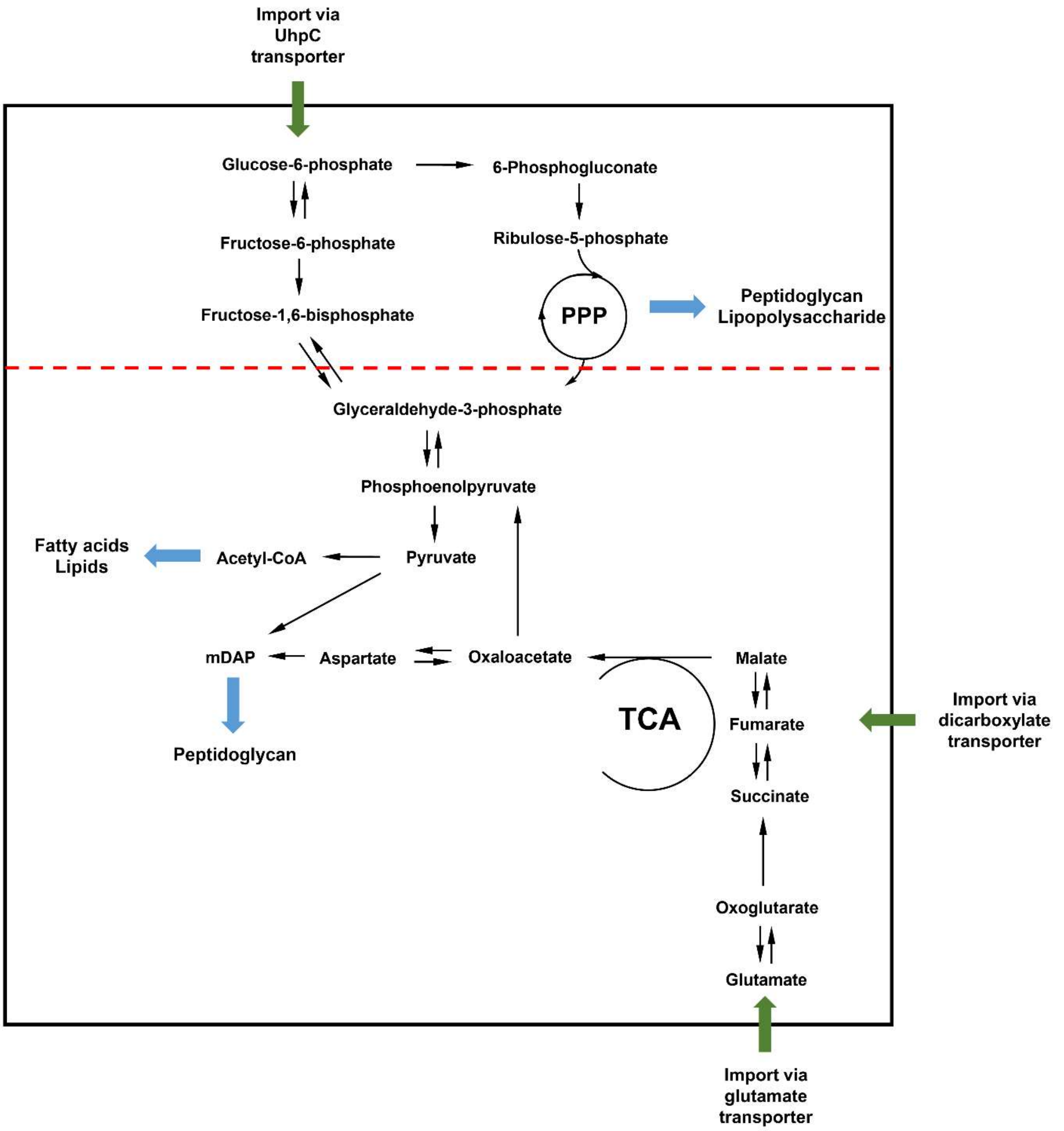

Figure 7: Model of the central carbon metabolism of *C. trachomatis*. The import of exogenous substrates *via* transporters is indicated by green arrows; the synthesis of metabolites is indicated by blue arrows; the bipartite metabolism is indicated by the red dashed line. TCA tricarboxylic acid cycle, PPP pentose phosphate pathway. Based on (Eisenreich et al., 2017; Mehlitz et al., 2017).

Reprogramming of host cell metabolism during infection with *C. trachomatis*

The constant supply of essential host-derived nutrients that cannot be produced by IBPs is crucial for the survival/persistence and efficient replication of these species in host cells. However, mammalian cells react on bacterial intrusions with different defence mechanisms like producing reactive oxygen species or inducing autophagy (Eisenreich et al., 2019). One example for an antimicrobial response to bacterial infections is the production of neutrophils. These host-produced immune cells invade pathogens in order to limit bacterial spread. However, pathogens try to counteract the intrusion by secreting/releasing specific substances. For example, the obligate intracellular human pathogen *C. trachomatis* secrets a protease-like activating factor that prevents the activation of neutrophils by interacting with their formyl peptide receptors. This leads to an inhibition of the signalling pathway downstream and enables the intracellular survival of these pathogens by preventing the generation of neutrophil extracellular traps (Rajeeve et al., 2018). Furthermore, bacteria try to manipulate the metabolism of host cells in order to fulfil their specific substrate requirements (Eisenreich et al., 2019). Although the detailed mechanism of metabolic reprogramming in host cells is still poorly understood, infections caused by *C. trachomatis* often lead to an enhanced glucose uptake by the host and hence also to an upregulated production of different metabolites (e.g. glucose-6-phosphate, pyruvate, lactate), whereas an observed downregulation in protein biosynthesis seems to be a cellular stress response of the host cells (Ohmer et al., 2019; Rother et al., 2019). Interestingly, no significant changes in the ATP consumption at different time-points after infection were detected in epithelial cells, even if glycolysis and oxidative phosphorylation are two essential pathways required for *chlamydial* proliferation (N'Gadjaga et al., 2022). Additionally, an upregulation of the glutamate transporter genes ASCT2/SLC1A5, glutaminase 1 and the amino acid transporters SLC43A1, SLC7A11 and SLC7A1 during infection could be observed using western blots and RNA-sequencing analysis. These results suggested a modulation of the glutamine metabolism in host cells and further demonstrated that host-derived glutamine is an essential metabolite for *chlamydial* growth (Rajeeve et al., 2020). Furthermore, a significant enrichment of the host enzymes aldolase A, pyruvate kinase and lactate dehydrogenase in the inclusion membrane of *C. trachomatis* and a decreased inclusion size after depletion of aldolase A indicated that the mentioned host glycolytic enzymes beneficially support the intracellular growth and replication of this bacterium (Ende and Derré, 2020). Moreover, fluorescence measurements demonstrated the ability of *C. trachomatis* to suppress the store-opened Ca^{2+} entry of host cells, which is an important regulator for Ca^{2+} homeostasis, by interacting with the endoplasmic reticulum, resulting in an inhibition of the signalling pathway (Chamberlain et al., 2022). Even if genes encoding enzymes for the generation of ATP are present in *chlamydiae*, the proliferation through the different life stages strongly depends on the supply of nucleotides (e.g. ATP, GTP, UTP) from the host. Therefore, *C. trachomatis* influences the mitochondrial morphology while inducing a mitochondrial elongation which is activated by phosphorylation of the dynamin-related protein 1. This elongation results in an upregulation of mitochondrial oxygen consumption and higher amounts of ATP (Kurihara et al., 2019).

Although *C. trachomatis* is able to synthesise some fatty acids on its own, host-derived lipids (e.g. sphingomyelin, phosphatidylcholine (PC), cholesterol) and acyl-CoA-synthetases from the host are incorporated into the inclusion in order to guaranty the survival of this bacterium. Because genes encoding for the synthesis of unsaturated fatty acids like oleate are absent in *C. trachomatis*, these lipids are efficiently utilized from the host cells, whereas saturated fatty acids may be derived from host or pathogen for the biosynthesis of phospholipids (Yao et al., 2015a). According to a recent finding, *chlamydial* growth also depends on the direct import of host-produced lipid droplets containing cholesteryl esters into the *chlamydial* membrane-bound compartment which can further be converted by bacterial-specific enzymes into cholesterol and free fatty acids for additional usage as carbon nutrients. Therefore, eukaryotic acyl-CoA:cholesterol acyltransferases seem to be essential enzymes for the replication of *C. trachomatis* as they catalyze the esterification of cholesterol in the lumen of the endoplasmic reticulum of the host (Peters and Byrne, 2015). Moreover, gene microarray analysis demonstrated that *C. trachomatis* manipulates the lipid metabolism of cervical epithelial cells in order to provide favourable conditions for its intracellular growth. During infection, several effects like the release of arachidonic acid from host membrane-bound phospholipids, a higher expression of cyclooxygenases which in turn catalyse the conversion of arachidonic acid into prostaglandins leading to inflammatory reactions, as well as the stimulation of cervical epithelial cells to produce and release interleukin-8 could be observed (Fukuda et al., 2005). According to different studies, there is evidence that these microorganisms seem to regulate the exact composition of phospholipids by replacing host-specific unsaturated fatty acids with bacterial-specific branched-chain fatty acids (Hatch and McClarty, 1998; Recuero-Checa et al., 2016; Wylie et al., 1997). However, results of labelling experiments from other research groups did not verify the suggestion of modifying host phospholipids with branched-chain fatty acids during infection with *C. trachomatis*, even if an increase of the phospholipids phosphatidylglycerol (PG), phosphatidylethanolamine (PE) and cardiolipin in infected host cells could be detected (Yao et al., 2015b). Additionally, PC – a mammalian specific phospholipid essential for bacterial growth – seems to be incorporated into the bacterial inclusion membrane using host-specific transporters without any previous modification (Cox et al., 2016). Taken together, further research analysis is required to shed more insight into metabolically changes in the pathways of mammalian host cells during *chlamydial* infections.

1.5 Isotopologue profiling as powerful tool for metabolic flux analysis

Antimicrobial resistance of bacteria is an ubiquitous issue as it causes several hundred thousand of human deaths each year (Mancuso et al., 2021). Interestingly, only few cases of antimicrobial resistance associated with clinical treatment failure of *C. trachomatis* infections are documented in the literature, whereas no resistance could be determined in strains from human isolates (Sandoz and Rockey, 2010; Somani et al., 2000). Nevertheless, a detailed characterisation of the central carbon metabolism of pathogen and its host cells is urgently needed as it might open new possibilities to avoid antibiotic resistance and to evolve new suitable drug targets for the treatment of bacterial infections.

The first flux analyses for discovering metabolic pathways were performed in the early 1990's using ^{13}C-NMR and MS measurements. Further improvements regarding experimental setting, measurement possibilities and mathematical data analysis enabled its application in various fields like cancer research, drug discovery, food science and nutrition research (Beger, 2013; Wiechert, 2001; Wishart, 2008; Wishart, 2016). Nowadays, ^{13}C-metabolic flux analysis (^{13}C-MFA) using stable isotope tracers has become an important mathematical approach for the detection of unknown pathways and reconstruction of the general metabolic network from different species especially in biological systems (Antoniewicz, 2021). Generally, ^{13}C-MFA is performed under the assumption that the amount of utilization and production of metabolites are in the same order of magnitude; meaning metabolic fluxes and incorporations of isotopes are constant in time which is termed metabolic and isotopic steady state (de Falco et al., 2022). Further assumptions are: no distinction between unlabelled and labelled carbon atoms during enzymatic conversions, no direct transformation of metabolites between different enzymes, no contamination of ^{13}C-tracers with other substances, an ideally composited intracellular surrounding in a homogenous cell culture, no turnover of metabolites and a complete metabolomic network model (Long and Antoniewicz, 2019). Because the nucleus ^{13}C has a low natural abundance of 1.1%, isotopic labelling is often used in order to increase sensitivity while producing more ^{13}C nuclei (Clendinen et al., 2015). By performing labelling experiments with different ^{13}C-tracers like [U-$^{13}C_6$]glucose, [U-$^{13}C_4$]malate or [U-$^{13}C_5$]glutamate, the labelled carbons are distributed into various intermediates and metabolites of an organism leading to different isotopologues. The synthesis and consumption rates can then be quantitatively analysed by NMR, LC-MS or GC-MS (Antoniewicz, 2021; Wiechert, 2001). Basically, isotopologues are "molecules with identical chemical structures but differences in mass due to the presence of different isotopes" (Langenhan et al., 2022), such as CH_3-CO-CoA and $^{13}CH_3$-CO-CoA. Isotopomers are a subcategory of isotopologues and are defined as "molecules of the same chemical species showing a specific labelling pattern" (Schmidt et al., 1997), such as CH_3-^{13}CO-CoA and $^{13}CH_3$-CO-CoA. The molecule consisting only of ^{12}C atoms is called M, whereas the isotopomers of this molecule containing ^{13}C labelled atoms are prescribed with M+1, M+2, M+3, et cetera (Hellerstein and Neese, 1999).

The application of GC-MS is the most widely used technique for metabolomic profiling as it enables an efficient separation of substances in a complex mixture, a sensitive and selective identification as well as a precise and accurate quantification of compounds (Fiehn, 2016; Wittmann, 2007). Additionally, commercially available mass spectra libraries (e.g. NIST, Wiley MSforID, Massbank) with a large number of data including compound name, molecular weight, retention time and fragmentation pattern from various references can simplify and verify the identification of unknown substances easily and quickly (Kind et al., 2018).

For the calculation of the relative isotopologue distribution of a metabolite, the absolute mass isotopomer patterns measured by GC-MS are corrected by subtracting the natural abundance of the characteristic distributions M, M+1, M+2, M+3, et cetera of unlabelled references from the analysed metabolite (Hellerstein and Neese, 1999). The total excess value – defined as the percentage of overall enrichment – for a specific isotope within a molecule can then be calculated from the isotopologue data with the following formula (Lee et al., 1991).

$$^{13}C - Excess = \frac{[(M+1)\ x\ 1] + [(M+2)\ x\ 2] + [(M+3)\ x\ 3] + \cdots + [(M+n)\ x\ n]}{n}$$

with n = number of carbon atoms

The beneficial characteristics of NMR spectroscopy like the simultaneously identification of unknown metabolites, the usage of only one internal standard for the quantitative analysis of many substances in a single NMR spectrum, the high reproducibility and the easy sample processing without any previous time-consuming preparation steps (e.g. harsh chemical treatment, separation, derivatization) make this analytical method an attractive alternative tool for metabolomic research (Nagana Gowda and Raftery, 2021). According to a summary of published review and research articles, the interest in metabolomics using NMR spectroscopy has gained more attention since the year 2000 in various fields like cells, plants and food (Larive et al., 2015). Although the nuclei ^{31}P, ^{15}N and ^{19}F are more and more frequently applied for the quantification of metabolites, one-dimensional ^{1}H-NMR and ^{13}C-NMR spectra are the most common used applications for metabolomic analyses (Crook and Powers, 2020). By recording a proton NMR spectrum, the integrated satellite signals from ^{13}C atoms that are directly bound to the proton of a specific metabolite provide informations about the labelling enrichment beyond its natural abundance. The ^{13}C-excess of a specific metabolite can therefore be determined using the following formula (Strauss et al., 1992).

$$^{13}C - Excess = \frac{I(^{13}C - satellites)}{I(^{13}C - satellites) + I(metabolite)}$$

with I = integral of signals from ^{13}C-satellites; I = integral of signal from metabolite

Taken together, the combination of GC-MS and NMR spectroscopy enables a precise and reproducible flux analysis in various research areas by providing comprehensive informations of ^{13}C-marked positions in a metabolite acquired by NMR spectra as well as mass isotopologue distributions obtained from MS spectra (de Falco et al., 2022). In the following, some results of flux analyses from labelling experiments in the context with the pathogen *C. trachomatis* are described in more detail.

Reconstruction of *C. trachomatis* general metabolism and discovery of interactions with host cells by performing labelling experiments

Due to its high clinical relevance, metabolic adaption of *C. trachomatis* to different host cells was intensively studied in the past decades. For example, a flux modelling of the common pathways in *C. trachomatis* was reconstructed based on data obtained from proteomic and quantitative real-time PCR experiments at different time-points during infection. By comparing mRNA expression rates of selected enzymes, a higher activity of the pathways in the RB form could be determined in contrast to the EB form. Thus, the constructed model of the metabolism describe pathway activity changes during infections and might build a foundation for further detailed research studies (Yang et al., 2019b). In order to get more information about how *C. trachomatis* influences host lipid metabolism and which specific host-derived nutrients are constantly utilized for *chlamydial* lipid biosynthesis, experiments using [U-^{14}C]isoleucine and [U-^{14}C]glucose were performed. The highest enrichment was detected in PE of infected HeLa cells, followed by PC and PG, whereas other phospholipids (e.g. phosphatidylserine, phosphatidylinositol, sphingomyelin) contained only minor incorporations of radioactivity (Wylie et al., 1997). Radiolabelled glucose was efficiently metabolized for the fatty acid biosynthesis in bacterial and host cells. It was further suggested that only a small amount from the conversion of labelled isoleucine into acetyl-CoA, the precursor for the biosynthesis of fatty acids, was incorporated into the lipid fraction of uninfected host cells. In contrast, isoleucine incorporation into fatty acids of infected cells was associated with the FASII pathway of *C. trachomatis*, as mammalian cells do not have the ability to produce branched-chain fatty acids from the precursor isoleucine (Yao et al., 2014). The analysis of uninfected and infected HeLa cells which were pre-labelled with [^{3}H]arachidonic acid, demonstrated a higher release of this fatty acid into the medium and a smaller incorporation in PE of infected host cells. Hence, host-derived polyunsaturated fatty acids from PE were selectively cleaved in order to adjust the PE composition in host cells infected with *C. trachomatis* (Yao et al., 2015b). Furthermore, isotopologue labelling of lauric acid, myristic acid and ethanolamine in the medium revealed that exogenous fatty acids can be elongated and incorporated into phospholipids by *C. trachomatis*, whereas ethanolamine does not serve as a precursor for the biosynthesis of PE in this pathogen, but is used for the production of host specific phospholipids (Yao and Rock, 2018). Labelling experiments of infected HeLa and CaCo-2 cells with ^{13}C-marked glucose, malate and glutamine revealed a *de novo* synthesis of the amino acids alanine, aspartate and glutamate from host-derived metabolites whereas other amino acids and nutrients were directly scavenged from the host cell. Additionally, ESI-FT-ICR-MS analysis of bacteria pellets revealed that *C. trachomatis* is able to assimilate host produced glucose-6-phosphate efficiently into LPS (Mehlitz et al., 2017). Furthermore, a recent study using [U-^{13}C$_5$]glutamine in axenic cultures demonstrated its efficient metabolization *via* glutaminolysis into the TCA intermediates, the amino acid alanine as well as the peptidoglycan component mDAP. Hence, the glutamine metabolism of host cells seems to play an important role for *chlamydial* replication, as upregulations of glutamine transporters and glutaminase during infection were observed (Rajeeve et al., 2020). Taken together, the incorporation of different labelled tracers demonstrated that *C. trachomatis* is able to utilize various carbon substrates and metabolites in a bipartite-like metabolism for the synthesis of cell wall components, LPS, fatty acids and the production of energy (Mehlitz et al., 2017).

2. Material and Methods

2.1 Materials

2.1.1 Laboratory equipment

Table 1: Overview of laboratory equipment

Item	Description	Manufacturer
Centrifuges	A-14	Jouan GmbH (Unterhaching, Germany)
	Biofuge primo R	Heraeus (Traunstein, Germany)
	Sigma Type 2-16KL	Sigma GmbH (Osterode am Harz, Germany)
	Beckman Coulter Life Sciences System Allegra X.30R	Beckman Coulter GmbH (Krefeld, Germany)
Drying oven		Binder GmbH (Tuttlingen, Germany)
Freeze-dryer	Christ Alpha 2-4 LD	Christ (Osterrode am Harz, Germany)
		Vacuubrand GmbH & Co. KG (Staufen, Germany)
	Pfeiffer Vacuum Duoline pump Duo3	Pfeiffer Vacuum GmbH (Asslar, Germany)
GC-MS	Gas Chromatograph GC-2010 Mass	Shimadzu (Neufahrn, Germany)
	Spectrometer QP-2010	Shimadzu (Neufahrn, Germany)
	Auto Injector: AOC-20i	Shimadzu (Neufahrn, Germany)
	Auto Sampler: AOC-20s	Shimadzu (Neufahrn, Germany)
	GC Column: EquityTM-5, FUSED SILICA Capillary Column, 30 m x 0.25 mm x 0.25 µm film thickness	SUPELCO (Bellefonte, USA)
Heating block	Techne DRI-Block® DB 2A	Thermo-DUX GmbH (Wertheim, Germany)
Micro scales	VWR-503B	VWR (Radnor, USA)
	Model SBC 31	Scaltec Instruments GmbH (Goettingen, Germany)
	Typ MSX (SD EE)	Sartorius AG (Goettingen, Germany)
NMR spectrometer	Bruker AVANCE II 400 MHz, 500 MHz, 600 MHz	Bruker GmbH (Rheinstetten, Germany)
NMR tubes	NORELL®; LOT: PD101614C	NORELL (Morganton, USA)
Pear shaped flask	25 ml, 50 ml	Carl Roth GmbH (Karlsruhe, Germany)
pH meter	780 pH Meter (Metrohm)	Mettler Toledo GmbH (Gießen, Germany)

Table 1 (*continued*): Overview of laboratory equipment

Item	Description	Manufacturer
Pipettes	Eppendorf Research® (0.5µl - 10 µl; 10 µl - 200 µl, 100 µl - 1000 µl, 1 ml - 10 ml)	Eppendorf AG (Hamburg, Germany)
	MICROMAN® (100 µl - 1000 µl)	Gilson Inc. (Middleton,USA)
Ribolyser		Hybaid (Kalletal, Germany)
Ultrasonic bath	USC 300T	VWR (Radnor, USA)
Thermostat	IKATRON® ETS-D4 fuzzy	IKA-Werke GmbH & Co. KG (Staufen, Germany)
Vortex mixer	Vortex-Gene®2	Scientific Industries (New York, USA)

2.1.2 Software

Table 2: Overview of software used

Software	Manufacturer
ChemDraw Professional (Version 17.0)	CambridgeSoft (Massachusetts, USA)
EndNote (Version 20.0.1)	Clarivate Analytics (New York, USA)
GC-MS LabSolution (Version 4.11)	Shimadzu Corporation (Kyoto, Japan)
MestreNova (Version 12.0.0)	Mestrelab Research (Santiago de Compostela, Spain)
Microsoft Office 2016	Microsoft (Redmond, USA)
TopSpin (Version 3.6.1)	Bruker Biospin GmbH (Rheinstetten, Germany)

2.1.3 Chemicals

Chemicals used in this work were obtained from Acros organics (New Jersey, USA), Alfa Aesar (Karlsruhe, Germany), Carl Roth GmbH & Co. KG (Karlsruhe, Germany), Deutero GmbH (Kastellaun, Germany), Mast Group (Reinfeld, Germany), Merck KGaA (Darmstadt, Germany), MP Biomedicals (Illkirch, France), Sigma Aldrich Chemie GmbH (Steinheim, Germany), Supelco (Pennsylvania, USA), ThermoFisher GmbH (Kandel, Germany), Tokyo Chemical Industry TCI (Tokyo, Japan), Vitanatur GmbH (Stockstadt am Rhein, Germany), VWR (Pennsylvania, USA). Distilled water was obtained from an in-house purity water system.

2.2 Methods

2.2.1 Experiments with *Chlamydia trachomatis*

Isolation of human monocytes, differentiation to macrophages, infection of human fallopian tube cells as well as M1 and M2 polarized macrophages with *C. trachomatis*, labelling experiments with [U-$^{13}C_6$]glucose and sample collection were performed by Dr. Adriana Moldovan at the Chair of Microbiology at the Julius Maximilians University of Würzburg under the supervision of Prof. Dr. Thomas Rudel. Sample preparation for the analysis of protein-derived amino acids, TCA intermediates, fatty acids and supernatants, GC-MS and NMR measurements, isotopologue analysis and calculation were performed by Sandra Radziej at the Technical University of Munich under the supervision of Prof. Dr. Wolfgang Eisenreich.

2.2.2 Experiments with *Neisseria meningitidis*

Bacterial cultivation of *N. meningitidis* wildtype, cas9 and scaRNA, labelling experiments with [U-$^{13}C_6$]glucose, $^{15}NH_4Cl$ and ^{15}N-Glutamine and heat-inactivation of the samples were performed by Denise Müller at the Institute for Hygiene and Microbiology at the Julius Maximilians University of Würzburg under the supervision of Prof. Dr. Dr. Christoph Schoen. Sample preparation for the analysis of protein-derived amino acids and methanol-soluble polar metabolites, GC-MS measurements, isotopologue analysis and calculation were performed by Sandra Radziej at the Technical University of Munich under the supervision of Prof. Dr. Wolfgang Eisenreich.

2.2.3 Experiments with *Coxiella burnetii*

Bacterial cultivation, labelling experiment with [U-$^{13}C_6$]glucose and heat-inactivation of the samples were performed by Martha Ölke at the Medical University of Erlangen under the supervision of Prof. Dr. Anja Lührmann and Prof. Dr. Roland Lang. Sample preparation for the analysis of protein-derived amino acids, methanol-soluble polar metabolites and supernatants, GC-MS measurements, isotopologue analysis and calculation were performed by Sandra Radziej at the Technical University of Munich under the supervision of Prof. Dr. Wolfgang Eisenreich.

2.2.4 Sample preparation

2.2.4.1 Sample preparation for the analysis of thickening agents in food products and their premixtures (sections 4.1 and 4.2)

Detailed informations can be found in “Radziej, S.; Scherb-Forster, J.; Schlicht, C. and Eisenreich, W. Fast Identification of Food Thickeners by Nontargeted NMR-Spectroscopy. *J Agric Food Chem*, **2021**, 69 (12), 3761 – 3775.” and “Radziej, S.; Scherb-Forster, J.; Schlicht, C. and Eisenreich, W. NMR-based identification of thickeners in membrane-filtered food premixtures. *Eur Food Res Technol*, **2022**, 248, 1715 – 1720.”

2.2.4.2 Sample preparation and derivatization for isotopologue profiling (section 4.3)

2.2.4.2.1 Infection of host cells

Human fallopian tube cells and human M1 and M2 polarized macrophages were infected with *C. trachomatis* (MOI=1) and grown on RPMI-1640 medium. The medium was supplemented with HEPES (25 mM), FCS (10%; v/v) and [U-$^{13}C_6$]glucose (2 g/l; 11.11 mM). Plated containing cells (infected and uninfected) were washed with cold PBS 30h post infection and snap-frozen in liquid N_2. Supernatants were likewise collected, sterile-filtered with 0.2 µm-pore filters and snap-frozen. Plates were thawed on ice. The material was collected by washing and scraping with ice-cold methanol/H_2O (80/20; v/v) and the samples were immediately transferred to - 80°C. The samples were dried under a gentle stream of nitrogen gas and lyophilized over-night.

2.2.4.2.2 Sample preparation for the analysis of polar metabolites

The sample preparation was done as described earlier (Häuslein et al., 2017b). In brief, a part of the freeze-dried cell pellet was dissolved in 1 ml cold MeOH. 800 mg of glass beads were added. Cell lysis was done with a ribolyser system (1 x 20 sec. at 4.5 m/s; 2 x 20 sec. at 6 m/s). Then, the samples were centrifuged for 10 min at 7.000 rpm. The supernatants were dried under a gentle stream of nitrogen gas. The derivatization was done with 25 µl ACN (anhydrous) and 25 µl MTBSTFA for 1h at 70°C.

2.2.4.2.3 Sample preparation for the analysis of fatty acid methyl ester

The sample preparation was done as described earlier (Keymer et al., 2018). In brief, a part of the freeze-dried cell pellet was derivatized with 500 µl methanolic HCl (3N) at 80°C over-night. The solution was then dried under a gentle stream of nitrogen and dissolved in 50 µl hexane (anhydrous).

2.2.4.2.4 Sample preparation for the analysis of protein-derived amino acids and mDAP

The sample preparation was done as described earlier (Kunze et al., 2021). In brief, a part of the freeze-dried cell pellet was hydrolysed with 500 µl HCl (6M) at 105°C over-night. The solution was then dried under a gentle stream of nitrogen gas and the residue was dissolved in 200 µl acetic acid (50%). For purification, a cation exchange column of DOWEX 50WX5 (400 mesh, 5 x 10 mM) was prepared which was previously washed with 1 ml MeOH (70%) and 1 ml distilled water. After having added the dissolved amino acid solution, the column was washed twice with 800 µl distilled water. For elution of the amino acids, 1 ml ammonium hydroxide (4M) was used. The eluates were dried under a gentle stream of nitrogen gas. The derivatization was done with 25 µl ACN (anhydrous) and 25 µl MTBSTFA for 30 min at 70°C.

2.2.4.2.5 Sample preparation for the analysis of supernatants

1 ml of supernatant was lyophilized over-night. The freeze-dried residue was dissolved in 50 µl TSP solution (c = 2 mg/ml), 100 µl maleic acid solution (c = 1 mg/ml) and 450 µl D_2O. 550 µl of the solution was transferred to a 5-mm NMR tube.

2.2.5 GC-MS measurement parameters

All GC-MS spectra were recorded on a QP2010 Plus gas chromatograph mass spectrometer (Shimadzu) which was equipped with a fused silica capillary column (30m x 0.25 mm; 0.25 µm film thickness, SUPELCO) and a quadrupole detector (with electron impact ionization at 70 eV). The derivatized samples were measured three times (technical replicates) in selected ion monitoring (rate 0.5 s) at an interface temperature of 260°C and a helium inlet pressure of 70 kPa in split mode (1:5). For the analysis of polar metabolites, the column was heated to 100°C and held for 2 min. Then, the following temperature gradients were used: the first temperature gradient was 3°C/min to a final temperature of 234°C, the second gradient was 1°C/min to a final temperature of 237°C, the third gradient was 3°C/min to a final temperature of 260°C and the forth gradient was 10°C/min to a final temperature of 300°C, which was held for 2 min. For the analysis of protein-derived amino acids and mDAP, the column was heated to 150°C and held for 3 min. Then, a temperature gradient of 7°C/min was used to a final temperature of 280°C which was held for 3 min. For the analysis of fatty acids, the column was heated to 150°C and held for 3 min. Then, the following temperature gradients were used: the first gradient was 1°C/min to a final temperature of 187°C, the second gradient was 2°C/min to a final temperature of 220°C and the third gradient was 10°C/min to a final temperature of 300°C, which was held for 2 min. Data were processed with LabSolution Version 4.11

(Shimdazu, Duisburg, Germany). The calculation of ^{13}C-enrichment and distribution of isotopologues was done as previously described (Steffens et al., 2021).

2.2.6 NMR measurement parameters

2.2.6.1 NMR measurement parameters for the analysis of thickening agents in food products and their premixtures (sections 4.1 and 4.2)

Detailed informations can be found in "Radziej, S.; Scherb-Forster, J.; Schlicht, C. and Eisenreich, W. Fast Identification of Food Thickeners by Nontargeted NMR-Spectroscopy. *J Agric Food Chem*, **2021**, 69 (12), 3761 – 3775." and "Radziej, S.; Scherb-Forster, J.; Schlicht, C. and Eisenreich, W. NMR-based identification of thickeners in membrane-filtered food premixtures. *Eur Food Res Technol*, **2022**, 248, 1715 – 1720."

2.2.6.2 NMR measurement parameters for the analysis of supernatants (section 4.3)

All NMR spectra were recorded with a Bruker AVANCE II 500 MHz spectrometer equipped with a SEI probe using TopSpin Version 2.1 (Bruker Biospin GmbH, Rheinstetten, Germany). ^{1}H-NMR spectra were recorded with the Bruker pulse program "noesygppr1d" for suppression of the water signal during the relaxation period applying a narrow saturation pulse with a linewidth of about 25 Hz. The parameters were ns = 64, ds = 4, TE = 27°C, aq = 5.45 sec, td = 65536, si = 65536, sw = 12.0 ppm, p1 = 8.20 µsec. Prior to Fourier-transformation, the FIDs were multiplied with a mild Gaussian function (lb = -0.10; gb = 1.66). Chemical shifts were reported relative to the internal standard TSP at 0 ppm. The internal standard maleic acid was used for the quantification of glucose amount. Data were processed with MestreNova Version 12.0.0 (Mestrelab Research, Santiago de Compostela, Spain).

3. Aims of this work

Human health and well-being are influenced by several aspects like social and physical environment, individual personality and consumption behaviour (Hood et al., 2016). One important factor that affects the nutrient selection of customers is the labelling and presentation of the food product (Cecchini and Warin, 2016). Because of many mislabeled foodstuffs in the past decades, food monitoring is an essential tool for protecting consumers from food fraud and potential health risks (Pacholczyk-Sienicka et al., 2021). Therefore, the first part of this work focusses on the detection of thickening agents, a functional class of food additives that is increasingly used in various food products due to its stabilizing and water-binding properties. The 'gold standard' for the identification and quantification of food thickeners in different matrices is the officially accepted §64 LFGB method L 00.00-13 which is based on divers preparation steps and the measurement by GC-FID. More recently, several approaches are presented using NMR spectroscopy for untargeted and targeted analysis in complex mixtures. However, the detection and content determination of different food thickeners in various matrices is only enabled by combination of numerous (often time-consuming) sample-processing steps. Therefore, one aim of this work is the development of protocols containing simple and fast preparation steps that allow the unequivocally identification of thickening agents in different premixtures and food products according to their specific chemical shifts and correlation coefficients by performing NMR measurements.

Another factor influencing human health is the contact with pathogens. Bacterial infections often cause diseases like acute respiratory infections, diarrhoea and fever (Doron and Gorbach, 2008). Because bacteria develop mechanisms to become resistant to medicaments over time, the treatment of infections with prescribed conventional drug therapies might be less effective or even ineffective. Consequently, the detailed knowledge of the central metabolism is necessary for the determination of new potential drug targets (Eisenreich et al., 2022). Therefore, the second chapter of this work focusses on the detection of metabolic changes in the pathways of human host cells during infection with the Gram-negative obligate intracellular bacterium *C. trachomatis*. One of the most frequently applied techniques for the disclosure of carbon pathways is the ^{13}C-MFA which is based on feeding the pathogens with ^{13}C-marked tracers, performing labelling measurements at metabolic steady state and calculating the relative amount of ^{13}C-enrichment in metabolic products. Based on the generated data, adaptations of host cells to *chlamydial* infections can be determined. Thus, the second part of this work aims to get more insight into the interplay of *C. trachomatis* and its host cells (human M1 and M2 polarized macrophages, human fallopian tubes) by performing NMR and GC-MS measurements of protein-derived amino acids, TCA intermediates and fatty acids for ^{13}C-MFA.

4. Results

4.1 “Fast Identification of Food Thickeners by Nontargeted NMR-Spectroscopy”

Citation:

Radziej, S.; Scherb-Forster, J.; Schlicht, C. and Eisenreich, W. Fast Identification of Food Thickeners by Nontargeted NMR-Spectroscopy. *J Agric Food Chem*, **2021**, 69 (12), 3761 – 3775. DOI: https://doi.org/10.1021/acs.jafc.0c07760

Supporting information:

The Supporting Information can be found in 9.1.

Author contribution:

I was involved in planning the study design, performed the experiments and did the interpretation of the data. Furthermore, I wrote the first draft of the manuscript and was involved in all steps of preparing this published paper.

Summary:

Nowadays, the officially accepted §64 LFGB method L 00.00-13 and other well-established procedures from the literature are used for the analysis of thickening agents in food products and their premixtures. Because the methods are based on many time-consuming preparation steps, the aim of this study was to develop an easy protocol that allows a fast and simple screening of thickeners in different premixtures and food matrices by NMR spectroscopy.

Therefore, characteristic marker signals and diffusion coefficients for the thickeners gum arabic, carrageenan, agar-agar, locust bean gum, guar gum and pectin were determined by using one- and two-dimensional NMR spectroscopy and compared with data from the literature. The development of the presented protocol enabled the unequivocally identification of intact food thickeners in different premixtures and food systems using proton NMR spectroscopy and DOSY. In contrast to the §64 LFBG method, carrageenan and agar-agar could be distinguished from each other in the ^{1}H-NMR spectrum, whereas locust bean gum and guar gum were differentiated in the DOSY spectra. Although not all declared thickeners could be identified in all analyzed premixtures or food products with this protocol due to the complexity of food matrices and different concentrations of individual components, the combination of ^{1}H-NMR and DOSY spectroscopy might support standardized methods to determine thickening agents in food products and their premixtures.

JOURNAL OF AGRICULTURAL AND FOOD CHEMISTRY

pubs.acs.org/JAFC Article

Fast Identification of Food Thickeners by Nontargeted NMR-Spectroscopy

Sandra Radziej, Julia Scherb-Forster, Claus Schlicht, and Wolfgang Eisenreich*

Cite This: *J. Agric. Food Chem.* 2021, 69, 3761−3775 Read Online

ACCESS | Metrics & More | Article Recommendations | Supporting Information

ABSTRACT: Food thickeners are carbohydrate additives that can only be determined by long-term, multistep analysis. Fast methods to directly determine thickeners in food matrixes are therefore welcome. In this study, a rapid procedure based on the direct ^{1}H NMR analysis of food samples dissolved in deuterated water was developed. Individual thickeners were assigned due to specific marker signals gleaned from two-dimensional NMR analyses. The combination of one-dimensional ^{1}H NMR and DOSY experiments enabled unequivocal assignments of thickeners even in complex matrixes. Using this approach, gum arabic, carrageenan, agar−agar, galactomannans, and pectin could be identified in pastille, glaze, and fruit spread. Because of low concentrations (<0.5%−1%, w/w), the same thickeners and others such as xanthan gum and alginate could not be determined directly by NMR in curry sauce, rice pudding, choco milk drink, and lemon peel flavor. Moreover, NMR analyses of the hydrolysate did not reveal the specific monomeric units of the thickeners under study, as shown for the hydrolysate of lemon peel flavor. Nevertheless, the NMR approach could provide welcome means in the future to directly determine intact thickeners in food.

KEYWORDS: *food thickeners, NMR spectroscopy, gum arabic, carrageenan, agar−agar, locust bean gum, guar gum, pectin*

INTRODUCTION

In recent years, more and more consumers prefer food that is free of additives, so-called “clean labelling products”.[1] Nevertheless, food additives such as antioxidants, antimicrobials, or colorants are still often used because of their diverse functions.[2] Thickeners—another class of food additives—are also increasingly applied. As defined in regulation (EC) No. 1333/2008, thickeners are compounds that increase the viscosity of a foodstuff. Therefore, thickeners are widely used in foods to thicken these products, to adjust their texture, to attain a specific mouth feeling, to stabilize formulations, and to produce a consistent quality. Because of their ability to bind water, they often find application in foods like ice cream, desserts, cakes, jams, soups, and salad dressings in concentrations between 0.1% and 5%.[3,4] In 2014, the global market for thickeners used in food products was estimated as 2.1 million tons and 5.5 billion US$.[4] Thickeners are usually produced by a manufacturer and sold from business to business or directly to the final consumer. Therefore, premixtures containing thickeners represent another field of application. Typical thickeners are gum arabic, agar−agar, carrageenan, galactomannans (locust bean gum, guar gum, and tara gum), pectin, xanthan gum, and alginate. All of these carbohydrates are extracted from algae, plants, or trees, except for xanthan gum, which is obtained from extracts of the bacterium *Xanthomonas campestris*.[5,6]

Because of their large number of sugar units, thickeners belong to polysaccharides. The chemical structures (Figure 1) vary from linear chains with steady repeating units to alternating units with strongly branched side chains containing different sugars.[5] As the mentioned thickeners are natural products, the exact compositions frequently differ with their natural source, i.e., the structures can reflect different growth conditions for example due to variable soil, temperature, and moisture, as well as different extraction methods.[7] Therefore, sugars such as sucrose, fructose, or glucose are often added to thickeners before their usage in the food industry in order to guarantee a constant gelling behavior.[7,8]

For the analysis of natural thickeners in food, in Germany, the officially accepted method given in § 64 of the “Lebensmittel- und Futtermittelgesetzbuch” (LFGB) L 00.00-13 is usually applied. It is based on a multistep procedure including the removal of fat, starch, and proteins, precipitation of the thickeners, hydrolysis into individual sugar components, and subsequent measurement of the resultant monosaccharides by gas chromatography with flame ionization detection (GC-FID) after trimethylsilylation. As this method is time-consuming due to numerous individual steps during sample preparation, it is not appropriate for a fast screening. Furthermore, the thickeners agar−agar and carrageenan cannot be differed on this basis, as mentioned in the § 64 LFGB method (L 00.00-13 No. 8.2), since both thickeners contain the same monosaccharide units.

Nowadays, NMR spectroscopy has been established as a powerful analytical method in food chemistry.[9] Its main application is the structure elucidation of purified food components in a targeted approach. However, more recently, NMR spectroscopy has also been applied for the untargeted analysis of complex liquid mixtures, such as wine, juice, and beer.

Received: December 10, 2020
Revised: February 16, 2021
Accepted: March 4, 2021
Published: March 16, 2021

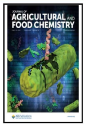

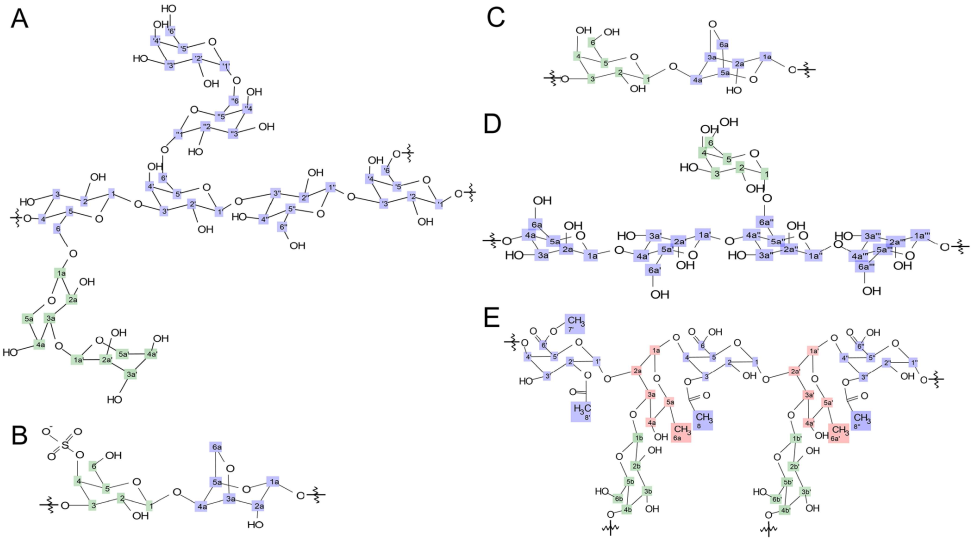

Figure 1. Chemical structures of thickeners. (A) Typical substructure of gum arabic (arabinose in green, galactopyranose in blue). (B) Typical moiety of κ-carrageenan (galactose-4-sulfate in green and 3,6-anhydrogalactose in blue). (C) Typical moiety of agar−agar (galactose in green and 3,6-anhydrogalactose in blue). (D) Typical moiety of the galactomannans locust bean gum and guar gum (mannose in blue and galactose in green). (E) Rhamnogalacturonan I, a typical substructure of pectin (galacturonic acid in blue, rhamnose in red, and galactose in green).

By combining it with different chemometric tools, for example, the authenticity, geographical origin, and ripeness of the applied raw materials could be defined by NMR following the concepts of metabolic footprinting.[10−12] In these protocols, two-dimensional diffusion ordered NMR spectroscopy (DOSY) has also been introduced for improving the identification of individual components in complex mixtures on the basis of different diffusion constants related to the molecular sizes of the components.[13,14]

The aim of this study was to develop a nontargeted ^{1}H NMR method for the fast identification of thickeners in foods and premixes for food manufacturing without time-consuming sample processing.

■ MATERIALS AND METHODS

Chemicals. Trifluoroacetic acid was obtained from Tokyo Chemical Industry TCI (Tokyo, Japan). Sodium hydroxide was purchased from Merck KGaA (Darmstadt, Germany). Galactose, rhamnose, arabinose, and glucuronic acid were obtained from Alfa Aesar ThermoFisher GmbH (Kandel, Germany). Deuterium oxide 99.9% with 0.03% TMSP-d_4 was purchased from Deutero GmbH (Kastellaun, Germany).

Alginic acid, gum arabic, and κ-carrageenan were obtained from Acros organics. The sodium salt of carboxymethyl cellulose (high viscosity) and xanthan gum were purchased from MP Biomedicals (Illkirch, France). Guar gum ∼5000 cP was obtained from Carl Roth GmbH & Co. (Karlsruhe, Germany). Locust bean gum was purchased from Vitanatur GmbH (Stockstadt am Rhein, Germany). Lipase from porcine pancreas type II (100−500 units/mg), pectin apple, and Phytagel were obtained from Sigma-Aldrich Chemie GmbH (Steinheim, Germany). Agar−agar was obtained from Mast Group (Reinfeld, Germany).

Samples. Commercially available pastilles (Bachblütenpastillen), cream pudding powder (Crèmepuddingpulver), egg replacer powder (Pflanzlicher Ei-Ersatz), fruit spread strawberry (Fruchtaufstrich Erdbeere), ice cream stabilizer (Speiseeis Stabilizator), almond milk (Mandeldrink), fitness whey (Fitnessmolke), fruit whey (Fruchtmolke), whey product (Molkenmischerzeugnis), milk (H-Vollmilch 3.5% Fett ultrahocherhitzt homogeniziert), whey (Reine Molke), milk drink (Milchdrink mit Bananen-Geschmack), clear cake glaze (Tortengusspulver klar ungezuckert), clear cake glaze (Tortengusspulver vegan and bio), curry sauce (Curry Sauce), dessert cream pudding powder with vanilla flavor (Dessert-Crèmepulver mit Vanille-Geschmack), dessert sauce with vanilla flavor (Dessertsoße mit Vanille-Geschmack), ice cream binding agent (Eisbindemittel für Milch- and Sahneeis), ice dessert strawberry (Erdbeere Eisdessert vegan and bio), low-calorie drink with mandarin flavor (kalorienarmes Erfrischungsgetränk mit Mandarinen-Geschmack), cream pudding powder (Crèmepuddingpulver mit Vanille-Geschmack), semolina pudding less sweet (Grießbrei weniger süß), bio oat drink chocolate (Haferdrink Schoko), yoghurt with 13.5% gooseberries-apple preparation (Joghurt Stachelbeere-Apfel), cream pudding powder for lemon-yoghurt dessert (Crèmespeisepulver), curry ketchup spicy (Curry Gewürz Ketchup scharf), coconut drink with rice (Kokosnussdrink mit Reis), rice pudding (Milchreis), cream pudding powder with lemon flavor (Crèmepuddingpulver mit Zitronen-Geschmack), milk drink with chocolate flavor 3.5% milk fat heat treated (Schokodrink), lemon peel flavor (Zitronenschalen-Aroma), premixtures for vitamin D3 preparation, meat preparation, emulsion type sausage, sauerkraut, stabilization of boiled sausages, and barbecue sauce were used as received unless otherwise stated.

Sample Preparation. *Preparing of Reference Thickener Samples.* Approximately 10 mg of a reference thickener was dissolved in 1 mL of D_2O with 0.03% trimethylsilylpropanoic acid (TMSP) and warmed up for 10 min at 80 °C for complete solving while stirring.

Solid Food or Premixture Samples. The premixture or food (10−300 mg) was dissolved in 1 mL of D_2O containing 0.03% TMSP and centrifuged at 14 000 rpm for 10 min at room temperature using a Beckman Coulter Allegra X.30R laboratory centrifuge. A volume of 550 μL was then transferred to a 5 mm NMR glass tube.

Table 1. Overview of Detected Thickener Signals in Different Foods and Premixtures by Nontargeted NMR Spectroscopy

name of the food product	thickener/gelling agent (according to the manufacturers specification)	comment on ^{1}H NMR spectrum
apple jelly (*self-made*)	E440 pectin	at a concentration of 150 mg/mL: pectin-signal at 5.08 ppm detectable
pastille (*Bachblütenpastille*)	E414 gum arabic	at a concentration of 30 mg/mL: gum arabic-signals at 5.30, 5.03, 4.74, 4.52, 4.42, and 4.30 ppm detectable
cream pudding powder (*Crèmepuddingpulver*)	E407 carrageenan	at a concentration of 300 mg/mL: κ-carrageenan-signals at 5.11, 4.87, and 4.54 ppm detectable
egg replacer powder (*pflanzlicher Ei-Ersatz*)	E410 locust bean gum	at a concentration of 20 mg/mL: galactomannan-signal at 5.03 ppm detectable
fruit spread strawberry (*Fruchtaufstrich Erdbeere*)	E440 pectin	at a concentration of 60 mg/mL: pectin-signal at 5.08 ppm detectable
ice cream stabilizer (*Speiseeis Stabilizator*)	E410 locust bean gum E412 guar gum E401 sodium alginate E406 agar−agar	at a concentration of 20 mg/mL: galactomannan-signals at 5.03 and 4.14 ppm detectable
almond milk (*Mandeldrink*)	E410 locust bean gum	after treatment of 1 mL almond milk with lipase, lyophilization and dissolving in 1 mL D_2O: galactomannan-signal at 5.03 ppm detectable
milk drinks: • fitness whey (*Fitnessmolke*) • fruit whey (*Fruchtmolke*) • whey product (*Molkenmischerzeugnis*)	E440 pectin	at a concentration of 500 μL/ml: pectin-signals at 5.08 and 4.96 ppm detectable
clear cake glaze (*Tortengusspulver, klar ungezuckert*)	E407 carrageenan	at a concentration of 20 mg/mL: κ-carrageenan-signals at 5.11, 4.87, 4.66, 4.54, and 4.15 ppm detectable
clear cake glaze, vegan and bio (*Tortengusspulver, vegan and bio*)	E406 agar−agar	at a concentration of 20 mg/mL: agar−agar-signals at 5.16, 4.57, and 4.14 ppm detectable
premixture (for meat preparation)	E412 guar gum	at a concentration of 5 mg/mL: galactomannan-signals at 5.03 and 4.14 ppm detectable
premixture (vitamin D3)	E414 gum arabic	at a concentration of 10 mg/mL: gum arabic-signals at 5.30, 5.03, 4.52, 4.42, and 4.30 ppm detectable

For spiking, similarly, 10−300 mg of the premixture or food was dissolved in 800 μL of D_2O with 0.03% TMSP. After having added 200 μL of the reference thickener sample, the mixture was centrifuged at 14 000 rpm for 10 min at room temperature using a Beckman Coulter Allegra X.30R laboratory centrifuge. A volume of 550 μL was transferred to a 5 mm NMR glass tube.

Liquid Samples. A volume of 500 μL of liquid food was diluted with 500 μL of D_2O containing 0.03% TMSP and centrifuged at 14 000 rpm for 10 min at room temperature using a Beckman Coulter Allegra X.30R laboratory centrifuge. A volume of 550 μL was then transferred to a 5 mm NMR glass tube.

For spiking, a volume of 500 μL of liquid food was diluted with 200 μL of the reference thickener sample and 300 μL of D_2O containing 0.03% TMSP and the mixture was centrifuged at 14 000 rpm for 10 min at room temperature using a Beckman Coulter Allegra X.30R laboratory centrifuge. A volume of 550 μL was then transferred to a 5 mm NMR glass tube.

Hydrolysis of Reference Thickeners and Food. Ten milligrams of the reference thickener or 10−300 mg of food were dissolved in 70 μL of D_2O and 30 μL of trifluoroacetic acid (TFA). The mixtures were stirred for 3 h at 80 °C. After cooling, the samples were neutralized with 1 M NaOH and centrifuged at 14 000 rpm for 10 min at room temperature using a Beckman Coulter Allegra X.30R laboratory centrifuge. A volume of 550 μL was transferred to a 5 mm NMR glass tube.

NMR Measurement Parameters. The apparent pH values of the NMR samples (dissolved in unbuffered D_2O) were determined (uncorrected values, see Tables S1 and S2) prior to NMR analysis. All NMR spectra were recorded with Bruker AVANCE III 400 and 600 MHz spectrometers equipped with a BBO and a cryo-TXO probehead, respectively, using TopSpin Version 3.6.1 (Bruker Biospin GmbH, Rheinstetten, Germany). ^{1}H NMR spectra were recorded with the Bruker pulse program "noesygppr1d" for the suppression of the water signal during the relaxation period, applying a narrow saturation pulse with a line width of about 25 Hz. The parameters were ns = 64 or 512, ds = 4, d1 = 4.0 s, TE = 27 °C, aq = 3.98 s, td = 65536, si = 131072, sw = 20.5 ppm, and p1 = 7.65 μs. Prior to Fourier-transformation, the FIDs were multiplied with a mild Gaussian function (lb = −0.10; gb = 1.76). DOSY spectra were recorded with the pulse program "stebpgp1s" or "ledbpgp2s". The parameters for DOSY were ns = 16 or 32, ds = 4, d1 = 10.0 s, d16 = 0.0002 s, d20 = 0.3 s, and d21 = 0.005 s. Chemical shifts were reported relative to the internal standard trimethylsilylpropanoic acid at 0 ppm. Data were processed with MestreNova Version 12.0.0 (Mestrelab Research, Santiago de Compostela, Spain) or TopSpin Version 3.6.1 (Bruker Biospin GmbH, Rheinstetten, Germany).

■ RESULTS AND DISCUSSION

Although foods are usually complex mixtures containing fats, proteins, and sugars (e.g., sucrose, glucose, and fructose) as main components and vitamins, phenolic components, and others as minor components, the untargeted NMR method described here was suitable to identify additives and especially thickeners in these complex matrixes without any previous sample preparation. To establish the method, the characteristic NMR signals of the pure thickeners under study (as obtained in pure form from commercial suppliers) were first assigned by one-dimensional and two-dimensional NMR experiments (^{1}H−^{1}H COSY, ^{1}H−^{13}C HSQC, ^{1}H−^{13}C HMBC) and diffusion spectroscopy (DOSY). Using the same NMR protocols, these thickeners were then identified in commercial premixtures according to the manufacturers' specifications. Finally, the method was exploited for the analysis of complex food matrixes, such as cream pudding powder, glaze, and pastille (see Table 1). In a typical setting, the combination of a one-dimensional ^{1}H NMR experiment and a DOSY experiment was sufficient to determine the thickeners. For a considerable number of examples, but not for all (see below), the NMR method turned out to be a rapid and useful alternative to the officially accepted methods, such as in Germany given in § 64 of the "Lebensmittel- und Futtermittelgesetzbuch" (LFGB) L 00.00-13.

In the following, the experimental approach with its benefits and limitations is illustrated with specific examples.

Gum Arabic (E414). Gum arabic is a complex polysaccharide extracted from the exudate of *Acacia senegal*. NMR experiments in the past few years indicated that the linear main chain consists of ß-(1 → 3)- and ß-(1 → 6)-galactopyranosyl residues with linked arabinose, rhamnose, and uronic acid moieties.[15,16] Figure 1A shows part of the arabinogalactan structure, a typical substructure found in gum arabic.

The ^{1}H NMR spectrum of a reference sample of this carbohydrate (Figure S1) revealed broad signals, as expected for a macromolecule with a typical molecular mass of 350 kDa. With the help of two-dimensional NMR-spectra (^{1}H−^{1}H COSY, ^{1}H−^{13}C HSQC, ^{1}H−^{13}C HMBC) and by comparing with data from the literature,[17] the detected signals could be assigned to protons of the rhamnose moieties, the arabinose units, and the galactopyranose units of the polymer (Table S3). Small deviations from the published chemical shift values[17] within ca. 0.03 ppm could be due to different temperature settings or calibration procedures. The characteristic signals at 5.42, 5.30 (H-1 in arabinose units), 5.03, 4.52 (H-1 in galactopyranose units), 4.74 (H-1 in rhamnose units), 4.42 (H-2 in arabinose units), 4.30 (H-4 in galactopyranose units), and 1.27 ppm (methyl H-6 in rhamnose units) served as a highly specific signal pattern for the detection of gum arabic in premixes and food samples under study (see below).

Carrageenan (E407) and Agar−Agar (E406). Carrageenan and agar−agar are polysaccharides that are extracted from red seaweeds (*Rhodophyta*). The chemical structures (Figure 1B,C) are characterized by linear chains of galactanes that contain galactopyranose residues with α-(1 → 3)- and β-(1 → 4)-glycosidic bonds and 3,6-anhydrogalactose residues linked to the 4-O-position of the galactose moiety.[18] Carrageenans contain sulfate residues at the galactopyranose units, and κ-carrageenan, ι-carrageenan, and λ-carrageenan differ in the numbers and the positions of these sulfate groups.[19]

In the ^{1}H NMR spectrum of the reference sample of κ-carrageenan (Figure S2)—as a representative of the carrageenan family—broad signals were assigned to the 3,6-anhydrogalactose units and galactose units according to the literature[20] and using the correlation patterns observed in the two-dimensional spectra. For the identification of carrageenan in food, the signals at 5.11 (H-1), 4.66 (H-4), 4.54 (H-3), and 4.15 ppm (H-2) of the 3,6-anhydrogalactose unit as well as the signal at 4.87 ppm (H-4 in the galactose unit) turned out to be useful marker signals (Table S4). Agar−agar—another red seaweed polysaccharide—showed a signal at 5.16 ppm belonging to H-1 of the 3,6-anhydrogalactopyranose unit.[18,21] In the ^{1}H NMR spectrum of the reference agar−agar (Figure S3), broad signals at 5.16, 4.57, and 4.14 ppm were defined as characteristic marker signals (Table S5).

Locust Bean Gum (E410) and Guar Gum (E412). Locust bean gum and guar gum are polysaccharides that contain a β-D-mannan backbone where galactose is linked at the O-6 position of the mannosyl residue (Figure 1D). Therefore, they both belong to the galactomannans and only differ in the ratio between the numbers of mannose and galactose. Locust bean gum usually shows a characteristic mannose/galactose ratio of 3.5/1, whereas the mannose/galactose ratio in guar gum is ca. 2/1.[22] The ^{1}H NMR spectrum of locust bean gum as a representative for the galactomannans (Figure S4) revealed broad signals that were assigned to the protons of the galactose units and mannose units by the procedures described above.[23] Due to signal overlap, the fraction of the mannose and galactose units could not be determined unequivocally.

The viscosity of the galactomannans can be increased by adding sugars like sucrose and glucose.[8] Thus, sucrose is often added to locust bean gum and guar gum before being used in the food industry to ensure a constant behavior in gel building. The sharp signals in the ^{1}H NMR spectra of many samples containing galactomannans including the ones shown in Figure S4 indeed indicated the presence of free sucrose. In many samples, the sucrose signals hampered the detection of most galactomannan signals. However, the signal at 5.03 ppm belonging to H-1 of the galactose unit as well as the broad and partially overlapping signal at 4.14 ppm belonging to H-2 of the mannose unit could be used as characteristic marker signals (Table S6) for the identification of galactomannans in premixtures and food. Because of their similar chemical structures, locust bean gum and guar gum could not be distinguished by the ^{1}H NMR approach.

Pectin (E440). Pectin (Figure 1E) is a complex class of heterogenic polysaccharides that are mainly found in cell walls of plants and classified in high-methoxy-pectin (>50% carboxyl groups are methylated) or low-methoxy-pectin (<50% carboxyl groups are methylated).[24−26] The three main motives in the core structure are described as homogalacturonan, rhamnogalacturonan I, and rhamnogalacturonan II. The homogalacturonan moiety is characterized by a linear chain of α-(1 → 4)-D-galacturonic acids whereby the carboxyl groups are eventually methylated and the hydroxyl groups are eventually acetylated. In contrast to the homogalacturonan moiety, the main chain of the rhamnogalacturonan I unit is interrupted by rhamnose residues with sugars like arabinose, galactose, and xylose as side chains. The rhamnogalacturonan II moiety also consists of a linear chain of α-(1 → 4)-D-galacturonic acids with branched side chains.[27]

By being compared with data from the literature[28] and two-dimensional NMR spectra (^{1}H−^{1}H COSY and ^{1}H−^{13}C HSQC) being used, the broad signals in the ^{1}H NMR spectrum of the intact pectin (Figure S5) were assigned to the galacturonic acid units, the rhamnose units, and the galactose units. The signals at 5.08 (H-1 of galacturonic acid) and 4.96 ppm (H-1 from galactose) were assigned as specific marker signals (Table S7) for pectin in food (see below).

Effect of the Temperature on the Quality of the ^{1}H NMR Spectra. The NMR analysis described above was performed at a temperature of 27 °C. Because of their high molecular weight, thickeners have the ability to build viscous solutions, also reflected by the broad signals in their ^{1}H NMR spectra. Cheng and Neiss in 2012 proposed to measure thickeners by ^{1}H NMR spectroscopy at higher temperatures in order to get better resolved spectra.[5] Therefore, we compared the ^{1}H NMR spectra of the reference thickeners described above also at temperatures up to 40 °C.

As an example, the effect of different temperatures is illustrated with the reference sample of gum arabic (Figure S6). As expected, at lower temperatures (i.e., < 25 °C), the signals were significantly broadened. Similar temperature effects could be observed for the spectra of the other thickeners. However, and disappointingly, at temperatures > 27 °C no further improvement of the spectral resolution could be achieved, and we therefore decided to identify the thickeners in premixtures and food at 27 °C (300 K), which is the default setting in many NMR applications.

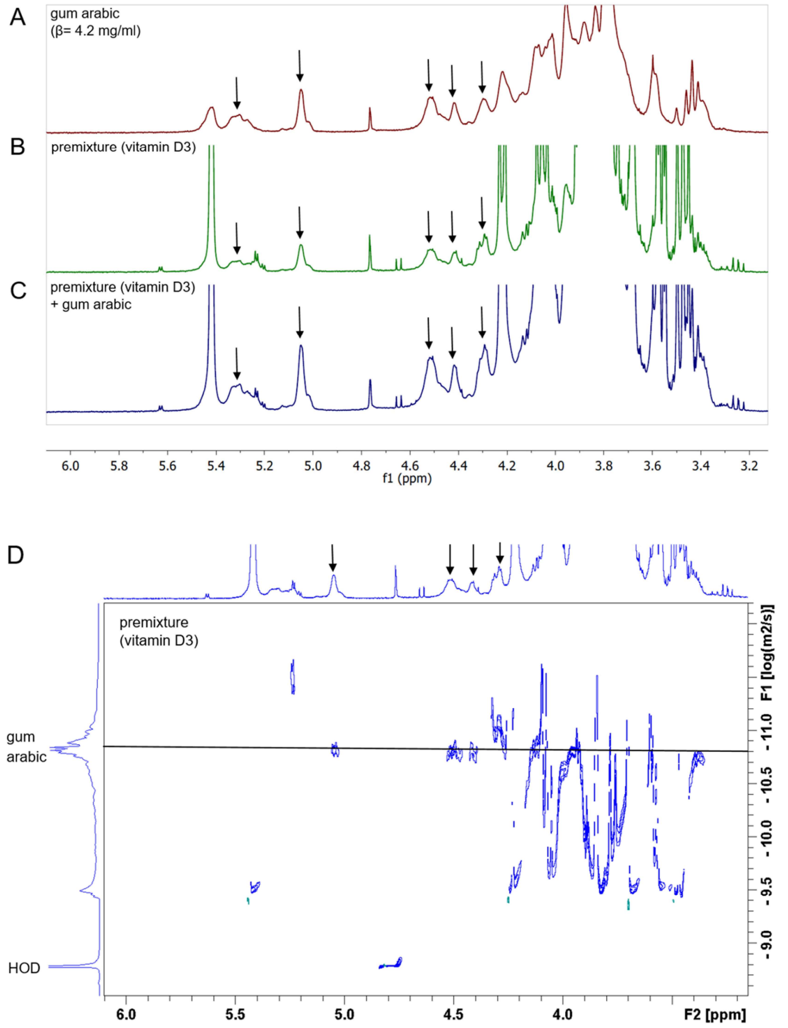

Figure 2. ^{1}H NMR spectra of (A) standard gum arabic, (B) the premixture vitamin D3, and (C) the premixture vitamin D3 spiked with standard gum arabic in D_2O. Measurement with ^{1}H NMR spectroscopy with water suppression (400 MHz, ns 64, ds 4, TE 27 °C). Gum arabic signals at 5.30, 5.03, 4.52, 4.42, and 4.30 ppm are indicated by black arrows. (D) DOSY spectrum of the premixture vitamin D3 in D_2O. Measurement with DOSY spectroscopy (400 MHz, ns 16, ds 4, TE 25 °C).

Identification of Thickeners in Premixtures and Food. To demonstrate the benefits and limits of the nontargeted NMR method for identifying thickeners in premixtures and food, some examples are now described in detail.

Gum Arabic in a Premixture (for vitamin D3 preparation) and in Pastilles. An amount of 10 mg of a premixture containing, according to the manufacturer, about 0.25% vitamin D3 and 20%−40% gum arabic was dissolved in 1 mL of D_2O and analyzed by the NMR protocol described above. The ^{1}H NMR spectrum (Figure 2B) displayed broad signals at 5.30, 5.03, 4.52, 4.42, and 4.30 ppm (indicated by the arrows) among others, which are characteristic for gum arabic (see also Figure 2A for the ^{1}H NMR spectrum of the reference sample). After spiking the sample with the reference, these signals increased (Figure 2C). In further support of these assignments, the DOSY spectrum of the premixture (Figure 2D) showed the same signals at 5.03, 4.52, 4.42, and 4.30 ppm with a diffusion coefficient of −10.82 log(m^2/s) (indicated by the straight line in

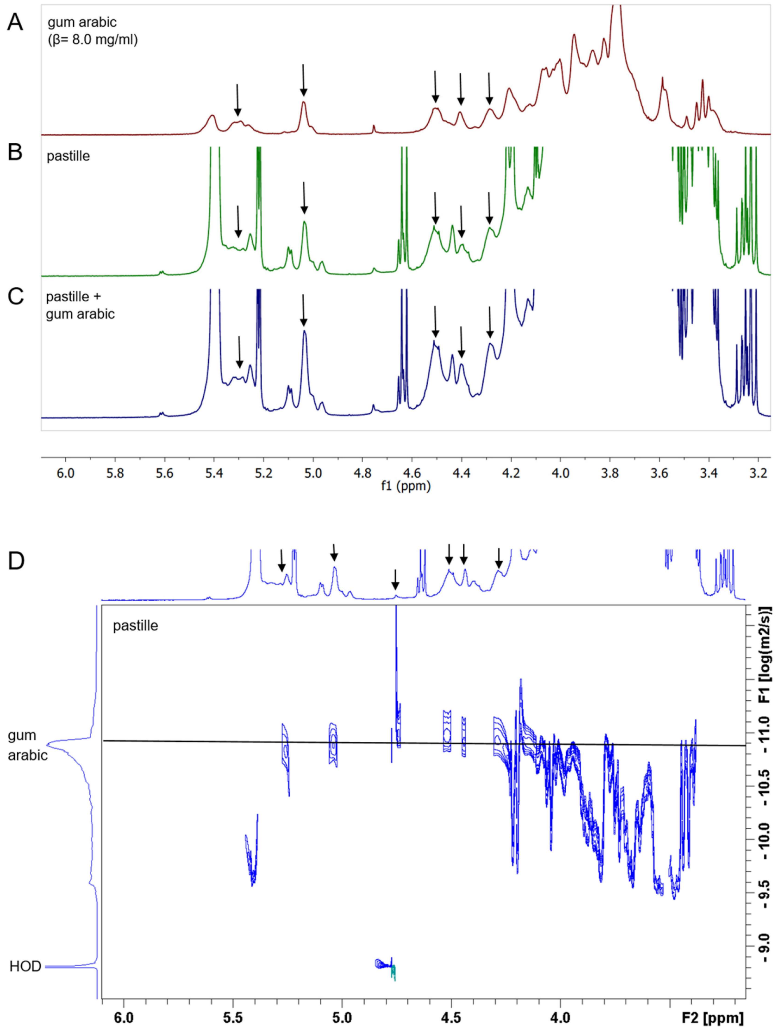

Figure 3. ^{1}H NMR spectra of (A) standard gum arabic, (B) the pastille, and (C) the pastille spiked with standard gum arabic in D_2O. Measurement with ^{1}H NMR spectroscopy with water suppression (400 MHz, ns 64, ds 4, TE 27 °C). Gum arabic signals at 5.30, 5.03, 4.74, 4.52, 4.42, and 4.30 ppm are indicated by black arrows. (D) DOSY spectrum of the pastille in D_2O. Measurement with DOSY spectroscopy (400 MHz, ns 32, ds 4, TE 25 °C).

the figure), which closely matched the corresponding value for the reference sample of gum arabic at −11.01 log(m^2/s). Thus, the DOSY spectrum verified that the detected signal pattern at 5.30, 5.03, 4.52, 4.42, and 4.30 ppm in the ^{1}H NMR spectrum of the premixture indeed belonged to the declared thickener gum arabic in this sample.

The food industry uses gum arabic not only as a thickening agent in premixtures but also in foods. The main application for gum arabic is its usage in pastilles, marshmallows, and toffees with concentrations of up to 55%.[29]

As a model food containing gum arabic, 30 mg of pastilles (Bach flowers) was dissolved in 1 mL of D_2O and measured by ^{1}H NMR and DOSY spectroscopy, again following the established protocol. The ^{1}H NMR spectrum (Figure 3B) displayed the characteristic signals at 5.30, 5.03, 4.74, 4.52, 4.42, and 4.30 ppm (cf. Figure 3A for the reference), which increased after being spiked with gum arabic (Figure 3C). Furthermore, the DOSY spectrum of the pastille revealed a diffusion coefficient of −10.91 log(m^2/s) for the signals at 5.30, 5.03, 4.74, 4.52, 4.42, and 4.30 ppm (Figure 3D), again similar to the

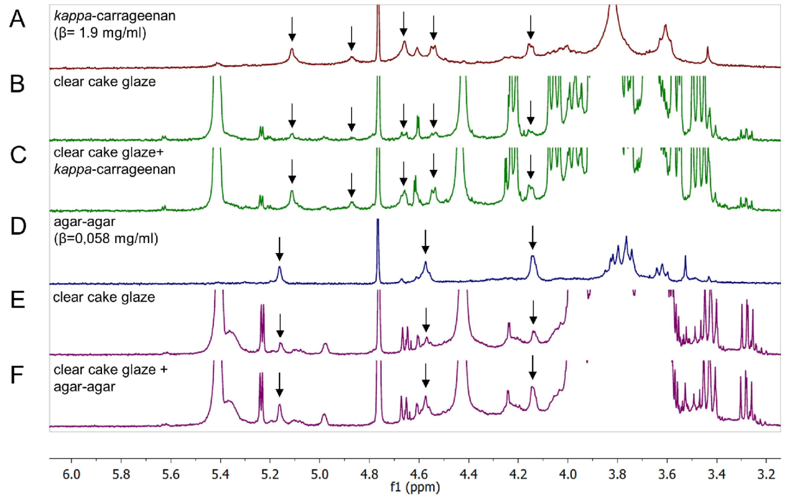

Figure 4. ^{1}H NMR spectra of (A) standard κ-carrageenan, (B) the clear cake glaze, (C) the clear cake glaze spiked with standard κ-carrageenan, (D) standard agar−agar, (E) the clear cake glaze, and (F) the clear cake glaze spiked with standard agar−agar in D_2O. Measurement with ^{1}H NMR spectroscopy with water suppression (400 MHz, ns 512, ds 4, TE 27 °C). κ-carrageenan signals at 5.11, 4.87, 4.66, 4.54, and 4.15 ppm as well as agar−agar signals at 5.16, 4.57, and 4.14 ppm are indicated by black arrows.

value of −11.01 log(m^2/s) for the reference. Thus, the chemical shifts of the marker signals and the diffusion coefficient provided solid evidence that the detected signals were indeed due to the declared thickener gum arabic.

Carrageenan and Agar−Agar in Clear Cake Glazes. Because of their thickening behavior, both polysaccharides are often used in food products like desserts, milk drinks and puddings.[30]

As an example, a clear cake glaze containing carrageenan as a thickening agent and another clear cake glaze containing the thickener agar−agar were analyzed by the NMR approach described above. Figure 4 shows the ^{1}H NMR spectra of both clear cake glazes with signals belonging to κ-carrageenan (Figure 4A) and agar−agar (Figure 4D). In the ^{1}H NMR spectrum of the glaze containing carrageenan (Figure 4B), among others, signals at 5.11, 4.87, 4.66, 4.54, and 4.15 ppm were detected, which were the characteristic marker signals for κ-carrageenan (Table S4). The same signals were increased after being spiked with the κ-carrageenan reference (Figure 4C). In contrast, the ^{1}H NMR spectrum of the other glaze (Figure 4E) showed the characteristic marker signals for agar−agar at 5.16, 4.57, and 4.14 ppm. Expectedly, spiking the glaze sample with the standard agar−agar led to increased signals at 5.16, 4.57, and 4.14 ppm (Figure 4F).

Galactomannans in Premixture (for meat preparation) and Ice Cream Stabilizer. Because of their gelling behavior, galactomannans are often applied as additives to ice cream, puddings, and soups in concentrations between 0.1% and 2%.[22] Before their usage in food, they are also often blended with other components. These so-called premixtures contain thickeners at higher concentrations than foods.

One example is a premixture for meat preparation that contains guar gum as a thickener. The ^{1}H NMR spectrum (Figure 5B) revealed, among others, two broad signals at 5.03 and 4.14 ppm, which are indeed characteristic for the galactomannans (Figure 5A and Table S6). These signals increased after the sample was spiked with the reference sample of guar gum (Figure 5C). Furthermore, the DOSY spectrum of this sample showed a diffusion coefficient of −11.60 log(m^2/s) for the broad signals at 5.03 and 4.14 ppm (Figure 5D), which exactly matched the value for the guar gum reference, whereas the diffusion coefficient for the signals of the standard locust bean gum was significantly higher [i.e., −11.31 log(m^2/s)].

The ice cream stabilizer containing the thickeners locust bean gum, guar gum, sodium alginate, and agar−agar was then subjected to NMR analysis. The ^{1}H NMR spectrum (Figure 6B) showed, among other sharp signals belonging to other ingredients, two broad weak signals at 5.03 and 4.14 ppm, which were in line with the chemical shifts of the characteristic galactomannan signals (Figure 6A and Table S6). Spiking the sample with standard locust bean gum or guar gum led to increased intensities of these signals (Figure 6C). Notably, the characteristic signals for agar−agar and alginate were not detected. Obviously, the concentrations of these thickeners were too low and therefore under the detection limit of the NMR method. Furthermore, the DOSY spectrum (Figure 6D) of the ice cream stabilizer revealed a diffusion coefficient of −11.31 log(m^2/s) for the galactomannan signals at 5.03 and 4.14 ppm, in line with the value for the standard locust bean gum. For the other declared thickeners guar gum, sodium alginate, and agar−agar, no characteristic DOSY signals or specific diffusion coefficients were detected.

Pectin in Milk Drinks. Because of its gelling behavior, pectin is often used in marmalades, bakery fillings, and ultrahigh temperature milk products.[25,26]

As a model food product, different commercially available milk drinks (fitness whey, fruit whey, and whey product) with declared pectin additives were analyzed. For this purpose, 500

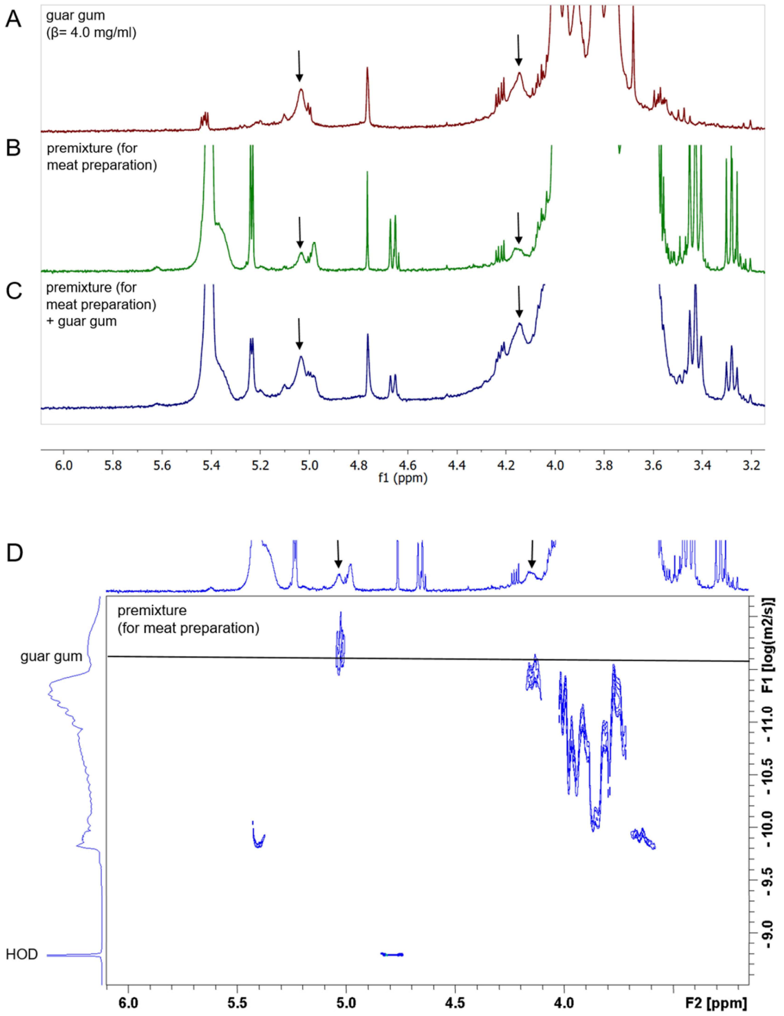

Figure 5. ^{1}H NMR spectra of (A) standard guar gum, (B) the premixture for meat preparation, and (C) the premixture for meat preparation spiked with standard guar gum in D_2O. Measurement with ^{1}H NMR spectroscopy with water suppression (400 MHz, ns 64, ds 4, TE 27 °C). Galactomannan signals at 5.03 and 4.14 ppm are indicated by black arrows. (D) DOSY spectrum of the premixture for meat preparation in D_2O. Measurement with DOSY spectroscopy (400 MHz, ns 16, ds 4, TE 25 °C).

μL of each drink was diluted with 500 μL of D_2O, and after centrifugation, they were directly subjected to ^{1}H NMR spectroscopy. As a negative control, commercially available milk drinks, which—according to the ingredients list—did not contain pectin, were also measured by ^{1}H NMR spectroscopy following the same protocol. Figure 7 shows the ^{1}H NMR spectra of the different milk drinks (with and without declared pectin as a thickening agent) and of the pectin reference on top. The ^{1}H NMR spectra of the fitness whey (Figure 7B) and the whey product (Figure 7F) displayed, apart from numerous sharp signals at high intensities, small broad signals at 5.08 and 4.96 ppm, which are indeed characteristic for pectin (Figure 7A and Table S7), as confirmed by spiking experiments with the pectin reference (Figure 7C,E,G). On the contrary, the fruit whey showed a significant signal at 5.08 ppm and a small signal at 4.96 ppm, however, at different intensities (Figure 7D), which was in contrast to the pectin standard displaying these signals at similar intensities. According to the ingredients list, the fruit whey contained not only pectin but also guar gum and locust bean gum as thickeners. As the two galactomannan standards showed

https://doi.org/10.1021/acs.jafc.0c07760
J. Agric. Food Chem. 2021, 69, 3761−3775

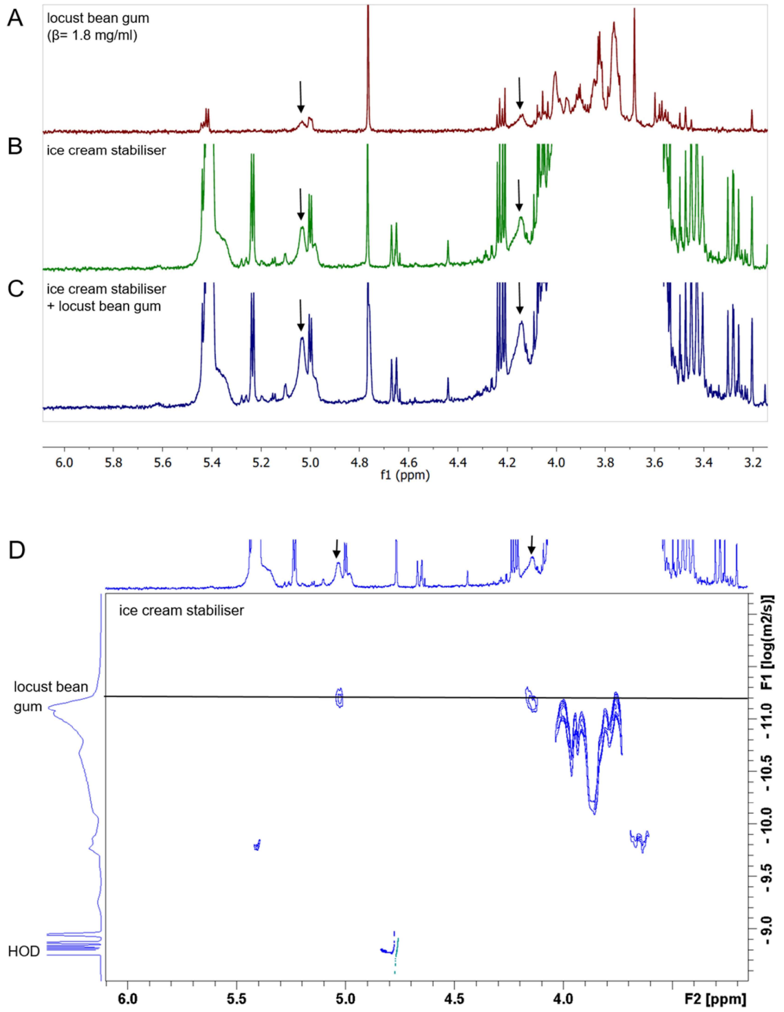

Figure 6. ^{1}H NMR spectra of (A) standard locust bean gum, (B) the ice cream stabilizer, and (C) the ice cream stabilizer spiked with standard locust bean gum in D_2O. Measurement with ^{1}H NMR spectroscopy with water suppression (400 MHz, ns 64, ds 4, TE 27 °C). Galactomannan signals at 5.03 and 4.14 ppm are indicated by black arrows. (D) DOSY spectrum of the ice cream stabilizer in D_2O. Measurement with DOSY spectroscopy (400 MHz, ns 32, ds 4, TE 25 °C).

characteristic signals at 5.03 ppm in the ^{1}H NMR spectra (Table S6), the broad signal at 5.08 ppm in the spectrum of the fruit whey could reflect an overlapping signal for pectin, locust bean gum, and guar gum. The characteristic galactomannan signal at 4.14 ppm was not detectable because of overlapping intense signals belonging to other ingredients. In the ^{1}H NMR spectra of milk, whey, and milk drink (Figure 7H,J,L), characteristic pectin signals at 5.08 and 4.96 ppm could not be detected. Therefore, these samples either did not contain any pectin or the concentration of pectin was below the detection limit. This was supported by the observation that spiking the samples with standard pectin (final concentration of 2.1 mg/mL corresponding to about 0.4%, w/w) led to resolved signals at 5.08 and 4.96 ppm (Figure 7I,K,M).

Carrageenan in Cream Pudding Powders and in Choco Milk Drinks. Shops often offer a wide product range of cream pudding powders with various ingredients and flavors. The ^{1}H NMR spectrum of the cream pudding powder (Figure 8B) showed characteristic κ-carrageenan signals at 5.11, 4.87, and 4.54 ppm (Figure 8A), which increased after being spiked with

https://doi.org/10.1021/acs.jafc.0c07760
J. Agric. Food Chem. 2021, 69, 3761−3775

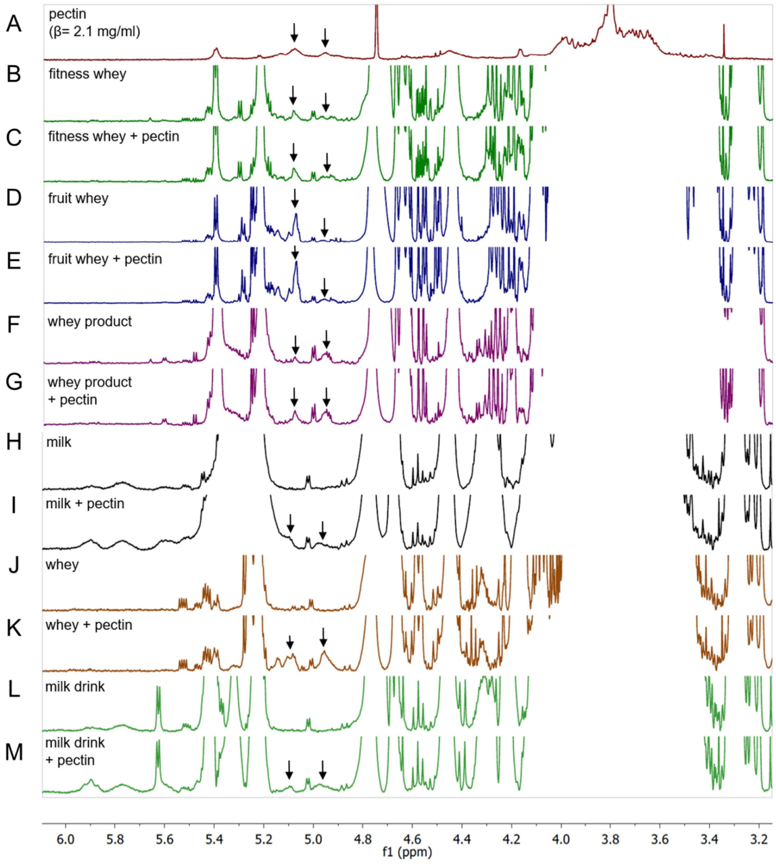

Figure 7. ^{1}H NMR spectra of (A) standard pectin, (B) the fitness whey, (C) the fitness whey spiked with standard pectin, (D) the fruit whey, (E) the fruit whey spiked with standard pectin, (F) the whey product, (G) the whey product spiked with standard pectin, (H) milk, (I) milk spiked with standard pectin, (J) whey, (K) whey spiked with standard pectin, (L) the milk drink, and (M) the milk drink spiked with standard pectin in D_2O. Measurement with ^{1}H NMR spectroscopy with water suppression (400 MHz, ns 64, ds 4, TE 27 °C). Pectin signals at 5.08 and 4.96 ppm are indicated by black arrows.

standard κ-carrageenan (Figure 8C). In contrast, κ-carrageenan signals at 5.11, 4.87, and 4.54 ppm were not identified in the ^{1}H NMR spectrum of another cream pudding powder (Figure 8D). This was due to other signals at high intensities in the area from 4.50 to 5.20 ppm that belonged to other major ingredients of this powder.

Unfortunately, no characteristic κ-carrageenan signals were detected in the DOSY spectrum (Figure S7). However, spiking the sample with κ-carrageenan (final concentration of 1.9 mg/mL corresponding to about 1%, w/w) led to some signals at the expected chemical shifts (Figure 8E). It can be concluded that the cream pudding powder under study did not contain carrageenan at a concentration >1%.

Carrageenan is used not only in solid food but also in liquid products. As an example, the choco milk drink, which contains—according to the manufacturer's specification—carrageenan as a stabilizer, is described.

Figure 8F shows the ^{1}H NMR spectrum of the choco milk drink showing sharp signals at high intensities belonging to free sugars as well as broadened signals at 5.30 and 4.30 ppm probably belonging to the glycerolipids of the milk fat. Characteristic marker signals for κ-carrageenan at 5.11 and 4.87 ppm in the anomeric sugar region were missing. Furthermore, a large overlapping region from 3.52 to 4.16 ppm prevented the detection of the other characteristic κ-carrageenan signals in the ^{1}H NMR spectrum. In addition, the DOSY spectrum did not reveal significant marker signals (Figure S8A). Spiking the choco milk drink with κ-carrageenan (final concentration of 1.9 mg/mL) resulted in a highly viscous solution and precipitates resulting in a poor resolution of the ^{1}H NMR signals (Figure 8G). Although the standard κ-carrageenan

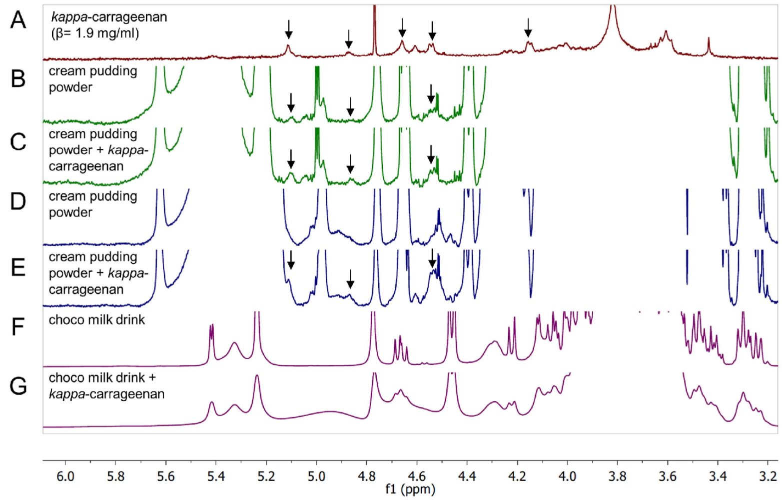

Figure 8. ^{1}H NMR spectra of (A) standard κ-carrageenan, (B) the cream pudding powder, (C) the cream pudding powder spiked with standard κ-carrageenan, (D) the cream pudding powder, (E) the cream pudding powder spiked with κ-carrageenan, (F) the choco milk drink, and (G) the choco milk drink spiked with κ-carrageenan in D_2O. Measurement with ^{1}H NMR spectroscopy with water suppression (400 MHz, ns 512, ds 4, TE 27 °C). κ-carrageenan signals at 5.11, 4.87, 4.66, 4.54, and 4.15 ppm are indicated by black arrows.

was added in an otherwise detectable amount (1.9 mg/mL), no marker signals were detected in the proton spectrum (Figure S8B) of the spiked sample. Because of its conformation, κ-carrageenan can interact with milk proteins, thereby forming gels.[31] Thus, it seemed that the added κ-carrageenan reference interacted with the protein from the milk in the choco milk drink and led to ^{1}H NMR data with worsened resolution. Therefore, the NMR method was unsuitable for the identification of carrageenan in milk drinks. It seems that the analysis of this matrix still has to rely on the classical methods, for example using GC-FID.[32]

Some limits of the NMR method became also clear when analyzing other premixtures and foods, where low concentrations (<0.5%−1%, w/w) prevented the NMR-based identification of the declared thickeners, at least with the NMR equipment used in this study. For these negative examples (summarized in Table 2), we therefore evaluated whether the hydrolysis of the polymers and subsequent NMR analysis of the resulting monomeric sugars could help to identify the thickeners.

Hydrolysis of Reference Thickeners and Food Products. In contrast to polysaccharides that usually show broad signals in their ^{1}H NMR spectra, monosaccharides like rhamnose, glucose, and arabinose result in sharp NMR signals and therefore in a spectral resolution that should facilitate unequivocal assignments.[5,33] Capitalizing on this possibility, the standard thickeners and some food products were hydrolyzed with trifluoroacetic acid (TFA) to break the glycosidic bonds in polysaccharides with reference to Merkx et al.[34] As an example for this approach, the spectrum of the hydrolyzed gum arabic is described in more detail. Parts A and B of Figure 9 show the ^{1}H NMR spectra of the polymeric gum arabic and its hydrolysate, respectively. The spectra of galactose (Figure 9C), rhamnose (Figure 9D), arabinose (Figure 9E), and glucuronic acid (Figure 9F) are shown for comparison. In contrast to the ^{1}H NMR spectrum of the intact gum arabic, the ^{1}H NMR spectrum of the hydrolyzed compound showed, as expected, sharp signals in the spectral region for anomeric protons from 5.28 to 4.52 ppm at high intensities and excellent resolution. Comparing the chemical shifts of the reference monosaccharides, the detected signals of the hydrolysate could be assigned as follows: H-1 of galactose at 5.27 (α-form) and 4.60 ppm (β-form), H-1 of arabinose at 5.24 (α-form) and 4.52 ppm (β-form), H-1 of rhamnose at 5.12 ppm, and H-6 of rhamnose at 1.29 ppm (Figure 10). Signals belonging to glucuronic acid were not detectable. Therefore, only the sharp signals in the anomeric region and the signal at 1.29 ppm belonging to H-6 of rhamnose could be used for the identification in food products. Nevertheless, in principle, the hydrolysis of the reference sample clearly enabled the detection of the expected monosaccharide units from the thickener.

As a food model (listed as a negative example for the direct NMR detection of thickeners, see Table 2), lemon peel flavor containing gum arabic as a stabilizer was hydrolyzed under harsh conditions, and the resulting hydrolysate was measured by ^{1}H NMR, DOSY, ^{1}H−^{1}H COSY, ^{1}H−^{13}C HSQC, and ^{1}H−^{13}C HMBC spectroscopy. In contrast to the polymeric gum arabic, the ^{1}H NMR spectrum of the hydrolysate (Figure 9G) now showed many sharp signals reflecting low-molecular weight products of the hydrolysis. By comparing with the ^{1}H NMR spectra of glucose, maltodextrin, and sucrose, the signals at 5.41, 5.25, and 4.67 ppm were assigned to the anomeric protons of maltodextrin and glucose (Figure S9). Furthermore, the ^{1}H−^{1}H COSY, ^{1}H−^{13}C HSQC, and ^{1}H−^{13}C HMBC NMR spectra of the hydrolysate were consistent with the respective two-dimensional spectra of the glucose reference (Figures S10, S11, and S12 and Table S8). In further support of these assignments, the DOSY spectrum of the hydrolysate (Figure

Table 2. Overview of Analyzed Premixtures and Foods Where Thickener Signals Were Not Detectable by the ^1H NMR Method

name of the food product	thickener/gelling agent (according to the manufacturers specification)	comment on ^1H NMR spectrum
curry sauce (*Curry Sauce*)	E415 xanthan gum	at a concentration of 200 mg/mL: xanthan gum signals not detectable
dessert-cream powder with vanilla flavor (*Dessert-Crèmepuddingpulver mit Vanille-Geschmack*)	E407 carrageenan	at a concentration of 100 mg/mL: carrageenan signals not detectable
dessert sauce with vanilla flavor (*Dessertsoße mit Vanille-Geschmack*)	E407 carrageenan	at a concentration of 30 mg/mL: carrageenan and galactomannan signals not detectable
	E412 guar gum	
ice cream binding agent (*Eisbindemittel für Milch- and Sahneeis*)	E466 carboxymethyl cellulose	at a concentration of 50 mg/mL: carboxymethyl cellulose, galactomannan, and sodium alginate signals not detectable
	E417 tara gum	
	E401 sodium alginate	
ice dessert strawberry (*Erdbeere Eisdessert vegan and bio*)	E440 pectin	at a concentration of 100 mg/mL: pectin, galactomannan, and xanthan signals not detectable
	E412 guar gum	
	E415 xanthan gum	
	E410 locust bean gum	
low-calorie drink with mandarin flavor (*kalorienarmes Erfrischungsgetränk mit Mandarinen-Geschmack*)	E410 locust bean gum	at a volume of 20 mL, lyophilization and dissolving in 2 mL D_2O: galactomannan signals not detectable
cream pudding powder vanilla flavor (*Crèmepuddingpulver mit Vanille-Geschmack*)	E407 carrageenan	at a concentration of 200 mg/mL: carrageenan signals not detectable
semolina pudding less sweet (*Grießbrei weniger süß*)	E415 xanthan gum	at a concentration of 100 mg/mL: xanthan gum signals not detectable
bio oat drink chocolate (*Haferdrink Schoko*)	E412 guar gum	at a volume of 1 mL, lyophilization and dissolving in 1 mL D_2O: galactomannan signals not detectable
yoghurt with 13,5% gooseberries-apple preparation (*Joghurt Stachelbeere-Apfel*)	E440 pectin	After weighing 5 g, extraction with dichloromethane, lyophilization and dissolving in 1 mL D_2O: pectin signals not detectable
cream powder for lemon-yoghurt dessert (*Crèmespeisepulver*)	E412 guar gum	at a concentration of 100 mg/mL: galactomannan signals not detectable
curry ketchup spicy (*Curry Gewürz Ketchup scharf*)	E412 guar gum	at a concentration of 200 mg/mL: galactomannan signals not detectable
	E410 locust bean gum	
coconut drink with rice (*Kokosnussdrink mit Reis*)	E412 guar gum	after treatment of 1 mL coconut drink with lipase, lyophilization and dissolving in 1 mL D_2O: galactomannan, xanthan gum, and gellan gum signal not detectable
	E418 gellan gum	
	E415 xanthan gum	
rice pudding (*Milchreis*)	E415 xanthan gum	at a concentration of 20 mg/mL: xanthan gum signals not detectable
cream pudding powder with lemon flavor (*Crèmepuddingpulver mit Zitronen-Geschmack*)	E415 xanthan gum	at a concentration of 50 mg/mL: xanthan gum and galactomannan signals not detectable
	E410 locust bean gum	
"choco milk drink" milk drink with chocolate flavor, 3,5% milk fat, heat-treated (*Schokodrink*)	E407 carrageenan	at a concentration of 500 μL/mL: carrageenan signals not detectable
lemon peel flavor (*Zitronenschalen-Aroma*)	E414 gum arabic	at a concentration of 100 mg/mL: gum arabic signals not detectable
premixture (for emulsion type sausage)	E412 guar gum	at a concentration of 300 mg/mL: galactomannan signals not detectable
	E410 locust bean gum	
premixture (for sauerkraut)	E415 xanthan gum	at a concentration of 10 mg/mL: xanthan gum signals not detectable
premixture (for stabilization of boiled sausages)	E466 carboxymethyl cellulose	at a concentration of 20 mg/mL: carboxymethyl cellulose signals not detectable
premixture (for barbecue sauce)	E415 xanthan gum	at a concentration of 10 mg/mL: xanthan gum signals not detectable

S13) showed the same signals at 5.25 and 4.67 ppm with a diffusion coefficient of −9.36 $\log(m^2/s)$, which closely matched the corresponding value for the reference sample of glucose at −9.29 $\log(m^2/s)$. Furthermore, a diffusion coefficient of −9.56 $\log(m^2/s)$ for the signals at 5.41, 4.94, and from 4.00 to 3.17 ppm could be assigned to maltodextrin (diffusion coefficient in the reference sample at −9.96 $\log(m^2/s)$). Disappointingly, anomeric protons from monosaccharides released by the hydrolysis of the thickener gum arabic could not be unequivocally assigned. It is important to note that treatment with TFA and heating the samples leads not only to the hydrolysis of the polymeric thickeners but also to the hydrolysis of other components like sucrose and maltodextrin as well as the denaturation and partial hydrolysis of proteins. Together, this mixture could also result in additional reactions and afford multiple products such as Maillard products. Since other trials for an indirect NMR identification of thickeners after hydrolysis also failed, we abandoned this approach but rather focused on those thickeners and matrixes that could directly be analyzed by the nontargeted NMR approach, as shown above.

Benefits of the Method. Although thickeners are often used at low concentrations in food, the NMR method enabled their detection at approximate concentrations >0.5%−1% (w/w) in some premixtures and food. In contrast to the § 64 LFGB method and multistep procedures described in the literature,[34,35] we were able to identify the declared thickeners in their intact forms in the presence of other ingredients, as shown with premixtures for vitamin D3 formulations and for meat

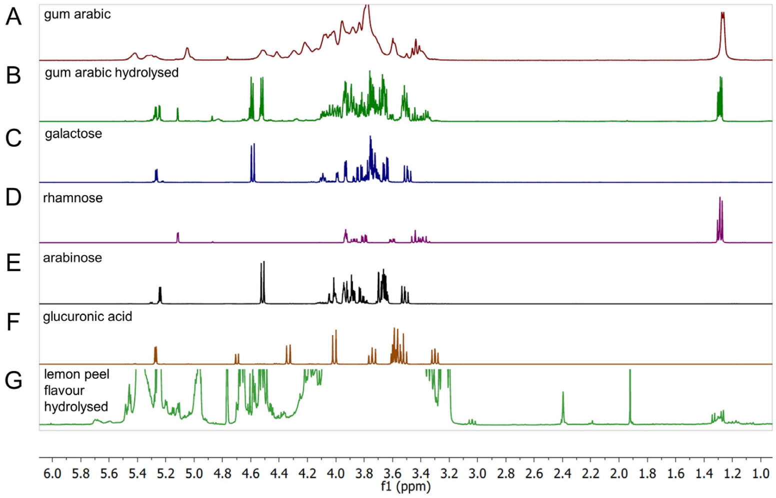

Figure 9. ^{1}H NMR spectra of (A) standard gum arabic, (B) gum arabic after hydrolysis in D_2O/TFA (70/30; w/w) for 3 h at 80 °C and after neutralization with 1 M NaOH, (C) standard galactose, (D) standard rhamnose, (E) standard arabinose, (F) glucuronic acid, and (G) the lemon peel flavor after hydrolysis in D_2O/TFA (70/30; w/w) for 3 h at 80 °C and after neutralization with 1 M NaOH in D_2O. Measurement with ^{1}H NMR spectroscopy with water suppression (400 MHz, ns 64, ds 4, TE 27 °C).

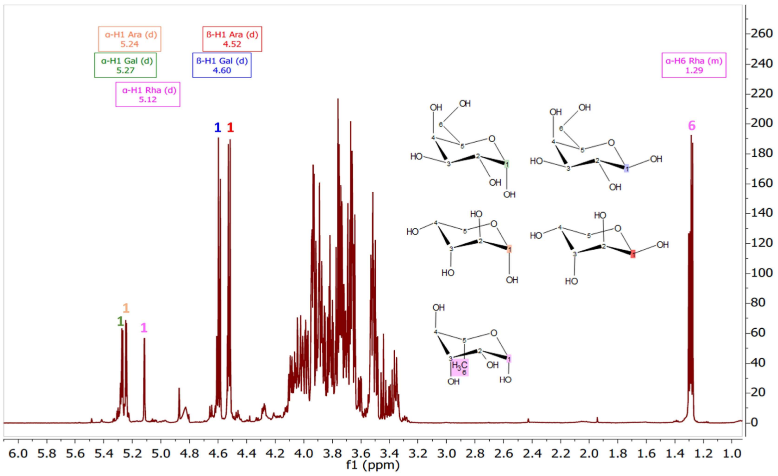

Figure 10. ^{1}H NMR spectrum of standard gum arabic after hydrolysis in D_2O/TFA (70/30; w/w) for 3 h at 80 °C and after neutralization with 1 M NaOH in D_2O. Measurement with ^{1}H NMR spectroscopy with water suppression (400 MHz, ns 64, ds 4, TE 27 °C). Protons and chemical structure of the monosaccharide units from gum arabic are shown in the insets. Signals are numbered according to the protons in the *α*-galactose moiety (in green), *β*-galactose moiety (in blue), *α*-arabinose moiety (in orange), *β*-arabinose moiety (in red), and *α*-rhamnose moiety (in magenta).

preparations. More examples comprise pastilles, clear cake glazes, ice cream stabilizer, and some milk drinks, without any previous time-consuming sample preparation such as a removal of major components like fat, proteins, and starch. We conclude that the novel protocol is superior to the established procedures considering the short time demand for the NMR measurements, which could even be done in full automation enabling high through-put. Therefore, the NMR approach is especially attractive for the fast screening of premixtures and food. Although thickeners in their natural state show broad NMR signals and at lower concentrations small intensities, they could be clearly identified by characteristic marker signals or patterns of characteristic signals in their ^{1}H NMR spectra (see Table 3). As the method enables the detection of intact thickeners, they

Table 3. Overview of Marker Signals from Different Thickeners Used for the Identification in Premixtures and Foods

name of thickener	chemical shifts μ of marker signals used for the identification
gum arabic (E414)	5.42, 5.30, 5.03, 4.74, 4.52, 4.42, 4.30, and 1.27 ppm
κ-carrageenan (E407)	5.11, 4.87, 4.66, 4.54, and 4.15 ppm
agar−agar (E406)	5.16, 4.57, and 4.14 ppm
galactomannans locust bean gum (E410) and guar gum (E412)	5.03 and 4.14 ppm
pectin (E440)	5.08 and 4.96 ppm

could also be distinguished from other components because of their high molecular weight and small diffusion constants as gleaned from DOSY. Because thickeners are built from monosaccharides like rhamnose, galactose, and arabinose, their chemical structures are often similar. Nevertheless, the method was able to even distinguish between the two galactomannans locust bean gum and guar gum in the described premixture and food by their specific diffusion constants, as revealed from the DOSY spectra. Due to the different chemical shifts of the characteristic marker signals for κ-carrageenan and agar−agar, the ^{1}H NMR method was also able to distinguish between these thickeners, as shown for glazes. This is superior in comparison to the established protocol described in § 64 LFGB method L 00.00-13. Together, the novel NMR method provides substantial progress and advantages in identifying thickeners in premixes and food.

Limitations of the Method. Even though thickeners could be clearly identified in different premixtures and food products by the NMR method, it is important to note that not all declared thickeners in the analyzed foods could be detected by this method (see Table 2 for negative results). Depending on the food class, many matrixes contain different components at varying quantities. This can also lead to a different solubility behavior as referred to the defined solvent volume of 1 mL of D_2O for the NMR analysis. At concentrations of thickeners below 0.5%−1% (w/w), these additives cannot be detected by the fast method. However, it should be noted that the detection limit can be lowered by the usage of high-field NMR magnets or sensitivity-improved "cryo-probes". Another problem could arise by differences in the concentration of the ingredients that could result in rather unpredictable conditions for the NMR analysis even within one food category. Thus, the novel method appears to be not generally applicable for any food matrix, and the failure to detect thickeners in these complex samples cannot be taken as evidence for the complete absence of these additives. However, whenever specific NMR signatures for thickeners can be observed, the benefits of the methods are obvious and significant.

■ ASSOCIATED CONTENT

Supporting Information

The Supporting Information is available free of charge at https://pubs.acs.org/doi/10.1021/acs.jafc.0c07760.

> Figures of ^{1}H NMR spectra, DOSY spectra, ^{1}H−^{1}H COSY spectra, ^{1}H−^{13}C HSQC spectra, and ^{1}H−^{13}C HMBC spectra and tables of overviews of the measured pH values and ^{1}H NMR signals and chemical shifts (PDF)

■ AUTHOR INFORMATION

Corresponding Author

Wolfgang Eisenreich − *Bavarian NMR Center − Structural Membrane Biochemistry, Department of Chemistry, Technische Universität München, D-85747 Garching, Germany*; orcid.org/0000-0002-9832-8279;
Phone: +49-(0)89-289-13336;
Email: wolfgang.eisenreich@mytum.de; Fax: +49-(0)89-289-13363

Authors

Sandra Radziej − *Bayerisches Landesamt für Gesundheit und Lebensmittelsicherheit, D-85764 Oberschleißheim, Germany*
Julia Scherb-Forster − *Bayerisches Landesamt für Gesundheit und Lebensmittelsicherheit, D-85764 Oberschleißheim, Germany*
Claus Schlicht − *Bayerisches Landesamt für Gesundheit und Lebensmittelsicherheit, D-85764 Oberschleißheim, Germany*

Complete contact information is available at:
https://pubs.acs.org/10.1021/acs.jafc.0c07760

Funding

This work was financially supported by the Bavarian State Ministry of the Environment and Consumer Protection (StMUV).

Notes

The authors declare no competing financial interest.

■ ACKNOWLEDGMENTS

The authors would like to gratefully thank Christine Schwarz for recording the DOSY spectra, Tobias Kauer for technical support, and Dr. Nicholas Schramek for help with NMR spectroscopy and access to the spectrometers.

■ REFERENCES

(1) van Gunst, A.; Roodenburg, A. J. C. Consumer Distrust about E-numbers: A Qualitative Study among Food Experts. *Foods.* **2019**, *8* (5), 178.

(2) Carocho, M.; Morales, P.; Ferreira, I. C. F. R. Natural food additives: Quo vadis? *Trends Food Sci. Technol.* **2015**, *45*, 284−295.

(3) Saha, D.; Bhattacharya, S. Hydrocolloids as thickening and gelling agents in food: A critical review. *J. Food Sci. Technol.* **2010**, *47*, 587−597.

(4) Wüstenberg, T. General Overview of Food Hydrocolloids. In *Cellulose and Cellulose Derivatives in the Food Industry*; Wüstenberg, T., Ed.; Wiley-VCH Verlag GmbH & Co. KGaA: Germany, 2015; Vol. *1*, pp 1−68.

(5) Cheng, H. N.; Neiss, T. G. Solution NMR Spectroscopy of Food Polysaccharides. *Polym. Rev.* **2012**, *52*, 81−114.

(6) Jansson, P. E.; Kenne, L.; Lindberg, B. Structure of extracellular polysaccharide from Xanthomonas campestris. *Carbohydr. Res.* **1975**, *45*, 275−282.

(7) Nasseri, A.; Thibault, J. F.; Ralet-Renard, M. C. Citrus pectin: structure and application in acid dairy drinks. In *Tree and Forestry Science and Biotechnology*; Benkeblia, N., Tennant, P., Eds.; Global Science Books, 2008; Vol. *2*, pp 60−70.

(8) Elfak, A. M.; Pass, G.; Morley, R. G. The viscosity of dilute solutions of guar gum and locust bean gum with and without added sugars. *J. Sci. Food Agric.* **1977**, *28*, 895−899.

(9) Ohtsuki, T.; Sato, K.; Sugimoto, N.; Akiyama, H.; Kawamura, Y. Absolute quantitative analysis for sorbic acid in processed foods using proton nuclear magnetic resonance spectroscopy. *Anal. Chim. Acta* **2012**, *734*, 54−61.

(10) Cuny, M.; Vigneau, E.; Le Gall, G.; Colquhoun, I.; Lees, M.; Rutledge, D. N. Fruit juice authentication by 1H NMR spectroscopy in

combination with different chemometrics tools. *Anal. Bioanal. Chem.* **2008**, *390*, 419−427.

(11) Godelmann, R.; Fang, F.; Humpfer, E.; Schütz, B.; Bansbach, M.; Schäfer, H.; Spraul, M. Targeted and Nontargeted Wine Analysis by 1H NMR Spectroscopy Combined with Multivariate Statistical Analysis. Differentiation of Important Parameters: Grape Variety, Geographical Origin, Year of Vintage. *J. Agric. Food Chem.* **2013**, *61*, 5610−5619.

(12) Rodrigues, J. E.; Gil, A. M. NMR methods for beer characterization and quality control. *Magn. Reson. Chem.* **2011**, *49*, S37−S45.

(13) Johnson, C. S., Jr. Diffusion ordered nuclear magnetic resonance spectroscopy: principles and applications. *Prog. Nucl. Magn. Reson. Spectrosc.* **1999**, *34*, 203−256.

(14) Li, W.; Chung, H.; Daeffler, C.; Johnson, J. A.; Grubbs, R. H. Application of (1)H DOSY for Facile Measurement of Polymer Molecular Weights. *Macromolecules* **2012**, *45*, 9595−9603.

(15) Anderson, D. M. W.; Stoddart, J. F. Studies on uronic acid materials: Part XV. The use of molecular-sieve chromatography in studies on acacia senegal gum (gum arabic). *Carbohydr. Res.* **1966**, *2*, 104−114.

(16) Churms, S. C.; Merrifield, E. H.; Stephen, A. M. Some new aspects of the molecular structure of Acacia senegal gum (gum arabic). *Carbohydr. Res.* **1983**, *123*, 267−279.

(17) Nie, S. P.; Wang, C.; Cui, S. W.; Wang, Q.; Xie, M. Y.; Phillips, G. O. A further amendment to the classical core structure of gum arabic (Acacia senegal). *Food Hydrocolloids* **2013**, *31*, 42−48.

(18) Usov, A. I. NMR Spectroscopy of Red Seaweed Polysaccharides: Agars, Carrageenans, and Xylans. *Botanica Marina.* **1984**, *27* (5), 189−202.

(19) De Ruiter, G. A.; Rudolph, B. Carrageenan biotechnology. *Trends Food Sci. Technol.* **1997**, *8*, 389−395.

(20) Tojo, E.; Prado, J. A simple 1H NMR method for the quantification of carrageenans in blends. *Carbohydr. Polym.* **2003**, *53*, 325−329.

(21) Dai, B.; Matsukawa, S. Elucidation of gelation mechanism and molecular interactions of agarose in solution by 1H NMR. *Carbohydr. Res.* **2013**, *365*, 38−45.

(22) Dea, I. C. M.; Morrison, A.; Tipson, R. S.; Horton, D. Chemistry and Interactions of Seed Galactomannans. *Adv. Carbohydr. Chem. Biochem.* **1975**, *31*, 241−312.

(23) Muschin, T.; Yoshida, T. Structural analysis of galactomannans by NMR spectroscopy. *Carbohydr. Polym.* **2012**, *87*, 1893−1898.

(24) Carpita, N. C.; Gibeaut, D. M. Structural models of primary cell walls in flowering plants: consistency of molecular structure with the physical properties of the walls during growth. *Plant J.* **1993**, *3* (1), 1−30.

(25) May, C. D. Industrial pectins: Sources, production and applications. *Carbohydr. Polym.* **1990**, *12*, 79−99.

(26) Rolin, C.; De Vries, J. Pectin. In *Food Gels*; Harris, P., Ed.; Springer Netherlands: Dordrecht, Germany, 1990; Vol. *1*, pp 401−434.

(27) Ridley, B. L.; O'Neill, M. A.; Mohnen, D. Pectins: structure, biosynthesis, and oligogalacturonide-related signaling. *Phytochemistry* **2001**, *57*, 929−967.

(28) Zhi, Z.; Chen, J.; Li, S.; Wang, W.; Huang, R.; Liu, D.; Ding, T.; Linhardt, R.; Chen, S.; Ye, X. Fast preparation of RG-I enriched ultra-low molecular weight pectin by an ultrasound accelerated Fenton process. *Sci. Rep.* **2017**, *7* (1), 541.

(29) Phillips, G.; Williams, P. Gum arabic. In *Handbook of Hydrocolloids*; Phillips, G., Williams, P., Eds.; Woodhead Publishing in Food Science and Technology, 2000; Vol. *1*, pp 155−168.

(30) Glicksman, M. Utilization of seaweed hydrocolloids in the food industry. In *Twelfth International Seaweed Symposium*; Ragan, M. A., Bird, C. J., Eds.; Springer Netherlands: Dordrecht, Germany, 1987; Vol. *41*, pp 31−47.

(31) Puvanenthiran, A.; Goddard, S. J.; Mckinnon, I. R.; Augustin, M. A. Milk-based Gels Made with κ-Carrageenan. *J. Food Sci.* **2003**, *68*, 137−141.

(32) Glück, U.; Thier, H. P. Quantitative Bestimmung einiger Dickungsmittel in Milchprodukten. *Z. Lebensm.-Unters. Forsch.* **1980**, *170*, 272−279.

(33) Roslund, M. U.; Säwén, E.; Landström, J.; Rönnols, J.; Jonsson, K. H.; Lundborg, M.; Svensson, M. V.; Widmalm, G. Complete (1)H and (13)C NMR chemical shift assignments of mono-, di-, and trisaccharides as basis for NMR chemical shift predictions of polysaccharides using the computer program casper. *Carbohydr. Res.* **2011**, *346*, 1311−1319.

(34) Merkx, D.; Westphal, Y.; Velzen, E. J. J.; Thakoer, K.; Roo, N.; Duynhoven, J. Quantification of food polysaccharide mixtures by 1 H NMR. *Carbohydr. Polym.* **2018**, *179*, 379−385.

(35) Grün, C. H.; Sanders, P.; van der Burg, M.; Schuurbiers, E.; van Adrichem, L.; van Velzen, E. J. J.; de Roo, N.; Brunt, K.; Westphal, Y.; Schols, H. A. Strategy to identify and quantify polysaccharide gums in gelled food concentrates. *Food Chem.* **2015**, *166*, 42−49.

4.2 “NMR-based identification of thickeners in membrane-filtered food premixtures”

Citation:

Radziej, S.; Scherb-Forster, J.; Schlicht, C. and Eisenreich, W. NMR-based identification of thickeners in membrane-filtered food premixtures. *Eur Food Res Technol*, **2022**, 248, 1715 – 1720. DOI: https://doi.org/10.1007/s00217-022-03998-w

Supporting information:

The Supporting Information can be found in 9.2.

Author contribution:

I was involved in planning the study design, performed the experiments and interpreted the data. Furthermore, I wrote the first draft of the manuscript and was involved in all steps of preparing this published paper.

Notation:

Due to an error during the type-setting process, many first and family names were mixed. The reply letter to the journal and the originally submitted reference list can be found in 9.3.

Summary:

Food thickeners are broadly used in different premixtures due to their ability of increasing the viscosity and shelf-life of products. In our previous work, an easy and fast protocol was developed which enabled the identification of intact thickening agents without any time-consuming sample preparation. Although the combination of ^{1}H-NMR spectroscopy and DOSY allowed a separation of high molecular weight food thickeners and low molecular weight substances like sucrose or glucose in different premixtures and food matrices, not all labelled thickening agents could be unequivocally determined.

Therefore, this work focused on the development of a simple sample preparation. By using centrifugal concentrators (cut-off 100 kDa), the declared food thickeners guar gum, locust bean gum, *kappa*-carrageenan, gum arabic and pectin could be fast and easy concentrated. According to their characteristic marker signals, these polysaccharides were unequivocally identified in the ^{1}H-NMR spectra of the filter residue from different premixtures (e.g. bakery mix, first infant milk powder, instant flavored drink), whereas the filtrates contained substances with molecular weight below 100 kDa like sucrose and glucose. Although a successful thickener concentration always depends on the exact composition of the premixture, the application of centrifugal concentrators might accomplish standardized methods.

European Food Research and Technology
https://doi.org/10.1007/s00217-022-03998-w

ORIGINAL PAPER

NMR-based identification of thickeners in membrane-filtered food premixtures

Sandra Radziej[1,2] · **Julia Scherb-Forster**[1] · **Claus Schlicht**[1] · **Wolfgang Eisenreich**[2]

Received: 16 December 2021 / Accepted: 26 February 2022

Abstract
Premixtures for food production are complex mixtures typically containing thickeners due to their water binding capacity. Here, we report an improved protocol for the fast identification of food thickeners by ^{1}H-NMR spectroscopy. The method is based on four steps: (i) dissolving of the dry premixture in water, (ii) centrifugation of the solution using centrifugal concentrators with a cut-off of 100 kDa, (iii) re-dissolving of the freeze-dried filtrate and the filter residue in small volumes of deuterated water, respectively, and (iv) ^{1}H-NMR analysis of these fractions focusing on specific marker signals. Using this procedure, the high molecular weight thickeners (above 100 kDa) κ-carrageenan, galactomannans, gum arabic and pectin were unequivocally identified in the NMR spectra of the filter residues from different premixtures, whereas low molecular substances (below 100 kDa) including sucrose and glucose were determined in the filtrates.

Graphical abstract

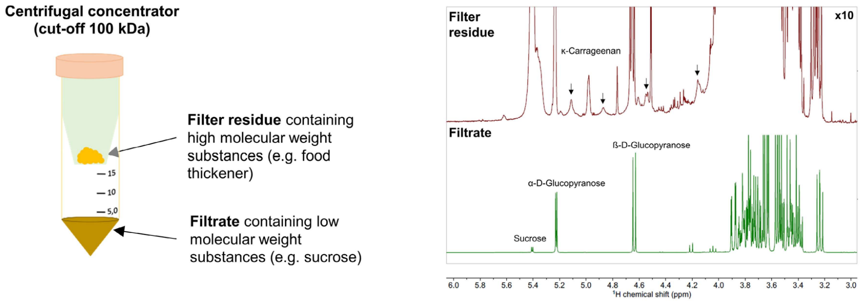

Keywords Premixtures · Food thickeners · NMR spectroscopy · Centrifugal concentrators

Introduction

In recent years, food fortification using supplements of vitamins and minerals has become an increasing trend in an attempt to provide health benefits for the consumers [1]. In the food industry, the application of formulations or blendings is a simple and cheap technology for the production of foodstuff [2]. Fine powders can be produced using different methods like pressure agglomeration, extrusion agglomeration or steam jet agglomeration [3]. The composition of these so-called premixtures differs and depends on the

---

✉ Wolfgang Eisenreich
wolfgang.eisenreich@mytum.de

[1] Bayerisches Landesamt Für Gesundheit Und Lebensmittelsicherheit, Veterinärstraße 2, 85764 Oberschleißheim, Germany

[2] Department of Chemistry, Bavarian NMR Center – Structural Membrane Biochemistry, Technische Universität München, Lichtenbergstraße 4, 85747 Garching, Germany

intended use in the food product. For instance, a formulation of different multiple components like soy protein isolates and wheat gluten is often used for the production of meat analogs, whereas sucrose, wheat flour and fats are important for the texture, volume and conservation of bakery products [4, 5]. Final consumers are also able to purchase premixtures like clear cake glaze powder, cake mix, spice mixture or sauce thickener in the supermarket. Further on, thickening agents containing starch or gums are offered for sale to increase the viscosity of liquids or food, which is especially important for persons with dysphagia [6]. All of these mentioned mixtures often contain food thickeners like carrageenan, guar gum or locust bean gum which are considered as food additives [5, 6]. The allowed usage and concentration of food additives in premixtures and food are defined in regulation (EC) No. 1333/2008 [7], whereas the specification—containing definition, purity and identification—of these substances is described in regulation (EU) No. 231/2012 [8]. In general, food thickeners are natural high molecular weight polysaccharides carrying various monosaccharide units [9]. The exact structures and hence the molecular weights depend on their biological source, the extraction method and the ripening point of the raw material [10]. For instance, modifications of pectin like alkylation of carboxyl and hydroxyl groups, amidation, thiolation and sulfation are often used to increase the molecular size [11]. The chemical composition and molecular weight from different food thickeners (locust bean gum, guar gum, κ-carrageenan, pectin and gum arabic) are listed in Table 1.

Because of their thickening, stabilizing and emulsifying characteristics, food thickeners are often used in emulsion food (e.g. dairy products, salad dressing), restructured food and frozen food [12]. In Germany, the compulsory method for the official food control is the so-called §64 LFGB method (here L 00.00-13), which has to be used in case of legal disputes [13]. This procedure is based on degradation of the polysaccharides and the determination of the resulting sugar units. Further time-consuming methods are described in the literature to analyse food thickeners in food products. Nevertheless, all of these methods are not appropriate for a fast screening, as they include numerous steps [14–16].

In our earlier study [17], a fast determination of some intact thickeners could be achieved by a combination of ^{1}H-NMR spectroscopy and Diffusion Ordered Spectroscopy (DOSY) without time-consuming sample preparation. However, this rapid procedure was not suitable for all analysed matrices mainly because of the low concentration of thickeners in the food or premixtures under study [17]. Here, we describe a simple addition to our earlier protocol which allowed to concentrate and to detect galactomannans, pectin, κ-carrageenan and gum arabic in premixtures.

Materials and methods

Chemicals

Deuterium oxide 99.9% with 0.03% trimethylsilylpropanoic acid (TMSP) was purchased from Deutero GmbH (Kastellaun, Germany). κ-Carrageenan and gum arabic were obtained from Acros organics (New Jersey, USA). Guar gum ~ 5000 cP was obtained from Carl Roth GmbH & Co. KG (Karlsruhe, Germany). Locust bean gum was purchased from Vitanatur GmbH (Stockstadt am Rhein, Germany). Apple pectin was obtained from Sigma Aldrich Chemie GmbH (Steinheim, Germany). Vivaspin Turbo 15, Membrane 100.000 MWCO Ultrafiltration Centrifugal

Table 1 Food thickeners with typical molecular weights and chemical composition

Name of thickener	Chemical composition	Molecular weight
Galactomannan locust bean gum (E410)	Mannose and galactose (ratio 4:1) [23]	50–1000 kDa [23]
Galactomannan guar gum (E412)	Mannose and galactose (ratio 2:1) [24]	2000–3000 kDa [24]
κ-carrageenan (E407)	Galactose-4-sulfate, 3,6-anhydrogalactose [25]	200–800 kDa [25]
Pectin (E440)	Three polysaccharide structures isolated from primary cell walls: Homogalacturonan Rhamnogalacturonan I Rhamnogalacturonan II containing galacturonic acid as main chain and rhamnose, arabinose, galactose, xylose as side chains; carboxyl groups can be methylated, hydroxyl groups can be acetylated [26]	50–150 kDa [27]
Gum arabic (E414)	Three fractions: Arabinogalactan (main component), Arabinogalactan-protein complex Glycoprotein containing galactose, rhamnose, arabinose, glucoronic acid and proteins [21, 28]	~ 380 kDa (from *Acacia senegal*) ~ 850 kDa (from *Acacia seyal*) [21]

Concentrators were obtained from Sartorius Stedim Biontech GmbH (Goettingen, Germany).

Samples

Bakery mix, premixture for compound sauce, premixture for brine supplement, premixture for ice dessert strawberry, gelling agent, standardized thickening agent, first infant milk powder, ice cream mix and instant flavored drink.

Sample preparation

- Preparing of reference thickener samples:
    - o Approx. 10 mg of a reference thickener were dissolved in 1 ml D_2O with 0.03% TMSP and warmed up for 10 min at 80 °C for complete solving while stirring.
- Premixture samples:
    - o 50—300 mg of the premixture were dissolved in 2 ml H_2O and centrifuged with ultrafiltration centrifugal concentrators (cut-off 100 kDa) at 2.000 rpm for 1 h at room temperature. The filter residue was resolved in approx. 3 ml H_2O and quantitatively transferred to a pear-shaped flask. The filter residue and the filtrate were placed in a freezer for 1 h and freeze-dried overnight. The dry samples were dissolved in 1 ml D_2O containing 0.03% TMSP and a volume of 550 µl was transferred to a 5-mm NMR glass tube.
    - o Spiking: Similarly, 50—300 mg of the premixture were dissolved in 2 ml H_2O. After having added 200 µl of the reference thickener sample, the mixture was centrifuged with ultrafiltration centrifugal concentrators (cut off 100 kDa) at 2.000 rpm for 1 h at room temperature. The filter residue was resolved in approx. 3 ml H_2O and quantitatively transferred to a pear-shaped flask. The filter residue and the filtrate were placed in a freezer for 1 h and freeze-dried overnight. The dry samples were dissolved in 1 ml D_2O containing 0.03% TMSP and a volume of 550 µl was transferred to a 5-mm NMR glass tube.

NMR acquisition parameters

All NMR spectra were recorded with a Bruker AVANCE III 400 MHz spectrometer equipped with a BBO probe using TopSpin Version 3.6.1 (Bruker Biospin GmbH, Rheinstetten, Germany). ^{1}H-NMR spectra were recorded applying the Bruker pulse program "noesygppr1d" for suppression of the HDO signal during the relaxation period applying a narrow saturation pulse with a bandwidth of about 25 Hz. The parameters were number of scans (ns) = 512, number of dummy scans (ds) = 4, relaxation delay (d1) = 4.0 s, temperature (TE) = 27 °C, acquisition time (aq) = 3.98 s, data points size of fid (td) = 65,536, data points size of real spectrum (si) = 131,072, spectral width (sw) = 20.50 ppm, 90 degree pulse (p1) = 7.65 µsec. Prior to Fourier-transformation, the free induction decays (FIDs) were multiplied with a mild Gaussian function (line broadening lb = − 0.10; gaussian maximal position gb = 1.76). Chemical shifts were reported relative to the internal standard TMSP at 0.00 ppm. Data were processed with MestreNova Version 12.0.0 (Mestrelab Research, Santiago de Compostela, Spain).

Results

Food thickeners are polysaccharides with high molecular weight. In food or food premixtures, they are typically used in low concentrations between 0.1 and 5% [18]. The method presented here enables the simple and fast concentrating of these polysaccharides from food premixtures followed by NMR analysis. By ultrafiltration using centrifugal concentrators with a cut-off of 100 kDa, low molecular constituents like sucrose, glucose and vitamins pass through the filter, whereas substances with high molecular weight (above 100 kDa) remain in the filter and are subsequently dissolved in deuterated water for NMR analysis. Starting from different premixtures (e.g. compound sauce, gelling agent, instant flavored drink), the declared food thickeners could be unequivocally identified in the ^{1}H-NMR spectra based on their characteristic marker signals (Table 2). This procedure was successful for the identification of the thickeners gum arabic, pectin and κ-carrageenan. In the following, the method is illustrated with the specific example of a

Table 2 Overview of marker signals from food thickeners used for the identification in premixtures [17]

Name of thickener	Chemical shifts δ of marker signals used for the identification
Galactomannans locust bean gum (E410) and guar gum (E412)	4.14 ppm and 5.03 ppm
κ-carrageenan (E407)	4.15 ppm, 4.54 ppm, 4.66 ppm, 4.87 ppm and 5.11 ppm
Pectin (E440)	4.96 ppm and 5.08 ppm
Gum arabic (E414)	1.27 ppm, 4.30 ppm, 4.42 ppm, 4.52 ppm, 5.03 ppm, 5.30 ppm and 5.42 ppm

bakery mix containing guar gum. For other examples, see Supporting information.

Bakery products often contain guar gum as an additive due to its ability to improve mixing tolerance and to prevent syneresis in frozen products [19]. For the NMR-based identification of the galactomannan guar gum, characteristic marker signals at 5.03 ppm (H1 of the galactose unit) and at 4.14 ppm (H2 of the mannose unit) can be used, as previously described [17].

To identify the declared thickener guar gum in a bakery mix, an amount of 100 mg of this premixture was dissolved in 1 ml D_2O and directly measured by ^{1}H-NMR spectroscopy. In the ^{1}H-NMR spectrum (Fig. 1B) many signals belonging to ingredients like sucrose, dextrose and malt extract were detected. The characteristic marker signal for galactomannans at 5.03 ppm could hardly be identified due to signal overlap with a sharp doublet signal belonging to another substance. To enable the detection of guar gum in this premixture, 100 mg were dissolved in 2 ml H_2O, centrifuged with ultrafiltration centrifugal concentrators (cut-off 100 kDa) and freeze-dried. The filter residue was then dissolved in 1 ml D_2O and analysed by ^{1}H-NMR spectroscopy. The spectrum (Fig. 1C) now revealed a broad signal at 5.03 ppm which is a characteristic marker signal for galactomannans like guar gum [17]. Spiking this sample with standard guar gum indeed led to an increase of the 5.03 ppm signal in the ^{1}H-NMR spectrum of the filter residue (Fig. 1C). As expected, the ^{1}H-NMR spectra of the filtrates (Fig. 1D, E) showed many sharp signals belonging to low molecular weight substances (e.g. sucrose). The characteristic NMR signals of the galactomannan guar gum at 5.03 ppm and 4.14 ppm were missing.

Discussion

Centrifugal concentrators are often used for biological sample preparation like desalting or concentration of proteins in cell lysates, serum and tissue homogenates [20]. However, they are also suitable for the separation of high molecular weight food thickeners from substances with molecular weight below 100 kDa. In contrast to the §64 LFGB method L 00.00–13 [13] and previously described methods in the literature [14–16], the sample preparation presented here seems to be especially appropriate for a fast screening of thickeners in food premixtures by means of NMR spectroscopy when the direct identification of these additives is not possible due to their low concentration [17]. We here show with various examples that high molecular weight thickeners predominantly remained in the filter residues as no broad

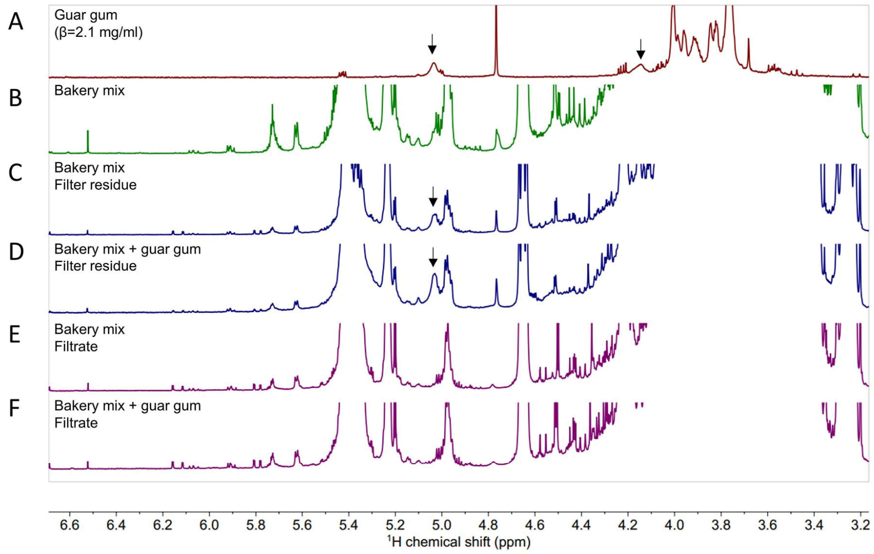

Fig. 1 ^{1}H-NMR spectra of standard guar gum (**A**), bakery mix (**B**), the filter residue of the bakery mix (**C**), the filter residue of the bakery mix spiked with guar gum (**D**), the filtrate of the bakery mix (**E**) and the filtrate of the bakery mix spiked with guar gum (**F**) in D_2O. Measurement with ^{1}H-NMR spectroscopy with water suppression (400 MHz, ns 512, ds 4, TE 27 °C). Guar gum signals at 5.03 ppm and 4.14 ppm are indicated by black arrows

signals were detected in the ^{1}H-NMR spectra of the filtrates. Although the declared food thickeners were unequivocally identified in the ^{1}H-NMR spectra of the filter residues, it seemed that the high molecular weight substances were not completely separated from low molecular weight substances as the ^{1}H-NMR spectra of the filter residues also contained some residual sharp signals albeit at small intensities. It should also be noted that premixtures could contain other ingredients with high molecular weight like starch and maltodextrin or additives like herbs or cocoa powder which could make the separation of the thickeners as well as their NMR detection more difficult. Furthermore, the molecular weight of food thickeners varies depending on seed source, production process and climatic conditions [21, 22]. Using food thickeners with molecular weight smaller 100 kDa for the production of premixtures, the polysaccharides will pass through the filter and no separation will be achieved. In this case, centrifugal filters with a different cut-off (e.g. 30 kDa) have to be used to guaranty a successful thickener concentration. Nevertheless, the application of centrifugal concentrators appeared to be a highly useful tool for concentrating food thickeners from premixtures allowing for their fast identification by NMR spectroscopy.

Supplementary Information The online version contains supplementary material available at https://doi.org/10.1007/s00217-022-03998-w.

Acknowledgements We gratefully thank Tobias Kauer for technical support and Dr. Nicholas Schramek for help with NMR spectroscopy.

Funding Open Access funding enabled and organized by Projekt DEAL. The authors acknowledge the financial support from the project of the Bavarian State Ministry of the Environment and Consumer Protection (StMUV).

Declarations

Conflict of interest The authors declare that they have no conflict of interest.

Ethical approval This article does not contain any studies with human or animals.

Informed consent Informed consent is not applicable.

References

1. Datta M, Mz V (2016) Food fortification and supplement use-are there health implications? Crit Rev Food Sci Nutr 56(13):2149–2159
2. Bigliardi B, Galati F (2013) Innovation trends in the food industry: the case of functional foods. Trends Food Sci Technol 31(2):118–129
3. Dhanalakshmi K, Ghosal S, Bhattacharya S (2011) Agglomeration of food powder and applications. Crit Rev Food Sci Nutr 51(5):432–441
4. Wittek P, Hp Karbstein, Ma Emin (2021) Blending proteins in high moisture extrusion to design meat analogues: rheological properties morphology development and product properties. Foods 10(7):1501–1518
5. Peris M, Rubio-Arraez S, Ml Castelló, Ortolá Md (2019) From the laboratory to the kitchen: new alternatives to healthier bakery products. Foods 8(12):661–627
6. Ja C (2013) Thickening agents used for dysphagia management: effect on bioavailability of water, medication and feelings of satiety. Nutr J 12(54):51–58
7. Regulation (EC) No 1333/2008 of the European parliament and of the council of 16 December 2008 on food additives. Off J Eur Union
8. Commision Regulation (EU) No 231/2012 of 9 March 2012 Laying down specifications for food additives listed in annexes Ii And Iii to regulation (EC) No 1333/2008 of the European parliament and of the council. Off J Eur Union
9. Cheng H, Neiss T (2012) Solution NMR spectroscopy of food polysaccharides. Polym Rev 52:81–114
10. Naseri A, Jf Thibault, Mc Ralet-Renard (2008) Citrus Pectin: structure and application in acid dairy drinks. In: Benkeblia N, Tennant P (eds) Tree and forestry science and biotechnology, vol 2. Global Science Books, pp 60–70
11. Chen J, Liu W, Cm L, Li T, Liang Rh, Sj L (2015) Pectin modifications: a review. Crit Rev Food Sci Nutr 55(12):1684–1698
12. Yang X, Li A, Li X, Sun L, Guo Y (2020) An overview of classifications, properties of food polysaccharides and their links to applications in improving food textures. Trends Food Sci Technol 102:1–15
13. §64 Lebensmittel- und Futtermittelgesetzbuch (LFGB) Method L 00.00–13 Nachweis von natürlichen Dickungsmitteln In Lebensmitteln. Methodensammlung BVL
14. Dwh M, Westphal Y, Ejj VV, Kv T, De Roo N, Jpm VD (2018) Quantification of food polysaccharide mixtures by (1)H NMR. Carbohydr Polym 179:379–385
15. Grün C, Sanders P, Van Der Burg M, Schuurbiers E, Adrichem L, Ejj Velzen, Roo N, Brunt K, Westphal Y, Ha Schols (2015) Strategy to identify and quantify polysaccharide gums in gelled food concentrates. Food Chem 166c:42–49
16. Glück U, Thier H-P (1980) Quantitative Bestimmung einiger Dickungsmittel in Milchprodukten. Z Lebensm-Unters Forsch 170(4):272–279
17. Radziej S, Scherb-Forster J, Schlicht C, Eisenreich W (2021) Fast identification of food thickeners by nontargeted NMR-spectroscopy. J Agric Food Chem 69(12):3761–3775
18. Saha D, Bhattacharya S (2010) Hydrocolloids as thickening and gelling agents in food: a critical review. J Food Sci Technol 47(6):587–597
19. Ae E, Mohammed A, Mustafa MHE (2007) Use of guar gum and gum arabic as bread improvers for the production of bakery products from sorghum flour. Food Sci Technol Res 13(4):327–331

20. Chernokalskaya E, Gutierrez S, Am P, Jt L (2004) Ultrafiltration for proteomic sample preparation. Electrophoresis 25(15):2461–2468
21. Mahendran T, Pa W, Go P, Al-Assaf S, Tc B (2008) New insights into the structural characteristics of the arabinogalactan-protein (AGP) fraction of gum arabic. J Agric Food Chem 56(19):9269–9276
22. Barak S, Mudgil D (2014) Locust bean gum: processing, properties and food applications-a review. Int J Biol Macromol 66:74–80
23. Pa D, Blecker C, Robert C, Wathelet B, Paquot M (2008) Composition and physicochemical properties of locust bean gum extracted from whole seeds by acid or water dehulling pre-treatment. Food Hydrocoll 22(5):807–818
24. Gupta S, Ck S, Ps V, Sharma A (2015) Comparative analysis of dietary fiber activities of enzymatic and gamma depolymerized guar gum. Food Hydrocoll 48:149–154
25. Mckim JM, Willoughby JA, Sr. lakemore WR, Weiner ML (2019) Clarifying the confusion between poligeenan, degraded carrageenan, and carrageenan: a review of the chemistry, nomenclature, and in vivo toxicology by the oral route. Crit Rev Food Sci Nutr 59(19):3054–3073
26. Bl Ridley, Oneill MA, Mohnen D (2001) Pectins: structure, biosynthesis and oligogalacturonide-related signaling. Phytochemistry 57(6):929–967
27. Mudgil D (2017) The interaction between insoluble and soluble fiber. In: Ra Samann (ed) Dietary fiber for the prevention of cardiovascular disease. Academic Press Elsevier, pp 35–59
28. Ali Bh, Ziada A, Blunden G (2009) Biological effects of gum arabic: a review of some recent research. Food Chem Toxicol 47(1):1–8

4.3 "Dual Isotopologue Profiling of Bacterial Pathogens and their Host Cells: Metabolic Adaptation of Human Macrophages and Fallopian Tube Cells to Intracellular *Chlamydia trachomatis*"

4.3.1 Abstract

The obligate intracellular human pathogen *C. trachomatis* uses multiple host-derived substrates for its growth and survival. While the intracellular metabolism of this bacterium has been extensively studied in recent decades, very little is known about the general carbon metabolism of primary host cells and their metabolic adaptation during infection. Therefore, uninfected and with *C. trachomatis* infected human fallopian tube cells as well as M1 and M2 polarized human macrophages were cultivated for 30h in RPMI-1640 medium (supplemented with 10% fetal calf serum and 11 mM [U-$^{13}C_6$]glucose) and analysed without previous separation of bacteria and host cells. By performing GC-MS and NMR measurements, the relative ^{13}C-enrichments and isotopologue distributions in different metabolites (protein-derived amino acids, cell wall components, TCA intermediates and fatty acids) were determined. The ^{13}C-excess values of uninfected and infected host cells revealed a higher utilization of labelled glucose *via* glycolysis, whereas only a minor part was used to feed the TCA cycle in infected human fallopian tube cells and the human M2 polarized macrophages. Furthermore, more lactate was secreted during infection and the bacterial specific metabolites anteiso-C15:0, iso-C15:0 and mDAP could be detected in the infected host cells. In contrast, no significant differences in the ^{13}C-excess values between uninfected and infected human M1 polarized macrophages could be determined. Additionally, characteristic bacterial specific metabolites were missing in the infected M1 phenotype. Thus, the human fallopian tube cells and the human M2 polarized macrophages seemed to allow an efficient replication of *C. trachomatis*, whereas the human M1 polarized macrophages seemed to be inappropriate to serve as host cells for this pathogen.

4.3.2 Introduction

The human pathogen *C. trachomatis* is a Gram-negative, obligate intracellular bacterium which causes trachoma, urinary tract infections and rectum infections (O'Connell and Ferone, 2016). The life cycle of *C. trachomatis* is characterized by two morphologically different phases, the infectious non-replicative EB and the non-infectious metabolically active RB form. At the beginning of the cycle, EBs bind on the host cells by forming a trimolecular bridging of bacterial adhesins, host heparan sulfate-like glycosaminoglycans and different host receptors like CFTR, ITGB1 and 3'SGL. Upon invasion, an inclusion is formed, where EBs convert into RBs and start to replicate. After reorganization back to the EB stage, the bacteria are extruded or released from the host cells and might infect new ones (Corsaro and Venditti, 2004; Gitsels et al., 2019; Sun et al., 2012). Under stress conditions (e.g. amino acid starvation, treatment with interferon-gamma), *C. trachomatis* is able to convert from the RB form into a persistent aberrant reticulate body (ARB) form (Wyrick, 2010). In this "persistent state", the bacteria are viable, but not replicating. When the unfavourable conditions change into better ones, a transition back to the RB form can be observed (Panzetta et al., 2018). Due to the lack of isocitrate dehydrogenase, aconitase and citrate synthase, the TCA cycle of *C. trachomatis* is incomplete (Stephens et al., 1998). Although substrates like malate or glutamine can directly fill the TCA cycle, survival and growth strongly depend on the supply of multiple nutrient sources from the host cells (Bastidas et al., 2013; Mehlitz et al., 2017; Rajeeve et al., 2020). Due to its fast proliferation rate, the cervical epithelial HeLa cell line is often used to study cell response during infection with *C. trachomatis* (Lin et al., 2019; Tang et al., 2021). However, also human macrophages can serve as primary host cells for this pathogen (Herweg and Rudel, 2016). Human macrophages can be divided into two main forms, the M1 and M2 polarized macrophages. The M1 phenotype is activated by bacterial lipopolysaccharides and cytokines like interferon-gamma or tumour necrosis factor-alpha. This pro-inflammatory subtype is involved in the activation of NADPH oxidase and, thus, in the production of reactive oxygen species (Castoldi et al., 2015; Shapouri-Moghaddam et al., 2018). In contrast, the anti-inflammatory M2 macrophages - activated by interleukin 4 as well as interleukin 13 - promote cell proliferation and tissue repair (Atri et al., 2018; Shapouri-Moghaddam et al., 2018). Another suitable primary host cells for studying cellular responses upon infections with *C. trachomatis* are human fallopian tube (HFT) cells (McQueen et al., 2020). In this study, human M1 and M2 polarized macrophages as well as HFT cells were infected with *C. trachomatis* and subsequently labelled with [U-$^{13}C_6$]glucose. Without prior separation of the cell pellet into host and bacteria fraction, ^{13}C-labelling patterns of specific key metabolites either from the host cells or the bacteria served to reconstruct crucial metabolic fluxes in the bacteria, and also in the host cells in response to the bacterial infection.

4.3.3 Results

In order to guaranty survival, *C. trachomatis* optimizes the supply of nutrients by modulating the metabolism of its host (Rother et al., 2019). Although recent studies focused on the investigation of the intracellular metabolism of *Chlamydia*, very little is known about the metabolic reprogramming of primary host cells during infection (Eisenreich et al., 2017). For a better understanding of how *C. trachomatis* affects the metabolism of primary hosts, labelling experiments with HFT cells as well as human M1 and M2 polarized macrophages were performed. The samples were analysed by GC-MS and NMR spectroscopy.

Carbon fluxes in HFT cells

To study the carbon metabolism of HFT cells, labelling experiments with [U-$^{13}C_6$]glucose were performed. In the following, the results of the protein-derived amino acids, the TCA intermediates, the fatty acids and the supernatants of uninfected and with *C. trachomatis* infected HFT cells are discussed in more detail.

Statistical analysis: All experiments were performed two or three times with different samples batches (biological replicates) and further measured three times in a row (technical replicates). However, the calculated absolute ^{13}C-excess values showed high variations (approx. 10%) in the biological replicates, whereas the variations of ^{13}C-excess values were less than 1% in the technical replicates. In the following, this observation is discussed in more detail for the protein-derived amino acid alanine based on three biological replicates (R1, R2, R3). The amino acid alanine from the uninfected HFT cells showed ^{13}C-excess values (Figure 8A) of 9.6% in R1, 11.2% in R2 and 20.1% in R3, resulting in a mean value of 13.6% (± 5.7%). A similar effect was observed for the protein-derived amino acid alanine from infected HFT cells (^{13}C-enrichment of 11.2% for R1, 13.8% for R2 and 21.7% for R3, resulting in a mean value of 15.5% ± 5.5%). Therefore, it can be concluded that these host cells (obtained from different female donors) were in different states and thus utilizing different amounts of exogenous glucose leading to high variations in the ^{13}C-enrichments of the analysed metabolites. Notably, the increased labelling rates in infected HFT cells compared to the uninfected HFT cells from the same sample batch were similar for all three biological replicates. Additionally, the isotopologue profiles (Figure 8B) of the protein-derived amino acid alanine from uninfected and with *C. trachomatis* infected HFT cells were similar in the biological replicates R1, R2 and R3 displaying mainly M+3 fractions. Thus, it can be assumed that the metabolic pathways were identical in the various sample batches.

Due to the high variations in the absolute ^{13}C-excess values in the biological replicates, we will not compare the metabolic fluxes based on the calculated mean ^{13}C-excess values of the three biological replicates, but rather discuss the ^{13}C-enrichments and isotopologue profiles of uninfected and infected host cells from one specific sample batch. The data from the other biological replicates can be found in the Supporting information (section 9.4).

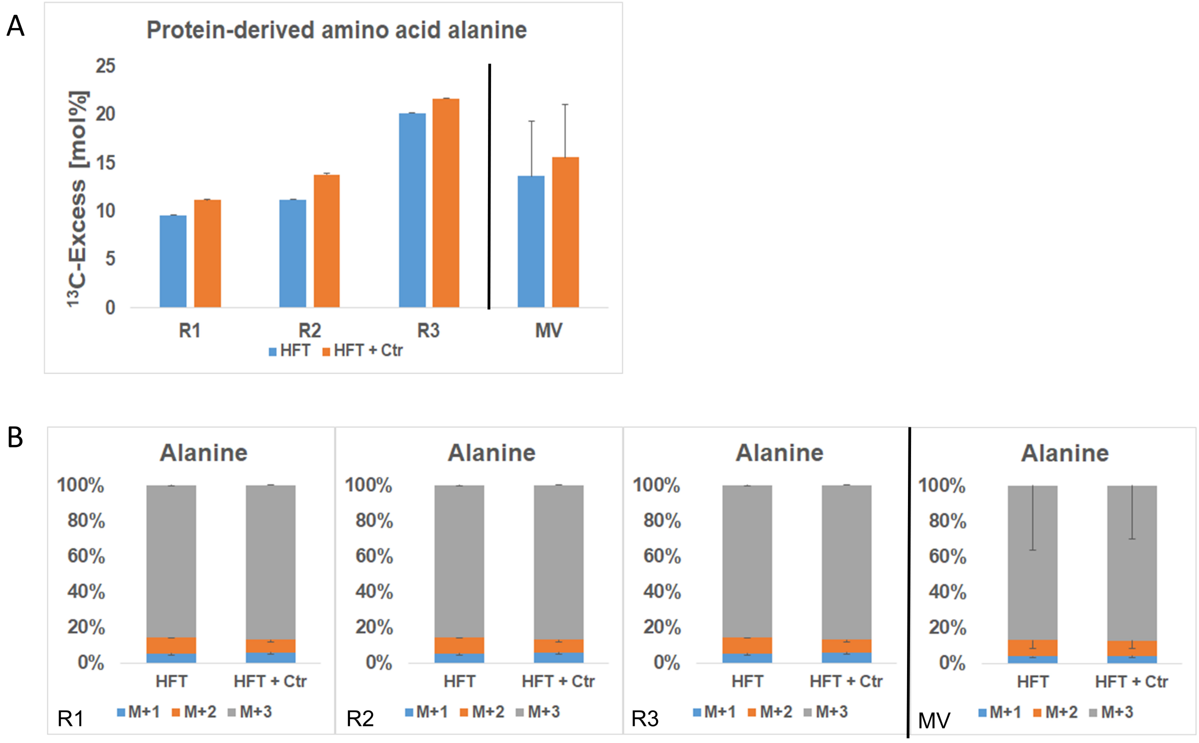

Figure 8: ^{13}C-Excess in mol% (A) and isotopologue profiles (B) of the protein-derived amino acid alanine from uninfected HFT cells and with *C. trachomatis* infected HFT cells. M+X represents the isotopologue profiles with X ^{13}C-atoms incorporated into the protein-derived amino acid. Error bars show the standard deviations from three separate biological replicates (R1, R2 and R3) with three technical replicates as well as the mean value (MV) from three biological replicates with three technical replicates.

Incorporation of ^{13}C into protein-derived amino acids from [U-^{13}C$_6$]glucose

The essential amino acids leucine, isoleucine, valine, threonine, phenylalanine, histidine and lysine showed ^{13}C-excess values under 1%. In contrast, the non-essential protein-derived amino acid alanine showed a high ^{13}C-incorporation (9.6% in the uninfected HFT cells; 11.2% in the infected HFT cells) with about 90% M+3 isotopologue fraction (Figure 9). The high percentage of fully labelled alanine demonstrates that this amino acid was formed from the fully labelled precursor pyruvate mainly deriving from glycolysis. In contrast, the protein-derived amino acids aspartate und glutamate showed a significant lower ^{13}C-enrichment (Figure 9A) for the uninfected HFT cells (aspartate 0.8%; glutamate 1.0%) and infected HFT cells (aspartate 1.4%; glutamate 1.2%). Both amino acids derived from the fully labelled precursor acetyl-CoA which was incorporated into the TCA cycle leading to metabolites with two labelled carbon atoms (Figure 9B). The high ^{13}C-enrichment of alanine and the low ^{13}C-excess values of aspartate as well as glutamate indicate that glucose was mainly used for glycolysis and only a minor part was utilized to feed the TCA cycle.

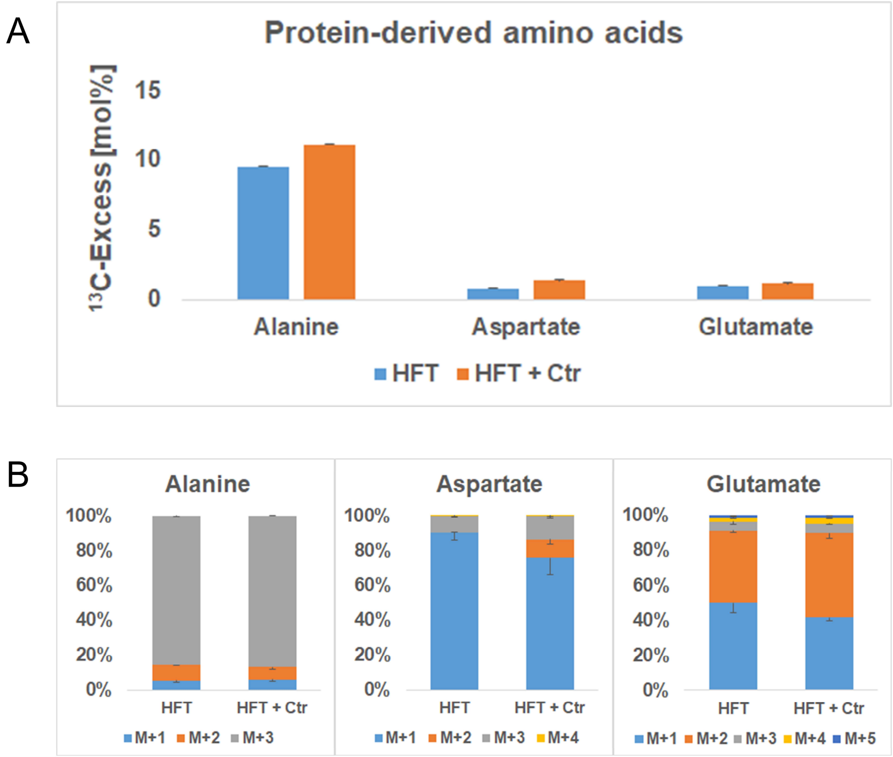

Figure 9: ^{13}C-Excess in mol% (A) and isotopologue profiles (B) of protein-derived amino acids from uninfected HFT cells and with *C. trachomatis* infected HFT cells. M+X represents the isotopologue profiles with X ^{13}C-atoms incorporated into the protein-derived amino acids. Error bars show the standard deviations from one biological replicate with three technical replicates.

Incorporation of ^{13}C in TCA intermediates from [U-$^{13}C_6$]glucose

Due to a lack of the enzymes isocitrate dehydrogenase, aconitase and citrate synthase in *C. trachomatis,* citrate can only be produced by human host cells and represents therefore a host-specific metabolite (Stephens et al., 1998). GC-MS measurements demonstrated that the TCA intermediates fumarate, malate, and citrate acquired ^{13}C-excess values above 2% (Figure 10A). As the isotopologue profile displayed mainly M+2 fractions (Figure 10B), it can be assumed that fully labelled acetyl-CoA was used for the synthesis of citrate. When the HFT cells were infected with *C. trachomatis*, the enrichments increased indicating a higher carbon flux into the TCA cycle during infection. However, no significant differences in the isotopologue profiles between uninfected and infected HFT cells were observed. Thus, multiple cycling *via* the TCA cycle did not increase during infection.

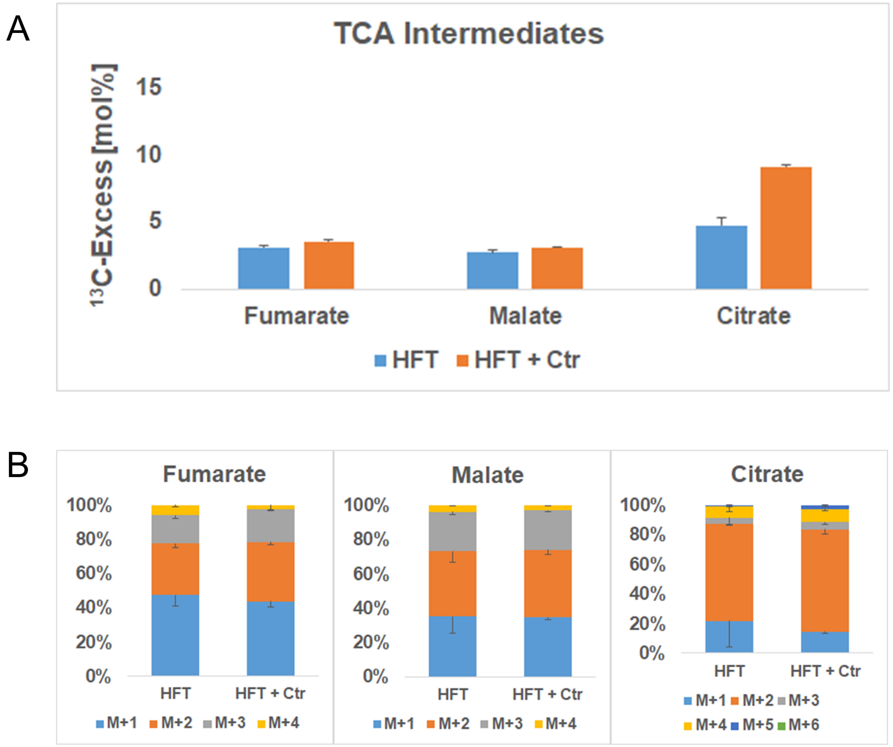

Figure 10: ^{13}C-Excess in mol% (A) and isotopologue profiles (B) of TCA intermediates from uninfected HFT cells and with *C. trachomatis* infected HFT cells. M+X represents the isotopologue profiles with X ^{13}C-atoms incorporated into the TCA intermediates. Error bars show the standard deviations from one biological replicate with three technical replicates.

Incorporation of ^{13}C in fatty acids from [U-^{13}C$_6$]glucose

By performing GC-MS measurements of the lipid fraction, the fatty acids C16:0 – C24:0 with ^{13}C-excess values below 10% could be observed for the HFT cells (Figure 11A). Of special interest were the host-derived unsaturated fatty acids C18:1 and C24:1 since *C. trachomatis* is not able to form unsaturated fatty acids (Yao and Rock, 2018). Moreover, the isotopologue profiles were characterized by M+2, M+4, M+6 et cetera reflecting the fatty acid formation from various units of [U-^{13}C$_2$]acetyl-CoA which were obtained from fully labelled glucose. Additionally, no significant differences in the ^{13}C-enrichments and isotopologue profiles between uninfected and with *C. trachomatis* infected HFT cells could be observed except for the fatty acid C20:0 which revealed a significant higher ^{13}C-enrichment of 34.6% in the infected HFT cells in contrast to the ^{13}C-excess value of 2.6% in the uninfected HFT cells (Figure 11A). Furthermore, the isotopologue distribution of C20:0 from the uninfected HFT cells showed mainly M+2 (Figure 11B) whereas the isotopologue profile of this fatty acid from the infected cells was shifted to higher fractions of M+4, M+6, M+8 et cetera. Thus, the observed increased formation of C20:0 could demonstrate that eicosanoids (C20 fatty acids) serve as precursor for the formation of prostaglandins and cytokines as response to acute inflammation and fever (Fukuda et al., 2005; Ricciotti and FitzGerald, 2011). Fukuda et al. showed that the key enzyme cyclooxygenase 2 (COX 2) - which is involved in the biosynthesis of prostaglandins from C20:4 - was upregulated during infection with *C. trachomatis* and was responsible for the conversion of arachidonic acid into prostaglandins (Fukuda et al., 2005). Furthermore, the branched-chain fatty acids anteiso-C15:0 and iso-C15:0 with ^{13}C-excess values of approx. 34% could only be detected in the GC-MS spectra of the infected HFT cells, but not in the spectra of the uninfected HFT cells (Figure S1). This verified that the detected branched-chain fatty acids were produced by *C. trachomatis* due to its branched-chain ketoacid dehydrogenase (Yao et al., 2015b). The isotopologue profiles of both fatty acids displayed a maximum of ten labelled carbon atoms resulting from five [U-$^{13}C_2$]acetyl-CoA units (Figure 11B). Therefore, it can be assumed that the C5-moieties of these fatty acids were obtained from unlabelled leucine and isoleucine.

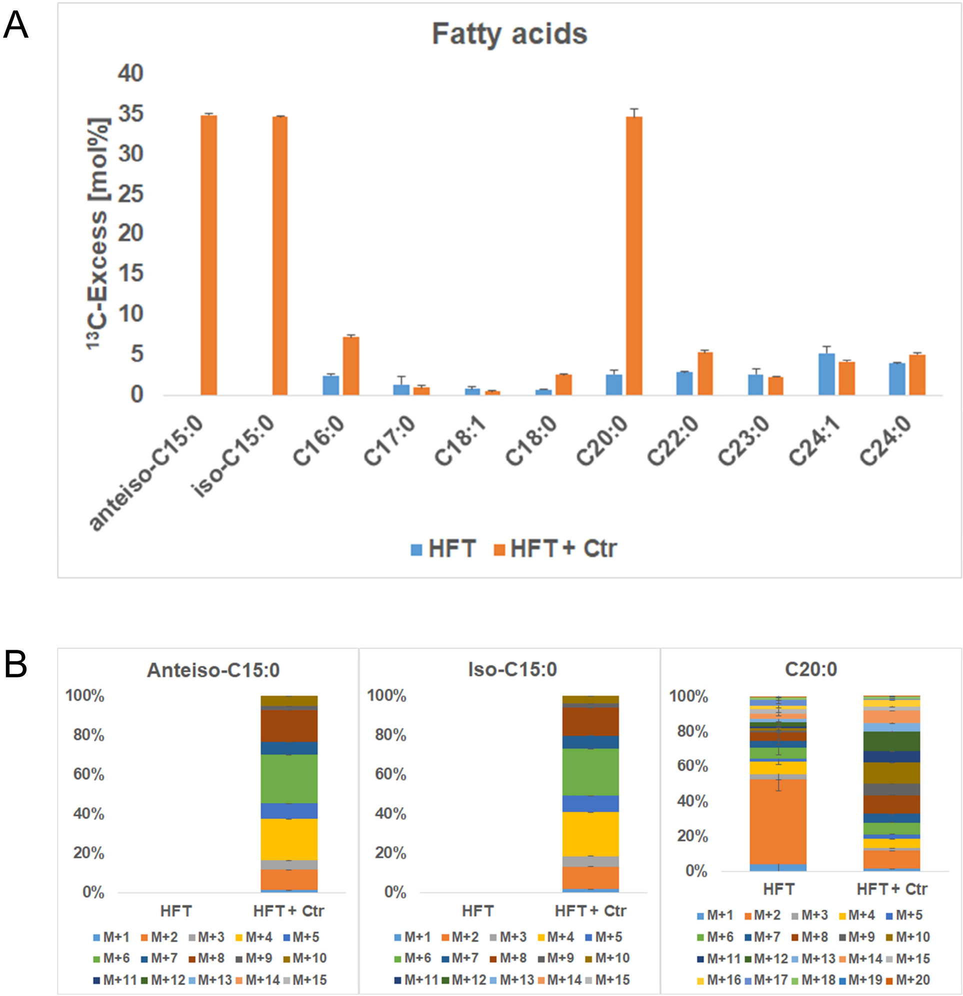

Figure 11: ^{13}C-Excess in mol% (A) and isotopologue profiles (B) of fatty acids from uninfected HFT cells and with *C. trachomatis* infected HFT cells. M+X represents the isotopologue profiles with X ^{13}C-atoms incorporated into the fatty acids. Error bars show the standard deviations from one biological replicate with three technical replicates.

Analysis of supernatants by NMR spectroscopy

The ^{1}H-NMR spectrum of the supernatant from uninfected HFT cells (Figure 12A) showed among others α-glucose with a characteristic signal for H-1 at 5.24 ppm (i.e. attached to a ^{12}C-1) and the ^{13}C-coupled satellites at 5.40 ppm and 5.06 ppm ($^{1}J_{CH}$, 83.8 Hz; reflecting H-1 attached to a ^{13}C-1) as well as the signal for H-1 of ß-glucose at 4.65 ppm (H-1 attached to ^{12}C-1) with the corresponding ^{13}C satellite at 4.49 ppm ($^{1}J_{CH}$, 82.3 Hz; reflecting H-1 attached to ^{13}C-1). The second ^{13}C satellite of ß-glucose could not be detected due to overlap with the water signal at 4.80 ppm. Furthermore, a doublet at 1.33 ppm for the methyl group of lactate (^{12}C-3 of lactate) with ^{13}C-coupled satellites at 1.45 ppm and 1.20 ppm ($^{1}J_{CH}$, 65.2 Hz; reflecting ^{13}C-3 of lactate) could be observed. In contrast, the ^{13}C-coupled satellites of glucose and lactate showed higher ^{1}H-NMR signal intensities in the spectrum of the supernatant from with *C. trachomatis* infected HFT cells (Figure 12B), whereas other signals were in the same order of magnitude. The higher ^{13}C-enrichment of lactate (74.3%) and the lower amount of glucose (1.3 mg/ml) in the supernatant of with *C. trachomatis* infected HFT cells in contrast to the ^{13}C-excess of 68.5% in lactate and 1.4 mg/ml glucose amount in the supernatant of the uninfected HFT cells implied that more glucose was utilized and glycolysis was increased resulting in the production of more labelled lactate and its secretion due to the infection.

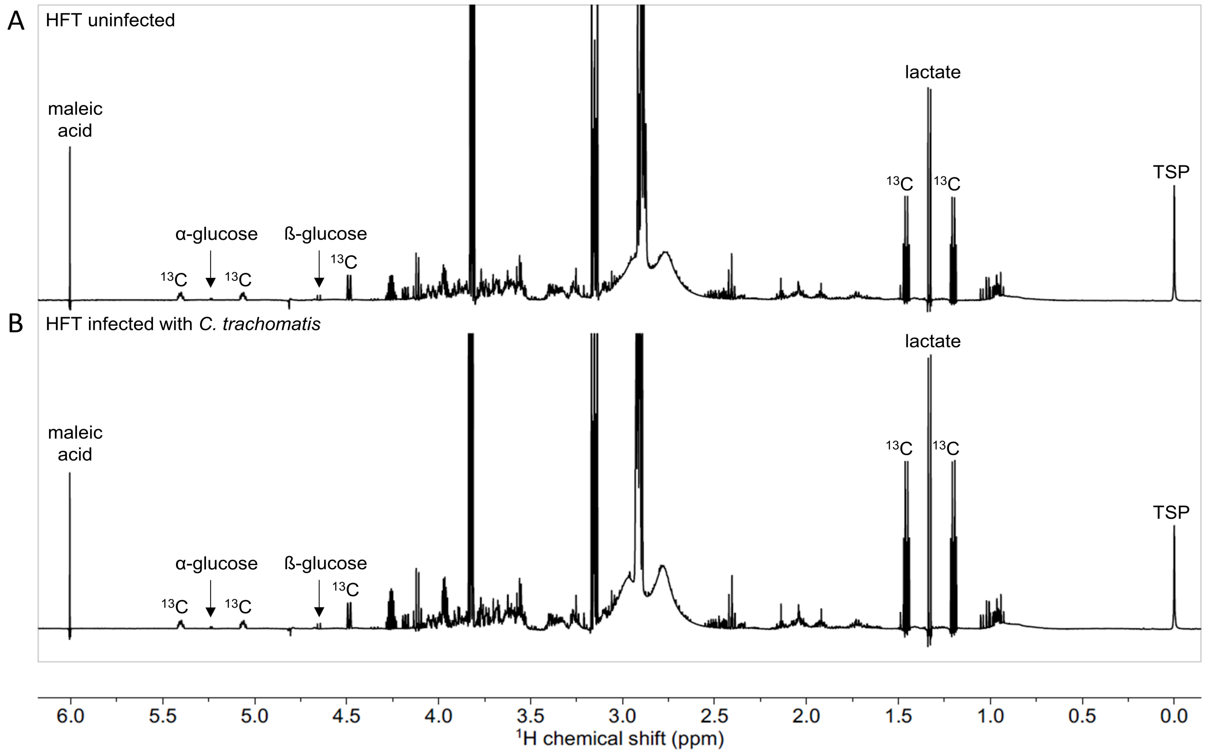

Figure 12: ^{1}H-NMR spectra of supernatants of uninfected HFT cells (A) and with *C. trachomatis* infected HFT cells (B) in D_2O. The labelling experiment was done with [U-$^{13}C_6$]glucose. Maleic acid was used as an internal standard for the quantification of glucose. TSP was used for chemical shift referencing.

Carbon fluxes in human M1 and M2 polarized macrophages

To study the carbon metabolism of human M1 and M2 polarized macrophages, labelling experiments with [U-$^{13}C_6$]glucose were performed. In the following, the results of the protein-derived amino acids, the TCA metabolites, the fatty acids and the supernatants of uninfected and with *C. trachomatis* infected M1 and M2 phenotypes are discussed in more detail.

Incorporation of ^{13}C in protein-derived amino acids from [U-$^{13}C_6$]glucose

As previously described for the HFT cells, the essential amino acids leucine, isoleucine, valine, threonine, phenylalanine, histidine and lysine showed ^{13}C-excess values under 1% in both macrophage subtypes (data not shown). However, the ^{13}C-enrichment for alanine was significant lower in the M1 phenotype (uninfected: 3.2%; infected: 3.3%) and in the M2 phenotype (uninfected: 1.5%; infected: 2.3%) than in the HFT cells (uninfected: 9.6%; infected: 11.2%). Interestingly, the protein-derived amino acids aspartate and glutamate showed similar ^{13}C-excess values as in the HFT cells. Therefore, it can be assumed that the macrophages utilized significant less labelled glucose for glycolysis that the HFT cells, whereas a similar small amount of ^{13}C-marked glucose was used to feed the TCA cycle.

In contrast to the labelling data of the HFT cells, no significant differences in ^{13}C-enrichments (Figure 13A) and isotopologue profiles (Figure 13C) of alanine, glutamate and aspartate could be observed between uninfected and infected M1 polarized macrophages. Furthermore, the bacterial cell wall component mDAP could not be detected in the GC-MS spectrum of the infected M1 phenotype (data not shown). Therefore, it can be assumed that M1 polarized human macrophages seemed to be inappropriate to serve as host for *C. trachomatis*.

The infected M2 phenotype showed a small increase in the ^{13}C-enrichments for alanine, aspartate and glutamate in contrast to the uninfected M2 macrophages (Figure 13B). Additionally, the isotopologue profiles displayed high fractions of M+3 in alanine (Figure 13D) Therefore, it can be concluded that more ^{13}C-labelled glucose was utilized *via* glycolysis for the synthesis of protein-derived amino acids during infection, as previously described for the infected HFT cells. Moreover, the bacteria specific metabolite mDAP was detected with a high ^{13}C-excess value of 32.6%. The isotopologue profile of mDAP (Figure 13D) revealed that it was synthesized from fully labelled pyruvate and unlabelled aspartate leading to M+3 and from unlabelled pyruvate and fully labelled aspartate mainly leading to M+2. Taken together, the higher ^{13}C-enrichments of the amino acids alanine, aspartate and glutamate as well as the detection of the bacteria specific metabolite mDAP in the infected M2 macrophages demonstrated an active metabolism of *C. trachomatis* in these host cells.

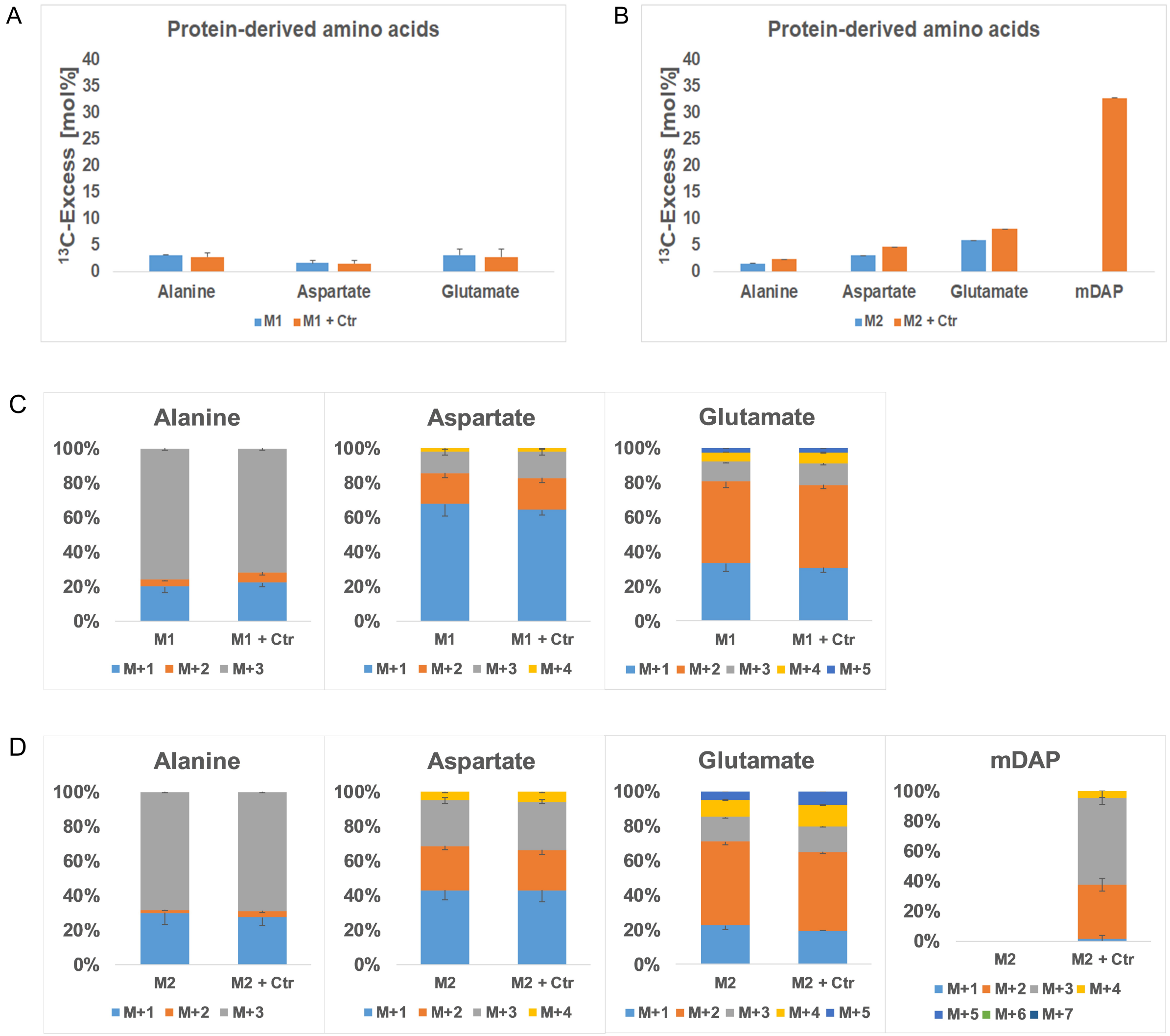

Figure 13: ^{13}C-Excess in mol% of protein-derived amino acids and mDAP from uninfected and with *C. trachomatis* infected M1 phenotype (A) and M2 phenotype (B) as well as the isotopologue profiles of protein-derived amino acids and mDAP from uninfected and with *C. trachomatis* infected M1 phenotype (C) and M2 phenotype (D). M+X represents the isotopologue profiles with X ^{13}C-atoms incorporated into the amino acids. Error bars show the standard deviations from one biological replicate with three technical replicates.

Incorporation of ^{13}C in TCA intermediates from [U-$^{13}C_6$]glucose

The lower ^{13}C-excess values (Figure 14A) of the TCA intermediates fumarate (uninfected: 5.9%; infected: 6.0%), malate (uninfected: 6.0%; infected: 5.7%) and citrate (uninfected: 3.0%; infected: 2.6%) in the M1 macrophages displayed that labelled glucose was mainly used for glycolysis and less for the TCA cycle. Again, the ^{13}C-enrichments (Figure 14A) and the isotopologue fractions (Figure 14C) of these metabolites in uninfected and infected M1 macrophages were in the same order of magnitude. Therefore, the results verified that an infection with *C. trachomatis* had no effect on the metabolic pathway of the M1 macrophages. The infected M2 polarized macrophages showed a significant decrease in the ^{13}C-excess values (Figure 14B) for the TCA intermediates in contrast to the uninfected M2 phenotype whereas the isotopologue profiles displayed similar fractions (Figure 14D). Hence, the metabolism seemed to be slowed down during infection.

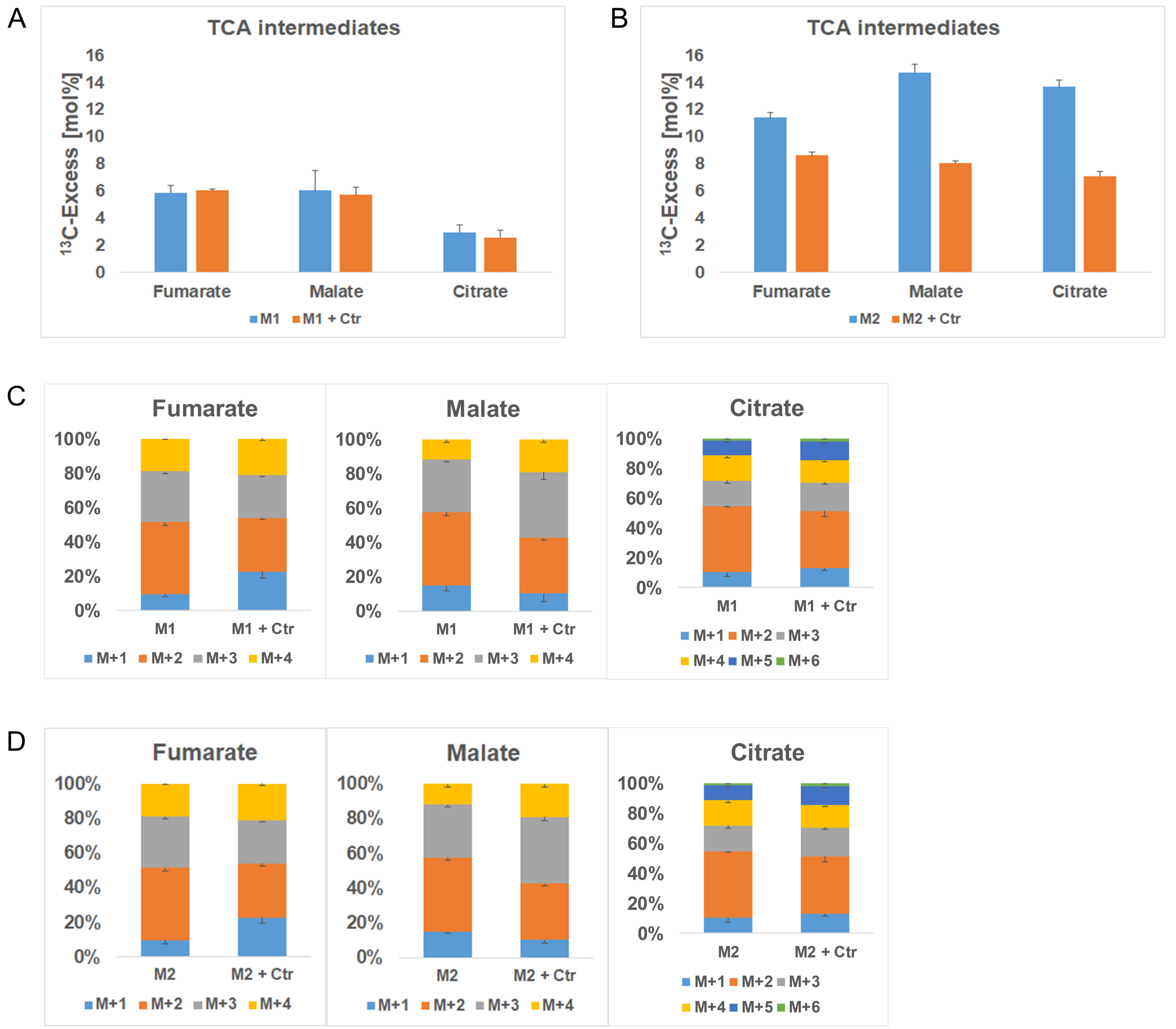

Figure 14: ^{13}C-Excess in mol% of TCA intermediates from uninfected and with *C. trachomatis* infected M1 phenotype (A) and M2 phenotype (B) as well as the isotopologue profiles of TCA intermediates from uninfected and with *C. trachomatis* infected M1 phenotype (C) and M2 phenotype (D). M+X represents the isotopologue profiles with X ^{13}C-atoms incorporated into the TCA intermediates. Error bars show the standard deviations from one biological replicate with three technical replicates.

Incorporation of ^{13}C in fatty acids from [U-$^{13}C_6$]glucose

The infected M1 phenotype revealed a decrease in the ^{13}C-excess (Figure 15A) of the fatty acid C20:0, whereas the enrichment of the fatty acids C22:0 and C23:0 were in the same order of magnitude. Furthermore, no significant differences in the isotopologue fractions between uninfected and infected M1 macrophages (Figure 15C) could be determined.

In comparision to the M1 phenotype, the infected M2 macrophages showed a significant increase in the ^{13}C-enrichment (Figure 15B) of arachidic acid in contrast to the uninfected M2 phenotype. Moreover, the istopologue distributions of C20:0 were different between uninfected and infected host cells (Figure 15D). The increased incorporation of ^{13}C into the arachidic acid during infection suggested that the M2 polarized human macrophages allowed an efficient replication of *C. trachomatis.* Notably, the bacteria specific branched-chain fatty acids anteiso-C15:0 and iso-C15:0 could not be detected in the GC-MS spectra of infected M2 macrophages.

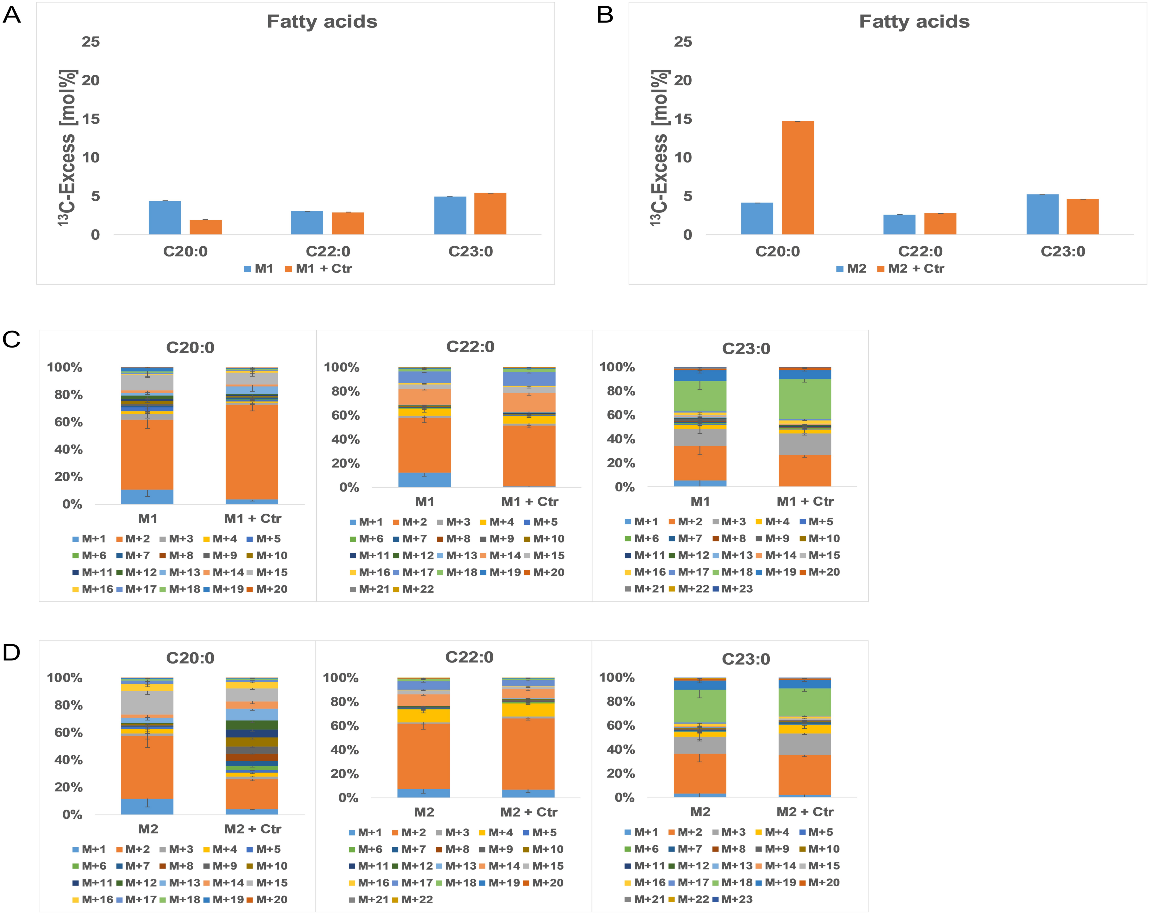

Figure 15: ^{13}C-Excess in mol% of fatty acids of uninfected and with *C. trachomatis* infected M1 phenotype (A) and M2 phenotype (B) as well as the isotopologue profiles of fatty acids of uninfected and with *C. trachomatis* infected M1 phenotype (C) and M2 phenotype (D). M+X represents the isotopologue profiles with X ^{13}C-atoms incorporated into the fatty acids. Error bars show the standard deviations from one biological replicate with three technical replicates.

Analysis of supernatants by NMR spectroscopy

The ^{1}H-NMR spectrum of the infected M2 phenotype (Figure 16B) displayed lactate at 1.33 ppm with significant higher ^{13}C satellites at 1.45 ppm and 1.20 ppm in contrast to the spectrum of the uninfected M2 macrophage (Figure 16A), whereas no difference could be revealed in the ^{1}H-NMR spectra between uninfected (Figure 16C) and infected (Figure 16D) M1 phenotype. This observation was verified by the calculated ^{13}C-excess values of lactate. The enrichment of lactate (72.7%) for the infected M2 phenotype was significantly higher than the lactate enrichment of 60.2% in the uninfected M2. The calculated ^{13}C-excess values for the uninfected and infected M1 macrophages were in the same order of magnitude (uninfected: 51.6%; infected: 51.7%). Furthermore, the glucose amount in the supernatant of the infected M2 phenotype was significantly lower (2.0 mg/ml) than in the supernatant of the uninfected M2 macrophages (2.4 mg/ml). Again, no significant difference in the glucose concentration could be determined between uninfected and infected M1 phenotype (both approx. 2.2 mg/ml).
The higher ^{13}C-excess value and the lower glucose amount in the infected M2 macrophages indicated that more glucose was used for glycolysis and more lactate was secreted during infection. In contrast, *C. trachomatis* had no influence on the glucose uptake and lactate production in the M1 phenotype as no significant differences could be noticed.

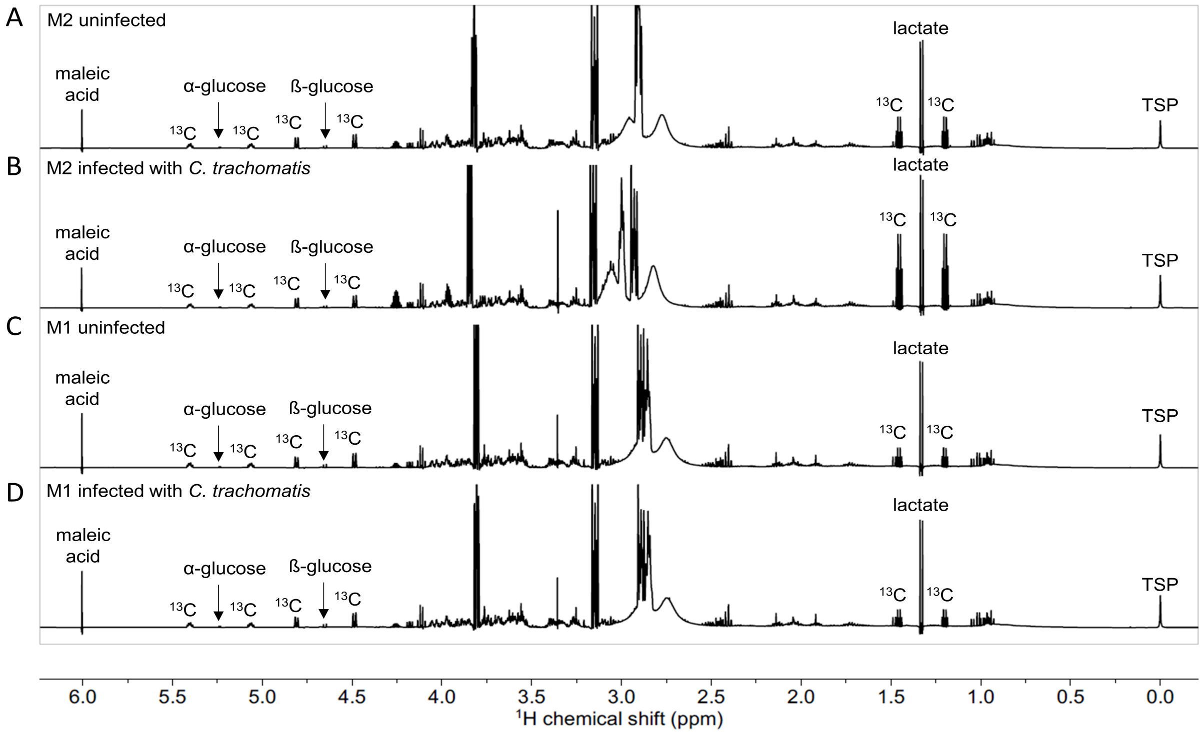

Figure 16: ^{1}H-NMR spectra of supernatants of uninfected M2 phenotype (A), with *C. trachomatis* infected M2 phenotype (B), uninfected M1 phenotype (C) and with *C. trachomatis* infected M1 phenotype (D) in D_2O. The labelling experiment was done with [U-$^{13}C_6$]glucose. Maleic acid was used as an internal standard for the quantification of glucose. TSP was used for chemical shift referencing.

4.3.4 Discussion

While the intracellular metabolism of *C. trachomatis* has been studied intensively in recent decades, the reprogramming of host cells during infection is still poorly understood. Therefore, we investigated on the general carbon metabolism of HFT cells as well as human M1 and M2 polarized macrophages and further on metabolic adaptations during infection by performing dual isotopologue profiling. In the following, the results obtained from the labelling experiment with [U-$^{13}C_6$]glucose for the uninfected and with *C. trachomatis* infected host cells are discussed in more detail.

Metabolic fluxes in uninfected and infected HFT cells

Based on the labelling experiment with [U-$^{13}C_6$]glucose, a high ^{13}C-excess value for the protein-derived amino acid alanine (with mainly M+3 fraction) and low ^{13}C-enrichments of the protein-derived amino acids glutamate and aspartate as well as the TCA intermediates citrate, fumarate and malate (with mainly M+2 fraction) could be determined in the uninfected HFT cells (Figure 17A). Therefore, it can be concluded that exogenous [U-$^{13}C_6$]glucose was efficiently utilized *via* glycolysis to [U-$^{13}C_3$]pyruvate and further used for the synthesis of alanine, whereas only a minor part was used to drive the TCA cycle leading to intermediates with two labelled carbon atoms. Additionally, small glucose amounts were utilized to form fatty acids resulting in small ^{13}C-excess values. In contrast to the labelling rates observed in the uninfected HFT cells, the ^{13}C-enrichments of the protein-derived amino acid alanine and the fatty acid C20:0 was significantly increased in the infected HFT cells (Figure 17B), whereas the ^{13}C-excess values of the TCA intermediates were in the same order of magnitude. Of special interest was the intermediate citrate which can only be produced by the host cells. The similar excess values and isotopologue profiles of uninfected and infected host cells clearly demonstrated that the labelling data mainly represented the metabolic pathway of the host cells. Moreover, a higher enrichment of lactate and a lower amount of glucose were determined in the supernatants of the infected cells. Thus, it could be assumed that more glucose was used *via* glycolysis for the production of alanine, lactate and the fatty acid C20:0 during infection, whereas *C. trachomatis* seemed to have no influence on the TCA cycle of the host. Furthermore, the bacterial specific branched-chain fatty acids anteiso-C15:0 and iso-C15:0 with a maximum of ten labelled carbon atoms were detected in the GC-MS spectra of the infected HFT cells. Because *C. trachomatis* is not able to utilize glucose directly, it can be assumed that host-derived glucose-6-phosphate was efficiently taken up by the *UhpC*-transporter and further converted to [U-$^{13}C_2$]-acetly-CoA units. The reaction of fully labelled acetyl-CoA units and exogenous unlabelled leucine and isoleucine resulted in the formation of the branched-chain fatty acids with maximal ten labelled carbon atoms and mainly odd numbers of ^{13}C-atoms (Figure 20A). The detection of bacterial specific fatty acids and the increased metabolic fluxes in the upper part of the glycolytic pathways indicated that HFT cells allowed an efficient replication of *C. trachomatis*.

Metabolic fluxes in uninfected and infected human M1 polarized macrophages

Low ^{13}C-excess values for the protein-derived amino acids alanine, aspartate and glutamate, for the fatty acids and the TCA intermediates were observed in the uninfected M1 macrophages (Figure 18A). Generally, the pro-inflammatory M1 phenotype is characterized by a “Warburg” metabolism with an increased uptake of glucose leading to higher rates of glycolysis, lactate production for energy regeneration and a decrease in TCA cycling (Eisenreich et al., 2020; Nonnenmacher and Hiller, 2018; Ó Maoldomhnaigh et al., 2021). Interestingly, the ^{13}C-enrichments in the protein-derived amino acids, TCA intermediates and fatty acids in the M1 polarized macrophages (Figure 18B) as well as the labelling rates in lactate and glucose amount in the supernatant of the infected phenotype were in the same order of magnitude. Additionally, no bacterial specific metabolites were detected. Thus, it was suggested that *C. trachomatis* had no influence on the metabolic pathway of the M1 macrophages and was further not able to replicate and grow within this host cell.

Metabolic fluxes in uninfected and infected human M2 polarized macrophages

Low ^{13}C-enrichments in the protein-derived amino acids alanine, aspartate and glutamate and fatty acids of the uninfected human M2 polarized macrophages (Figure 19A) were observed, whereas the TCA intermediates displayed higher ^{13}C-excess values. Furthermore, the analysis of the supernatants revealed a high enrichment in lactate. Hence, exogenous [U-$^{13}C_6$]glucose was mainly used to produce lactate and to feed the TCA cycle, whereas the production of protein-derived amino acids seemed to be less active in this phenotype. In contrast to the uninfected M2 macrophages, the analysis of the infected M2 phenotype (Figure 19B) revealed an increased incorporation into the protein-derived amino acid alanine, the fatty acid C20:0 and lactate, but a decrease in the ^{13}C-excess values of the TCA intermediates. Furthermore, the bacterial specific cell wall component mDAP could be detected in the GC-MS spectra of the infected host cells. The isotopologue profile of mDAP with mainly M+3 revealed its biosynthesis from fully labelled pyruvate and unlabelled aspartate (Figure 20B). Additionally, host-derived glutamate or other carboxylates with two labelled carbon atoms were efficiently taken up and incorporated into the amino acid aspartate which was further used resulting in the formation of mDAP with two labelled carbon atoms. Taken together, it was concluded that an infection with *C. trachomatis* led to an increased uptake of glucose in the M2 macrophages resulting in higher labelling rates of alanine, lactate and arachidic acid, whereas the TCA cycle seemed to be downregulated during infection. Moreover, it was suggested that the human M2 polarized macrophages seemed to be suitable to serve as host cells for an intracellular growth of *C. trachomatis*.

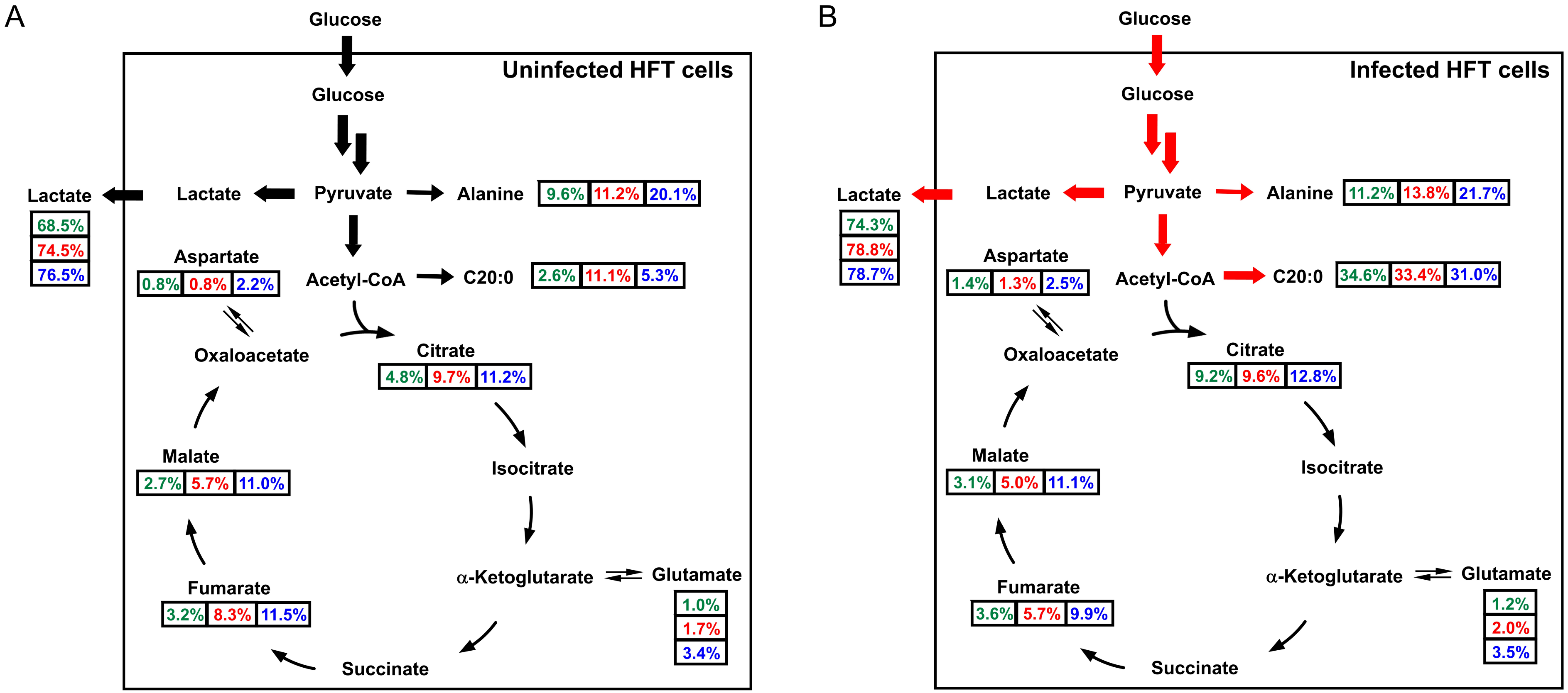

Figure 17: Model for the carbon metabolism of uninfected HFT cells (A) and with *C. trachomatis* infected HFT cells (B) based on the labelling experiment with [U-$^{13}C_6$]glucose. The thickness of the arrows shows the approximate relative amount of ^{13}C-incorporation. The total ^{13}C-enrichments from replicate one (*green*), replicate two (*red*) and replicate three (*blue*) are framed. Red arrows indicate an increase in the enrichment during infection.

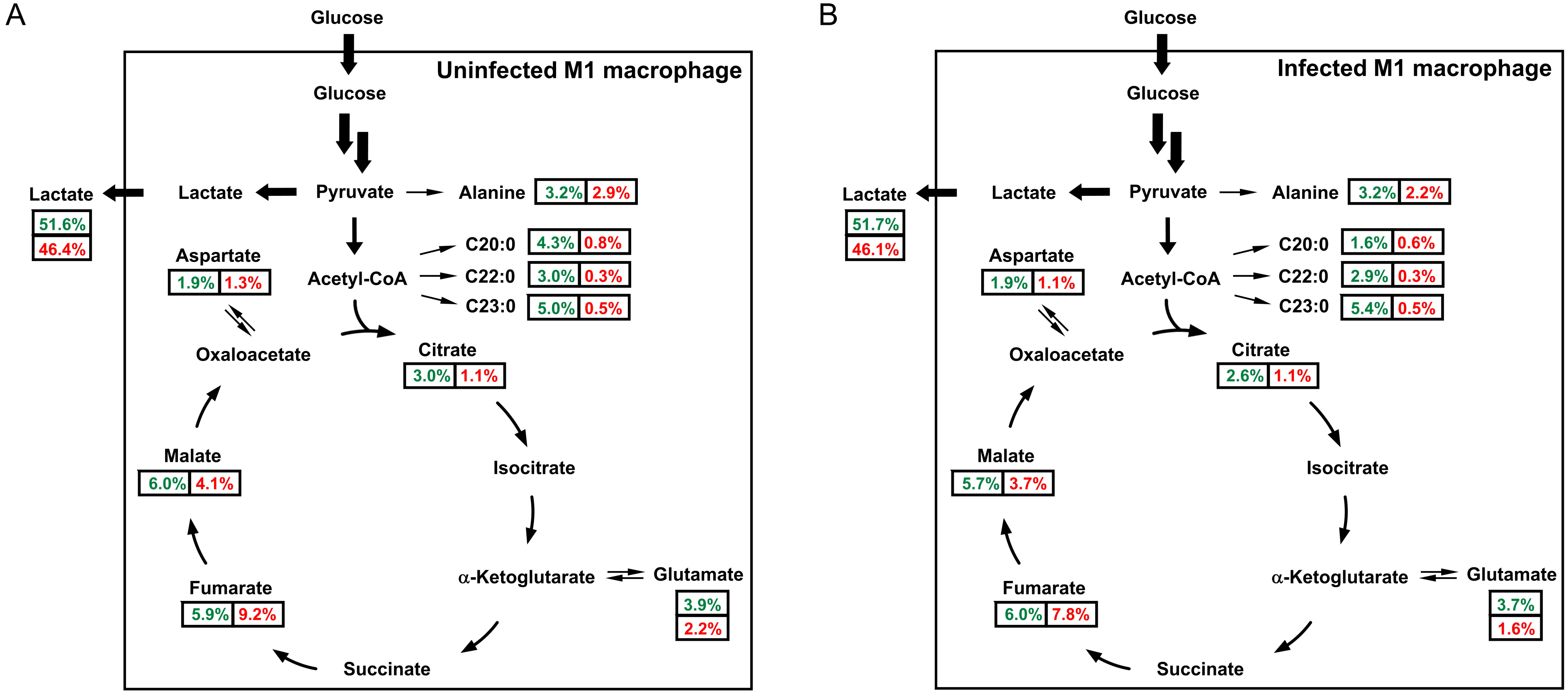

Figure 18: Model for the carbon metabolism of uninfected M1 macrophage (A) and with *C. trachomatis* infected M1 macrophage (B) based on the labelling experiment with [U-$^{13}C_6$]glucose. The thickness of the arrows shows the approximate relative amount of ^{13}C-incorporation. The total ^{13}C-enrichments from replicate one (*green*) and replicate two (*red*) are framed.

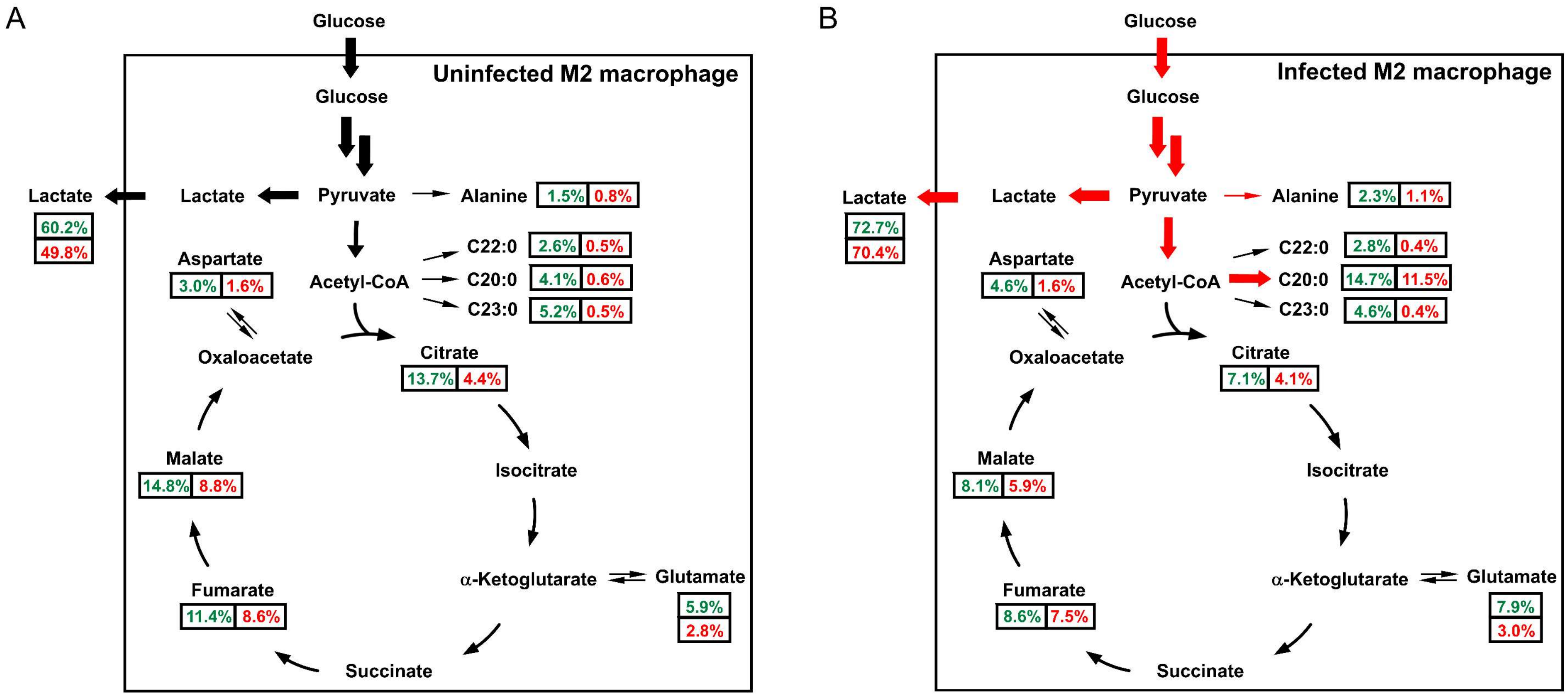

Figure 19: Model for the carbon metabolism of uninfected M2 macrophage (A) and with *C. trachomatis* infected M2 macrophage (B) based the labelling experiment with [U-$^{13}C_6$]glucose. The thickness of the arrows shows the approximate relative amount of ^{13}C-incorporation. The total ^{13}C-enrichments from replicate one (*green*) and replicate two (*red*) are framed. Red arrows indicate an increase in the enrichment during infection.

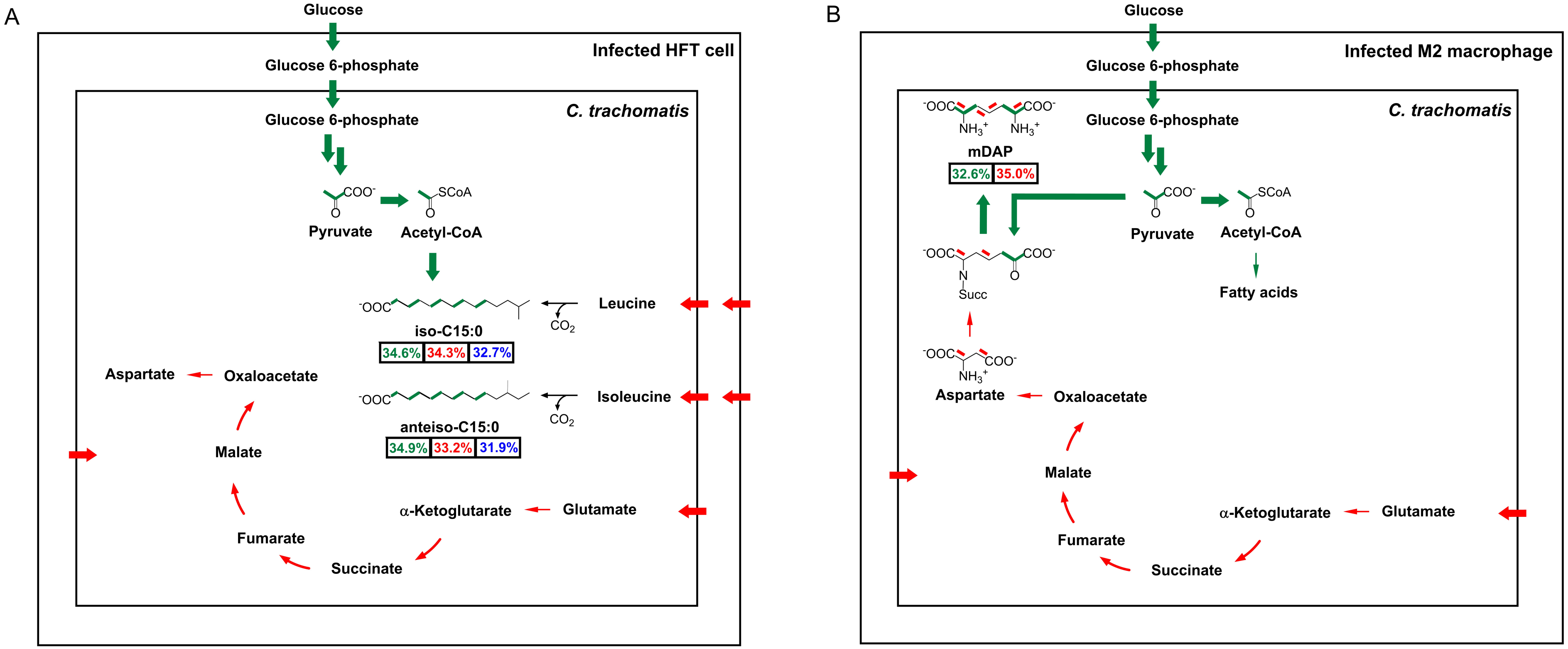

Figure 20: Model for the carbon metabolism of *C. trachomatis* in HFT cell (A) and M2 macrophage (B) based on the labelling experiment with [U-$^{13}C_6$]glucose. The thickness of the arrows shows the approximate relative amount of ^{13}C-incorporation. The total ^{13}C-enrichments from replicate one (*green*), two (*red*) and three (*blue*) are framed. The incorporation of exogenous subtrates *via* transporters is indicated by red thick arrows.

5. Conclusion

The first chapter of this work deals with the development of fast and easy methods for the identification of thickening agents, a functional class of food additives, in various food products and their premixtures using NMR spectroscopy. In contrast to previous published methods using time-consuming preparation steps for the identification and quantification of food thickeners by NMR spectroscopy (Grün et al., 2015; Merkx et al., 2018), the presented protocols in this work enabled the unequivocally identification of intact food thickeners in different complex matrices without any previous long-delayed sample processing steps. By measuring DOSY spectra, thickening agents could be spectrometrically separated from other compounds in a single sample batch based on different molecular weights without any prior processing steps (Radziej et al., 2021). Additionally, a fast and easy separation of high-molecular weight thickeners from low-molecular weight substances was achieved using centrifugal concentrators (Radziej et al., 2022). However, the limits of the developed procedures (low concentrations of applied thickening agents, presence of other compounds) were also demonstrated in this work. Therefore, the suitability of identifying food thickeners in food products and their premixtures with these protocols has to be examined for each matrix individually. Taken together, the methods presented in this work can support the officially accepted §64 LFGB method L 00.00-13 as well as other well-established methods in determining thickening agents in premixtures and food products.

The second chapter of this work deals with different metabolic reactions of various host cells to infections with *C. trachomatis*. By performing labelling experiment with [U-$^{13}C_6$]glucose, differences in the general carbon metabolism of HFT cells as well as human M1 and M2 polarized macrophages could be revealed. Moreover, the detection of bacterial specific metabolites in infected HFT cells and M2 polarized macrophages demonstrated the suitability of these cells to serve as host cells for an efficient replication of *C. trachomatis*. In contrast, this bacterium was not able to grow and replicate within the human M1 polarized macrophages as no significant differences between uninfected as well as infected host cells were observed and no bacterial specific metabolites could be detected. Taken together, the labelling experiments presented in this work provided more insight into the general metabolic network of HFT cells and macrophages. Additionally, the ^{13}C-excess values and isotopologue distributions illustrated how *C. trachomatis* influences the pathways of its host cells. Based on these settings, new therapeutic approaches can be tested for the treatment of infections.

6. Outlook

In the following, preliminary results of ongoing studies (*Neisseria meningitidis, Coxiella burnetii*) are briefly discussed.

6.1 The intracellular pathogen *Neisseria meningitidis*

The human pathogen *Neisseria meningitidis* (*N. meningitidis)* is a Gram-negative bacterium that was first isolated from a cerebrospinal fluid by Anton Weichselbaum in 1887 (Yazdankhah and Caugant, 2004). It is the causative agent of the meningococcal disease, which is known for its high lethality and morbidity rates with over 500 000 reported cases each year (Batista et al., 2017; Brigham and Sandora, 2009). An infection with *N. meningitidis* can also lead to other serious illnesses like severe sepsis, pneumonia or conjunctivitis (Yazdankhah and Caugant, 2004). For the treatment of infections with this type of pathogen, antibiotics like penicillin, chloramphenicol or dexamethasone are usually administered parenterally (Ferguson et al., 2002; Hill et al., 2010). People who may be at risk of contracting a meningococcal disease can receive rifampin, ceftriaxone or ciprofloxacin for prophylaxis (Ferguson et al., 2002). *N. meningitidis* is spread directly from person to person and colonizes the nasopharynx by adhesion on the membrane-located receptor CD46 of the host cell (Trivedi et al., 2011). By modulating the host cell machinery, it is able to cross the epithelial barrier and persists in the bloodstream (Barrile et al., 2015). According to experimental studies and a genome-scale flux model based on genomic data, *N. meningitidis* is adapted to grow on a minimal medium with glucose, pyruvate or lactate as sole carbon sources (Baart et al., 2007). Moreover, the performance of NMR measurements from labelling experiments with 3-[^{13}C]pyruvate demonstrated that this tracer was efficiently utilized for the synthesis of various protein-derived amino acids. Furthermore, the investigation of enzyme activities in cell-free extracts revealed that all enzymes are present to drive the TCA cycle in *N. meningitidis* except the NAD-dependent malate dehydrogenase (Leighton et al., 2001). However, very little is known about the detailed pathways in this pathogen (Schoen et al., 2014). Additionally, there is evidence that the CRISPR/Cas system influences the bacterial adhesion to human epithelial cells, even if further analysis for the discovery of the exact molecular mechanism is required (Heidrich et al., 2019). In order to study the influence of the CRISPR/Cas system on the pathway of *N. meningitidis*, the wildtype as well as the cas9 and scaRNA mutants were incubated for 2h at 37°C on ENEM +++ medium (supplemented with sodium pyruvate, non-essential amino acids and fetal calf serum). For the flux analysis, 20% [U-^{13}C$_6$]glucose, ^{15}NH$_4$Cl or ^{15}N-Glutamine were used as tracers. After heat inactivation (120°C, 20 min) and lyophilisation of the cell pellets, the protein-derived amino acids and methanol-soluble polar metabolites were analysed by GC-MS as previously described (section 2.2). In the following, the preliminary results are discussed in more detail.

Incorporation of ^{13}C in protein-derived amino acids from [U-$^{13}C_6$]glucose

The protein-derived amino acids alanine, aspartate, glutamate, glycine, serine and valine showed total ^{13}C-excess values between 2% (glutamate) and 7% (serine) from the labelling experiment with 20% [U-$^{13}C_6$]glucose (Figure 21A). The isotopologue profiles displayed mainly M+3 in alanine and serine, mainly M+2 in glycine and mainly M+1 in aspartate and glutamate (Figure 21B). In contrast, the amino acids leucine, isoleucine, phenylalanine, proline, threonine and tyrosine displayed ^{13}C-enrichments under 1% (data not shown). Additionally, no significant differences in the ^{13}C-excess values (Figure 21A) and isotopologue distributions (Figure 21B) between wildtype, cas9 and scaRNA could be observed.

Incorporation of ^{13}C in methanol-soluble polar metabolites from [U-$^{13}C_6$]glucose

From the labelling experiment with 20% [U-$^{13}C_6$]glucose, high ^{13}C-enrichments were detected in ethanolamine (approx. 10%) with about 80% M+2, lactate (approx. 12%) with about 80% M+3 and glyceraldehyde (approx. 15%) with about 90% M+3 (Figure 22). Furthermore, ^{13}C-excess values between 3% and 7% were determined in the free amino acids alanine, glycine, serine, glutamate, the TCA intermediates fumarate and glutamate as well as in the fatty acid myristate. Low ^{13}C-enrichments were observed in valine (approx. 1%) with an isotopologue distribution of about 30% M+1, 30% M+2 and 40% M+3 as well as in aspartate (approx. 2%) with mainly M+1 (about 70%). In contrast, the free amino acids leucine, isoleucine, phenylalanine, proline, threonine and tyrosine displayed ^{13}C-enrichments under 1% (data not shown). Again, no significant differences in the ^{13}C-excess values (Figure 22A) and isotopologue distributions (Figure 22B) between wildtype, cas9 and scaRNA could be observed.

Carbon flux in *N. meningitidis* wildtype (Labelling experiment with 20% [U-$^{13}C_6$]glucose)

Labelling experiments revealed significant ^{13}C-excess values (5% - 15%) and isotopologue distributions with mainly M+3 (70% - 90%) for the metabolites glyceraldehyde, serine, alanine, lactate and valine. In contrast, the amino acids phenylalanine and tyrosine showed no significant ^{13}C-enrichments (below 1%). Therefore, it can be concluded that fully labelled glucose was mainly utilized *via* the Entner-Doudoroff pathway for the synthesis of lactate (approx. 11% ^{13}C-excess value; 90% M+3) and less *via* the pentose phosphate pathway for the synthesis of phenylalanine and tyrosine. These results confirmed the genome-based model of the central carbon metabolism (Schoen et al., 2014). The isotopologue distribution of myristate with about 60% M+2 and a ^{13}C-excess value of approx. 5% demonstrated that this fatty acid was mainly built from the fully labelled precursor acetyl-CoA. Interestingly, the amino acid aspartate showed an isotopologue profile with about 60% M+1, about 30% M+3 and less than 5% M+2. Hence, it can be assumed that the intermediate oxaloacetate was mainly synthetized from labelled hydrogen carbonate and unlabelled phosphoenolpyruvate *via* the enzyme phosphoenolpyruvate carboxylase and further converted to aspartate leading to one labelled carbon atom. Additionally, the reaction of unlabelled hydrogen carbonate with fully labelled phosphoenolpyruvate led to oxaloacetate and aspartate with three labelled carbon atoms. The synthesis of aspartate from fully labelled acetyl-CoA *via* the TCA cycle seemed to be less active as the isotopologue distribution showed about only 5% of the M+2 fraction. The TCA intermediates fumarate and malate displayed similar isotopologue profiles (mainly M+1 and M+3) indicating that these intermediates were mainly built from aspartate *via* the aspartate ammonia lyase and only a minor part was synthesized *via* the TCA cycle. Furthermore, the labelling experiment implied that malate (with one labelled carbon atom) was converted to pyruvate *via* the NADP-dependent malic enzyme leading to alanine with about 15% M+1. Due to a high ^{13}C-excess value of approx. 15% in glyceraldehyde and low ^{13}C-excess values of approx. 6% in the TCA intermediates, a bipartite metabolism in *N. meningitidis* wildtype was deduced. A schematic model of the general carbon metabolism based on the labelling experiment with 20% [U-$^{13}C_6$]glucose is demonstrated in Figure 24.

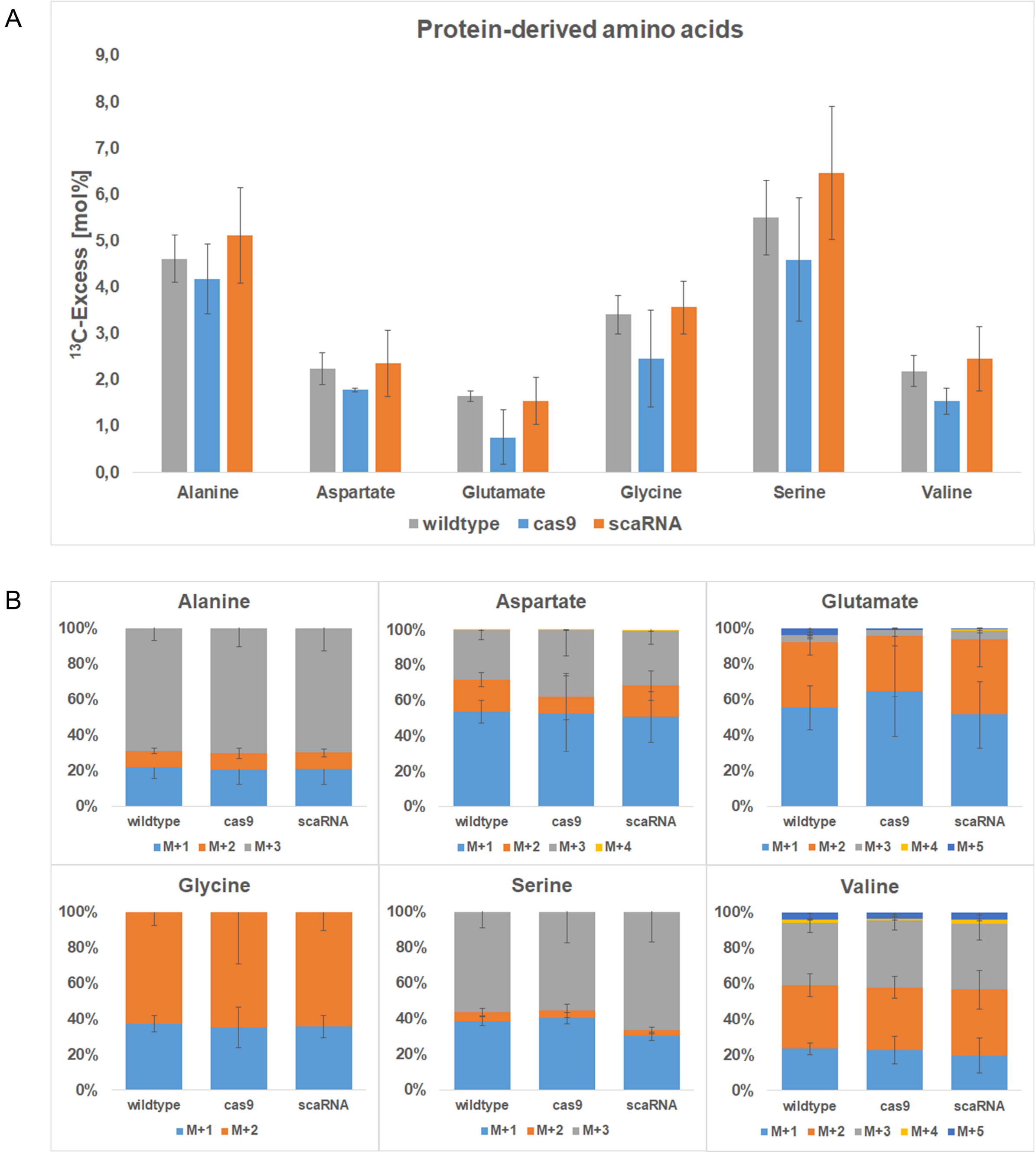

Figure 21: ^{13}C-Excess in mol% (A) and isotopologue profiles (B) of protein-derived amino acids from *N. meningitidis* wildtype, cas9 and scaRNA based on labelling experiments with 20% [U-$^{13}C_6$]glucose. M+X represents the isotopologue profiles with X ^{13}C-atoms incorporated into the protein-derived amino acids. Error bars show the standard deviations from three biological replicates (wildtype, scaRNA) with three technical replicates and from two biological replicates (cas9) with three technical replicates.

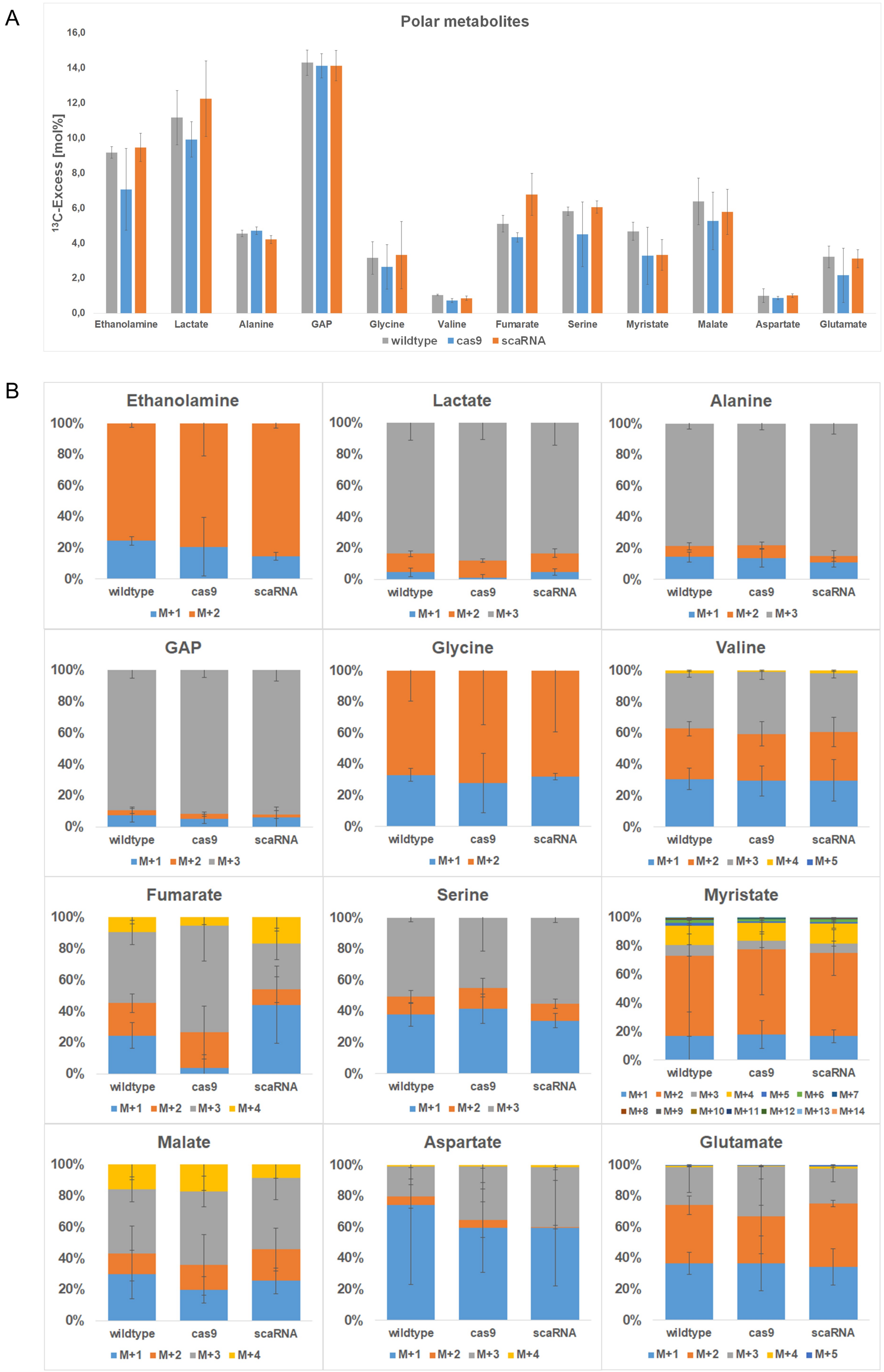

Figure 22: ^{13}C-Excess in mol% (A) and isotopologue profiles (B) of polar metabolites from *N. meningitidis* wildtype, cas9 and scaRNA based on labelling experiments with 20% [U-$^{13}C_6$]glucose. M+X represents the isotopologue profiles with X ^{13}C-atoms incorporated into the polar metabolites. Error bars show the standard deviations from three biological replicates (wildtype, scaRNA) with three technical replicates and from two biological replicates (cas9) with three technical replicates.

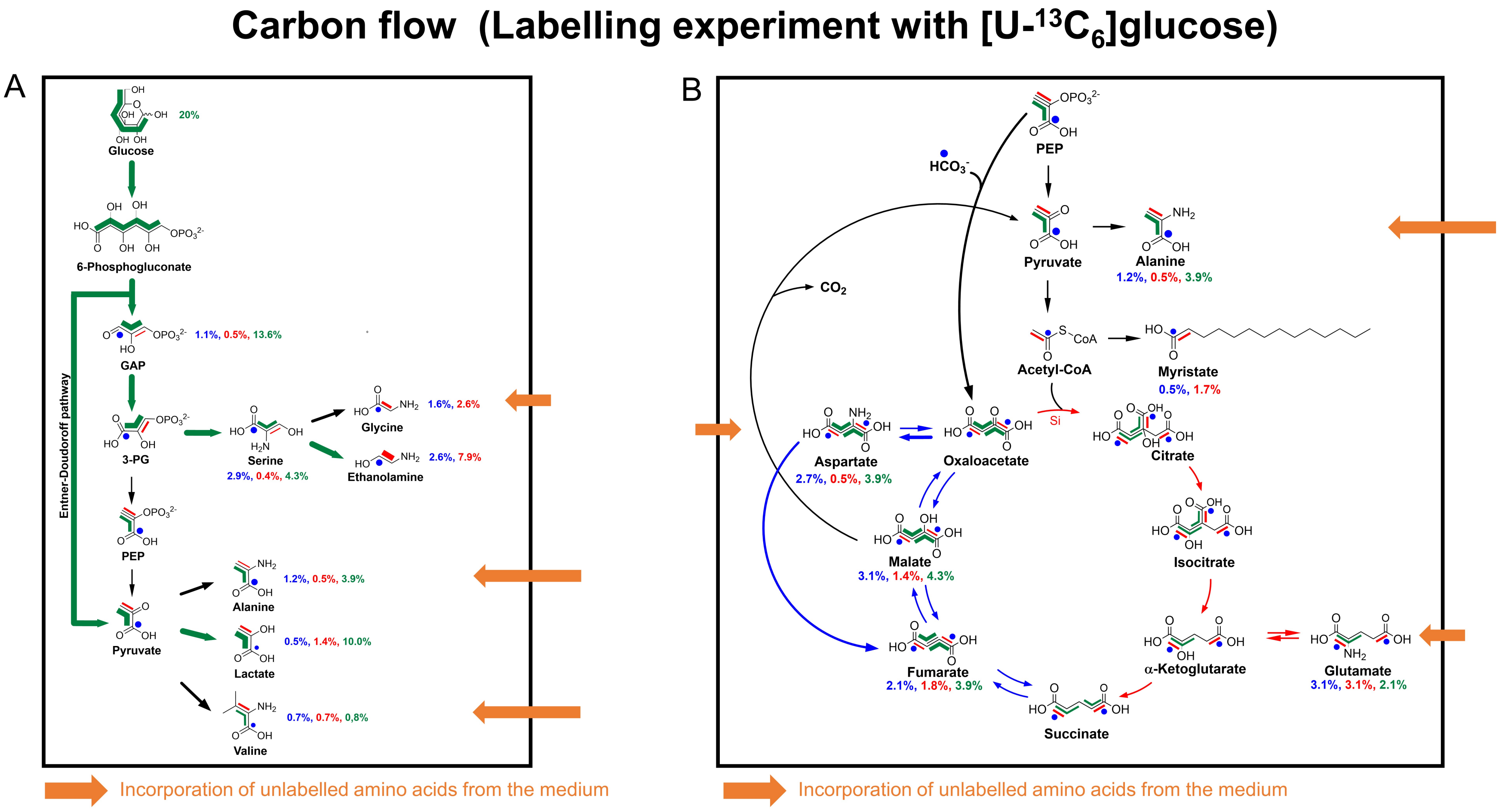

Figure 23: Scheme of the carbon fluxes in the upper part (A) and the lower part (B) of the central carbon metabolism in *N. meningitidis* wildtype based on labelling experiments with 20% [U-$^{13}C_6$]glucose. The incorporation of exogenous substrates *via* transporters is indicated by orange thick arrows; the carbon flux from [U-$^{13}C_6$]glucose *via* the Entner-Doudoroff pathway is indicated by green arrows; the carbon flux *via* the tricarboxylic acid cycle (leading to two labelled carbon atoms) is indicated by red arrows; the carbon flux from hydrogen carbonate (leading to one labelled carbon atom) is indicated by blue arrows. GAP glyceraldehyde-3-phosphate, 3-PG 3-phosphoglycerate, PEP phosphoenolpyruvate.

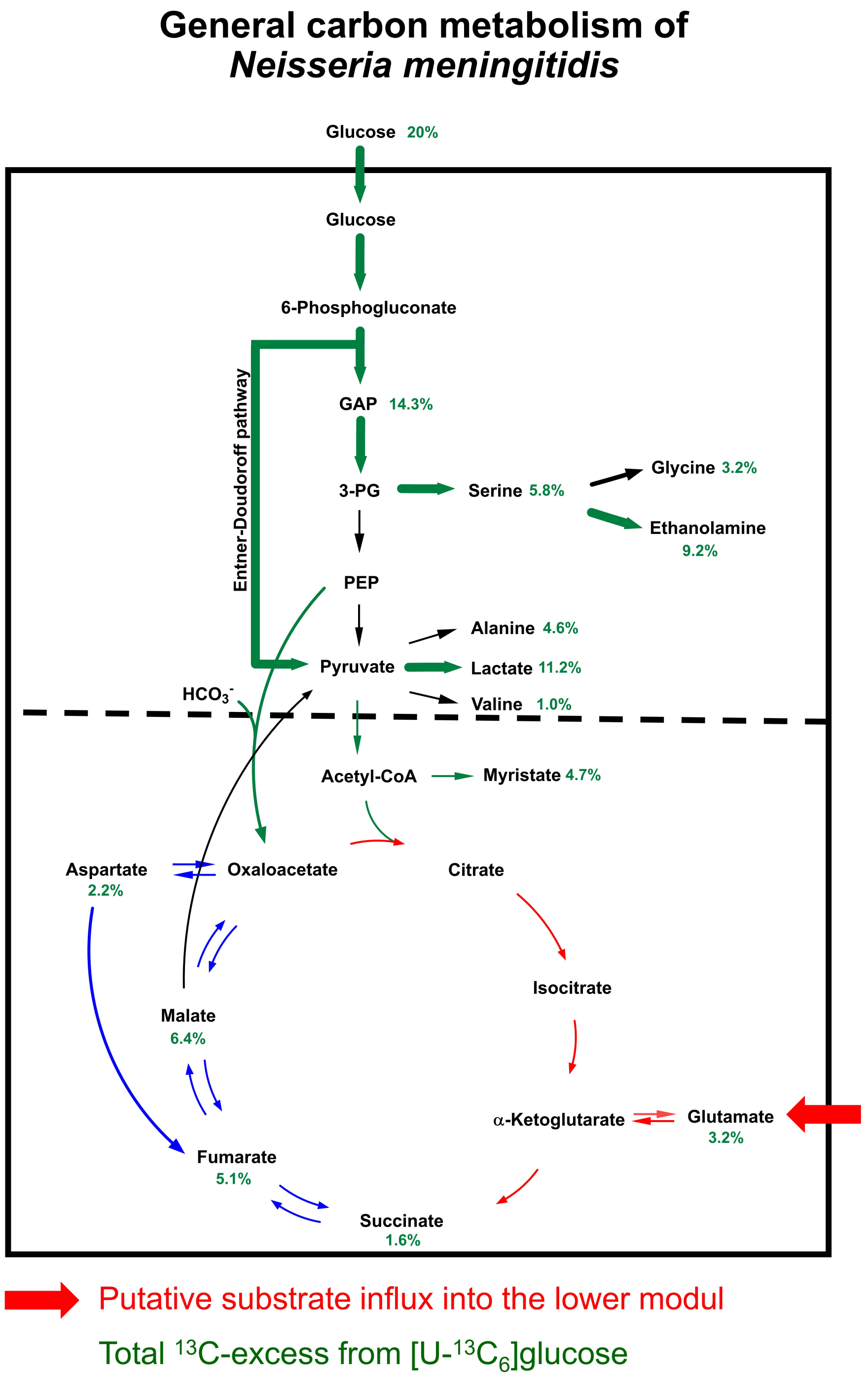

Figure 24: Model for the central carbon metabolism of *N. meningitidis* wildtype based on labelling experiments with 20% [U-$^{13}C_6$]glucose. The import of exogenous substrates *via* transporters into the tricarboxylic acid cycle is indicated by the red thick arrow; the carbon flux from [U-$^{13}C_6$]glucose *via* the Entner-Doudoroff pathway is indicated by green arrows; the carbon flux *via* the tricarboxylic acid cycle (leading to two labelled carbon atoms) is indicated by red arrows; the carbon flux from hydrogen carbonate (leading to one labelled carbon atom) is indicated by blue arrows; the bipartite metabolism is indicated by the black dashed line. The values represented in green display the overall ^{13}C-incorporation in the respective metabolite beyond their natural ^{13}C abundance. GAP glyceraldehyde-3-phosphate, 3-PG 3-phosphoglycerate, PEP phosphoenolpyruvate.

^{15}N-Incorporation in protein-derived amino acids of wildtype (Labelling experiments with $^{15}NH_4Cl$ and ^{15}N-Glutamine)

The protein-derived amino acids showed total ^{15}N-excess values between 3% (lysine) and 19% (alanine, aspartate, mDAP) in the labelling experiment with $^{15}NH_4Cl$ (Figure 25A). In contrast, lower ^{15}N-enrichments between 2% (lysine) and 14% (glutamate) were observed in the labelling experiment with ^{15}N-Glutamine (Figure 25B). The isotopologue profile of alanine (displaying only M+1) as a representative for all protein-derived amino acids with one nitrogen atom as well as the isotopologue distributions of lysine and mDAP with two nitrogen atoms are illustrated in Figure 26. Interestingly, lysine and mDAP showed an isotopologue profile with about 30% M+2 in the labelling experiment with $^{15}NH_4Cl$ (Figure 26A), whereas the M+2 fraction in these metabolites was significant lower (approx. 5%) in the labelling experiment with ^{15}N-Glutamine (Figure 26B).

Comparison of ^{15}N-enrichments in protein- derived amino acids of wildtype, cas9 and scaRNA

By studying the labelling data from $^{15}NH_4Cl$ using a Student's T-test analysis, a significant decrease in the ^{15}N-excess values of the protein-derived amino acids in cas9 could be determined compared to the wildtype, whereas no significant variations in ^{15}N-labelled metabolites of wildtype and scaRNA were observed. Interestingly, the ^{15}N-excess values of glutamate, glycine, isoleucine and leucine of wildtype and cas9 showed no significant differences according to the Student's T-test when ^{15}N-Glutamine was used as tracer, whereas a significant increase in the enrichment of the other amino acids in cas9 in contrast to the wildtype could be observed. Again, the ^{15}N-enrichments of the amino acids in wildtype and scaRNA were in the same order of magnitude (except alanine and mDAP). The differences in the total ^{15}N-enrichments of *N. meningitidis* wildtype and cas9 are schematically demonstrated in Figure 27 (labelling experiment with $^{15}NH_4Cl$) and Figure 28 (labelling experiment with ^{15}N-Glutamine).

Conclusion

Based on the performed labelling experiments, it can be assumed that glutamate could be efficiently taken up or synthesized from ammonium *via* the NADPH-specific glutamate dehydrogenase. These results confirmed the genome-based model of the nitrogen metabolism in *N. meningitidis* (Schoen et al., 2014). Furthermore, the nitrogen assimilation and metabolization seemed to be regulated by cas9 as significant differences in the enrichments could be determined. It can further be concluded that scaRNA had no influence on the nitrogen pathways as no variations could be detected compared to the wildtype. However, further investigations are required to verify these results.

A

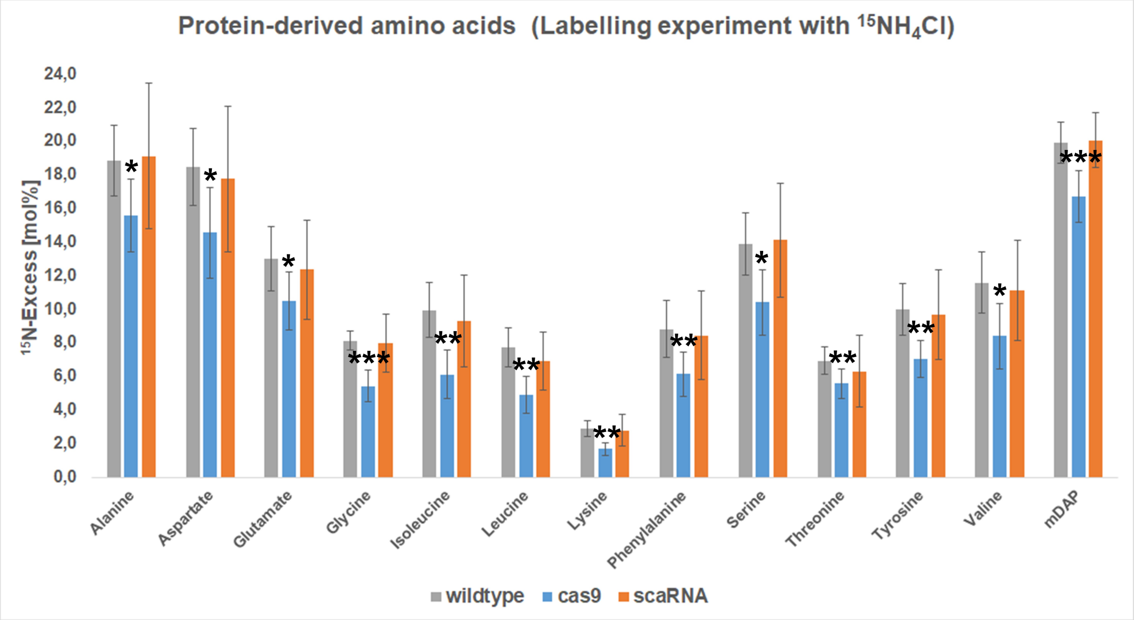

*** $p<0.001$; ** $p<0.01$; * $p<0.05$

B

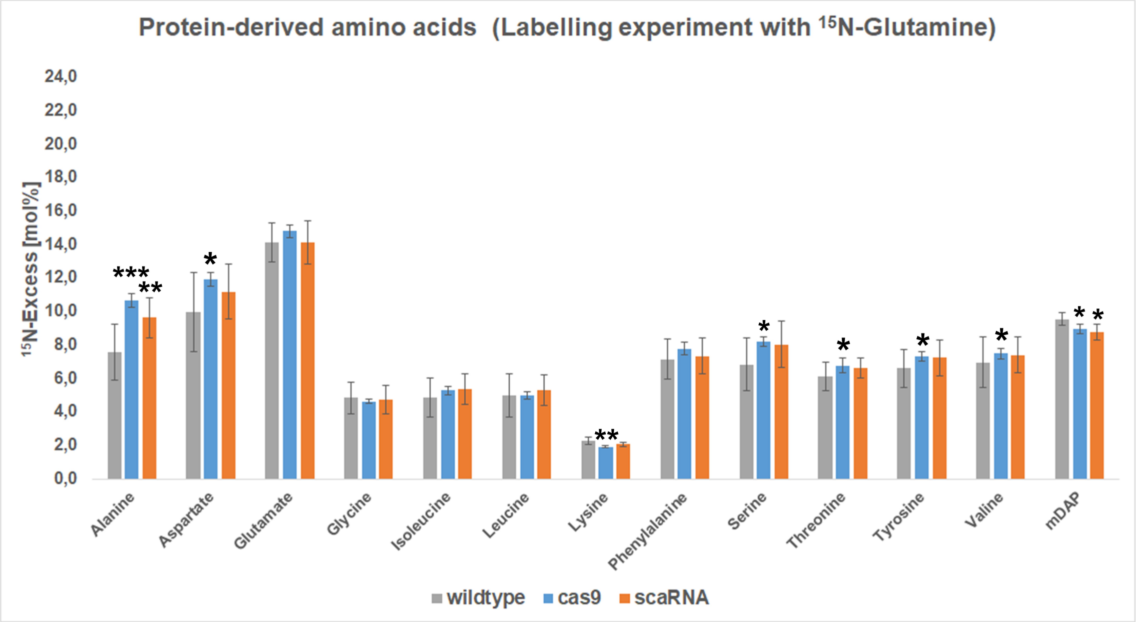

*** $p<0.001$; ** $p<0.01$; * $p<0.05$

Figure 25: ^{15}N-Excess in mol% of protein-derived amino acids from *N. meningitidis* wildtype, cas9 and scaRNA based on labelling experiments with $^{15}NH_4Cl$ (A) and ^{15}N-Glutamine (B). Error bars show the standard deviations from three biological replicates with three technical replicates. Statistical significance was determined using Student's T-test analysis (*** $p<0.001$; ** $p<0.01$; * $p<0.05$).

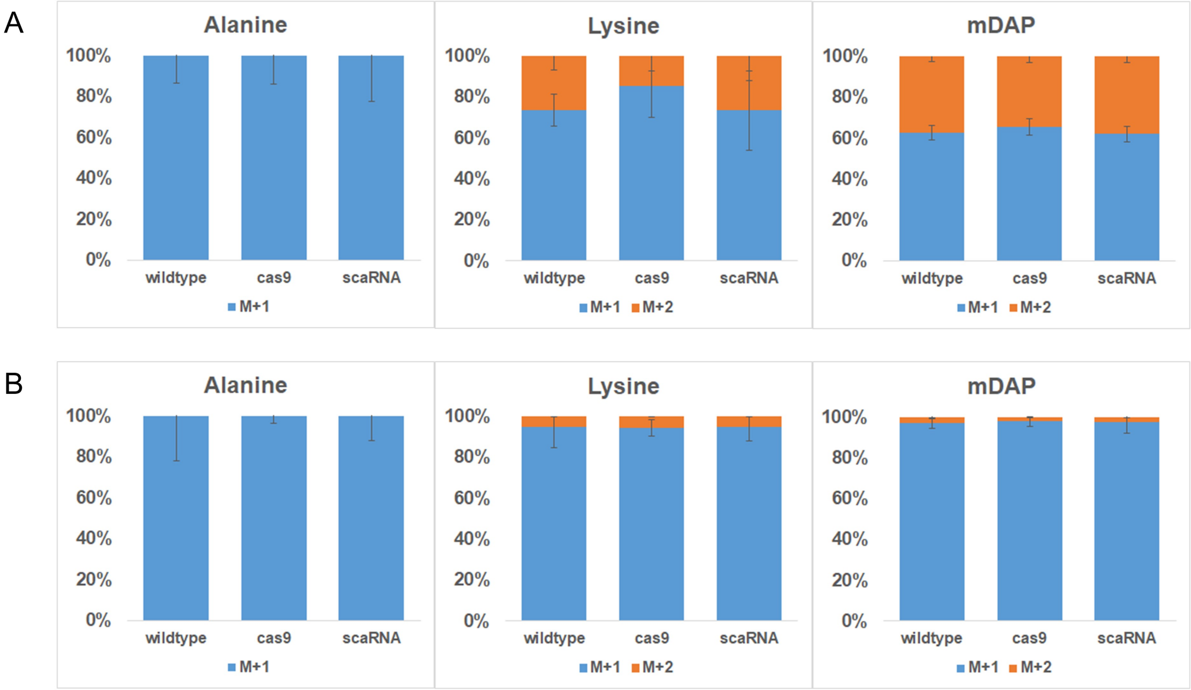

Figure 26: Isotopologue profiles of the protein-derived amino acids alanine, lysine and the cell wall component mDAP from *N. meningitidis* wildtype, cas9 and scaRNA based on labelling experiments with $^{15}NH_4Cl$ (A) and ^{15}N-Glutamine (B). M+X represents the isotopologue profiles with X ^{15}N-atoms incorporated into the protein-derived amino acids. Error bars show the standard deviations from three biological replicates with three technical replicates.

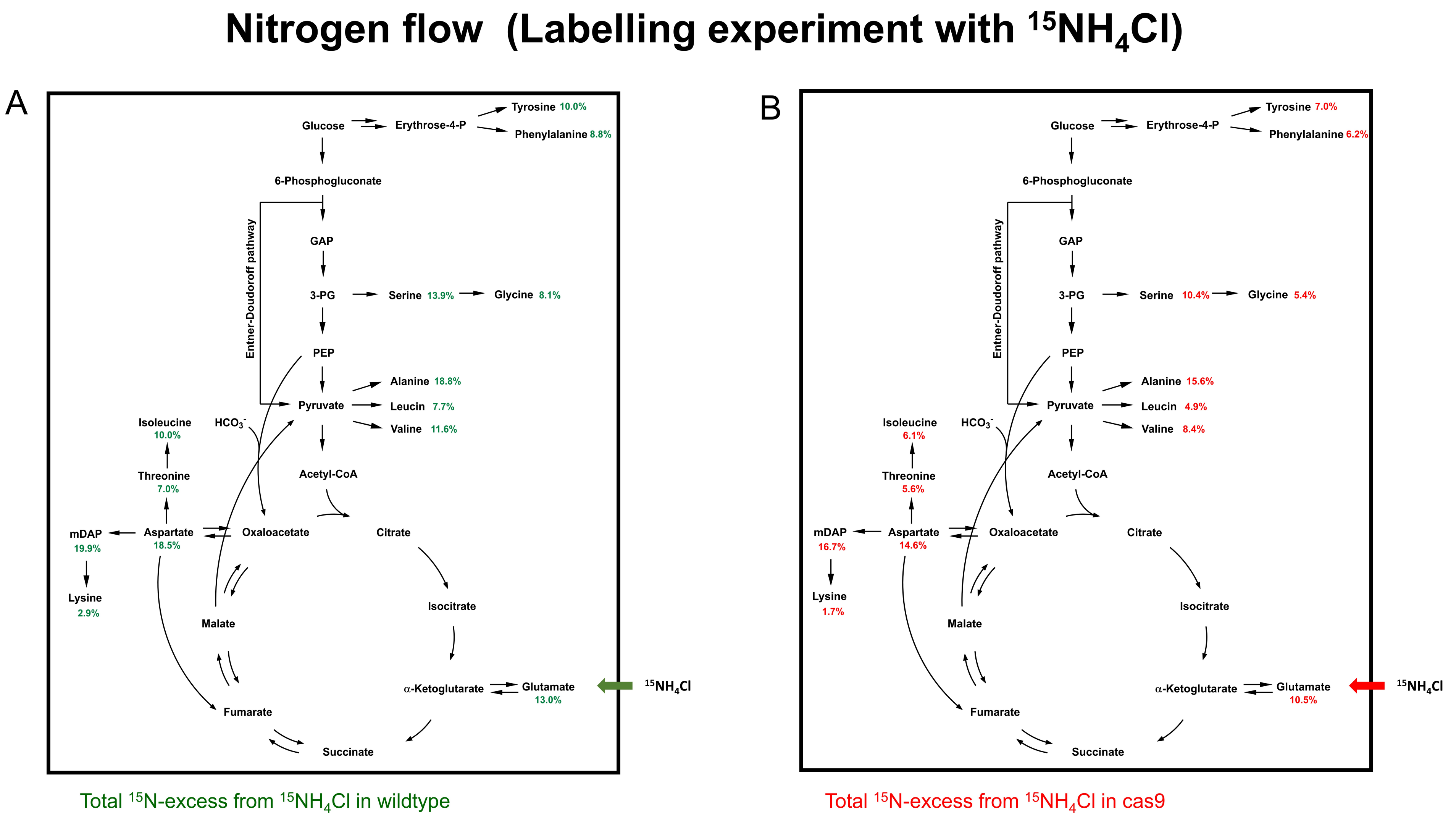

Figure 27: Scheme of the carbon fluxes in the central carbon metabolism of *N. meningitidis* wildtype (A) and cas9 (B) based on labelling experiments with $^{15}NH_4Cl$. GAP glyceraldehyde-3-phosphate, 3-PG 3-phosphoglycerate, PEP phosphoenolpyruvate.

Nitrogen flow (Labelling experiment with ^{15}N-Glutamine)

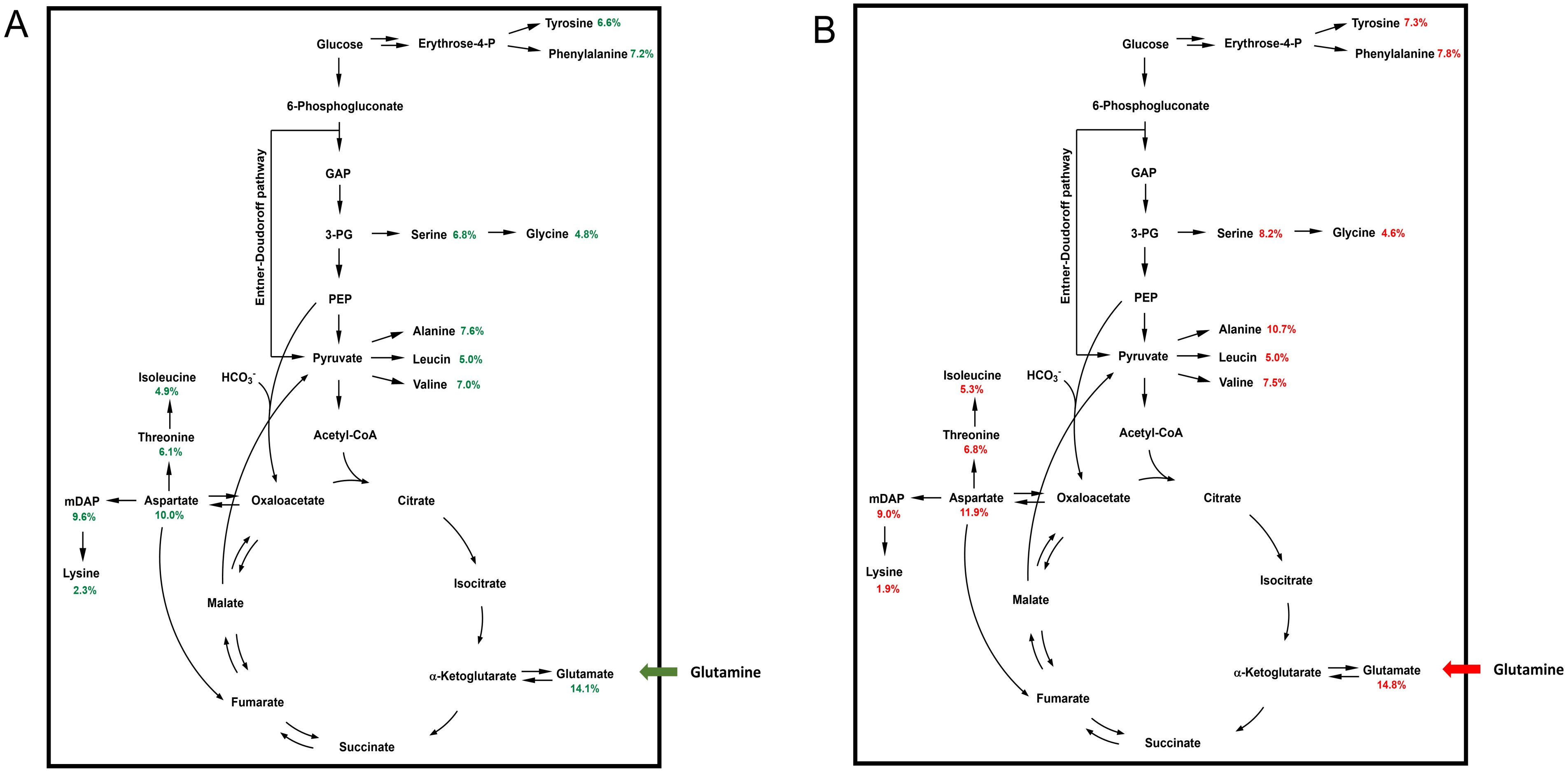

Total ^{15}N-excess from ^{15}N-Glutamine in wildtype

Total ^{15}N-excess from ^{15}N-Glutamine in cas9

Figure 28: Scheme of the carbon fluxes in the central carbon metabolism of *N. meningitidis* wildtype (A) and cas9 (B) based on labelling experiments with ^{15}N-Glutamine. GAP glyceraldehyde-3-phosphate, 3-PG 3-phosphoglycerate, PEP phosphoenolpyruvate.

6.2 The intracellular pathogen *Coxiella burnetii*

The obligate intracellular bacterium *Coxiella burnetii (C. burnetii)* is the causative agent of the Q-fever disease, which was first described by Edward Holbrook Derrick in 1935 (Ullah et al., 2022). *C. burnetii* occurs in various animal species like goats, sheep, cats and dogs and can be transmitted to humans by direct contact, inhalation of polluted air, blood transfusion or consumption of contaminated food products (Celina and Cerný, 2022). An infection with *C. burnetii* can remain asymptomatically, but might also lead to acute or chronic diseases like fever, pneumonia or endocarditis (Knobel et al., 2013). Bacterial infections with this type of pathogen are usually treated with antibiotics like doxycycline, minocycline or clarithromycin (Eldin et al., 2017). Similar to the pathogen *C. trachomatis*, the developmental cycle of *C. burnetii* consists of two infectious morphological forms, the small cell variant (SCV) and the large cell variant (LCV). After binding of the SCV form on the integrin receptor of the host cell, a nascent phagosome fuses with autophagosomes, endosomes and lysosomes leading to formation of a parasitophorous vacuole. In this state, the SCVs differentiate into LCVs, replicate intracellular while using host-derived nutrient sources and reorganize back into SCVs after six days (Dragan and Voth, 2020; Heinzen et al., 1999). Although little is known about the exact metabolism of *C. burnetii*, recent proteomic studies provided detailed informations about the structures and functions of its proteins (Toman et al., 2009). Additionally, an elegant study by Häuslein et al. (2017a) analyzed the highly complex central carbon metabolism of *C. burnetii* by performing labelling experiments with [U-$^{13}C_6$]glucose, [U-$^{13}C_3$]serine and [U-$^{13}C_3$]glycerol. Isotopologue profiling approaches revealed that *C. burnetii* uses multiple substrates in a bipartite metabolic network for its intracellular survival and growth (Häuslein et al., 2017a). Thus, the knowledge of the general metabolic network lays the foundation for the discovery of new therapeutic targets to treat infections with *C. burnetii*. Furthermore, experimental settings demonstrated that itaconate – a derivate produced from cis-aconitate by host cells – inhibits the growth of IBPs like *C. burnetii* (Kohl et al., 2022). However, pathogens (e.g. *Pseudomonas aeruginosa, Yersinia pestis*) have the ability to metabolize itaconate leading to pyruvate and acetyl-CoA in order to guaranty their intracellular survival (Sasikaran et al., 2014).

With a focus on the influence of itaconate on the pathway of *C. burnetii*, the wildtype was grown in ACCM-2 medium for three days at 37°C. T, the samples were incubated for 30 min, 3h and 24h at 37°C after supplementation with [U-$^{13}C_6$]glucose and itaconate. Additionally, a negative control without itaconate (incubation times 30 min, 3h and 24h) was performed. After heat inactivation and lyophilisation of the cell pellets, the protein-derived amino acids, the methanol-soluble polar metabolites and the supernatants were analysed by GC-MS as previously described (section 2.2). In the following, the preliminary results are discussed in more detail.

Determination of [U-$^{13}C_6$]glucose amount in supernatants

By performing GC-MS measurements of the supernatants, [U-$^{13}C_6$]glucose amounts between 8 mg/ml and 10 mg/ml was determined for all time-points (Figure 29). Interestingly, no significant different concentrations in the supernatants of untreated and with itaconate treated cell pellets after 30 min, 3h and 24h could be observed. Therefore, it can be assumed that itaconate had no influence on the uptake of glucose by *C. burnetii*.

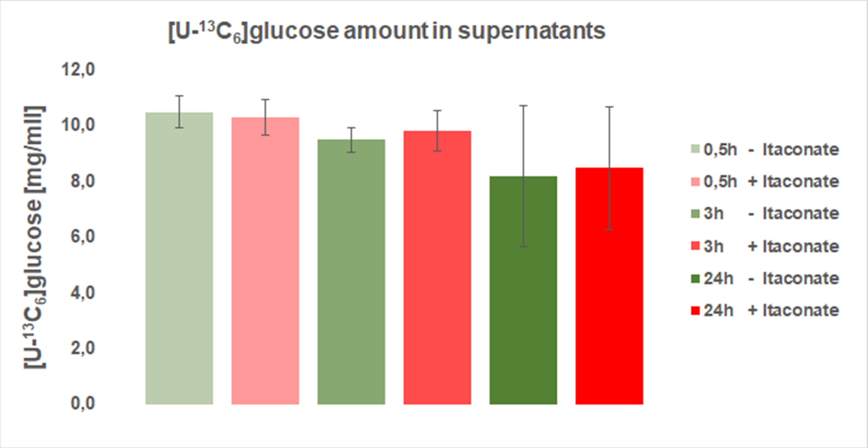

Figure 29: Calculated [U-$^{13}C_6$]glucose amounts [mg/ml] in supernatants of *C. burnetii* wildtype untreated and treated with itaconate after incubation for 30 min, 3h and 24h. Error bars show the standard deviations from three biological replicates with three technical replicates.

Incorporation of ^{13}C in metabolites from [U-$^{13}C_6$]glucose

By performing a time-course experiment (30 min, 3h and 24h) with [U-$^{13}C_6$]glucose, the highest ^{13}C-enrichments (Figure 30) could be determined in the samples after an incubation time of 24h indicating that more labelled glucose was utilized over time. The protein-derived amino acid alanine showed a ^{13}C-excess value of 4.0% in the untreated pellets and a decreased enrichment of 2.5% in the samples treated with itaconate at 24h, whereas no significant differences between untreated and with itaconate treated samples could be detected in this metabolite at 30 min and 3h. Similar effects were observed for the protein-derived amino acids aspartate, glutamate and serine as well as the cell wall component mDAP. Additionally, no significant differences in the isotopologue profiles (Figure 31) between untreated and with itaconate treated samples could be detected. Despite the large standard deviation, the ^{13}C-excess value (5.8%) in the fatty acid myristate of samples, which were previously treated with itaconate, was significant lower than the ^{13}C-enrichment (8.7%) in myristate of untreated samples at 24h. Interestingly, the fatty acid palmitate and the polar metabolite lactate showed similar ^{13}C-excess values (approx. 2%) in untreated and with itaconate treated samples at all time-points.

Influence of itaconate on the metabolic pathway of *C. burnetii*

The differences in the total ^{13}C-enrichments of untreated and with itaconate treated *C. burnetii* wildtype cell pellets after incubation for 24h are schematically demonstrated in Figure 32. Due to the decreased ^{13}C-excess values in the metabolites serine, alanine, myristate, glutamate, aspartate and mDAP of cell pellets treated with itaconate at 24h, it was suggested that itaconate was degraded into pyruvate (the precursor for the synthesis of serine, alanine and mDAP) and acetyl-CoA (the precursor for the synthesis of fatty acids and TCA-intermediates) leading to a dilution resulting in lower ^{13}C-excess values in the metabolites. In contrast, the treatment with itaconate seemed to have no influence on the upper part of the pathway as no significant differences in the amount of ^{13}C-marked lactate between untreated and treated samples could be observed. However, further labelling experiments (e.g. with [U-^{13}C$_5$]itaconic acid) should be performed to examine whether itaconate is efficiently degraded into pyruvate and acetyl-CoA leading to ^{13}C-labelled metabolites or whether itaconate shows inhibitory effects on the lower part of the carbon metabolism in *C. burnetii*.

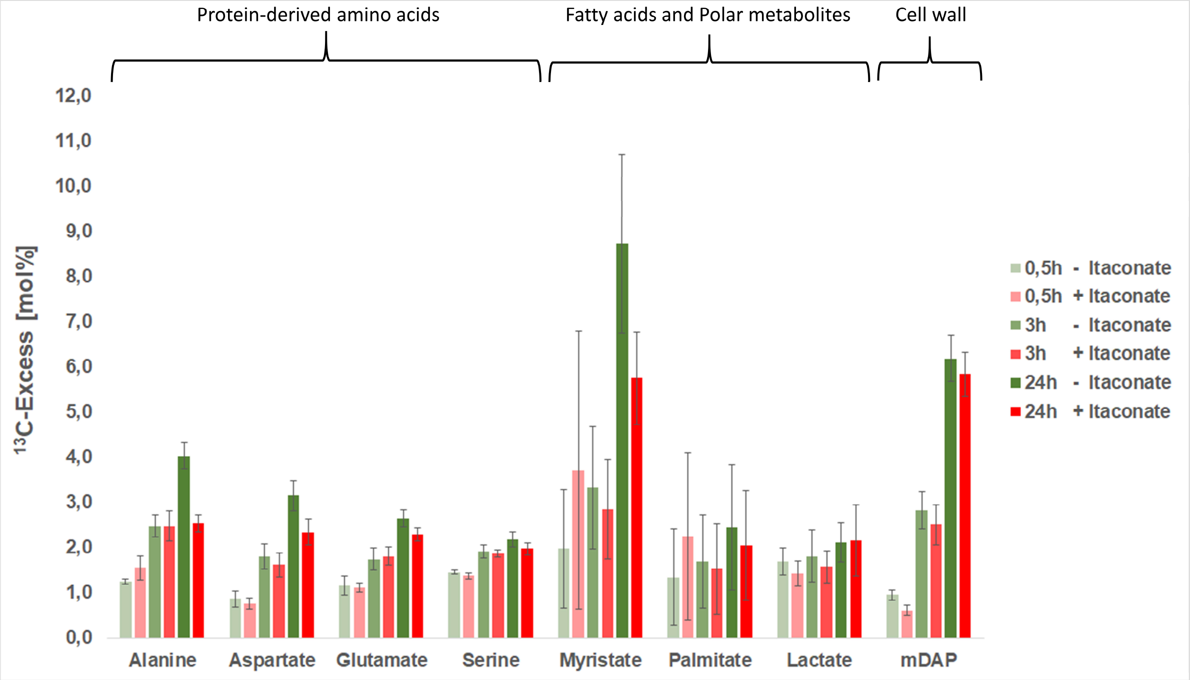

Figure 30: ^{13}C-Excess in mol% of the protein-derived amino acids alanine, aspartate, glutamate and serine, the fatty acids myristate and palmitate, the polar metabolite lactate and the cell wall component mDAP from *C. burnetii* wildtype untreated and treated with itaconate after incubation for 30 min, 3h and 24h based on labelling experiments with [U-^{13}C$_6$]glucose. Error bars show the standard deviations from three biological replicates with three technical replicates.

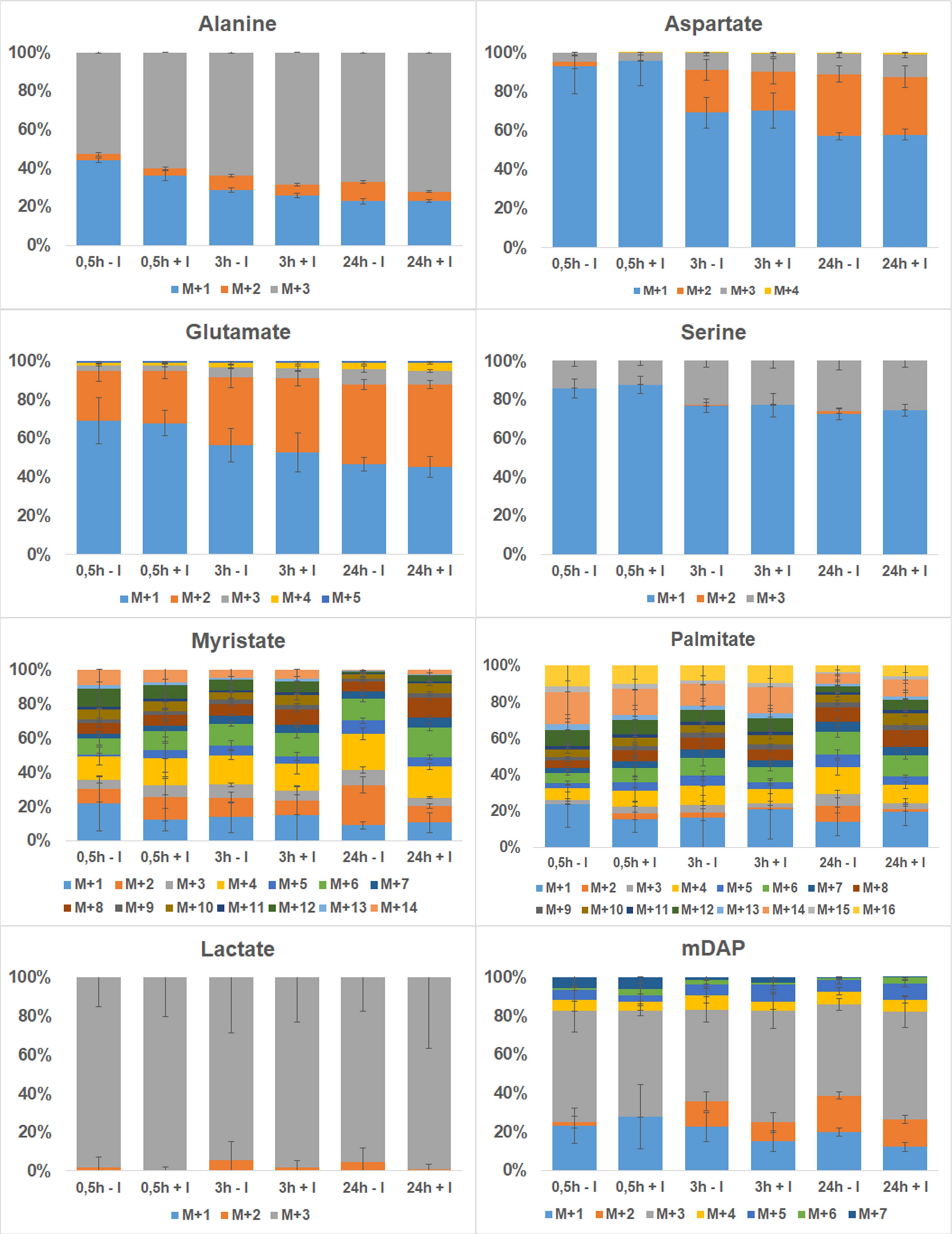

Figure 31: Isotopologue profiles of the amino acids alanine, aspartate, glutamate, serine, the fatty acids myristate and palmitate, the polar metabolite lactate and the cell wall component mDAP from *C. burnetii* wildtype untreated (- I) and treated with itaconate (+ I) after incubation for 30 min, 3h and 24h based on labelling experiments with [U-$^{13}C_6$]glucose. M+X represents the isotopologue profiles with X ^{13}C-atoms incorporated into the metabolites. Error bars show the standard deviations from three biological replicates with three technical replicates.

Carbon flow (Labelling experiment with [U-$^{13}C_6$]glucose)

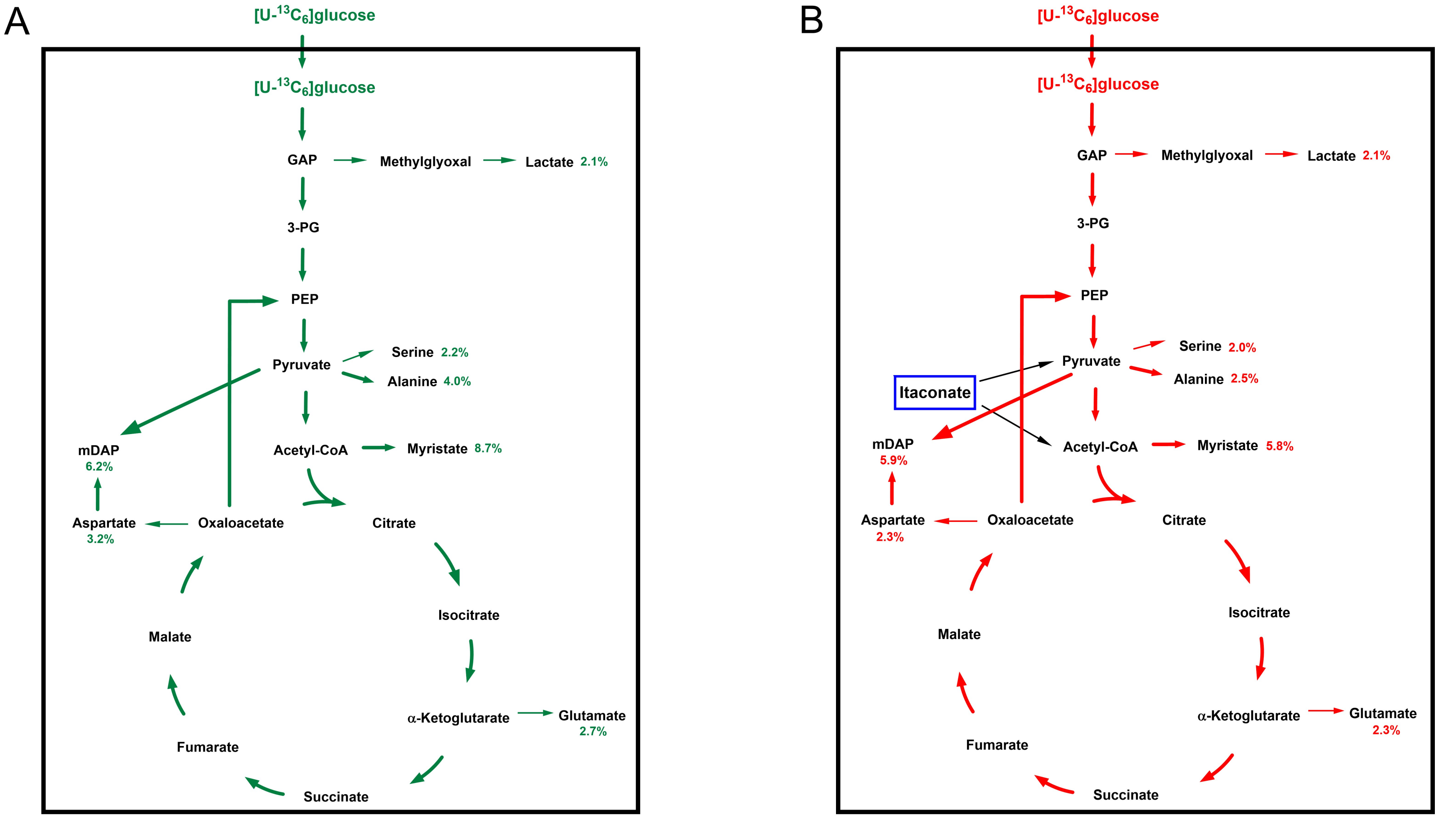

Total ^{13}C-excess from [U-$^{13}C_6$]glucose, 24h, without itaconate

Total ^{13}C-excess from [U-$^{13}C_6$]glucose, 24h, supplemented with itaconate

Figure 32: Scheme of the carbon fluxes in the central carbon metabolism of *C. burnetii* wildtype untreated (A) and treated with itaconate (B) after incubation for 24h based on labelling experiments with [U-$^{13}C_6$]glucose. GAP glyceraldehyde-3-phosphate, 3-PG 3-phosphoglycerate, PEP phosphoenolpyruvate.

7. List of figures

8. References

AbdelRahman, Y. M. and Belland, R. J. (2005). The *chlamydial* developmental cycle. *FEMS Microbiol Rev*, **29**(5), 949-959.

Adjei, J. K., Ahormegah, V., Boateng, A. K., Megbenu, H. K. and Owusu, S. (2020). Fast, easy, cheap, robust and safe method of analysis of Sudan dyes in chilli pepper powder. *Heliyon*, **6**(10), e05243.

Alfarouk, K. O., Ahmed, S. B. M., Elliott, R. L., Benoit, A., Alqahtani, S. S., Ibrahim, M. E., Bashir, A. H. H., Alhoufie, S. T. S., Elhassan, G. O., Wales, C. C., Schwartz, L. H., Ali, H. S., Ahmed, A., Forde, P. F., Devesa, J., Cardone, R. A., Fais, S., Harguindey, S. and Reshkin, S. J. (2020). The pentose phosphate pathway dynamics in cancer and its dependency on intracellular pH. *Metabolites*, **10**(7), 285.

Anderson, J. W., Baird, P., Davis, R. H., Jr., Ferreri, S., Knudtson, M., Koraym, A., Waters, V. and Williams, C. L. (2009). Health benefits of dietary fiber. *Nutr Rev*, **67**(4), 188-205.

Antimicrobial Resistance Collaborators (2022). Global burden of bacterial antimicrobial resistance in 2019: a systematic analysis. *Lancet*, **399**(10325), 629-655.

Antoniewicz, M. R. (2021). A guide to metabolic flux analysis in metabolic engineering: methods, tools and applications. *Metab Eng*, **63**, 2-12.

Arakawa, S., Ishihara, H., Nishio, O. and Isomura, S. (1991). A sandwich enzyme-linked immunosorbent assay for κ-carrageenan determination. *J Sci Food Agric*, **57**(1), 135-140.

Arana, V. A., Medina, J., Alarcon, R., Moreno, E., Heintz, L., Schäfer, H. and Wist, J. (2015). Coffee's country of origin determined by NMR: The Colombian case. *Food Chem*, **175**, 500-506.

Ashour, M. A., Fatima, W., Imran, M., Ghoneim, M. M., Alshehri, S. and Shakeel, F. (2022). A review on the main phytoconstituents, traditional uses, inventions, and patent literature of gum arabic emphasizing *Acacia seyal*. *Molecules*, **27**(4), 1171.

Atri, C., Guerfali, F. Z. and Laouini, D. (2018). Role of human macrophage polarization in inflammation during infectious diseases. *Int J Mol Sci*, **19**(6), 1801.

Aydin, S. (2015). A short history, principles, and types of ELISA, and our laboratory experience with peptide/protein analyses using ELISA. *Peptides*, **72**, 4-15.

Baart, G. J., Zomer, B., de Haan, A., van der Pol, L. A., Beuvery, E. C., Tramper, J. and Martens, D. E. (2007). Modeling *Neisseria meningitidis* metabolism: from genome to metabolic fluxes. *Genome Biol*, **8**(7), R136.

Barak, S. and Mudgil, D. (2014). Locust bean gum: processing, properties and food applications - a review. *Int J Biol Macromol*, **66**, 74-80.

Barak, S., Mudgil, D. and Taneja, S. (2020). Exudate gums: chemistry, properties and food applications – a review. *J Sci Food Agric*, **100**(7), 2828-2835.

Barding, G. A., Jr., Salditos, R. and Larive, C. K. (2012). Quantitative NMR for bioanalysis and metabolomics. *Anal Bioanal Chem*, **404**(4), 1165-1179.

REFERENCES

Barnes, R. C. (1989). Laboratory diagnosis of human *chlamydial* infections. *Clin Microbiol Rev*, **2**(2), 119-136.

Barreteau, H., Kovač, A., Boniface, A., Sova, M., Gobec, S. and Blanot, D. (2008). Cytoplasmic steps of peptidoglycan biosynthesis. *FEMS Microbiol Rev*, **32**(2), 168-207.

Barrile, R., Kasendra, M., Rossi-Paccani, S., Merola, M., Pizza, M., Baldari, C., Soriani, M. and Aricò, B. (2015). *Neisseria meningitidis* subverts the polarized organization and intracellular trafficking of host cells to cross the epithelial barrier. *Cell Microbiol*, **17**(9), 1365-1375.

Bastidas, R. J., Elwell, C. A., Engel, J. N. and Valdivia, R. H. (2013). *Chlamydial* intracellular survival strategies. *Cold Spring Harb Perspect Med*, **3**(5), a010256.

Batista, R. S., Gomes, A. P., Dutra Gazineo, J. L., Balbino Miguel, P. S., Santana, L. A., Oliveira, L. and Geller, M. (2017). Meningococcal disease, a clinical and epidemiological review. *Asian Pac J Trop Med*, **10**(11), 1019-1029.

Beger, R. D. (2013). A review of applications of metabolomics in cancer. *Metabolites*, **3**(3), 552-574.

Bertani, B. and Ruiz, N. (2018). Function and biogenesis of lipopolysaccharides. *EcoSal Plus*, **8**(1), 10.1128.

Bhattacharyya, S., O-Sullivan, I., Katyal, S., Unterman, T. and Tobacman, J. K. (2012). Exposure to the common food additive carrageenan leads to glucose intolerance, insulin resistance and inhibition of insulin signalling in HepG2 cells and C57BL/6J mice. *Diabetologia*, **55**(1), 194-203.

Blanco-Pérez, F., Steigerwald, H., Schülke, S., Vieths, S., Toda, M. and Scheurer, S. (2021). The dietary fiber pectin: health benefits and potential for the treatment of allergies by modulation of gut microbiota. *Curr Allergy Asthma Rep*, **21**(10), 43.

Błaszak, B., Gozdecka, G. and Shyichuk, A. (2018). Carrageenan as a functional additive in the production of cheese and cheese-like products. *Acta Sci Pol Technol Aliment*, **17**(2), 107-116.

Borsani, B., De Santis, R., Perico, V., Penagini, F., Pendezza, E., Dilillo, D., Bosetti, A., Zuccotti, G. V. and D'Auria, E. (2021). The role of carrageenan in inflammatory bowel diseases and allergic reactions: where do we stand? *Nutrients*, **13**(10), 3402.

Brigham, K. S. and Sandora, T. J. (2009). *Neisseria meningitidis*: epidemiology, treatment and prevention in adolescents. *Curr Opin Pediatr*, **21**(4), 437-443.

Bush, K. and Macielag, M. (2000). New approaches in the treatment of bacterial infections. *Curr Opin Chem Biol*, **4**(4), 433-439.

Carocho, M., Barreiro, M. F., Morales, P. and Ferreira, I. C. F. R. (2014). Adding molecules to food, pros and cons: a review on synthetic and natural food additives. *Compr Rev Food Sci Food Saf*, **13**(4), 377-399.

Castoldi, A., Naffah de Souza, C., Câmara, N. O. and Moraes-Vieira, P. M. (2015). The macrophage switch in obesity development. *Front Immunol*, **6**, 637.

REFERENCES

Cecchini, M. and Warin, L. (2016). Impact of food labelling systems on food choices and eating behaviours: a systematic review and meta-analysis of randomized studies. *Obes Rev*, **17**(3), 201-210.

Celina, S. S. and Cerný, J. (2022). *Coxiella burnetii* in ticks, livestock, pets and wildlife: A mini-review. *Front Vet Sci*, **9**, 1068129.

Cena, H. and Calder, P. C. (2020). Defining a healthy diet: evidence for the role of contemporary dietary patterns in health and disease. *Nutrients*, **12**(2), 334.

Chamberlain, N. B., Dimond, Z. and Hackstadt, T. (2022). *Chlamydia trachomatis* suppresses host cell store-operated Ca^{2+} entry and inhibits NFAT/calcineurin signaling. *Sci Rep*, **12**(1), 21406.

Chan, S. Y., Choo, W. S., Young, D. J. and Loh, X. J. (2017). Pectin as a rheology modifier: origin, structure, commercial production and rheology. *Carbohydr Polym*, **161**, 118-139.

Chauhan, P. S. and Saxena, A. (2016). Bacterial carrageenases: an overview of production and biotechnological applications. *3 Biotech*, **6**(2), 146.

Chazelas, E., Deschasaux, M., Srour, B., Kesse-Guyot, E., Julia, C., Alles, B., Druesne-Pecollo, N., Galan, P., Hercberg, S., Latino-Martel, P., Esseddik, Y., Szabo, F., Slamich, P., Gigandet, S. and Touvier, M. (2020). Food additives: distribution and co-occurrence in 126,000 food products of the French market. *Sci Rep*, **10**(1), 3980.

Chen, J., Liu, W., Liu, C. M., Li, T., Liang, R. H. and Luo, S. J. (2015). Pectin modifications: a review. *Crit Rev Food Sci Nutr*, **55**(12), 1684-1698.

Churms, S. C., Merrifield, E. H. and Stephen, A. M. (1983). Some new aspects of the molecular structure of *Acacia senegal* gum (gum arabic). *Carbohydr Res*, **123**(2), 267-279.

Cichero, J. A. (2013). Thickening agents used for dysphagia management: effect on bioavailability of water, medication and feelings of satiety. *Nutr J*, **12**, 54.

Cipolla, L., Gabrielli, L., Bini, D., Russo, L. and Shaikh, N. (2010). Kdo: a critical monosaccharide for bacteria viability. *Nat Prod Rep*, **27**(11), 1618-1629.

Clegg, M. E. and Shafat, A. (2014). The effect of agar jelly on energy expenditure, appetite, gastric emptying and glycaemic response. *Eur J Nutr*, **53**(2), 533-539.

Clendinen, C. S., Stupp, G. S., Ajredini, R., Lee-McMullen, B., Beecher, C. and Edison, A. S. (2015). An overview of methods using ^{13}C for improved compound identification in metabolomics and natural products. *Front Plant Sci*, **6**, 611.

Commission Regulation (EU) No 231/2012 of 9 March 2012 laying down specifications for food additives listed in Annexes II and III to Regulation (EC) No 1333/2008 of the European Parliament and of the Council

Corsaro, D. and Venditti, D. (2004). Emerging *chlamydial* infections. *Crit Rev Microbiol*, **30**(2), 75-106.

Cox, J. V., Abdelrahman, Y. M., Peters, J., Naher, N. and Belland, R. J. (2016). *Chlamydia trachomatis* utilizes the mammalian CLA1 lipid transporter to acquire host phosphatidylcholine essential for growth. *Cell Microbiol*, **18**(3), 305-318.

REFERENCES

Cox, S., Sandall, A., Smith, L., Rossi, M. and Whelan, K. (2021). Food additive emulsifiers: a review of their role in foods, legislation and classifications, presence in food supply, dietary exposure, and safety assessment. *Nutr Rev*, **79**(6), 726-741.

Crook, A. A. and Powers, R. (2020). Quantitative NMR-based biomedical metabolomics: current status and applications. *Molecules*, **25**(21), 5128.

Csáki, K. F. (2011). Synthetic surfactant food additives can cause intestinal barrier dysfunction. *Med Hypothese*, **76**(5), 676-681.

Czarnecka, K., Pilarz, A., Rogut, A., Maj, P., Szymańska, J., Olejnik, Ł. and Szymański, P. (2021). Aspartame - true or false? Narrative review of safety analysis of general use in products. *Nutrients*, **13**(6), 1957.

de Falco, B., Giannino, F., Carteni, F., Mazzoleni, S. and Kim, D.-H. (2022). Metabolic flux analysis: a comprehensive review on sample preparation, analytical techniques, data analysis, computational modelling, and main application areas. *RSC Advances*, **12**(39), 25528-25548.

Di Lorenzo, F., Duda, K. A., Lanzetta, R., Silipo, A., De Castro, C. and Molinaro, A. (2022). A journey from structure to function of bacterial lipopolysaccharides. *Chem Rev*, **122**(20), 15767-15821.

Dionísio, M. and Grenha, A. (2012). Locust bean gum: exploring its potential for biopharmaceutical applications. *J Pharm Bioallied Sci*, **4**(3), 175-185.

Doron, S. and Gorbach, S. L. (2008). Bacterial infections: overview. In *International Encyclopedia of Public Health*, 273-282.

Dragan, A. L. and Voth, D. E. (2020). *Coxiella burnetii:* international pathogen of mystery. *Microbes Infect*, **22**(3), 100-110.

du Preez, R., Paul, N., Mouatt, P., Majzoub, M. E., Thomas, T., Panchal, S. K. and Brown, L. (2020). Carrageenans from the red seaweed *Sarconema filiforme* attenuate symptoms of diet-induced metabolic syndrome in rats. *Mar Drugs*, **18**(2), 97.

Duvallet, S., Fenyo, J. C. and Vandevelde, M. C. (1989). Meaning of molecular weight measurements of gum arabic. *Polym Bull*, **21**(5), 517-521.

Eisenreich, W., Rudel, T., Heesemann, J. r. and Goebel, W. (2017). To eat and to be eaten: mutual metabolic adaptations of immune cells and intracellular bacterial pathogens upon infection. *Front Cell Infect Microbiol*, **7**, 316.

Eisenreich, W., Rudel, T., Heesemann, J. and Goebel, W. (2019). How viral and intracellular bacterial pathogens reprogram the metabolism of host cells to allow their intracellular replication. *Front Cell Infect Microbiol*, **9**, 42.

Eisenreich, W., Rudel, T., Heesemann, J. and Goebel, W. (2020). Persistence of intracellular bacterial pathogens - with a focus on the metabolic perspective. *Front Cell Infect Microbiol*, **10**, 615450.

Eisenreich, W., Rudel, T., Heesemann, J. and Goebel, W. (2022). Link between antibiotic persistence and antibiotic resistance in bacterial pathogens. *Front Cell Infect Microbiol*, **12**, 900848.

Eldin, C., Mélenotte, C., Mediannikov, O., Ghigo, E., Million, M., Edouard, S., Mege, J. L., Maurin, M. and Raoult, D. (2017). From Q fever to *Coxiella burnetii* infection: a paradigm change. *Clin Microbiol Rev*, **30**(1), 115-190.

Ende, R. J. and Derré, I. (2020). Host and bacterial glycolysis during *Chlamydia trachomatis* infection. *Infect Immun*, **88**(12), e00545.

Ernst, R. R. (1992). Nuclear magnetic resonance fourier transform spectroscopy (Nobel lecture). *Angew Chem Int Ed Engl*, **31**(7), 805-823.

Fadel, S. and Eley, A. (2008). Is lipopolysaccharide a factor in infectivity of *Chlamydia trachomatis*? *J Med Microbiol*, **57**(Pt 3), 261-266.

Ferguson, L. E., Hormann, M. D., Parks, D. K. and Yetman, R. J. (2002). *Neisseria meningitidis*: presentation, treatment, and prevention. *J Pediatr Health Care*, **16**(3), 119-124.

Fiehn, O. (2016). Metabolomics by gas chromatography-mass spectrometry: combined targeted and untargeted profiling. *Curr Protoc Mol Biol*, **114**, 30.34.31-30.34.32.

Fisher, D. J., Fernández, R. E. and Maurelli, A. T. (2013). *Chlamydia trachomatis* transports NAD via the Npt1 ATP/ADP translocase. *J Bacteriol*, **195**(15), 3381-3386.

Fonovich, T. M. (2013). Sudan dyes: are they dangerous for human health? *Drug Chem Toxicol*, **36**(3), 343-352.

Frediansyah, A. (2021). The antiviral activity of iota-, kappa-, and lambda-carrageenan against COVID-19: A critical review. *Clin Epidemiol Glob Health*, **12**, 100826.

Freitas, C. M. P., Coimbra, J. S. R., Souza, V. G. L. and Sousa, R. C. S. (2021). Structure and applications of pectin in food, biomedical, and pharmaceutical industry: A review. *Coatings*, **11**(8), 922.

Fukuda, E. Y., Lad, S. P., Mikolon, D. P., Iacobelli-Martinez, M. and Li, E. (2005). Activation of lipid metabolism contributes to interleukin-8 production during *Chlamydia trachomatis* infection of cervical epithelial cells. *Infect Immun*, **73**(7), 4017-4024.

Gaborieau, M. and Castignolles, P. (2011). Size-exclusion chromatography (SEC) of branched polymers and polysaccharides. *Anal Bioanal Chem*, **399**(4), 1413-1423.

Gallina, A., Fiorese, E., Pastore, P. and Magno, F. (2004). Identification and semi-quantitative determination of gum arabic in wines by GC-MS and size exclusion chromatography. *Ann Chim*, **94**(3), 177-184.

Genualdi, S., MacMahon, S., Robbins, K., Farris, S., Shyong, N. and DeJager, L. (2016). Method development and survey of sudan I-IV in palm oil and chilli spices in the Washington, DC, area. *Food Addit Contam Part A Chem Anal Control Expo Risk Assess*, **33**(4), 583-591.

Gerothanassis, I. P., Troganis, A., Exarchou, V. and Barbarossou, K. (2002). Nuclear magnetic resonance (NMR) spectroscopy: basic principles and phenomena, and their applications to chemistry, bioloy and medicine. *Chem Educ Res Pract*, **3**(2), 229-252.

Girond, S., Crance, J. M., Van Cuyck-Gandre, H., Renaudet, J. and Deloince, R. (1991). Antiviral activity of carrageenan on hepatitis A virus replication in cell culture. *Res Virol*, **142**(4), 261-270.

Gitsels, A., Sanders, N. and Vanrompay, D. (2019). *Chlamydial* infection from outside to inside. *Front Microbiol*, **10**, 2329.

Glück, U. and Thier, H.-P. (1980). Quantitative Bestimmung einiger Dickungsmittel in Milchprodukten. *Z Lebensm Unters Forsch*, **170**(4), 272-279.

Godelmann, R., Fang, F., Humpfer, E., Schütz, B., Bansbach, M., Schäfer, H. and Spraul, M. (2013). Targeted and nontargeted wine analysis by ^{1}H NMR spectroscopy combined with multivariate statistical analysis. Differentiation of important parameters: grape variety, geographical origin, year of vintage. *J Agric Food Chem*, **61**(23), 5610-5619.

Gómez Barrio, L. P., Cabral, E. M., Zhao, M., Álvarez García, C., Senthamaraikannan, R., Padamati, R. B., Tiwari, U., Curtin, J. F. and Tiwari, B. K. (2022). Comparison study of an optimized ultrasound-based method versus an optimized conventional method for agar extraction, and protein co-extraction, from *Gelidium sesquipedale*. *Foods*, **11**(6), 805.

Gostan, T., Moreau, C., Juteau, A., Guichard, E. and Delsuc, M. A. (2004). Measurement of aroma compound self-diffusion in food models by DOSY. *Magn Reson Chem*, **42**(6), 496-499.

Gottstein, V., Müller, M., Günther, J., Kuballa, T. and Vetter, W. (2019). Direct ^{1}H NMR quantitation of valuable furan fatty acids in fish oils and fish oil fractions. *J Agric Food Chem*, **67**(42), 11788-11795.

Gronow, S. and Brade, H. (2001). Lipopolysaccharide biosynthesis: which steps do bacteria need to survive? *J Endotoxin Res*, **7**(1), 3-23.

Grün, C. H., Sanders, P., van der Burg, M., Schuurbiers, E., van Adrichem, L., van Velzen, E. J. J., de Roo, N., Brunt, K., Westphal, Y. and Schols, H. A. (2015). Strategy to identify and quantify polysaccharide gums in gelled food concentrates. *Food Chem*, **166**, 42-49.

Gu, Y., Cheong, K.-L. and Du, H. (2017). Modification and comparison of three *Gracilaria* spp. agarose with methylation for promotion of its gelling properties. *Chem Cent J*, **11**(1), 104.

Haines, J. and Patel, P. D. (1997). Antibody- and lectin- based assays for the rapid analysis of food-grade gums and thickeners. *Trends Food Sci Technol*, **8**(12), 395-400.

Hammerschlag, M. R. (2004). *Chlamydia trachomatis* and *Chlamydia pneumoniae* infections in children and adolescents. *Pediatr Rev*, **25**(2), 43-51.

Hassan, R. A., Heng, L. Y. and Tan, L. L. (2019). Novel DNA biosensor for direct determination of carrageenan. *Sci Rep*, **9**(1), 6379.

Hassan, S. S. M., Meyerhoff, M. E., Badr, I. H. A. and Abd-Rabboh, H. S. M. (2002). Determination of carrageenan in food products using potentiometric polyion sensors. *Electroanalysis*, **14**(6), 439-444.

Hassoun, A., Måge, I., Schmidt, W. F., Temiz, H. T., Li, L., Kim, H.-Y., Nilsen, H., Biancolillo, A., Aït-Kaddour, A., Sikorski, M., Sikorska, E., Grassi, S. and Cozzolino, D. (2020). Fraud in animal origin food products: advances in emerging spectroscopic detection methods over the past five years. *Foods*, **9**(8), 1069.

Hatch, G. M. and McClarty, G. (1998). Phospholipid composition of purified *Chlamydia trachomatis* mimics that of the eucaryotic host cell. *Infect Immun*, **66**(8), 3727-3735.

Häuslein, I., Cantet, F., Reschke, S., Chen, F., Bonazzi, M. and Eisenreich, W. (2017a). Multiple substrate usage of *Coxiella burnetii* to feed a bipartite metabolic network. *Front Cell Infect Microbiol*, **7**, 285.

Häuslein, I., Sahr, T., Escoll, P., Klausner, N., Eisenreich, W. and Buchrieser, C. (2017b). *Legionella pneumophila* CsrA regulates a metabolic switch from amino acid to glycerolipid metabolism. *Open Biol*, **7**(11), 170149.

Heidrich, N., Hagmann, A., Bauriedl, S., Vogel, J. and Schoen, C. (2019). The CRISPR/Cas system in *Neisseria meningitidis* affects bacterial adhesion to human nasopharyngeal epithelial cells. *RNA Biol*, **16**(4), 390-396.

Heinzen, R. A., Hackstadt, T. and Samuel, J. E. (1999). Developmental biology of *Coxiella burnettii*. *Trends Microbiol*, **7**(4), 149-154.

Hellerstein, M. K. and Neese, R. A. (1999). Mass isotopomer distribution analysis at eight years: theoretical, analytic, and experimental considerations. *Am J Physiol*, **276**(6), E1146-1170.

Herweg, J. A. and Rudel, T. (2016). Interaction of *Chlamydiae* with human macrophages. *Febs j*, **283**(4), 608-618.

Hill, D. J., Griffiths, N. J., Borodina, E. and Virji, M. (2010). Cellular and molecular biology of *Neisseria meningitidis* colonization and invasive disease. *Clin Sci (Lond)*, **118**(9), 547-564.

Hilliou, L. (2021). Structure-elastic properties relationships in gelling carrageenans. *Polymers*, **13**(23), 4120.

Himashree, P., Sengar, A. S. and Sunil, C. K. (2022). Food thickening agents: sources, chemistry, properties and applications - a review. *Int J Gastron Food Sci*, **27**, 100468.

Hong, E., Lee, S. Y., Jeong, J. Y., Park, J. M., Kim, B. H., Kwon, K. and Chun, H. S. (2017). Modern analytical methods for the detection of food fraud and adulteration by food category. *J Sci Food Agric*, **97**(12), 3877-3896.

Hood, C. M., Gennuso, K. P., Swain, G. R. and Catlin, B. B. (2016). County health rankings: relationships between determinant factors and health outcomes. *Am J Prev Med*, **50**(2), 129-135.

Iliffe-Lee, E. R. and McClarty, G. (1999). Glucose metabolism in *Chlamydia trachomatis*: the 'energy parasite' hypothesis revisited. *Mol Microbiol*, **33**(1), 177-187.

Jaki, B. U., Bzhelyansky, A. and Pauli, G. F. (2021). Quantitative NMR (qNMR) for pharmaceutical analysis: the pioneering work of George Hanna at the US FDA. *Magn Reson Chem*, **59**(1), 7-15.

Jarrar, A. H., Stojanovska, L., Apostolopoulos, V., Feehan, J., Bataineh, M. F., Ismail, L. C. and Al Dhaheri, A. S. (2021). The effect of gum arabic (*Acacia senegal*) on cardiovascular risk factors and gastrointestinal symptoms in adults at risk of metabolic syndrome: a randomized clinical trial. *Nutrients*, **13**(1), 194.

Johnson, C. (1999). Diffusion ordered nuclear magnetic resonance spectroscopy: principles and applications. *Prog Nucl Magn Reson Spectrosc*, **34**, 203-256.

Jones, R. B. (1991). New treatments for *Chlamydia trachomatis*. *Am J Obstet Gynecol*, **164**(6), 1789-1793.

Kaplan, R. M. and Ries, A. L. (2007). Quality of life: concept and definition. *COPD: J Chronic Obstr Pulm Dis*, **4**(3), 263-271.

Keymer, A., Huber, C., Eisenreich, W. and Gutjahr, C. (2018). Tracking lipid transfer by fatty acid isotopolog profiling from host plants to *Arbuscular Mycorrhiza Fungi*. *Bio-protocol*, **8**(7), e2786.

Kind, T., Tsugawa, H., Cajka, T., Ma, Y., Lai, Z., Mehta, S. S., Wohlgemuth, G., Barupal, D. K., Showalter, M. R., Arita, M. and Fiehn, O. (2018). Identification of small molecules using accurate mass MS/MS search. *Mass Spectrom Rev*, **37**(4), 513-532.

Knobel, D. L., Maina, A. N., Cutler, S. J., Ogola, E., Feikin, D. R., Junghae, M., Halliday, J. E. B., Richards, A. L., Breiman, R. F., Cleaveland, S. and Njenga, M. K. (2013). *Coxiella burnetii* in humans, domestic ruminants, and ticks in rural western Kenya. *Am J Trop Med Hyg*, **88**(3), 513-518.

Kohanski, M. A., Dwyer, D. J. and Collins, J. J. (2010). How antibiotics kill bacteria: from targets to networks. *Nat Rev Microbiol*, **8**(6), 423-435.

Kohl, L., Siddique, M., Bodendorfer, B., Berger, R., Preikschat, A., Daniel, C., Ölke, M., Liebler-Tenorio, E., Schulze-Luehrmann, J., Mauermeir, M., Yang, K. T., Hayek, I., Szperlinski, M., Andrack, J., Schleicher, U., Bozec, A., Krönke, G., Murray, P. J., Wirtz, S., Yamamoto, M., Schatz, V., Jantsch, J., Oefner, P., Degrandi, D., Pfeffer, K., Mertens-Scholz, K., Rauber, S., Bogdan, C., Dettmer, K., Lührmann, A. and Lang, R. (2022). Macrophages inhibit *Coxiella burnetii* by the ACOD1-itaconate pathway for containment of Q fever. *EMBO Mol Med*, **7**, e15931.

Kosma, P. (1999). *Chlamydial* lipopolysaccharide. *Biochim Biophys Acta*, **1455**(2-3), 387-402.

Kunze, M., Steiner, T., Chen, F., Huber, C., Rydzewski, K., Stämmler, M., Heuner, K. and Eisenreich, W. (2021). Metabolic adaption of *Legionella pneumophila* during intracellular growth in *Acanthamoeba castellanii*. *Int J Med Microbiol*, **311**(4), 151504.

Kurihara, Y., Itoh, R., Shimizu, A., Walenna, N. F., Chou, B., Ishii, K., Soejima, T., Fujikane, A. and Hiromatsu, K. (2019). *Chlamydia trachomatis* targets mitochondrial dynamics to promote intracellular survival and proliferation. *Cell Microbiol*, **21**(1), e12962.

Kwan, E. E. and Huang, S. G. (2008). Structural elucidation with NMR spectroscopy: practical strategies for organic chemists. *Eur J Org Chem*, **2008**(16), 2671-2688.

Lai, V. M. F., Wong, P. A. L. and Lii, C. Y. (2000). Effects of cation properties on sol-gel transition and gel properties of κ-carrageenan. *J Food Sci*, **65**(8), 1332-1337.

Langendorff, V., Cuvelier, G., Michon, C., Launay, B., Parker, A. and De Kruif, C. G. (2000). Effects of carrageenan type on the behaviour of carrageenan/milk mixtures. *Food Hydrocoll*, **14**(4), 273-280.

Langenhan, J., Jaeger, C., Baum, K., Simon, M. and Lisec, J. (2022). A flexible tool to correct superimposed mass isotopologue distributions in GC-APCI-MS flux experiments. *Metabolites*, **12**(5), 408.

Larive, C. K., Barding, G. A., Jr. and Dinges, M. M. (2015). NMR Spectroscopy for metabolomics and metabolic profiling. *Anal Chem*, **87**(1), 133-146.

Leandro, A., Pacheco, D., Cotas, J., Marques, J. C., Pereira, L. and Gonçalves, A. M. M. (2020). Seaweed's bioactive candidate compounds to food industry and global food security. *Life*, **10**(8), 140.

Lee, W. K., Lim, Y. Y., Leow, A. T. C., Namasivayam, P., Ong Abdullah, J. and Ho, C. L. (2017). Biosynthesis of agar in red seaweeds: a review. *Carbohydr Polym*, **164**, 23-30.

Lee, W. N., Byerley, L. O., Bergner, E. A. and Edmond, J. (1991). Mass isotopomer analysis: theoretical and practical considerations. *Biol Mass Spectrom*, **20**(8), 451-458.

Leighton, M. P., Kelly, D. J., Williamson, M. P. and Shaw, J. G. (2001). An NMR and enzyme study of the carbon metabolism of *Neisseria meningitidis*. *Microbiology*, **147**(Pt 6), 1473-1482.

Lenoir-Wijnkoop, I., Sanders, M. E., Cabana, M. D., Caglar, E., Corthier, G., Rayes, N., Sherman, P. M., Timmerman, H. M., Vaneechoutte, M., Van Loo, J. and Wolvers, D. A. (2007). Probiotic and prebiotic influence beyond the intestinal tract. *Nutr Rev*, **65**(11), 469-489.

Li, W., Chung, H., Daeffler, C., Johnson, J. A. and Grubbs, R. H. (2012). Application of ^{1}H DOSY for facile measurement of polymer molecular weights. *Macromolecules*, **45**(24), 9595-9603.

Liao, Y. C., Chang, C. C., Nagarajan, D., Chen, C. Y. and Chang, J. S. (2021). Algae-derived hydrocolloids in foods: applications and health-related issues. *Bioengineered*, **12**(1), 3787-3801.

Liechti, G. W., Kuru, E., Hall, E., Kalinda, A., Brun, Y. V., VanNieuwenhze, M. and Maurelli, A. T. (2014). A new metabolic cell-wall labelling method reveals peptidoglycan in *Chlamydia trachomatis*. *Nature*, **506**(7489), 507-510.

Lin, J., Chen, L., Jiang, W., Zhang, H., Shi, Y. and Cai, W. (2019). Rapid detection of low-level HeLa cell contamination in cell culture using nested PCR. *J Cell Mol Med*, **23**(1), 227-236.

Liu, F., Hou, P., Zhang, H., Tang, Q., Xue, C. and Li, R. W. (2021). Food-grade carrageenans and their implications in health and disease. *Compr Rev Food Sci Food Saf*, **20**(4), 3918-3936.

Liu, Z., Gao, T., Yang, Y., Meng, F., Zhan, F., Jiang, Q. and Sun, X. (2019). Anti-cancer activity of porphyran and carrageenan from red seaweeds. *Molecules*, **24**(23), 4286.

Long, C. P. and Antoniewicz, M. R. (2019). High-resolution ^{13}C metabolic flux analysis. *Nature Protocols*, **14**(10), 2856-2877.

Louala, S. and Lamri-Senhadji, M. (2019). Beneficial effects of low-calorie-carbohydrate/high-agar diet on cardiometabolic disorders associated with non-alcoholic fatty liver disease in obese rats. *Prev Nutr Food Sci*, **24**(4), 400-409.

Lozano-Castellón, J., López-Yerena, A., Domínguez-López, I., Siscart-Serra, A., Fraga, N., Sámano, S., López-Sabater, C., Lamuela-Raventós, R. M., Vallverdú-Queralt, A. and Pérez, M. (2022). Extra virgin olive oil: a comprehensive review of efforts to ensure its authenticity, traceability, and safety. *Compr Rev Food Sci Food Saf*, **21**(3), 2639-2664.

REFERENCES

Mahfoudhi, N., Chouaibi, M. and Hamdi, S. (2014). Effectiveness of almond gum trees exudate as a novel edible coating for improving postharvest quality of tomato (*Solanum lycopersicum L.*) fruits. *Int J Food Sci Technol*, **20**(1), 33-43.

Mancuso, G., Midiri, A., Gerace, E. and Biondo, C. (2021). Bacterial antibiotic resistance: the most critical pathogens. *Pathogens*, **10**(10), 1310.

Marchetti, L., Pellati, F., Benvenuti, S. and Bertelli, D. (2019). Use of ^{1}H NMR to detect the percentage of pure fruit juices in blends. *Molecules*, **24**(14), 2592.

Martins, J. T., Cerqueira, M. A., Bourbon, A. I., Pinheiro, A. C., Souza, B. W. S. and Vicente, A. A. (2012). Synergistic effects between κ-carrageenan and locust bean gum on physicochemical properties of edible films made thereof. *Food Hydrocoll*, **29**(2), 280-289.

Matsuura, M. (2013). Structural modifications of bacterial lipopolysaccharide that facilitate gram-negative bacteria evasion of host innate immunity. *Front Immun*, **4**, 109.

McCoy, A. J., Adams, N. E., Hudson, A. O., Gilvarg, C., Leustek, T. and Maurelli, A. T. (2006). L,L-diaminopimelate aminotransferase, a trans-kingdom enzyme shared by *Chlamydia* and plants for synthesis of diaminopimelate/lysine. *Proc Natl Acad Sci USA*, **103**(47), 17909-17914.

McKim, J. M. (2014). Food additive carrageenan: Part I: a critical review of carrageenan in vitro studies, potential pitfalls, and implications for human health and safety. *Crit Rev Toxicol*, **44**(3), 211-243.

McQueen, B. E., Kiatthanapaiboon, A., Fulcher, M. L., Lam, M., Patton, K., Powell, E., Kollipara, A., Madden, V., Suchland, R. J., Wyrick, P., O'Connell, C. M., Reidel, B., Kesimer, M., Randell, S. H., Darville, T. and Nagarajan, U. M. (2020). Human fallopian tube epithelial cell culture model to study host responses to *Chlamydia trachomatis* infection. *Infect Immun*, **88**(9), e00105-00120.

Mehlitz, A., Eylert, E., Huber, C., Lindner, B., Vollmuth, N., Karunakaran, K., Goebel, W., Eisenreich, W. and Rudel, T. (2017). Metabolic adaptation of *Chlamydia trachomatis* to mammalian host cells. *Mol Microbiol*, **103**(6), 1004-1019.

Merkx, D. W. H., Westphal, Y., van Velzen, E. J. J., Thakoer, K. V., de Roo, N. and van Duynhoven, J. P. M. (2018). Quantification of food polysaccharide mixtures by ^{1}H NMR. *Carbohydr Polym*, **179**, 379-385.

Meyer, K., Rosa, C., Hischenhuber, C. and Meyer, R. (2001). Determination of locust bean gum and guar gum by polymerase chain reaction and restriction fragment length polymorphism analysis. *J AOAC Int*, **84**(1), 89-100.

Miller, K. E. (2006). Diagnosis and treatment of *Chlamydia trachomatis* infection. *Am Fam Physician*, **73**(8), 1411-1416.

Mishori, R., McClaskey, E. L. and WinklerPrins, V. J. (2012). *Chlamydia trachomatis* infections: screening, diagnosis, and management. *Am Fam Physician*, **86**(12), 1127-1132.

Mohnen, D. (2008). Pectin structure and biosynthesis. *Curr Opin Plant Biol*, **11**(3), 266-277.

Mooradian, A. D., Smith, M. and Tokuda, M. (2017). The role of artificial and natural sweeteners in reducing the consumption of table sugar: a narrative review. *Clin Nutr ESPEN*, **18**, 1-8.

Moreira, M. J., García-Díez, J., de Almeida, J. M. M. M. and Saraiva, C. (2021). Consumer knowledge about food labeling and fraud. *Foods*, **10**(5), 1095.

Mudgil, D., Barak, S. and Khatkar, B. S. (2014). Guar gum: processing, properties and food applications - a review. *J Food Sci Technol*, **51**(3), 409-418.

N'Gadjaga, M. D., Perrinet, S., Connor, M. G., Bertolin, G., Millot, G. A. and Subtil, A. (2022). *Chlamydia trachomatis* development requires both host glycolysis and oxidative phosphorylation but has only minor effects on these pathways. *J Biol Chem*, **298**(9), 102338.

Nagana Gowda, G. A. and Raftery, D. (2021). NMR-Based metabolomics. *Adv Exp Med Biol*, **1280**, 19-37.

Naseri, A., Thibault, J. F. and Ralet, M. C. (2008). Citrus pectin: structure and application in acid dairy drinks. In Benkeblia, N. and Tennant, P.: Tree and forestry science and biotechnology, *Global Science Book*, 60-70.

Newman, L., Rowley, J., Vander Hoorn, S., Wijesooriya, N. S., Unemo, M., Low, N., Stevens, G., Gottlieb, S., Kiarie, J. and Temmerman, M. (2015). Global estimates of the prevalence and incidence of four curable sexually transmitted infections in 2012 based on systematic review and global reporting. *PLoS One*, **10**(12), e0143304.

Nguyen, B. D., Cunningham, D., Liang, X., Chen, X., Toone, E. J., Raetz, C. R., Zhou, P. and Valdivia, R. H. (2011). Lipooligosaccharide is required for the generation of infectious elementary bodies in *Chlamydia trachomatis*. *Proc Natl Acad Sci USA*, **108**(25), 10284-10289.

Nicholson, T. L., Chiu, K. and Stephens, R. S. (2004). *Chlamydia trachomatis* lacks an adaptive response to changes in carbon source availability. *Infect Immun*, **72**(7), 4286-4289.

Nonnenmacher, Y. and Hiller, K. (2018). Biochemistry of proinflammatory macrophage activation. *Cell Mol Life Sci*, **75**(12), 2093-2109.

Nurminen, M., Rietschel, E. T. and Brade, H. (1985). Chemical characterization of *Chlamydia trachomatis* lipopolysaccharide. *Infect Immun*, **48**(2), 573-575.

O'Connell, C. M. and Ferone, M. E. (2016). *Chlamydia trachomatis* genital infections. *Microb Cell*, **3**(9), 390-403.

Ó Maoldomhnaigh, C., Cox, D. J., Phelan, J. J., Malone, F. D., Keane, J. and Basdeo, S. A. (2021). The warburg effect occurs rapidly in stimulated human adult but not umbilical cord blood derived macrophages. *Frontiers in Immunology*, **12**, 657261.

Ohmer, M., Tzivelekidis, T., Niedenführ, N., Volceanov-Hahn, L., Barth, S., Vier, J., Börries, M., Busch, H., Kook, L., Biniossek, M. L., Schilling, O., Kirschnek, S. and Häcker, G. (2019). Infection of HeLa cells with *Chlamydia trachomatis* inhibits protein synthesis and causes multiple changes to host cell pathways. *Cell Microbiol*, **21**(4), e12993.

Ohtsuki, T., Sato, K., Sugimoto, N., Akiyama, H. and Kawamura, Y. (2012a). Absolute quantitative analysis for sorbic acid in processed foods using proton nuclear magnetic resonance spectroscopy. *Anal Chim Acta*, **734**, 54-61.

Ohtsuki, T., Sato, K., Sugimoto, N., Akiyama, H. and Kawamura, Y. (2012b). Absolute quantification for benzoic acid in processed foods using quantitative proton nuclear magnetic resonance spectroscopy. *Talanta*, **99**, 342-348.

REFERENCES

Ohtsuki, T., Sato, K., Abe, Y., Sugimoto, N. and Akiyama, H. (2015). Quantification of acesulfame potassium in processed foods by quantitative ^{1}H NMR. *Talanta*, **131**, 712-718.

Omsland, A., Sager, J., Nair, V., Sturdevant, D. E. and Hackstadt, T. (2012). Developmental stage-specific metabolic and transcriptional activity of *Chlamydia trachomatis* in an axenic medium. *Proc Natl Acad Sci USA*, **109**(48), 19781-19785.

Otten, C., Brilli, M., Vollmer, W., Viollier, P. H. and Salje, J. (2018). Peptidoglycan in obligate intracellular bacteria. *Mol Microbiol*, **107**(2), 142-163.

Pacholczyk-Sienicka, B., Ciepielowski, G. and Albrecht, Ł. (2021). The application of NMR spectroscopy and chemometrics in authentication of spices. *Molecules*, **26**(2), 382.

Panzetta, M. E., Valdivia, R. H. and Saka, H. A. (2018). *Chlamydia* persistence: a survival strategy to evade antimicrobial effects *in-vitro* and *in-vivo*. *Front Microbiol*, **9**, 3101.

Partridge, D., Lloyd, K. A., Rhodes, J. M., Walker, A. W., Johnstone, A. M. and Campbell, B. J. (2019). Food additives: assessing the impact of exposure to permitted emulsifiers on bowel and metabolic health - introducing the FADiets study. *Nutr Bull*, **44**(4), 329-349.

Patel, S. and Goyal, A. (2015). Applications of natural polymer gum arabic: a review. *Int J Food Prop*, **18**(5), 986-998.

Pechanek, U., Blaicher, G., Pfannhauser, W. and Woidich, H. (2020). Electrophoretic method for qualitative and quantitative analysis of gelling and thickening agents. *J Assoc Off Anal Chem*, **65**(3), 745-752.

Peters, J. and Byrne, G. I. (2015). *Chlamydia trachomatis* growth depends on eukaryotic cholesterol esterification and is affected by acyl-CoA:cholesterol acyltransferase inhibition. *Pathog Dis*, **73**(6), ftv028.

Petrescu, D. C., Vermeir, I. and Petrescu-Mag, R. M. (2019). Consumer understanding of food quality, healthiness, and environmental impact: a cross-national perspective. *Int J Environ Res Public Health*, **17**(1), 169.

Petrovski, S. and Tillett, D. (2012). Back to the kitchen: food-grade agar is a low-cost alternative to bacteriological agar. *Anal Biochem*, **429**(2), 140-141.

Pettolino, F. A., Hoogenraad, N. J. and Stone, B. A. (2002). Application of a mannan-specific antibody for the detection of galactomannans in foods. *Food Hydrocoll*, **16**(6), 551-556.

Phillips, A. O. and Phillips, G. O. (2011). Biofunctional behaviour and health benefits of a specific gum arabic. *Food Hydrocoll*, **25**(2), 165-169.

Politi, M., Groves, P., Chávez, M. I., Cañada, F. J. and Jiménez-Barbero, J. (2006). Useful applications of DOSY experiments for the study of mushroom polysaccharides. *Carbohydr Res*, **341**(1), 84-89.

Quemener, B., Marot, C., Mouillet, L., Da Riz, V. and Diris, J. (2000). Quantitative analysis of hydrocolloids in food systems by methanolysis coupled to reverse HPLC. Part 2. Pectins, alginates and xanthan. *Food Hydrocoll*, **14**(1), 19-28.

Radziej, S., Scherb-Forster, J., Schlicht, C. and Eisenreich, W. (2021). Fast identification of food thickeners by nontargeted NMR-spectroscopy. *J Agric Food Chem*, **69**(12), 3761-3775.

REFERENCES

Radziej, S., Scherb-Forster, J., Schlicht, C. and Eisenreich, W. (2022). NMR-based identification of thickeners in membrane-filtered food premixtures. *Eur Food Res Technol*, **248**(7), 1715-1720.

Rajeeve, K., Das, S., Prusty, B. K. and Rudel, T. (2018). *Chlamydia trachomatis* paralyses neutrophils to evade the host innate immune response. *Nat Microbiol*, **3**(7), 824-835.

Rajeeve, K., Vollmuth, N., Janaki-Raman, S., Wulff, T. F., Baluapuri, A., Dejure, F. R., Huber, C., Fink, J., Schmalhofer, M., Schmitz, W., Sivadasan, R., Eilers, M., Wolf, E., Eisenreich, W., Schulze, A., Seibel, J. and Rudel, T. (2020). Reprogramming of host glutamine metabolism during *Chlamydia trachomatis* infection and its key role in peptidoglycan synthesis. *Nat Microbiol*, **5**(11), 1390-1402.

Ramay, B. M., Caudell, M. A., Cordón-Rosales, C., Archila, L. D., Palmer, G. H., Jarquin, C., Moreno, P., McCracken, J. P., Rosenkrantz, L., Amram, O., Omulo, S. and Call, D. R. (2020). Antibiotic use and hygiene interact to influence the distribution of antimicrobial-resistant bacteria in low-income communities in Guatemala. *Sci Rep*, **10**(1), 13767.

Recuero-Checa, M. A., Sharma, M., Lau, C., Watkins, P. A., Gaydos, C. A. and Dean, D. (2016). *Chlamydia trachomatis* growth and development requires the activity of host long-chain acyl-CoA synthetases (ACSLs). *Sci Rep*, **6**(1), 23148.

Regulation (EC) No 1333/2008 of the European Parliament and of the Council of 16 December 2008 on food additives

Reygaert, W. C. (2018). An overview of the antimicrobial resistance mechanisms of bacteria. *AIMS Microbiol*, **4**(3), 482-501.

Ricciotti, E. and FitzGerald, G. A. (2011). Prostaglandins and inflammation. *Arterioscler Thromb Vasc Biol*, **31**(5), 986-1000.

Rohasmizah, H. and Azizah, M. (2022). Pectin-based edible coatings and nanoemulsion for the preservation of fruits and vegetables: a review. *Applied Food Research*, **2**(2), 100221.

Rongai, D., Sabatini, N., Del Coco, L., Perri, E., Del Re, P., Simone, N., Marchegiani, D. and Fanizzi, F. P. (2017). ^{1}H NMR and multivariate analysis for geographic characterization of commercial extra virgin olive oil: a possible correlation with climate data. *Foods*, **6**(11), 96.

Rother, M., Teixeira da Costa, A. R., Zietlow, R., Meyer, T. F. and Rudel, T. (2019). Modulation of host cell metabolism by *Chlamydia trachomatis*. *Microbiol Spectr*, **7**(3), 1-10.

Rund, S., Lindner, B., Brade, H. and Holst, O. (1999). Structural analysis of the lipopolysaccharide from *Chlamydia trachomatis* serotype L2. *J Biol Chem*, **274**(24), 16819-16824.

Saha, D. and Bhattacharya, S. (2010). Hydrocolloids as thickening and gelling agents in food: a critical review. *J Food Sci Technol*, **47**(6), 587-597.

Sandoz, K. M. and Rockey, D. D. (2010). Antibiotic resistance in *Chlamydiae*. *Future Microbiol*, **5**(9), 1427-1442.

Sasikaran, J., Ziemski, M., Zadora, P. K., Fleig, A. and Berg, I. A. (2014). Bacterial itaconate degradation promotes pathogenicity. *Nat Chem Biol*, **10**(5), 371-377.

Schmidt, K., Carlsen, M., Nielsen, J. and Villadsen, J. (1997). Modeling isotopomer distributions in biochemical networks using isotopomer mapping matrices. *Biotechnol Bioeng*, **55**(6), 831-840.

Schmitt, C., Schneider, T., Rumask, L., Fischer, M. and Hackl, T. (2020). Food profiling: determination of the geographical origin of walnuts by ^{1}H NMR spectroscopy using the polar extract. *J Agric Food Chem*, **68**(52), 15526-15534.

Schneider, P. J., Grosche, O. and Engelhardt, H. (1999). Capillary electrophoretic identification of commercial gelling agents. *J High Resol Chromatogr*, **22**(2), 79-82.

Schoen, C., Kischkies, L., Elias, J. and Ampattu, B. J. (2014). Metabolism and virulence in *Neisseria meningitidis*. *Front Cell Infect Microbiol*, **4**, 114.

Schorsch, C., Garnier, C. and Doublier, J. L. (1997). Viscoelastic properties of xanthangalactomannan mixtures: comparison of guar gum with locust bean gum. *Carbohydr Polym*, **34**(3), 165-175.

Schwartz, K. L. and Morris, S. K. (2018). Travel and the spread of drug-resistant bacteria. *Curr Infect Dis Rep*, **20**(9), 29.

Shapouri-Moghaddam, A., Mohammadian, S., Vazini, H., Taghadosi, M., Esmaeili, S. A., Mardani, F., Seifi, B., Mohammadi, A., Afshari, J. T. and Sahebkar, A. (2018). Macrophage plasticity, polarization, and function in health and disease. *J Cell Physiol*, **233**(9), 6425-6440.

Siciliano, C., Belsito, E., De Marco, R., Di Gioia, M. L., Leggio, A. and Liguori, A. (2013). Quantitative determination of fatty acid chain composition in pork meat products by high resolution ^{1}H NMR spectroscopy. *Food Chem*, **136**(2), 546-554.

Simmler, C., Napolitano, J. G., McAlpine, J. B., Chen, S. N. and Pauli, G. F. (2014). Universal quantitative NMR analysis of complex natural samples. *Curr Opin Biotechnol*, **25**, 51-59.

Simon, R. A. (2003). Adverse reactions to food additives. *Curr Allergy Asthma Rep*, **3**(1), 62-66.

Singh, R., Slade, J. A., Brockett, M., Mendez, D., Liechti, G. W. and Maurelli, A. T. (2020). Competing Substrates for the Bifunctional Diaminopimelic Acid Epimerase/Glutamate Racemase Modulate Peptidoglycan Synthesis in *Chlamydia trachomatis*. *Infect Immun*, **89**(1), e00401.

Soedjak, H. S. (1994). Colorimetric determination of carrageenans and other anionic hydrocolloids with methylene blue. *Anal Chem*, **66**(24), 4514-4518.

Somani, J., Bhullar, V. B., Workowski, K. A., Farshy, C. E. and Black, C. M. (2000). Multiple drug-resistant *Chlamydia trachomatis* associated with clinical treatment failure. *J Infect Dis*, **181**(4), 1421-1427.

Spink, J. and Moyer, D. C. (2011). Defining the public health threat of food fraud. *J Food Sci*, **76**(9), 157-163.

Steffens, L., Pettinato, E., Steiner, T. M., Mall, A., König, S., Eisenreich, W. and Berg, I. A. (2021). High CO_2 levels drive the TCA cycle backwards towards autotrophy. *Nature*, **592**(7856), 784-788.

Stephens, R. S., Kalman, S., Lammel, C., Fan, J., Marathe, R., Aravind, L., Mitchell, W., Olinger, L., Tatusov, R. L., Zhao, Q., Koonin, E. V. and Davis, R. W. (1998). Genome sequence of an obligate intracellular pathogen of humans: *Chlamydia trachomatis*. *Science*, **282**(5389), 754-759.

Stincone, A., Prigione, A., Cramer, T., Wamelink, M. M., Campbell, K., Cheung, E., Olin-Sandoval, V., Grüning, N. M., Krüger, A., Tauqeer Alam, M., Keller, M. A., Breitenbach, M., Brindle, K. M., Rabinowitz, J. D. and Ralser, M. (2015). The return of metabolism: biochemistry and physiology of the pentose phosphate pathway. *Biol Rev Camb Philos Soc*, **90**(3), 927-963.

Strauss, G., Eisenreich, W., Bacher, A. and Fuchs, G. (1992). ^{13}C-NMR study of autotrophic CO_2 fixation pathways in the sulfur-reducing *Archaebacterium Thermoproteus* neutrophilus and in the phototrophic Eubacterium *Chloroflexus aurantiacus*. *Eur J Biochem*, **205**(2), 853-866.

Sun, H. S., Eng, E. W., Jeganathan, S., Sin, A. T., Patel, P. C., Gracey, E., Inman, R. D., Terebiznik, M. R. and Harrison, R. E. (2012). *Chlamydia trachomatis* vacuole maturation in infected macrophages. *J Leukoc Biol*, **92**(4), 815-827.

Swenson, H. A., Kaustinen, H. M., Kaustinen, O. A. and Thompson, N. S. (1968). Structure of gum arabic and its configuration in solution. *J Polym Sci A2 Polym Phys*, **6**(9), 1593-1606.

Tahir, H. E., Xiaobo, Z., Jiyong, S., Mahunu, G. K., Zhai, X. and Mariod, A. A. (2018). Quality and postharvest-shelf life of cold-stored strawberry fruit as affected by gum arabic (*Acacia senegal*) edible coating. *J Food Biochem*, **42**(3), e12527.

Tang, C., Liu, C., Maffei, B., Niragire, B., Cohen, H., Kane, A., Donnadieu, A. C., Levy-Zauberman, Y., Vernay, T., Hugueny, J., Vincens, E., Louis-Sylvestre, C., Subtil, A. and Wu, Y. (2021). Primary ectocervical epithelial cells display lower permissivity to *Chlamydia trachomatis* than HeLa cells and a globally higher pro-inflammatory profile. *Sci Rep*, **11**(1), 5848.

Taylor, P. L., Blakely, K. M., de Leon, G. P., Walker, J. R., McArthur, F., Evdokimova, E., Zhang, K., Valvano, M. A., Wright, G. D. and Junop, M. S. (2008). Structure and function of sedoheptulose-7-phosphate isomerase, a critical enzyme for lipopolysaccharide biosynthesis and a target for antibiotic adjuvants. *J Biol Chem*, **283**(5), 2835-2845.

Thakur, B. R., Singh, R. K. and Handa, A. K. (1997). Chemistry and uses of pectin - a review. *Crit Rev Food Sci Nutr*, **37**(1), 47-73.

Thomas, N. C. (1991). The early history of spectroscopy. *J Chem Educ*, **68**(8), 631-634.

Thrippleton, M. J., Loening, N. M. and Keeler, J. (2003). A fast method for the measurement of diffusion coefficients: one-dimensional DOSY. *Magn Reson Chem*, **41**(6), 441-447.

Tojo, E. and Prado, J. (2003). A simple ^{1}H NMR method for the quantification of carrageenans in blends. *Carbohydr Polym*, **53**(3), 325-329.

Toman, R., Skultety, L. and Ihnatko, R. (2009). *Coxiella burnetii* glycomics and proteomics - tools for linking structure to function. *Ann N Y Acad Sci*, **1166**, 67-78.

Trius, A. and Sebranek, J. G. (1996). Carrageenans and their use in meat products. *Crit Rev Food Sci Nutr*, **36**(1-2), 69-85.

Trivedi, K., Tang, C. M. and Exley, R. M. (2011). Mechanisms of meningococcal colonisation. *Trends Microbiol*, **19**(9), 456-463.

Ullah, Q., Jamil, T., Saqib, M., Iqbal, M. and Neubauer, H. (2022). Q Fever - A Neglected Zoonosis. *Microorganisms*, **10**(8), 1530.

Urdiain, M., Doménech-Sánchez, A., Albertí, S., Benedí, V. J. and Rosselló, J. A. (2004). Identification of two additives, locust bean gum (E-410) and guar gum (E-412), in food products by DNA-based methods. *Food Addit Contam*, **21**(7), 619-625.

Valado, A., Pereira, M., Caseiro, A., Figueiredo, J. P., Loureiro, H., Almeida, C., Cotas, J. and Pereira, L. (2019). Effect of carrageenans on vegetable jelly in humans with hypercholesterolemia. *Mar Drugs*, **18**(1), 19.

Wang, T. P., Chang, L. L., Chang, S.-N., Wang, E. C., Hwang, L. C., Chen, Y. H. and Wang, Y. M. (2012). Successful preparation and characterization of biotechnological grade agarose from indigenous Gelidium amansii of Taiwan. *Process Biochem*, **47**(3), 550-554.

Wang, X. and Quinn, P. J. (2010). Lipopolysaccharide: biosynthetic pathway and structure modification. *Prog Lipid Res*, **49**(2), 97-107.

Wiechert, W. (2001). ^{13}C metabolic flux analysis. *Metab Eng*, **3**(3), 195-206.

Wishart, D. S. (2008). Metabolomics: applications to food science and nutrition research. *Trends Food Sci Technol*, **19**(9), 482-493.

Wishart, D. S. (2016). Emerging applications of metabolomics in drug discovery and precision medicine. *Nat Rev Drug Discov*, **15**(7), 473-484.

Witkin, S. S., Minis, E., Athanasiou, A., Leizer, J. and Linhares, I. M. (2017). *Chlamydia trachomatis*: the persistent pathogen. *Clin Vaccine Immunol*, **24**(10), e00203.

Wittmann, C. (2007). Fluxome analysis using GC-MS. *Microb Cell Fact*, **6**(1), 6.

Wood, T. K., Knabel, S. J. and Kwan, B. W. (2013). Bacterial persister cell formation and dormancy. *Appl Environ Microbiol*, **79**(23), 7116-7121.

Wu, L., Zhang, C., Long, Y., Chen, Q., Zhang, W. and Liu, G. (2022). Food additives: From functions to analytical methods. *Crit Rev Food Sci Nutr*, **62**(30), 8497-8517.

Wu, Y., Ding, W., Jia, L. and He, Q. (2015). The rheological properties of tara gum (*Caesalpinia spinosa*). *Food Chem*, **168**, 366-371.

Wylie, J. L., Hatch, G. M. and McClarty, G. (1997). Host cell phospholipids are trafficked to and then modified by *Chlamydia trachomatis*. *J Bacteriol*, **179**(23), 7233-7242.

Wyrick, P. B. (2010). *Chlamydia trachomatis* persistence in vitro: an overview. *J Infect Dis*, **201**(Suppl 2), 88-95.

Xiao, C. and Anderson, C. (2013). Roles of pectin in biomass yield and processing for biofuels. *Front Plant Sci*, **4**, 67.

Xu, X., Ye, S., Zuo, X. and Fang, S. (2022). Impact of guar gum and locust bean gum addition on the pasting, rheological properties, and freeze-thaw stability of rice starch gel. *Foods*, **11**(16), 2508.

Xue, Y., Zheng, H., Mai, Z., Qin, X., Chen, W., Huang, T., Chen, D. and Zheng, L. (2017). An *in vitro* model of azithromycin-induced persistent *Chlamydia trachomatis* infection. *FEMS Microbiol Lett*, **364**(14), 1-8.

Yabe, Y., Ninomiya, T., Tatsuno, T. and Okada, T. (1991). Simple colorimetric determination of carrageenan in jellies and salad dressings. *J Assoc Off Anal Chem*, **74**(6), 1019-1022.

Yadav, M. P., Igartuburu, J. M., Yan, Y. and Nothnagel, E. A. (2007). Chemical investigation of the structural basis of the emulsifying activity of gum arabic. *Food Hydrocoll*, **21**(2), 297-308.

Yang, C., Briones, M., Chiou, J., Lei, L., Patton, M. J., Ma, L., McClarty, G. and Caldwell, H. D. (2019a). *Chlamydia trachomatis* lipopolysaccharide evades the canonical and noncanonical inflammatory pathways to subvert innate immunity. *mBio*, **10**(2), e00595.

Yang, M., Rajeeve, K., Rudel, T. and Dandekar, T. (2019b). Comprehensive flux modeling of *Chlamydia trachomatis* proteome and qRT-PCR data indicate biphasic metabolic differences between elementary bodies and reticulate bodies during infection. *Front Microbiol*, **10**, 2350.

Yao, J. and Rock, C. O. (2018). Therapeutic targets in *chlamydial* fatty acid and phospholipid synthesis. *Front Microbiol*, **9**, 2291.

Yao, J., Dodson, V. J., Frank, M. W. and Rock, C. O. (2015a). *Chlamydia trachomatis* scavenges host fatty acids for phospholipid synthesis via an acyl-acyl carrier protein synthetase. *J Biol Chem*, **290**(36), 22163-22173.

Yao, J., Cherian, P. T., Frank, M. W. and Rock, C. O. (2015b). *Chlamydia trachomatis* relies on autonomous phospholipid synthesis for membrane biogenesis. *J Biol Chem*, **290**(31), 18874-18888.

Yao, J., Abdelrahman, Y. M., Robertson, R. M., Cox, J. V., Belland, R. J., White, S. W. and Rock, C. O. (2014). Type II fatty acid synthesis is essential for the replication of *Chlamydia trachomatis*. *J Biol Chem*, **289**(32), 22365-22376.

Yazdankhah, S. P. and Caugant, D. A. (2004). *Neisseria meningitidis*: an overview of the carriage state. *J Med Microbiol*, **53**(9), 821-832.

Yubero-Serrano, E. M., Lopez-Moreno, J., Gomez-Delgado, F. and Lopez-Miranda, J. (2019). Extra virgin olive oil: more than a healthy fat. *Eur J Clin Nutr*, **72**(1), 8-17.

Yun, E. J., Yu, S., Kim, Y. A., Liu, J. J., Kang, N. J., Jin, Y. S. and Kim, K. H. (2021). *In Vitro* prebiotic and anti-colon cancer activities of agar-derived sugars from red seaweeds. *Mar Drugs*, **19**(4), 213.

Zhao, J., Li, A., Jin, X., Liang, G. and Pan, L. (2022). Discrimination of geographical origin of agricultural products from small-scale districts by widely targeted metabolomics with a case study on pinggu peach. *Front Nutr*, **9**, 891302.

Zhou, J., Wang, F., Chen, J., Yang, R., Chen, Y., Gu, D., Niu, T., Luo, Q., Yan, X., Chen, H. and Wu, W. (2021). Long-term *kappa*-carrageenan consumption leads to moderate metabolic disorder by blocking insulin binding. *Pharmacol Res*, **165**, 105417.

9. Supporting information

9.1 Supporting information to “Fast Identification of Food Thickeners by Nontargeted NMR-Spectroscopy”

Supporting information

Fast identification of food thickeners by non-targeted NMR-spectroscopy

Sandra Radziej[†], Julia Scherb-Forster[†], Claus Schlicht[†] and Wolfgang Eisenreich[‡*]

[†] Bayerisches Landesamt für Gesundheit und Lebensmittelsicherheit, Veterinärstraße 2, D-85764 Oberschleißheim, Germany

[‡] Technische Universität München, Bavarian NMR Center – Structural Membrane Biochemistry, Department of Chemistry, Lichtenbergstraße 4, D-85747 Garching, Germany

CORRESPONDING AUTHOR FOOTNOTE.

* Author to whom correspondence should be addressed [Tel.: +49-(0)89-289-13336. Fax: +49-(0)89-289-13363. E-mail: wolfgang.eisenreich@mytum.de]

Table S1. Overview of the measured pH values of analyzed premixtures and foods where thickener signals were detectable by ^{1}H-NMR-spectroscopy.

Name of the food product	**pH value (measured at 27°C)**	**Name of the food product**	**pH value (measured at 27°C)**
apple jelly (*self-made*)	3.7	almond milk (*Mandeldrink*)	7.6
pastille (*Bachblütenpastille*)	4.9	milk drinks: • fitness whey (*Fitnessmolke)* • fruit whey *(Fruchtmolke)* • whey product (*Molkenmisch-erzeugnis)*	 • 4.7 • 4.6 • 4.7
cream pudding powder (*Crèmepuddingpulver*)	6.4	clear cake glaze (*Tortengusspulver, klar ungezuckert)*	6.3
egg replacer powder (*pflanzlicher Ei-Ersatz*)	6.4	clear cake glaze, vegan and bio (*Tortengusspulver, vegan und bio*)	6.5
fruit spread strawberry (*Fruchtaufstrich Erdbeere*)	4.5	premixture (for meat preparation)	7.7
ice cream stabiliser (*Speiseeis Stabilisator*)	7.3	premixture (vitamin D3)	7.7

Table S2. Overview of the measured pH values of analyzed premixtures and foods where thickener signals were not detectable by ^{1}H-NMR-spectroscopy.

Name of the food product	pH value (measured at 27°C)	Name of the food product	pH value (measured at 27°C)
curry sauce (*Curry Sauce*)	5.2	curry ketchup spicy (*Curry Gewürz Ketchup scharf*)	5.5
dessert-cream powder with vanilla flavour *(Dessert-Crèmepuddingpulver mit Vanille-Geschmack)*	7.5	coconut drink with rice (*Kokosnussdrink mit Reis*)	7.4
dessert sauce with vanilla flavour *(Dessertsoße mit Vanille-Geschmack)*	7.7	rice pudding (*Milchreis*)	7.8
ice cream binding agent (*Eisbindemittel für Milch- und Sahneeis*)	7.5	cream pudding powder with lemon flavour (*Crèmepuddingpulver mit Zitronen-Geschmack)*	6.5
ice dessert strawberry (*Erdbeere Eisdessert vegan und bio*)	5.9	„choco milk drink“ milk drink with chocolate flavour, 3,5% milk fat, heat-treated (*Schokodrink*)	7.1
low-calorie drink with mandarin flavour (*kalorienarmes Erfrischungsgetränk mit Mandarinen-Geschmack*)	2.9	lemon peel flavour (*Zitronenschalen-Aroma*)	7.5
cream pudding powder vanilla flavour (*Crèmepuddingpulver mit Vanille-Geschmack*)	7.8	premixture (for emulsion type sausage)	5.2
semolina pudding less sweet (*Grießbrei weniger süß*)	7.1	premixture (for sauerkraut)	7.4
bio oat drink chocolate (*Haferdrink Schoko*)	7.1	premixture (for stabilisation of boiled sausages)	7.7
yoghurt with 13,5% gooseberries-apple preparation (*Joghurt Stachelbeere-Apfel*)	5.9	premixture (for barbecue sauce)	7.8
cream powder for lemon-yoghurt dessert (*Crèmespeisepulver*)	4.9		

Table S3. ^{1}H-NMR signals of gum arabic in D_2O. Chemical shifts of protons and carbons (in parentheses) are listed. Assignment by means of two-dimensional NMR-experiments. Comparison with chemical shifts from [1]. n.d. not detected; n.i. no information.

^{1}H (^{13}C)	chemical shift δ [ppm]	chemical shift δ [ppm] from literature [1]
H1 (C1) galactopyranose	5.03 (102.6) 4.52 (105.8)	5.03 – 4.49 (105.7 – 102.7)
H2 (C2) galactopyranose	3.83 (71.2) 3.39 (n.d.)	3.76 – 3.38 (76.4 – 71.9)
H3 (C3) galactopyranose	3.59 (77.1)	4.05 – 3.57 (81.4 – 71.6)
H4 (C4) galactopyranose	4.30 (85.6)	4.38 – 3.73 (85.4 – 71.4)
H5 (C5) galactopyranose	n.d.	3.97 – 3.63 (76.2 – 70.9)
H6 (C6) galactopyranose	n.d. (178.1)	3.82 – 3.62 (177.9)
H1 (C1) rhamnose	4.74 (103.6)	4.77 (103.4)
H2 (C2) rhamnose	3.96 (73.1)	3.95 (72.4)
H3 (C3) rhamnose	3.78 (72.9)	3.75 (72.1)
H4 (C4) rhamnose	3.43 (74.8)	3.41 (75.2)
H5 (C5) rhamnose	4.04 (71.8)	4.02 (71.1)
H6 (C6) rhamnose	1.27 (19.4)	1.26 (19.3)
H1 (C1) arabinose	5.42 (111.0) 5.30 (112.5)	5.39 (110.8) 5.32 (112.3)
H2 (C2) arabinose	4.22 (84.3) 4.42 (83.1)	4.18 (84.2) 4.39 (82.8)
H3 (C3) arabinose	n.d.	3.92 (76.2) 3.94 (87.6)
H4 (C4) arabinose	n.d.	4.07 (86.4) 4.26 (85.1)
H5 (C5) arabinose	n.d.	3.80 (64.1) 3.93 (64.0)
H6 (C6) arabinose	n.d.	3.70 (n.i.) 3.74 (n.i.)

Table S4. ^{1}H-NMR signals of *kappa*-carrageenan in D_2O. Chemical shifts of protons are listed. Assignment by means of two-dimensional NMR-experiments. Comparison with chemical shifts from [2]. n.d. not detected.

^{1}H	**chemcial shifts δ [ppm]**	**chemical shifts δ [ppm] from literature [2]**
H1 galactose	n.d.	4.70
H2 galactose	3.62	3.68
H3 galactose	n.d.	4.15
H4 galactose	4.87	4.94
H5 galactose	3.82	3.89
H6 galactose	3.82	3.89
H1 3,6-anhydrogalactose	5.11	5.17
H2 3,6-anhydrogalactose	4.15	4.22
H3 3,6-anhydrogalactose	4.54	4.61
H4 3,6-anhydrogalactose	4.66	4.73
H5 3,6-anhydrogalactose	4.61	4.68
H6 3,6-anhydrogalactose	4.24	4.30/4.16

Table S5. ^{1}H-NMR signals of agar-agar in D_2O. Chemical shifts of protons are listed. Assignment by means of two-dimensional NMR-experiments. Comparison with chemical shifts from [3]. n.d. not detected.

^{1}H	chemcial shifts δ [ppm]	chemical shifts δ [ppm] from literature [3]
H1 galactose	n.d.	4.56
H2 galactose	n.d.	3.63
H3 galactose	n.d.	3.76
H4 galactose	n.d.	4.12
H5 galactose	n.d.	3.71
H6 galactose	3.77	3.80/3.75
H1 3,6-anhydrogalactose	5.16	5.14
H2 3,6-anhydrogalactose	4.14	4.10
H3 3,6-anhydrogalactose	4.57	4.53
H4 3,6-anhydrogalactose	n.d.	4.66
H5 3,6-anhydrogalactose	n.d.	4.55
H6 3,6-anhydrogalactose	n.d.	4.19/4.02

Table S6. ^{1}H-NMR signals of galactomannans in D_2O. Chemical shifts of protons and carbons (in parentheses) are listed. Assignment by means of two-dimensional NMR-experiments. Comparison with chemical shifts from [4]. n.d. not detected; n.i. no information.

^{1}H (^{13}C)	chemcial shift δ [ppm]	chemical shift δ [ppm] from literature [4]
H1 (C1) galactose	5.03 (98.8)	5.03
H2 (C2) galactose	3.84 (68.4)	3.84
H3 (C3) galactose	3.95 (n.d.)	3.93 / 3.95
H4 (C4) galactose	n.d.	n.i.
H5 (C5) galactose	n.d.	n.i.
H6 (C6) galactose	n.d.	n.i.
H1 (C1) mannose	n.d.	4.77
H2 (C2) mannose	4.14 (69.7)	4.14
H3 (C3) mannose	n.d.	3.81
H4 (C4) mannose	n.d.	3.86
H5 (C5) mannose	n.d.	3.75
H6 (C6) mannose	3.76 (61.2)	3.96/3.78 or 3.91/3.75 (63.0/69.0)

Table S7. ^{1}H-NMR signals of pectin in D_2O. Chemical shifts of protons and carbons (in parentheses) are listed. Assignment by means of two-dimensional NMR-experiments. Comparison with chemical shifts from [5]. n.d. not detected.

^{1}H (^{13}C)	**chemical shift δ [ppm]**	**chemical shift δ [ppm] from literature [5]**
H7 (C7) at carboxyl group of galactuonic acid	3.80 (60.5)	3.73
H6 (C6) of rhamnose	1.32 (16.7)	1.22
H6 (C6) of rhamnose	1.25 (16.4)	1.16
acetyl group at 2-O and 3-O-galacturonic acid	n.d.	1.91
acetyl group at 2-O and 3-O-galacturonic acid	n.d.	1.82
H1 (C1) galacturonic acid	5.08 (99.7)	4.99
H2 (C2) galacturonic acid	3.76 (73.0)	3.63
H3 (C3) galacturonic acid	4.00 (67.7)	3.91
H4 (C4) galacturonic acid	4.17 (77.5)	4.08
H5 (C5) galacturonic acid	4.46 (78.4)	4.37
H1 (C1) rhamnose	5.13 (n.d.)	5.03
H1 (C1) galactose	4.96 (99.8)	4.88

Table S8. ^{1}H-NMR signals of the reference glucose and the lemon peel flavour hydrolysate in D_2O. Chemical shifts of protons and carbons (in parentheses) are listed. Assignments by means of two-dimensional NMR experiments. n.d. not detected.

^{1}H (^{13}C)	chemical shifts δ [ppm] from the reference glucose	chemcial shifts δ [ppm] from the hydrolysate
α-H1 (C1) glucose	5.23 (92.1)	5.25 (92.5)
α-H2 (C2) glucose	3.53 (71.5)	3.53 (71.7)
α-H3 (C3) glucose	3.71 (72.8)	n.d.
α-H4 (C4) glucose	3.42 (69.7)	3.45 (69.5)
α-H5 (C5) glucose	n.d.	n.d.
α-H6 (C6) glucose	3.90 (60.5)	3.91 (60.8)
ß-H1 (C1) glucose	4.65 (95.9)	4.67 (96.7)
ß-H2 (C2) glucose	3.25 (74.2)	3.22 (74.6)
ß-H3 (C3) glucose	n.d.	n.d.
ß-H4 (C4) glucose	n.d.	n.d.
ß-H5 (C5) glucose	n.d.	n.d.
ß-H6 (C6) glucose	3.78 (60.5)	3.75 (60.8)

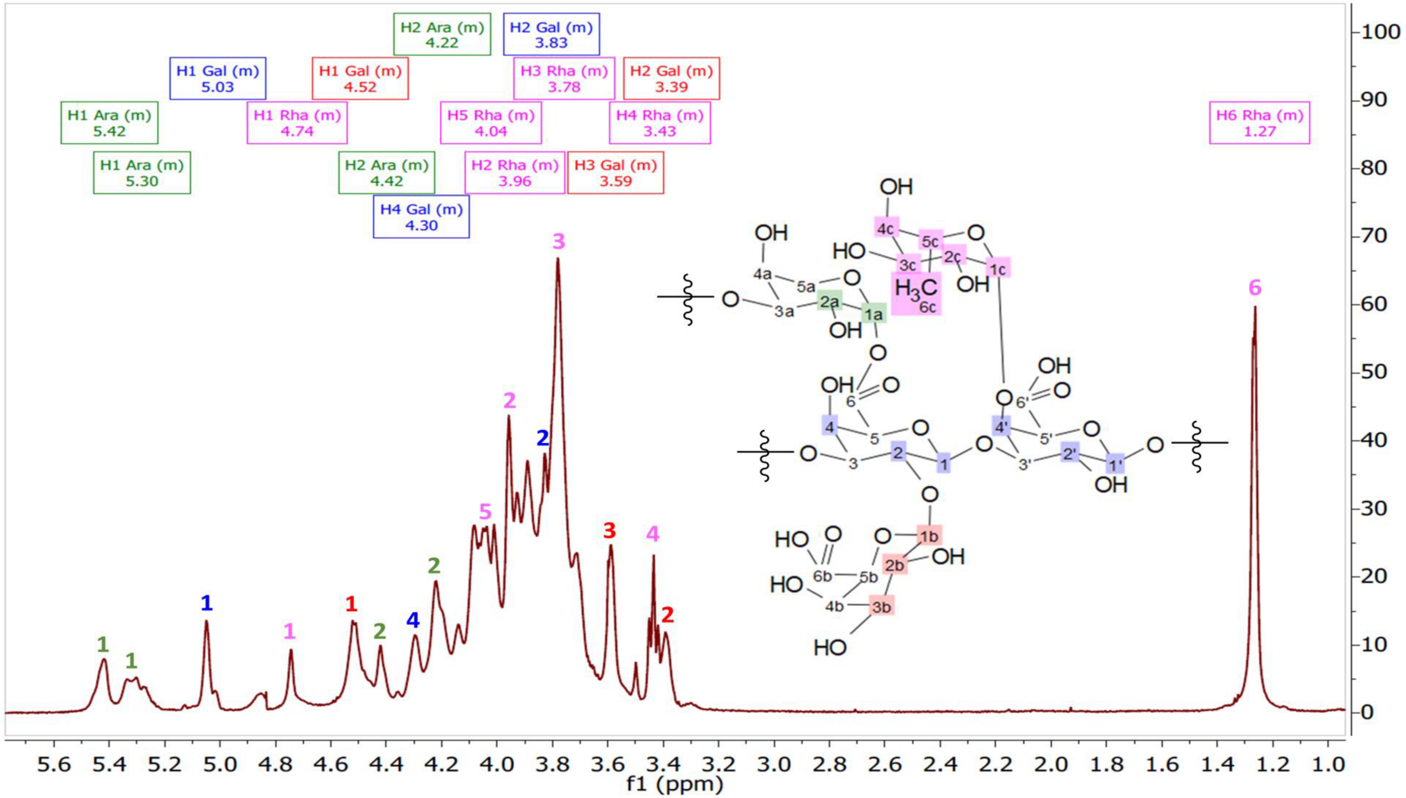

Figure S1. ^{1}H-NMR spectrum of gum arabic in D_2O (400 MHz, water suppression, ns 64, ds 4, TE 27°C). The typical substructure of gum arabic is shown in the inset. Signals are numbered according to the protons in the arabinose moiety (*green*), galactopyranose moiety (*blue* and *red*), and rhamnose moiety (*magenta*). Assignments are made by means of two-dimensional NMR-spectra.

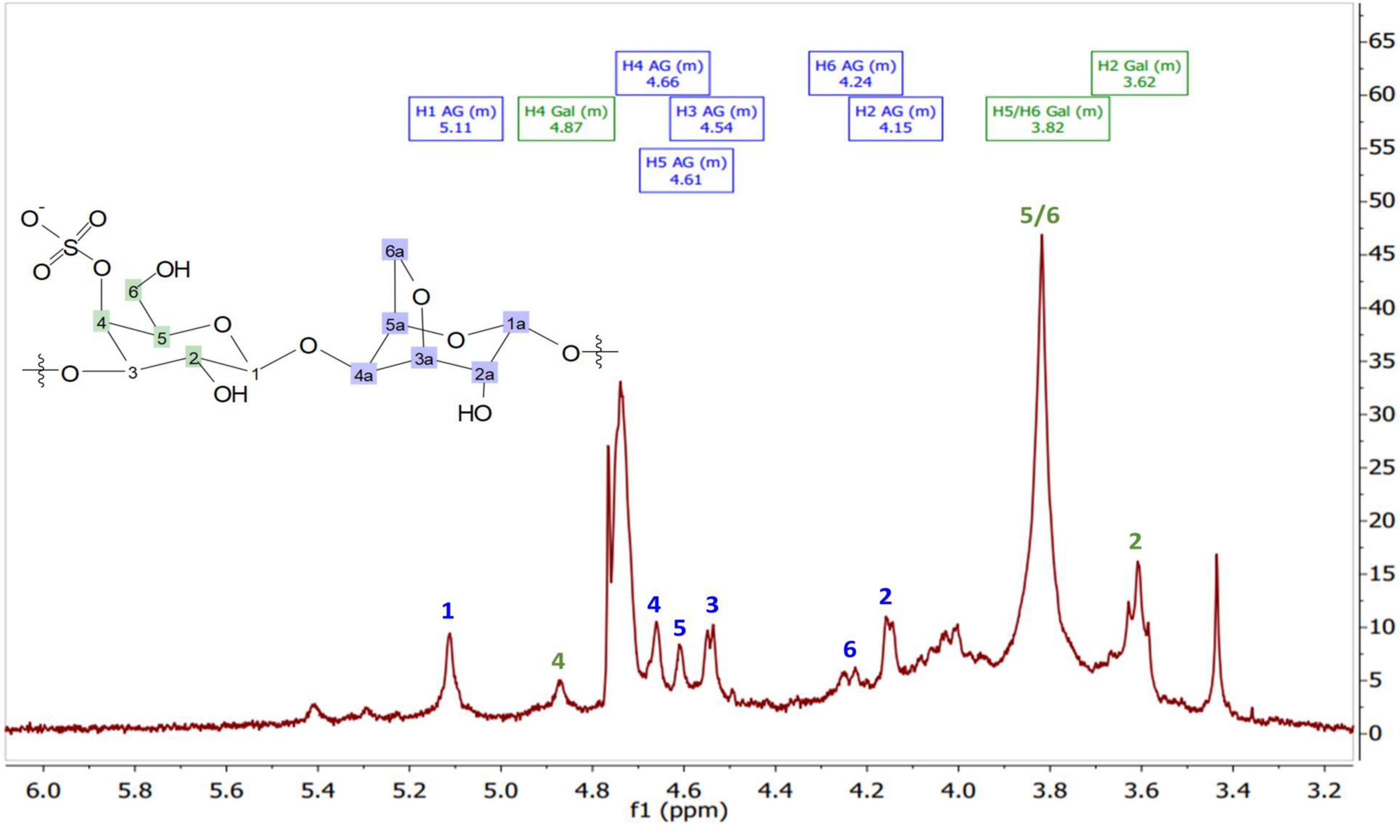

Figure S2. ^{1}H-NMR spectrum of *kappa*-carrageenan in D_2O. Signals are numbered according to the protons in the galactose-4-sulphate moiety (*green*) and 3,6-anhydrogalactose moiety (*blue*). For more details, see Legend to Figure S1.

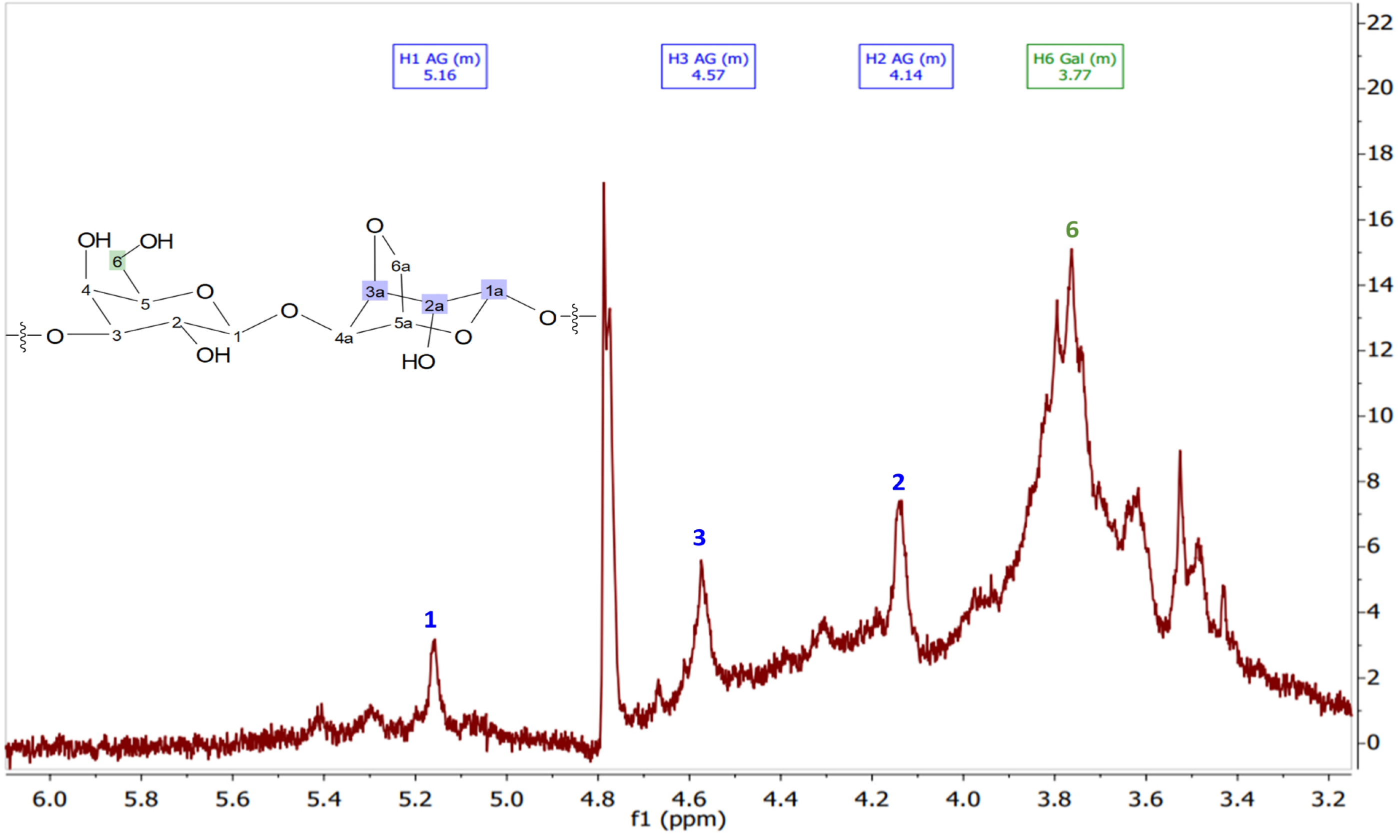

Figure S3. ^{1}H-NMR spectrum of agar-agar in D_2O. Signals are numbered according to the protons in the galactose moiety (*green*) and 3,6-anhydrogalactose moiety (*blue*). For more details, see Legend to Figure S1.

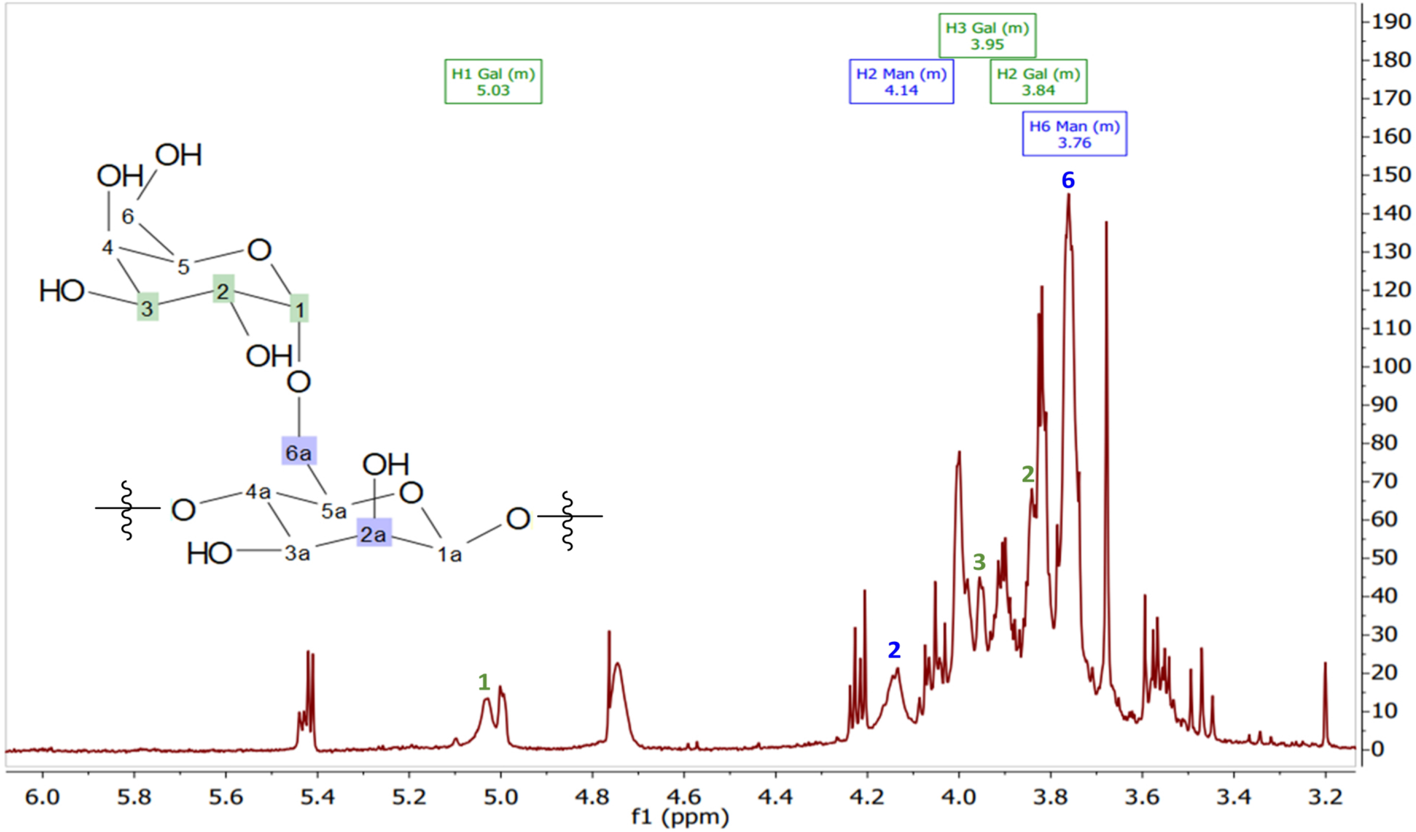

Figure S4. ^{1}H-NMR spectrum of locust bean gum in D_2O as a representative for the galactomannans. Signals are numbered according to the protons in the galactose moiety (*green*) and mannose moiety (*blue*). For more details, see Legend to Figure S1.

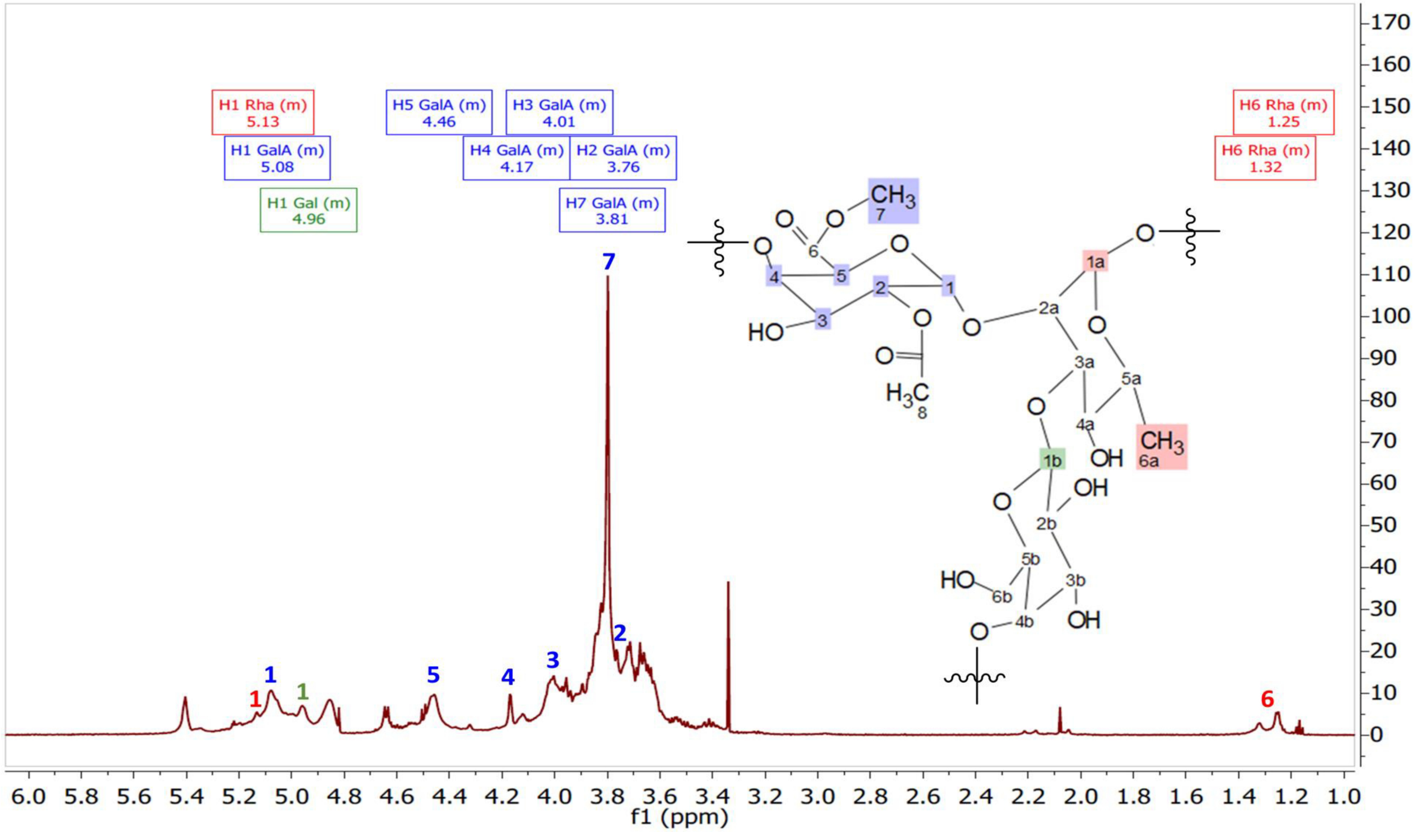

Figure S5. ^{1}H-NMR spectrum of pectin in D_2O. Signals are numbered according to the protons in the galactose moiety (*green*), rhamnose moiety (*red*) and galacturonic acid moiety (*blue*). For more details, see Legend to Figure S1.

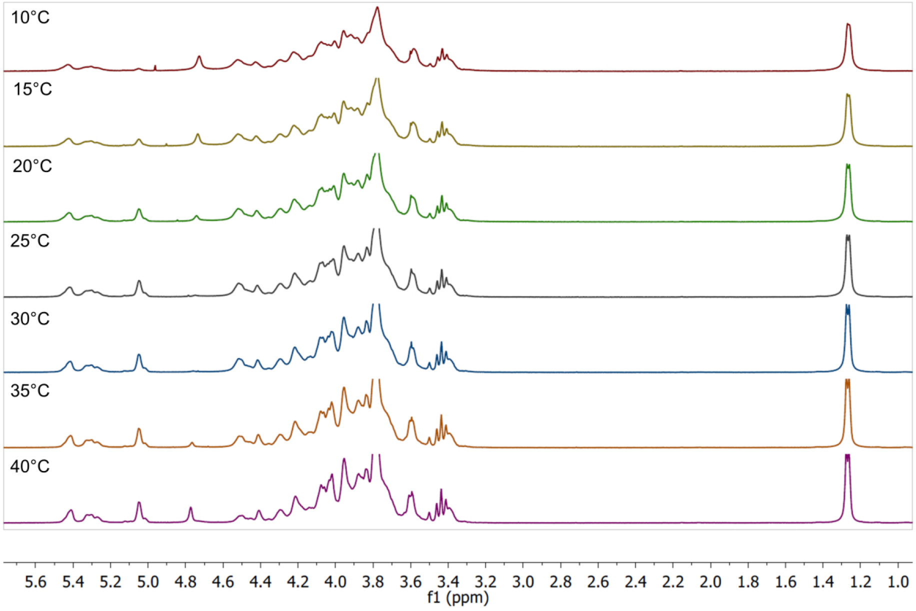

Figure S6. ^{1}H-NMR spectra of standard gum arabic in D_2O recorded at different temperatures (10°C, 15°C, 20°C, 25°C, 30°C, 35°C and 40°C). Measurement with ^{1}H-NMR spectroscopy with water suppression (400 MHz, ns 64, ds 4).

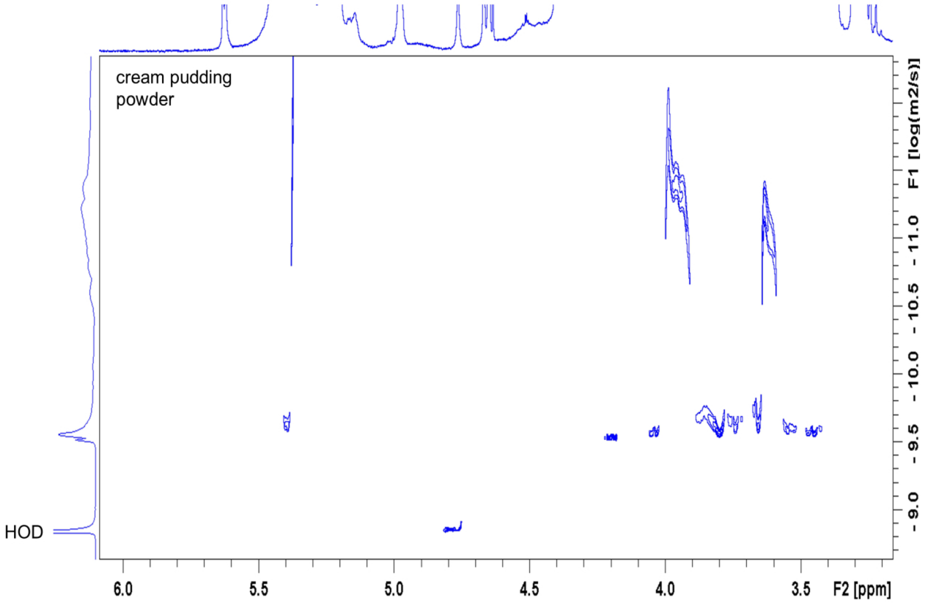

Figure S7. DOSY spectrum of the cream pudding powder in D_2O. Measurement with DOSY spectroscopy (400 MHz, ns 16, ds 4, TE 25°C).

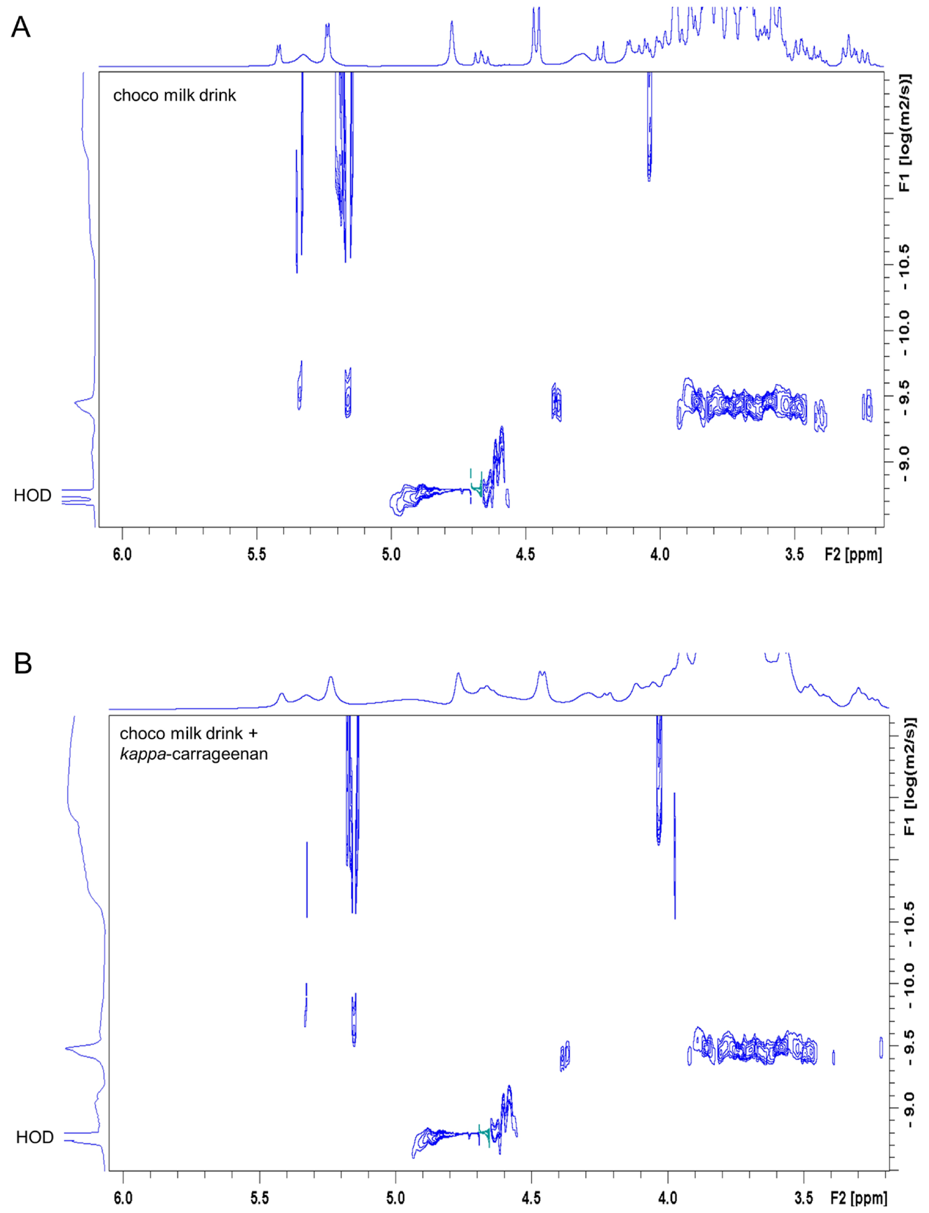

Figure S8. DOSY spectra of the choco milk drink (A) and choco milk drink spiked with standard *kappa*-carrageenan (B) in D_2O. Measurement with DOSY spectroscopy (400 MHz, ns 16, ds 4, TE 25°C).

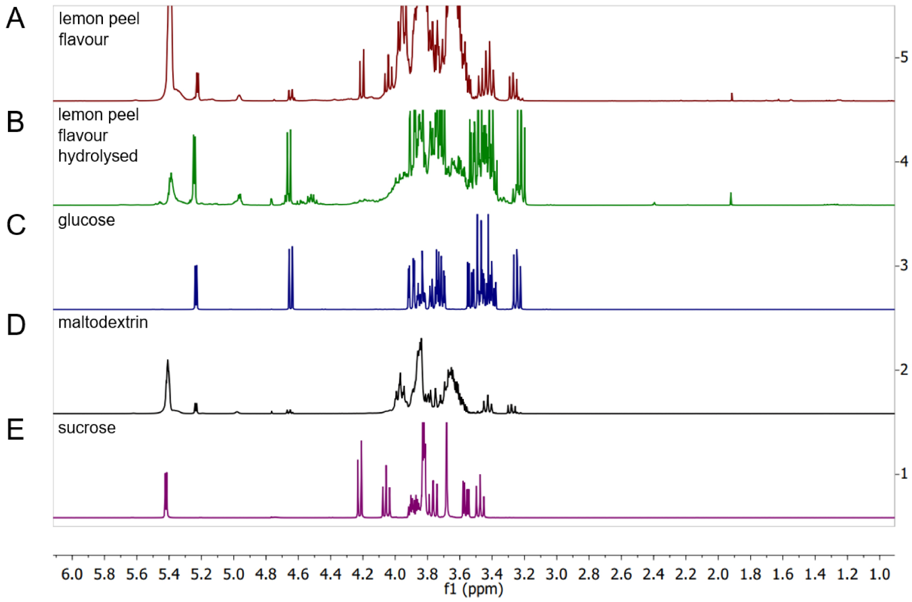

Figure S9. ^{1}H-NMR spectra of lemon peel flavour (A), lemon peel flavour after hydrolysis in D_2O/TFA (70/30; w:w) for 3h at 80°C and neutralization with 1M NaOH (B), standard glucose (C), standard maltodextrin (D) and standard sucrose (E) in D_2O. Measurement with ^{1}H-NMR spectroscopy with water suppression (400 MHz, ns 64, ds 4, TE 27°C).

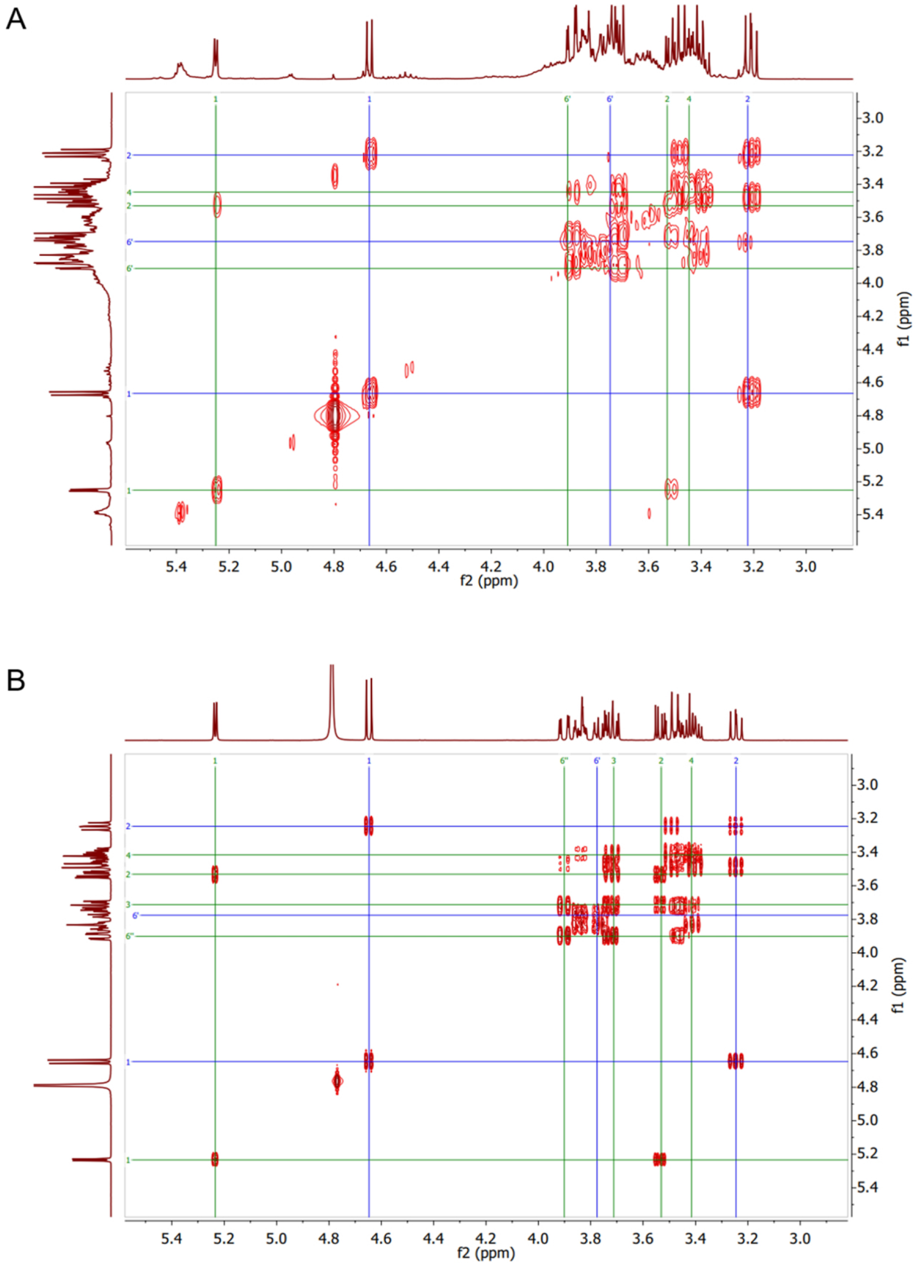

Figure S10. ^1H-^1H-COSY spectra of lemon peel flavour after hydrolysis in D_2O/TFA (70/30; w:w) for 3h at 80°C and neutralization with 1M NaOH (A) and standard glucose (B) in D_2O. Measurement with ^1H-^1H-COSY spectroscopy (400 MHz, ns 16, ds 32, TE 25°C).

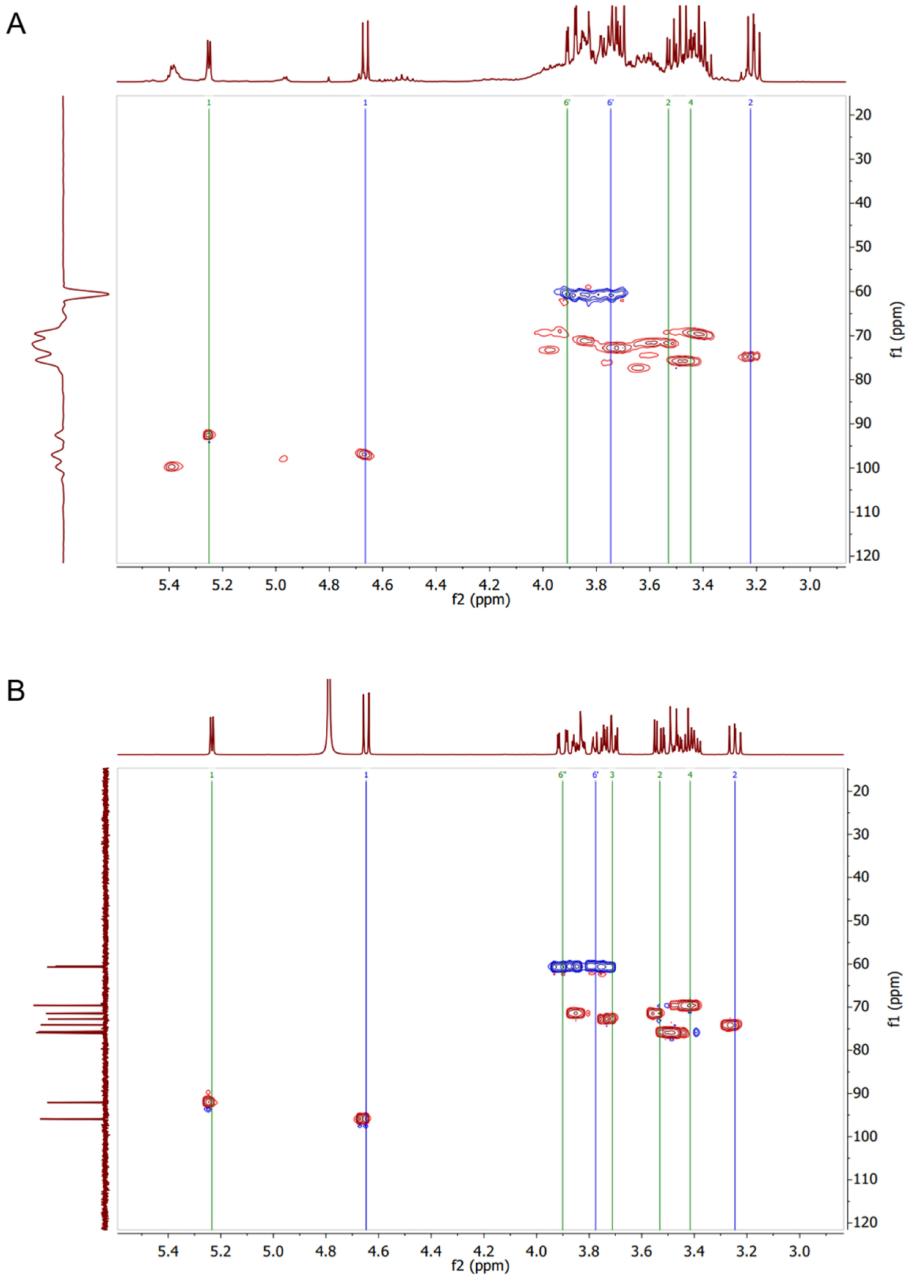

Figure S11. ^1H-^{13}C-HSQC spectra of lemon peel flavour after hydrolysis in D_2O/TFA (70/30; w:w) for 3h at 80°C and neutralization with 1M NaOH (A) and standard glucose (B) in D_2O. Measurement with ^1H-^{13}C-HSQC spectroscopy (400 MHz, ns 16, ds 32, TE 25°C).

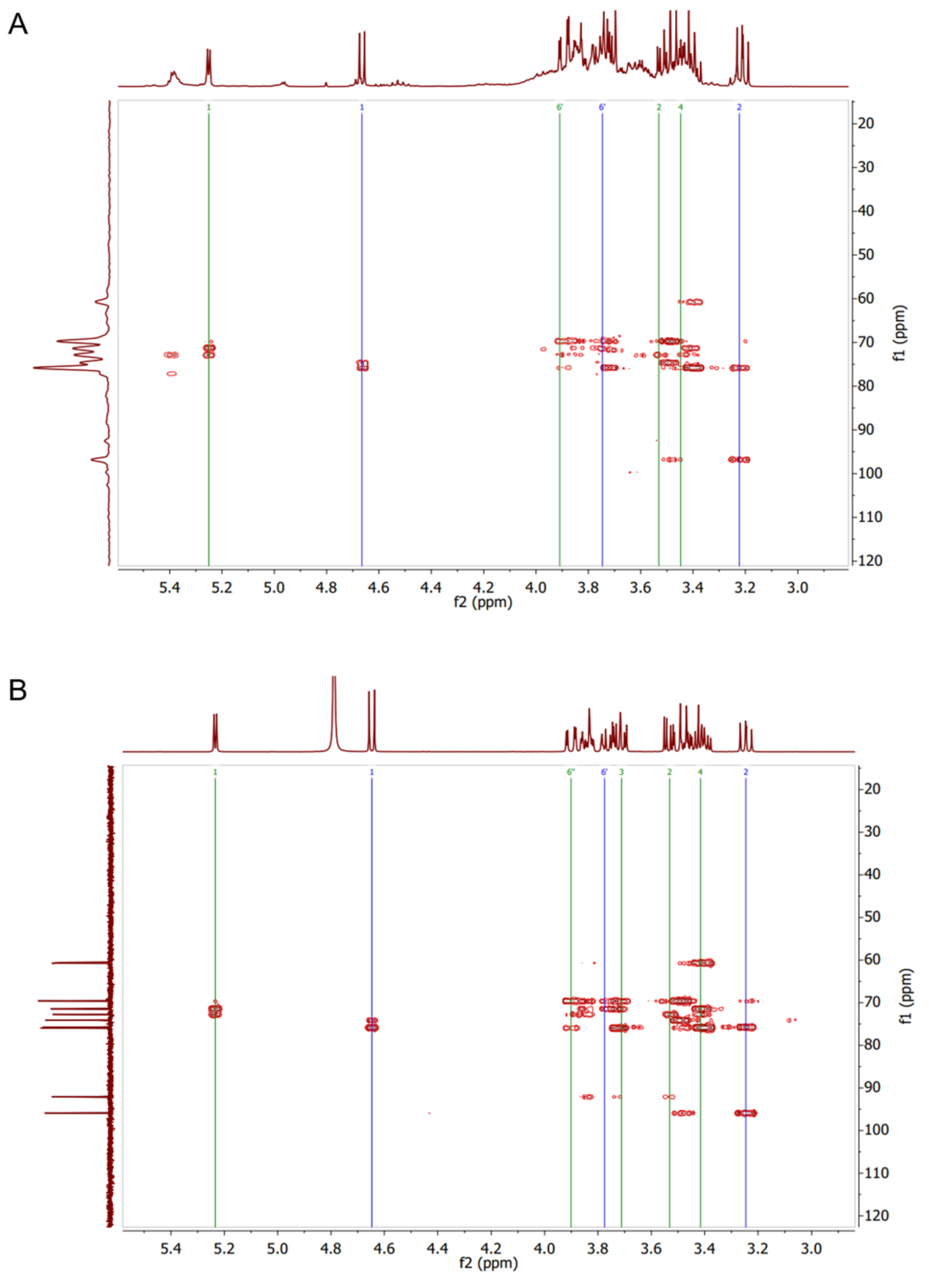

Figure S12. ^{1}H-^{13}C-HMBC spectra of lemon peel flavour after hydrolysis in D_2O/TFA (70/30; w:w) for 3h at 80°C and neutralization with 1M NaOH (A) and standard glucose (B) in D_2O. Measurement with ^{1}H-^{13}C-HMBC spectroscopy (400 MHz, ns 16, ds 32, TE 25°C).

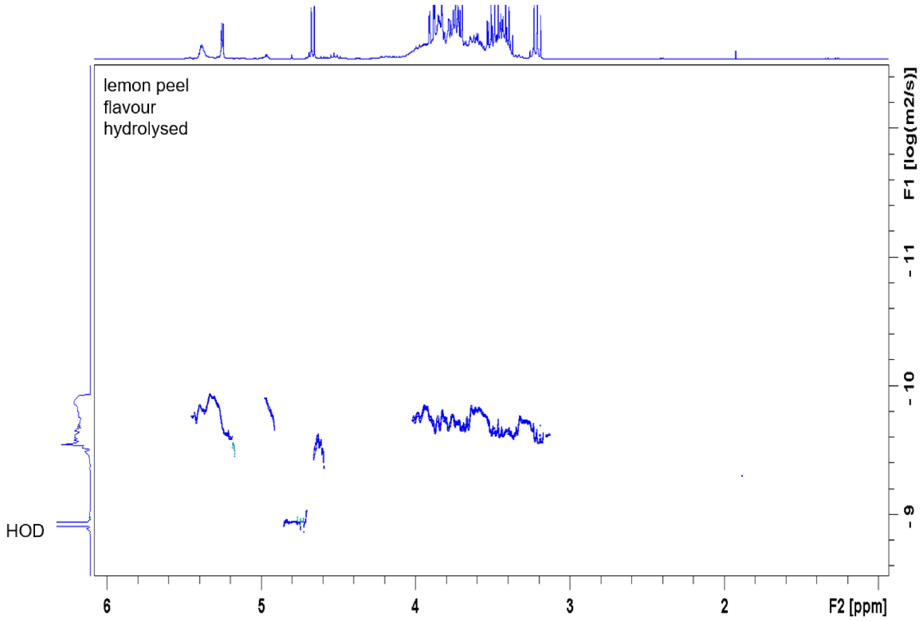

Figure S13. DOSY spectrum of the lemon peel flavour after hydrolysis in D_2O/TFA (70/30; w:w) for 3h at 80°C and neutralization with 1M NaOH in D_2O. Measurement with DOSY spectroscopy (400 MHz, ns 16, ds 4, TE 25°C).

REFERENCES

[1] Nie, S. P., Wang, C., Cui, S. W., Wang, Q., Xie, M. Y., Phillips, G. O. A further amendment to the classical core structure of gum arabic (Acacia senegal). *Food Hydrocoll.* **2013**, 31, 42-48.

[2] Tojo, E., Prado, J. A simple 1H NMR method for the quantification of carrageenans in blends. *Carbohydr. Polym*. **2003**, 53, 325-329.

[3] Usov, A. I. NMR Spectroscopy of Red Seaweed Polysaccharides: Agars, Carrageenans, and Xylans. *Botanica Marina*. **1984**, 27, 189-202.

[4] Muschin, T., Yoshida, T. Structural analysis of galactomannans by NMR spectroscopy. *Carbohydr. Polym*. **2012**, 87, 1893-1898.

[5] Zhi, Z., Chen, J., Li, S., Wang, W., Huang, R., Liu, D., Ding, T., Linhardt, R., Chen, S., Ye, X. Fast preparation of RG-I enriched ultra-low molecular weight pectin by an ultrasound accelerated Fenton process. *Sci. Rep*. **2017**, 7, 1-11.

9.2 Supporting information to "NMR-based identification of thickeners in membrane-filtered food premixtures"

Supporting information

NMR-based identification of thickeners in membrane-filtered food premixtures

Sandra Radziej[†‡], Julia Scherb-Forster[†], Claus Schlicht[†] and Wolfgang Eisenreich[‡*]

[†] Bayerisches Landesamt für Gesundheit und Lebensmittelsicherheit, Veterinärstraße 2, D-85764 Oberschleißheim, Germany

[‡] Technische Universität München, Bavarian NMR Center – Structural Membrane Biochemistry, Department of Chemistry, Lichtenbergstraße 4, D-85747 Garching, Germany

CORRESPONDING AUTHOR FOOTNOTE.

* Author to whom correspondence should be addressed [Tel.: +49-(0)89-289-13336. Fax: +49-(0)89-289-13363. E-mail: wolfgang.eisenreich@mytum.de]

Compound sauce (containing guar gum)

Because of its ability to enhance the viscosity of the water phase, guar gum is not only used in bakery products or salad dressings, but also in sauces like tomato ketchup [1].

As a model premixture, a compound sauce containing maize starch, glucose syrup, wholemeal rice flour and guar gum was directly measured by ^{1}H-NMR spectroscopy. Further on, 100 mg of the compound sauce were prepared as previously described and filtrate and filter residue were measured by NMR spectroscopy. The ^{1}H-NMR spectrum of the directly measured compound sauce (Fig. S1B) revealed many overlapping signals not only from 4.60 ppm to 3.20 ppm, but also from 5.40 ppm to 4.80 ppm. It seemed that the compound sauce contained high concentrations of different sugar components as the anomeric protons usually appear in this range (5.40 ppm to 4.60 ppm). Nevertheless, characteristic signals from the declared thickener guar gum were not detected. Conversely, the ^{1}H-NMR spectrum of the filter residue of the compound sauce (Fig. S1C) displayed among others, a broad signal at 5.03 ppm, which increased after spiking the compound sauce with standard guar gum (Fig. S1D). Again, the ^{1}H-NMR spectra of the filtrate from the compound sauce (Fig. S1E) and the compound sauce spiked with guar gum (Fig. S1F) showed sharp signals belonging to low molecular substances (below 100 kDa), whereas the thickener guar gum could not be detected.

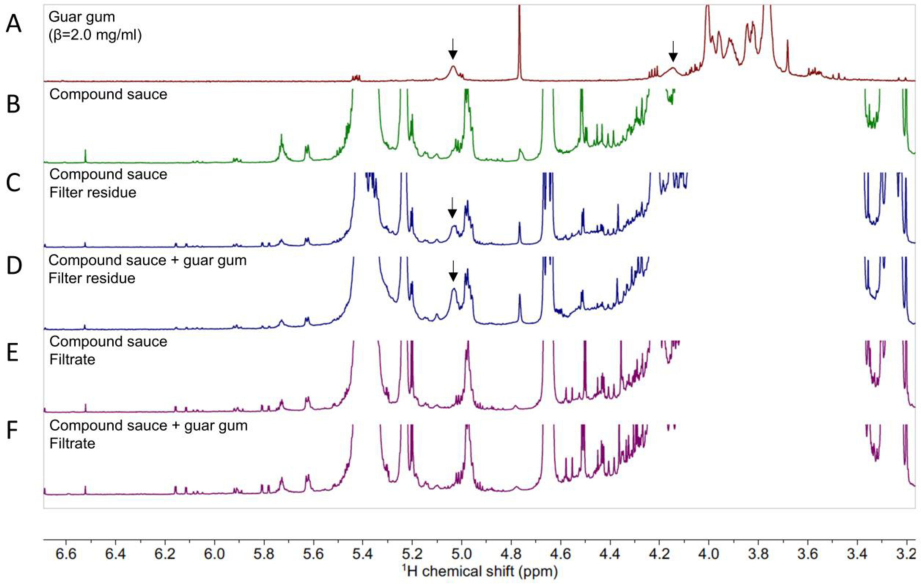

Fig. S1. ^{1}H-NMR spectra of standard guar gum (A), compound sauce (B), the filter residue of the compound sauce (C), the filter residue of the compound sauce spiked with guar gum (D), the filtrate of the compound sauce (E) and the filtrate of the compound sauce spiked with guar gum (F) in D_2O. Measurement with ^{1}H-NMR spectroscopy with water suppression (400 MHz, ns 512, ds 4, TE 27°C). Guar gum signals at 5.03 ppm and 4.14 ppm are indicated by black arrows.

First infant milk powder (containing locust bean gum)

For treatment of excessive regurgitation, locust bean gum is often applied as a thickening agent in commercially available infant formulas [2].

One example is the first infant milk powder for the dietary management of frequent regurgitation, which contained – according to the ingredients list – lactose, vegetable oils, skimmed milk, whey and locust bean gum as main components. For the analysis of the declared thickener locust bean gum, 50 mg of the milk powder were dissolved in 1 ml D_2O for the direct NMR measurement. Additionally, a sample preparation using the centrifugal concentrators was processed before measuring filter residue and filtrate by NMR spectroscopy. The ^{1}H-NMR spectrum of the directly measured milk powder (Fig. S2B) showed a slight rise of the baseline under the sharp doublet signal at 5.01 ppm, but the declared thickener locust bean gum could not be unequivocally identified. In the ^{1}H-NMR spectrum of the filter residue from the milk powder (Fig. S2C) a broad signal at 5.03 ppm could be detected, although a minor residue of the sharp doublet signal was also determined and led to an overlapping. Because the centrifugal concentrations had a built-in deadstop feature [3], it can be assumed that about 10% of the low molecular weight substances (below 100 kDa) remained in the filter residue and resulted in these sharp signals. Nevertheless, the ^{1}H-NMR spectrum of the filter residue from the milk powder spiked with the reference locust bean gum (Fig. S2D) revealed a broad galactomannan signal at 5.03 ppm with a small sharp doublet signal on top. Again, no broad signal at 5.03 ppm could be detected in the ^{1}H-NMR spectra of the filtrate from the milk powder (Fig. S2E) and the milk powder spiked with the reference locust bean gum (Fig. S2F).

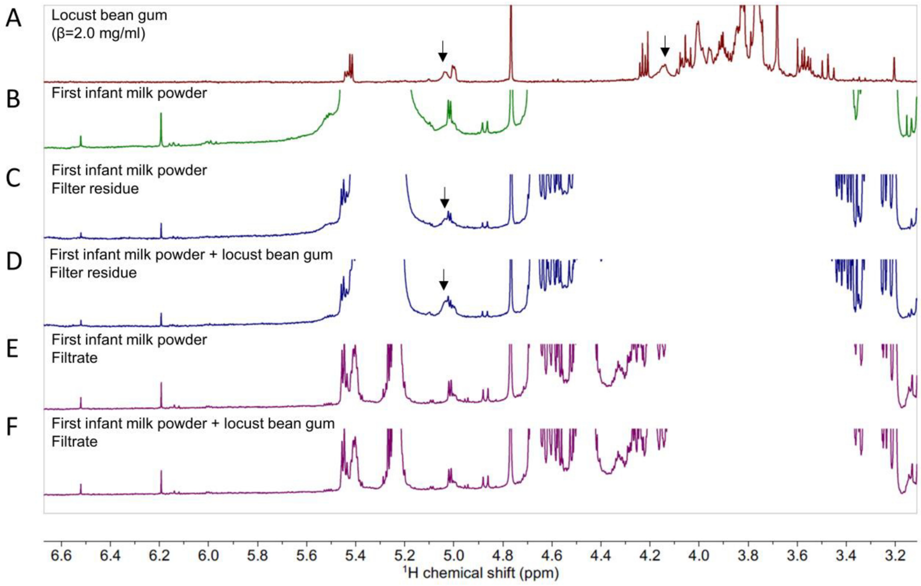

Fig. S2. ^{1}H-NMR spectra of standard locust bean gum (A), first infant milk powder (B), the filter residue of the first infant milk powder (C), the filter residue of the first infant milk powder spiked with locust bean gum (D), the filtrate of the first infant milk powder (E) and the filtrate of the first infant milk powder spiked with locust bean gum (F) in D_2O. Measurement with ^{1}H-NMR spectroscopy with water suppression (400 MHz, ns 512, ds 4, TE 27°C). Locust bean gum signals at 5.03 ppm and 4.14 ppm are indicated by black arrows.

Ice cream mix (containing locust bean gum)

For the inhibition of ice recrystallization, locust bean gum is often applied in frozen dairy products [4]. As a model premixture, 50 mg of an ice cream mix was directly measured by NMR spectroscopy and additionally centrifuged using centrifugal concentrators. The ^{1}H-NMR spectrum of the directly measured ice cream mix (Fig. S3B) showed sharp signals with high intensities, but no characteristic marker signal for galactomannans. In contrast, a characteristic marker signal at 5.03 ppm could be detected in the ^{1}H-NMR spectrum of the filter residue from the ice cream mix (Fig. S3C) which showed a higher intensity after spiking the premixture with the reference locust bean gum (Fig. S3D). As expected, the ^{1}H-NMR spectra of the filtrate from the ice cream mix (Fig. S3E) and the ice cream mix spiked with locust bean gum (Fig. S3F) showed sharp signals belonging to low molecular substances.

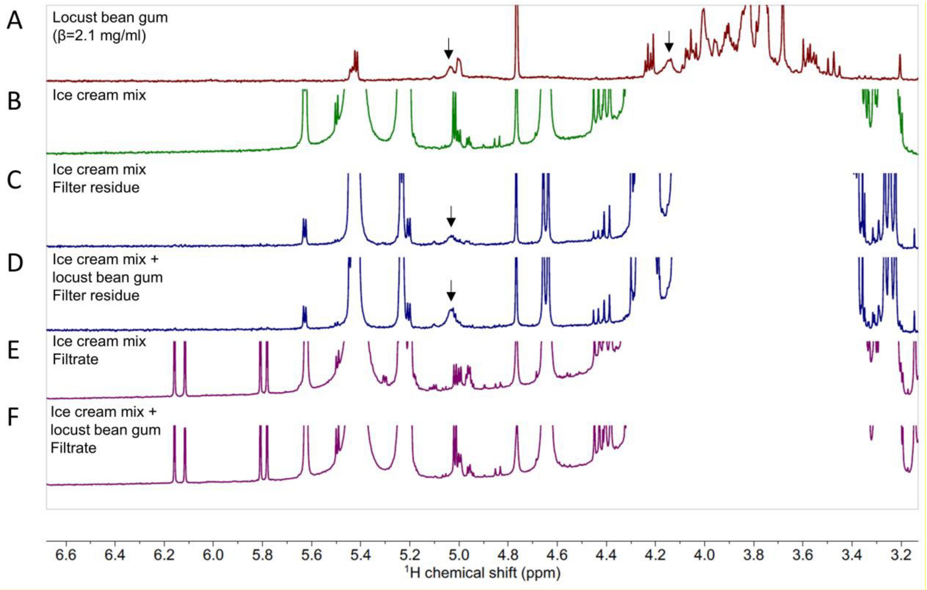

Fig. S3. ^{1}H-NMR spectra of standard locust bean gum (A), ice cream mix (B), the filter residue of the ice cream mix (C), the filter residue of the ice cream mix spiked with locust bean gum (D), the filtrate of the ice cream mix (E) and the filtrate of the ice cream mix spiked with locust bean gum (F) in D_2O. Measurement with ^{1}H-NMR spectroscopy with water suppression (400 MHz, ns 512, ds 4, TE 27°C). Locust bean gum signals at 5.03 ppm and 4.14 ppm are indicated by black arrows.

Ice dessert strawberry (containing pectin, guar gum and xanthan)

A small size of ice crystals is important for a smooth texture and depends on different processing factors and the presence of stabilizers. For this purpose, the stabilizer pectin, a polysaccharide mainly obtained from citrus peels and apple pomace, is often used for quality improvement of ice cream and other milk products [5-7].

One example for a premixture is the commercially available ice dessert strawberry which contained the thickeners pectin, guar gum and xanthan gum. Because of too low concentration, the ^{1}H-NMR spectrum of the directly measured premixture did not reveal any characteristic marker signals for the declared thickeners [8]. Therefore, the ice dessert strawberry was dissolved in 2 ml H_2O, centrifuged with centrifugal concentrators and freeze-dried overnight. Then, filtrate and filter residue were dissolved in 1 ml D_2O and measured by ^{1}H-NMR spectroscopy.

In contrast to the ^{1}H-NMR spectrum of the directly measured ice dessert (Fig. S4D), the ^{1}H-NMR spectrum of the filter residue from the ice dessert (Fig. S4E) revealed among other signals a characteristic pectin signal at 5.08 ppm and a characteristic guar gum signal at 5.03 ppm. Xanthan gum signals were missing. Solutions with xanthan gum usually show a high viscosity even at low concentrations. Therefore, applications often contain xanthan gum in concentrations between 0.05% and 0.5% [9]. It seemed that the used concentration of xanthan gum in the ice dessert was too low for a detection by NMR spectroscopy. Spiking the ice dessert with the reference pectin led to an increased signal at 5.08 ppm in the ^{1}H-NMR spectrum of the filter residue (Fig. S4F), whereas the characteristic galactomannan signal at 5.03 ppm showed a higher intensity in the ^{1}H-NMR spectrum of the filter residue after spiking the ice dessert with the reference guar gum (Fig. S4G). Further on, the ^{1}H-NMR spectra of the filtrate from the ice dessert (Fig. S4H) and the ice dessert spiked with pectin (Fig. S4I) and guar gum (Fig. S4J) did not show any broad signals for these thickeners.

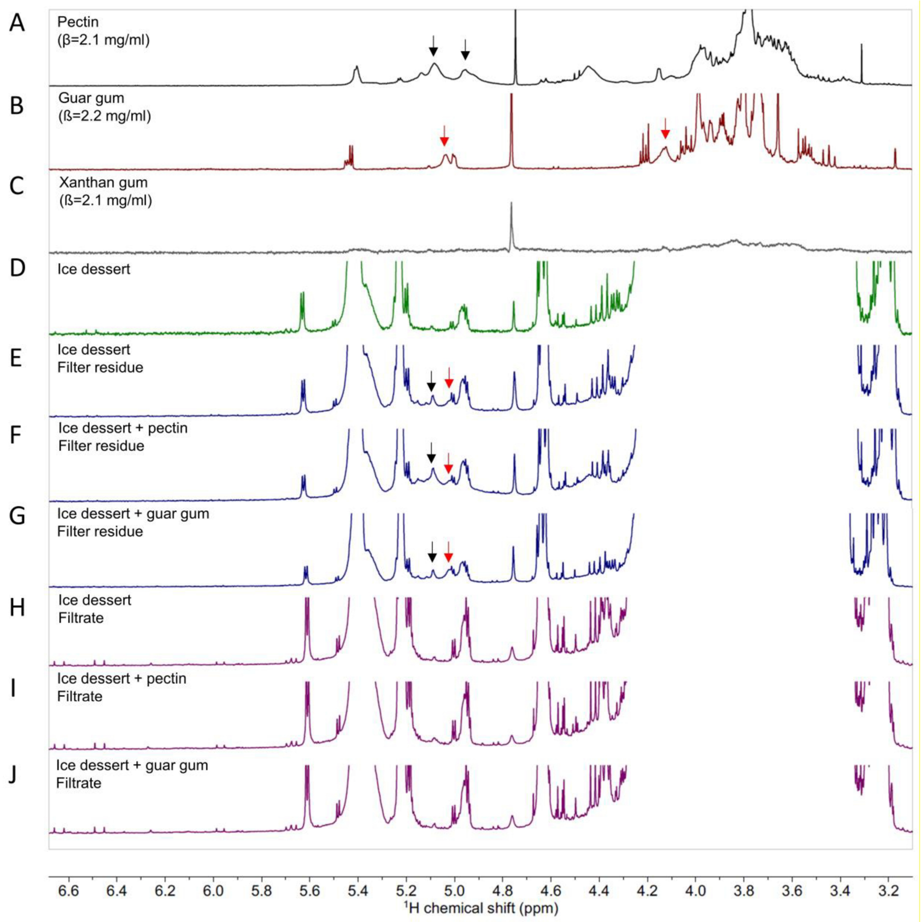

Fig. S4. ^{1}H-NMR spectra of standard pectin (A), standard guar gum (B), standard xanthan gum (C), ice dessert (D), the filter residue of the ice dessert (E), the filter residue of the ice dessert spiked with pectin (F), the filter residue of the ice dessert spiked with guar gum (G), the filtrate of the ice dessert (H), the filtrate of the ice dessert spiked with pectin (I) and the filtrate of the ice dessert spiked with guar gum (J) in D_2O. Measurement with ^{1}H-NMR spectroscopy with water suppression (400 MHz, ns 512, ds 4, TE 27°C). Pectin signals at 5.08 ppm and 4.96 ppm are indicated by black arrows. Guar gum signals at 5.03 ppm and 4.14 ppm are indicated by red arrows.

Standardized thickening agent (containing κ-carrageenan)

κ-Carrageenan has the ability to build strong gels not only with other thickeners like locust bean gum or gellan, but can also interact with milk proteins. Therefore, it is often used as a stabilizer and suspending agent in dairy products. In order to guaranty a constant dispersion behavior and gel stability in ready to sale food, it is further standardized with sugars [10].

An example for a standardized thickening agent is now described in detail. For the identification of the declared thickener carrageenan, the standardized thickening agent was first directly measured by NMR spectroscopy and then additionally centrifuged with centrifugal concentrations in order to achieve a separation of ingredients on the basis of different molecular weights. Although the standardized thickening agent only consisted of carrageenan and wheat dextrose, the ^{1}H-NMR spectrum of the directly measured standardized thickening agent (Fig. S5B) showed broad overlapping signals with poor resolution. Characteristic marker signals for κ-carrageenan could not be unequivocally determined because the combination of carrageenan and dextrose led to a solution with high viscosity due to synergistic effects. In contrast, broad signals at 5.11 ppm, 4.87 ppm, 4.54 ppm and 4.15 ppm were detected in the ^{1}H-NMR spectrum of the filter residue from the standardized thickening agent (Fig. S5C), which are marker signals for κ-carrageenan. Further on, spiking the thickening agent with standard κ-carrageenan led to increased signals in the ^{1}H-NMR spectrum of the filter residue (Fig. S5D). The ^{1}H-NMR spectra of the filtrate from the standardized thickening agent (Fig. S5E) and standardized thickening agent spiked with κ-carrageenan (Fig. S5F) contained numerous sharp signals with high resolution belonging to the wheat dextrose, but no signals belonging to the high molecular weight κ-carrageenan.

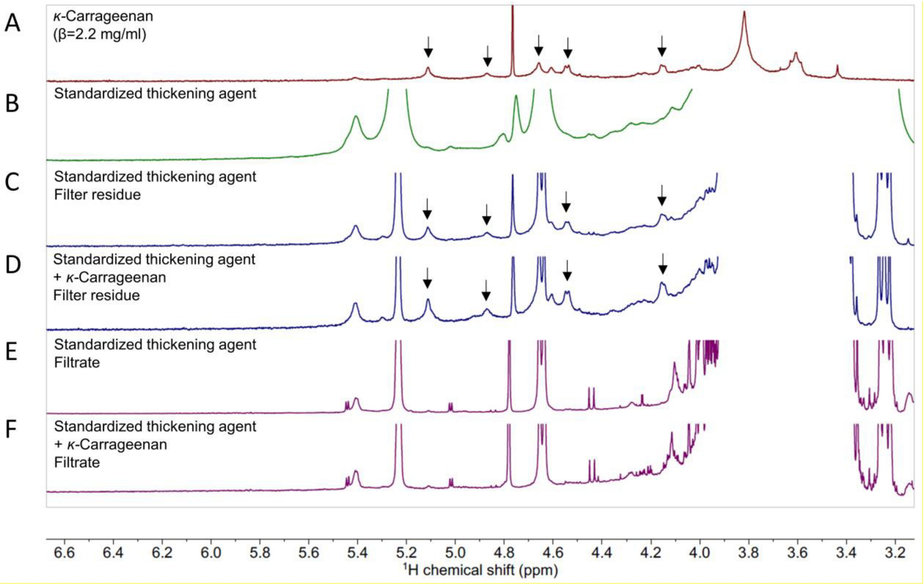

Fig. S5. ^{1}H-NMR spectra of standard κ-carrageenan (A), standardized thickening agent (B), the filter residue of the standardized thickening agent (C), the filter residue of the standardized thickening agent spiked with κ-carrageenan (D), the filtrate of the standardized thickening agent (E) and the filtrate of the standardized thickening agent spiked with κ-carrageenan (F) in D_2O. Measurement with ^{1}H-NMR spectroscopy with water suppression (400 MHz, ns 512, ds 4, TE 27°C). κ-Carrageenan signals at 5.11 ppm, 4.87 ppm, 4.66 ppm, 4.54 ppm and 4.15 ppm are indicated by black arrows.

Brine supplement (containing κ-carrageenan)

Carrageenan is a food thickener which increases the water binding capacity and changes the texture of meat products like sausages [11]. Therefore, brine supplements often contain among other substances also carrageenan as food additive. In the following, the analysis of a brine supplement is described in more detail.

An amount of 50 mg brine supplement was dissolved in 1 ml D_2O and directly measured by ^{1}H-NMR spectroscopy. Additionally, 50 mg of the brine supplement were centrifuged following the established protocol (see sample preparation) and measured by ^{1}H-NMR spectroscopy. Although the ^{1}H-NMR spectrum of the brine supplement (Fig. S6B) revealed many sharp signals with high intensities belonging to sugars, characteristic κ-carrageenan signals were not detected. It seemed that the applied concentration of κ-carrageenan in the premixture was too low for a direct identification by NMR spectroscopy. In contrast, broad low intensity signals at 5.11 ppm, 4.87 ppm, 4.54 ppm and 4.15 ppm were detectable in the ^{1}H-NMR spectrum of the filter residue from the brine supplement (Fig. S6C) which are characteristic for κ-carrageenan. These signals increased after spiking the brine supplement with standard κ-carrageenan (Fig. S6D). Again, the ^{1}H-NMR spectra of the filtrates (Fig. S6E, Fig. S6F) did not show any broad signals belonging to high molecular substances, but many sharp signals with high intensity sugar signals.

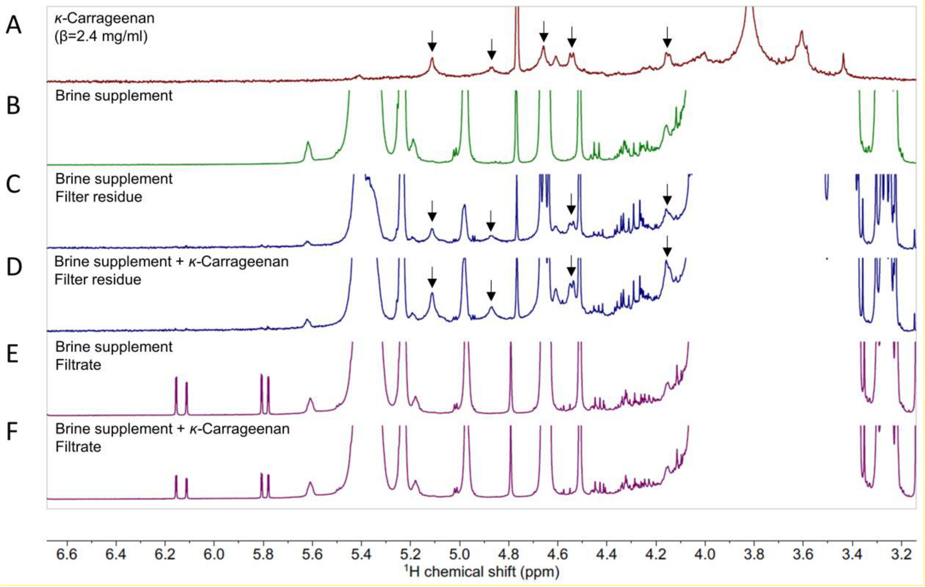

Fig. S6. ^{1}H-NMR spectra of standard κ-carrageenan (A), brine supplement (B), the filter residue of the brine supplement (C), the filter residue of the brine supplement spiked with κ-carrageenan (D), the filtrate of the brine supplement (E) and the filtrate of the brine supplement spiked with κ-carrageenan (F) in D_2O. Measurement with ^{1}H-NMR spectroscopy with water suppression (400 MHz, ns 512, ds 4, TE 27°C). κ-Carrageenan signals at 5.11 ppm, 4.87 ppm, 4.66 ppm, 4.54 ppm and 4.15 ppm are indicated by black arrows.

Gelling agent (containing κ-carrageenan and locust bean gum)

Because κ-carrageenan shows synergistic effects with locust bean gum, the combination of both thickeners is often used in food products like glaze or cooked meat [12,13].

As a model premixture containing carrageenan and locust bean gum, 100 mg of a gelling agent were dissolved in 1 ml D_2O and directly measured by ^{1}H-NMR spectroscopy. In another experimental setup, the ingredients of the gelling agent were separated by centrifugal concentrators according to their molecular weight and then measured by ^{1}H-NMR spectroscopy. The ^{1}H-NMR spectrum of the directly measured gelling agent (Fig. S7C) included many sharp signals belonging to sucrose (e.g. anomeric proton at 5.40 ppm) and glucose (e.g. anomeric protons at 5.20 ppm and 4.60 ppm), but no characteristic marker signals for κ-carrageenan or locust bean gum were detectable. Again, characteristic marker signals for κ-carrageenan at 5.11 ppm, 4.87 ppm, 4.54 ppm and 4.15 ppm and characteristic marker signals for locust bean gum at 5.03 ppm and 4.14 ppm were detected in the ^{1}H-NMR spectrum of the filter residue from the gelling agent (Fig. S7D). Because of similar chemical shifts, the broad signal at 4.15 ppm could reflect an overlapping signal for both thickeners. Spiking experiments with standards led to the same broad signals with increased intensities in the ^{1}H-NMR spectra of the filter residue (Fig. S7E, Fig. S7F), although the ^{1}H-NMR spectrum of the filter residue from the premixture spiked with κ-carrageenan showed a worse resolution due to high viscosity. Again, the ^{1}H-NMR spectrum of the filtrate from the gelling agent (Fig. S7G). as well as the ^{1}H-NMR spectra of the filtrates from the gelling agent spiked with standard κ-carrageenan (Fig. S7H) or locust bean gum (Fig. S7I) displayed the same sharp signals with similar signal intensities belonging to substances with molecular weight below

100 kDa, whereas the macromolecular standards κ-carrageenan and locust bean gum were not detectable.

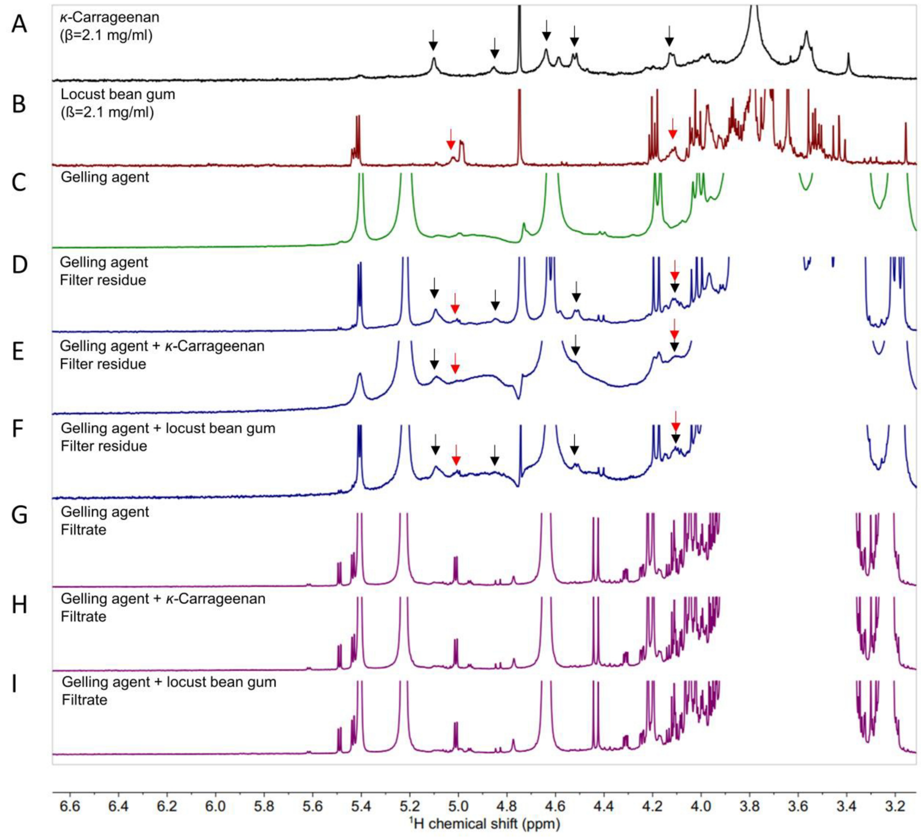

Fig. S7. ^{1}H-NMR spectra of standard κ-carrageenan (A), standard locust bean gum (B), gelling agent (C), the filter residue of the gelling agent (D), the filter residue of the gelling agent spiked with κ-carrageenan (E), the filter residue of the gelling agent spiked with locust bean gum (F), the filtrate of the gelling agent (G), the filtrate of the gelling agent spiked with κ-carrageenan (H) and the filtrate of the gelling agent spiked with locust bean gum (I) in D_2O. Measurement with ^{1}H-NMR spectroscopy with water suppression (400 MHz, ns 512, ds 4, TE 27°C). κ-Carrageenan signals at 5.11 ppm, 4.87 ppm, 4.66 ppm, 4.54 ppm and 4.15 ppm are indicated by black arrows. Locust bean gum signals at 5.03 ppm and 4.14 ppm are indicated by red arrows.

Instant flavoured drink (containing gum arabic)

Because of its high content of arabinogalactan (about 90%), gum arabic is often used as a stabilizer and emulsifier in beverages [14]. One example for a premixture is the instant flavoured drink, which contained – according to the ingredients list – gum arabic as a thickener.

Although the ^{1}H-NMR spectrum of the directly measured instant flavoured drink (Fig. S8B) showed among others a broad signal at 5.03 ppm, other characteristic marker signals from gum arabic could not be unequivocally detected due to overlapping with signals belonging to other ingredients. In contrast, broad signals at 5.03 ppm, 4.52 ppm and 4.42 ppm could be determined in the ^{1}H-NMR spectrum of the filter residue from the instant flavoured drink (Fig. S8C). Further on, the ^{1}H-NMR spectrum of the filter residue from the instant flavoured drink spiked with gum arabic (Fig. S8D) displayed the same broad signals with increased intensities. The ^{1}H-NMR spectra of the filtrate from the instant flavoured drink (Fig. S8E) and instant flavoured drink spiked with gum arabic (Fig. S8F) contained numerous sharp signals with high resolution belonging to small molecular weight substances, but no signals belonging to the high molecular weight thickener gum arabic.

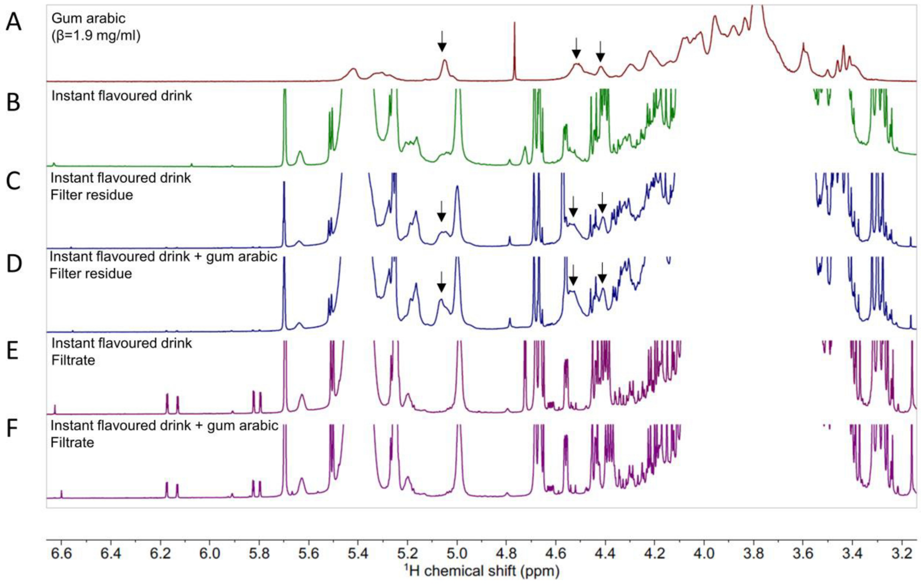

Fig. S8. ^{1}H-NMR spectra of standard gum arabic (A), instant flavoured drink (B), the filter residue of the instant flavoured drink (C), the filter residue of the instant flavoured drink spiked with gum arabic (D), the filtrate of the instant flavoured drink (E) and the filtrate of the instant flavoured drink spiked with gum arabic (F) in D_2O. Measurement with ^{1}H-NMR spectroscopy with water suppression (400 MHz, ns 512, ds 4, TE 27°C). Gum arabic signals at 5.03 ppm, 4.52 ppm and 4.42 ppm are indicated by black arrows.

REFERENCES

1. Mudgil D, Barak S, Khatkar BS (2014) Guar gum: processing, properties and food applications-A Review. J Food Sci Technol 51 (3):409-418

2. Meunier L, Garthoff JA, Schaafsma A, Krul L, Schrijver J, van Goudoever JB, Speijers G, Vandenplas Y (2014) Locust bean gum safety in neonates and young infants: An integrated review of the toxicological database and clinical evidence. Regulatory Toxicology and Pharmacology 70 (1):155-169

3. McRae R, Hannes L (2018) Application Note: Concentration to a defined final volume with Vivaspin® Turbo 15, Vivaspin® Tubro 4 and Vivaspin® 500. Sartorius Lab Instruments GmbH & Co. KG. https://www.sartorius.com/en/pr/lab-filtration/concentration-to-a-defined-final-volume-with-vivaspin-turbo-15-vivaspin-turbo-4-vivaspin-500/concentration-to-a-defined-final-volume-with-vivaspin-turbo-15-vivaspin-turbo-4-and-vivaspin-500-thank-you. Accessed 28.07.2021

4. Zhu BJ, Zayed MZ, Zhu HX, Zhao J, Li SP (2019) Functional polysaccharides of carob fruit: a review. Chin Med 14:40-40

5. Hagiwara T, Hartel RW (1996) Effect of Sweetener, Stabilizer, and Storage Temperature on Ice Recrystallization in Ice Cream. J Dairy Sci 79 (5):735-744

6. Park SH, Hong G-P, Kim JY, Choi M, Min S-G (2006) The influence of food hydrocolloids on changes in the physical properties of ice cream. Food Sci Biotechnol 15:721-727

7. Thakur BR, Singh RK, Handa AK (1997) Chemistry and uses of pectin-a review. Crit Rev Food Sci Nutr 37 (1):47-73

8. Radziej S, Scherb-Forster J, Schlicht C, Eisenreich W (2021) Fast Identification of Food Thickeners by Nontargeted NMR-Spectroscopy. J Agric Food Chem 69 (12):3761-3775

9. García-Ochoa F, Santos VE, Casas JA, Gómez E (2000) Xanthan gum: production, recovery, and properties. Biotechnol Adv 18 (7):549-579

10. Hotchkiss S, Brooks M, Campbell R, Philp K, Trius A (2016) The use of carrageenan in food. In: Pereira L (ed) Carrageenans. Nova Science Publishers, pp 229-243

11. Ayadi M, Kechaou A, Makni I, Attia H (2009) Influence of carrageenan addition on turkey meat sausage properties. J Food Eng 93:278-283

12. Arda E, Kara S, Pekcan Ö (2009) Synergistic effect of the locust bean gum on the thermal phase transitions of κ-carrageenan gels. Food Hydrocoll 23 (2):451-459

13. Saha D, Bhattacharya S (2010) Hydrocolloids as thickening and gelling agents in food: a critical review. J Food Sci Technol 47 (6):587-597

14. Reiner SJ, Reineccius GA, Peppard TL (2010) A Comparison of the Stability of Beverage Cloud Emulsions Formulated with Different Gum Acacia- and Starch-Based Emulsifiers. J Food Sci 75 (5):236-246

9.3 Notation to “NMR-based identification of thickeners in membrane-filtered food premixtures”

Reply letter to the journal

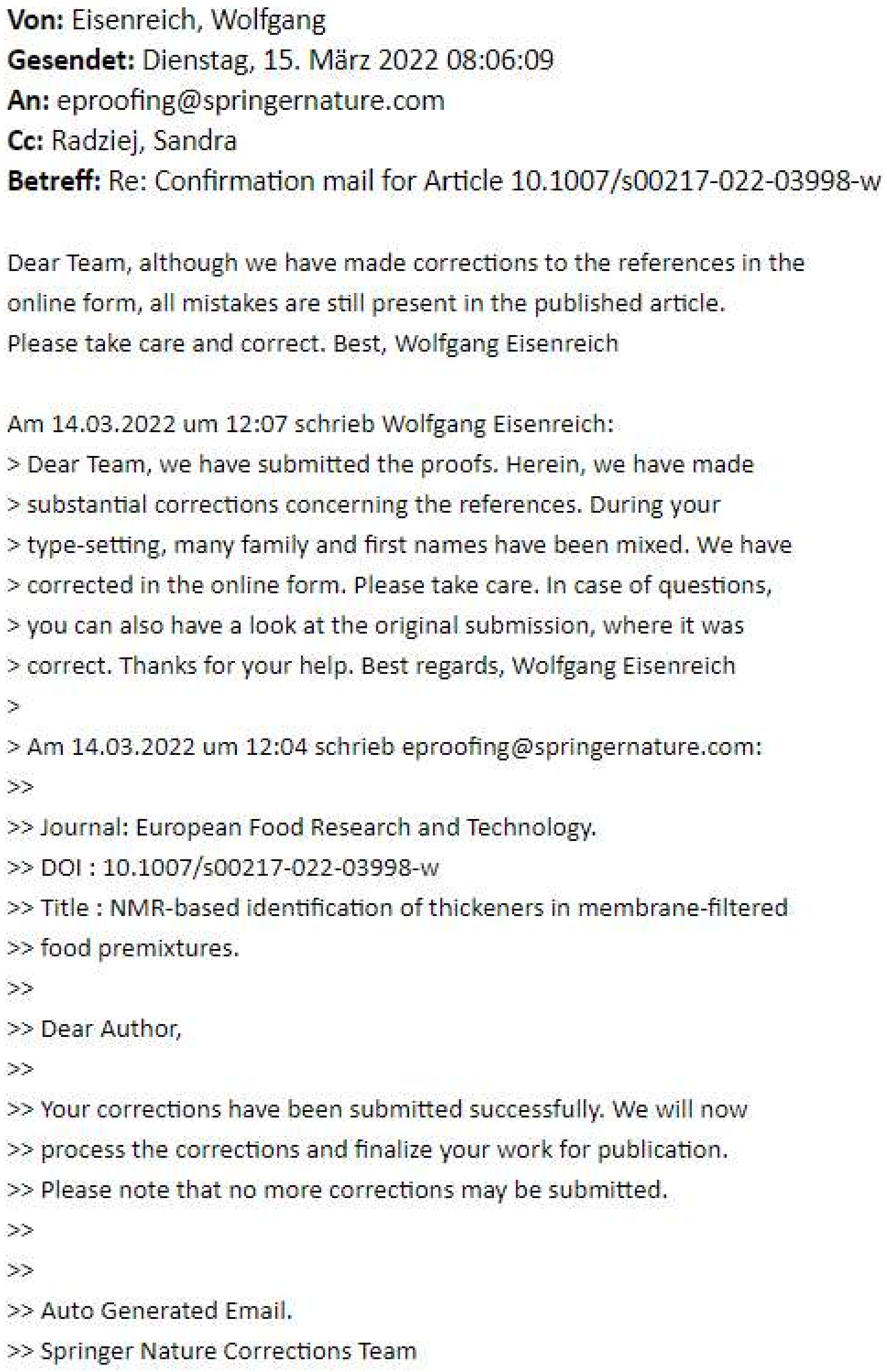

Von: Eisenreich, Wolfgang
Gesendet: Dienstag, 15. März 2022 08:06:09
An: eproofing@springernature.com
Cc: Radziej, Sandra
Betreff: Re: Confirmation mail for Article 10.1007/s00217-022-03998-w

Dear Team, although we have made corrections to the references in the
online form, all mistakes are still present in the published article.
Please take care and correct. Best, Wolfgang Eisenreich

Am 14.03.2022 um 12:07 schrieb Wolfgang Eisenreich:
> Dear Team, we have submitted the proofs. Herein, we have made
> substantial corrections concerning the references. During your
> type-setting, many family and first names have been mixed. We have
> corrected in the online form. Please take care. In case of questions,
> you can also have a look at the original submission, where it was
> correct. Thanks for your help. Best regards, Wolfgang Eisenreich
>
> Am 14.03.2022 um 12:04 schrieb eproofing@springernature.com:
>>
>> Journal: European Food Research and Technology.
>> DOI : 10.1007/s00217-022-03998-w
>> Title : NMR-based identification of thickeners in membrane-filtered
>> food premixtures.
>>
>> Dear Author,
>>
>> Your corrections have been submitted successfully. We will now
>> process the corrections and finalize your work for publication.
>> Please note that no more corrections may be submitted.
>>
>>
>> Auto Generated Email.
>> Springer Nature Corrections Team

Originally submitted reference list

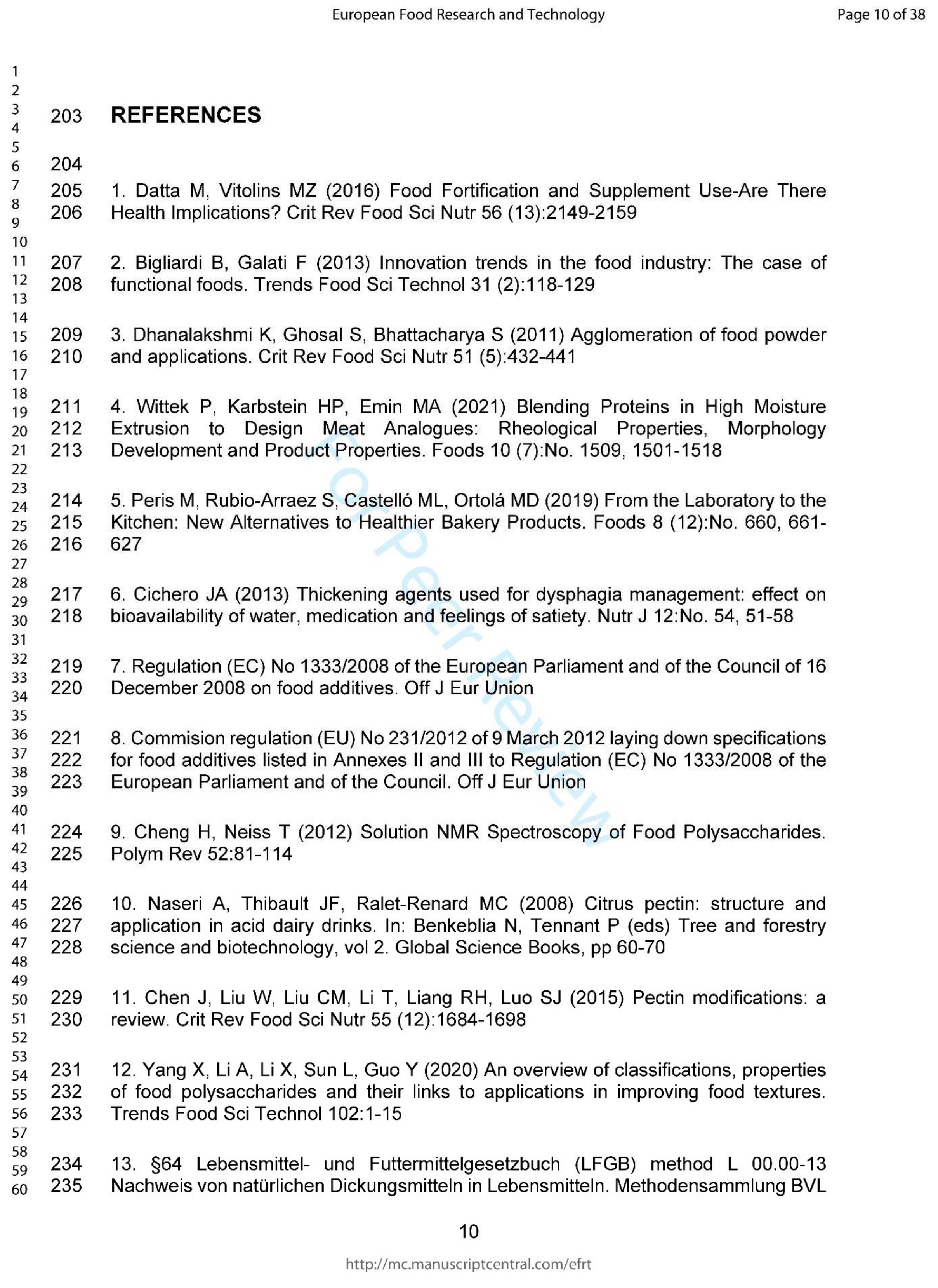

REFERENCES

1. Datta M, Vitolins MZ (2016) Food Fortification and Supplement Use-Are There Health Implications? Crit Rev Food Sci Nutr 56 (13):2149-2159

2. Bigliardi B, Galati F (2013) Innovation trends in the food industry: The case of functional foods. Trends Food Sci Technol 31 (2):118-129

3. Dhanalakshmi K, Ghosal S, Bhattacharya S (2011) Agglomeration of food powder and applications. Crit Rev Food Sci Nutr 51 (5):432-441

4. Wittek P, Karbstein HP, Emin MA (2021) Blending Proteins in High Moisture Extrusion to Design Meat Analogues: Rheological Properties, Morphology Development and Product Properties. Foods 10 (7):No. 1509, 1501-1518

5. Peris M, Rubio-Arraez S, Castelló ML, Ortolá MD (2019) From the Laboratory to the Kitchen: New Alternatives to Healthier Bakery Products. Foods 8 (12):No. 660, 661-627

6. Cichero JA (2013) Thickening agents used for dysphagia management: effect on bioavailability of water, medication and feelings of satiety. Nutr J 12:No. 54, 51-58

7. Regulation (EC) No 1333/2008 of the European Parliament and of the Council of 16 December 2008 on food additives. Off J Eur Union

8. Commision regulation (EU) No 231/2012 of 9 March 2012 laying down specifications for food additives listed in Annexes II and III to Regulation (EC) No 1333/2008 of the European Parliament and of the Council. Off J Eur Union

9. Cheng H, Neiss T (2012) Solution NMR Spectroscopy of Food Polysaccharides. Polym Rev 52:81-114

10. Naseri A, Thibault JF, Ralet-Renard MC (2008) Citrus pectin: structure and application in acid dairy drinks. In: Benkeblia N, Tennant P (eds) Tree and forestry science and biotechnology, vol 2. Global Science Books, pp 60-70

11. Chen J, Liu W, Liu CM, Li T, Liang RH, Luo SJ (2015) Pectin modifications: a review. Crit Rev Food Sci Nutr 55 (12):1684-1698

12. Yang X, Li A, Li X, Sun L, Guo Y (2020) An overview of classifications, properties of food polysaccharides and their links to applications in improving food textures. Trends Food Sci Technol 102:1-15

13. §64 Lebensmittel- und Futtermittelgesetzbuch (LFGB) method L 00.00-13 Nachweis von natürlichen Dickungsmitteln in Lebensmitteln. Methodensammlung BVL

14. Merkx DWH, Westphal Y, van Velzen EJJ, Thakoer KV, de Roo N, van Duynhoven JPM (2018) Quantification of food polysaccharide mixtures by (1)H NMR. Carbohydr Polym 179:379-385

15. Grün C, Sanders P, van der Burg M, Schuurbiers E, Adrichem L, Velzen EJJ, Roo N, Brunt K, Westphal Y, Schols HA (2015) Strategy to identify and quantify polysaccharide gums in gelled food concentrates. Food chem 166C:42-49

16. Glück U, Thier H-P (1980) Quantitative Bestimmung einiger Dickungsmittel in Milchprodukten. Z Lebensm-Unters Forsch 170 (4):272-279

17. Radziej S, Scherb-Forster J, Schlicht C, Eisenreich W (2021) Fast Identification of Food Thickeners by Nontargeted NMR-Spectroscopy. J Agric Food Chem 69 (12):3761-3775

18. Saha D, Bhattacharya S (2010) Hydrocolloids as thickening and gelling agents in food: a critical review. J Food Sci Technol 47 (6):587-597

19. Elkhalifa AE, Mohammed A, Mustafa M, H E (2007) Use of Guar Gum and Gum Arabic as Bread Improvers for the Production of Bakery Products from Sorghum Flour. Food Sci Technol Res 13 (4):327-331

20. Chernokalskaya E, Gutierrez S, Pitt AM, Leonard JT (2004) Ultrafiltration for proteomic sample preparation. Electrophoresis 25 (15):2461-2468

21. Mahendran T, Williams PA, Phillips GO, Al-Assaf S, Baldwin TC (2008) New insights into the structural characteristics of the arabinogalactan-protein (AGP) fraction of gum arabic. J Agric Food Chem 56 (19):9269-9276

22. Barak S, Mudgil D (2014) Locust bean gum: processing, properties and food applications-a review. Int J Biol Macromol 66:74-80

23. Dakia PA, Blecker C, Robert C, Wathelet B, Paquot M (2008) Composition and physicochemical properties of locust bean gum extracted from whole seeds by acid or water dehulling pre-treatment. Food Hydrocoll 22 (5):807-818

24. Gupta S, Saurabh CK, Variyar PS, Sharma A (2015) Comparative analysis of dietary fiber activities of enzymatic and gamma depolymerized guar gum. Food Hydrocoll 48:149-154

25. McKim JM, Willoughby JA, Sr., Blakemore WR, Weiner ML (2019) Clarifying the confusion between poligeenan, degraded carrageenan, and carrageenan: A review of the chemistry, nomenclature, and in vivo toxicology by the oral route. Crit Rev Food Sci Nutr 59 (19):3054-3073

26. Ridley BL, O'Neill MA, Mohnen D (2001) Pectins: structure, biosynthesis, and oligogalacturonide-related signaling. Phytochemistry 57 (6):929-967

27. Mudgil D (2017) The Interaction Between Insoluble and Soluble Fiber. In: Samann RA (ed) Dietary Fiber for the Prevention of Cardiovascular Disease. Academic Press Elsevier, pp 35-59

28. Ali BH, Ziada A, Blunden G (2009) Biological effects of gum arabic: A review of some recent research. Food Chem Toxicol 47 (1):1-8

9.4 Supporting information to “Dual Isotopologue Profiling of Bacterial Pathogens and their Host Cells: Metabolic Adaptation of Human Macrophages and Fallopian Tube Cells to Intracellular *Chlamydia trachomatis*”

HFT cells: Analysis of fatty acids by GC-MS

A HFT uninfected

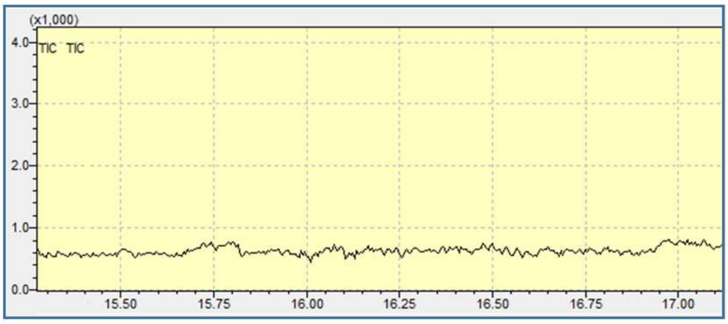

B HFT infected with *C. trachomatis*

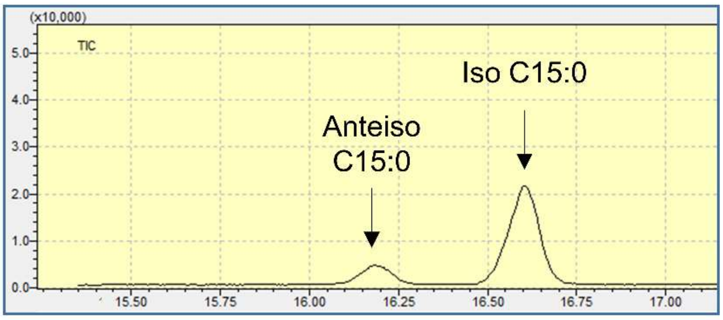

Figure S1: Part of the GC-MS chromatograms (15.0 min – 17.50 min) of the branched-chain fatty acids anteiso-C15:0 and iso-C15:0 from uninfected HFT cells (A) and with *C. trachomatis* infected HFT cells (B).

HFT cells - Biological Replicate 2 (R2): Incorporation of ^{13}C into protein-derived amino acids

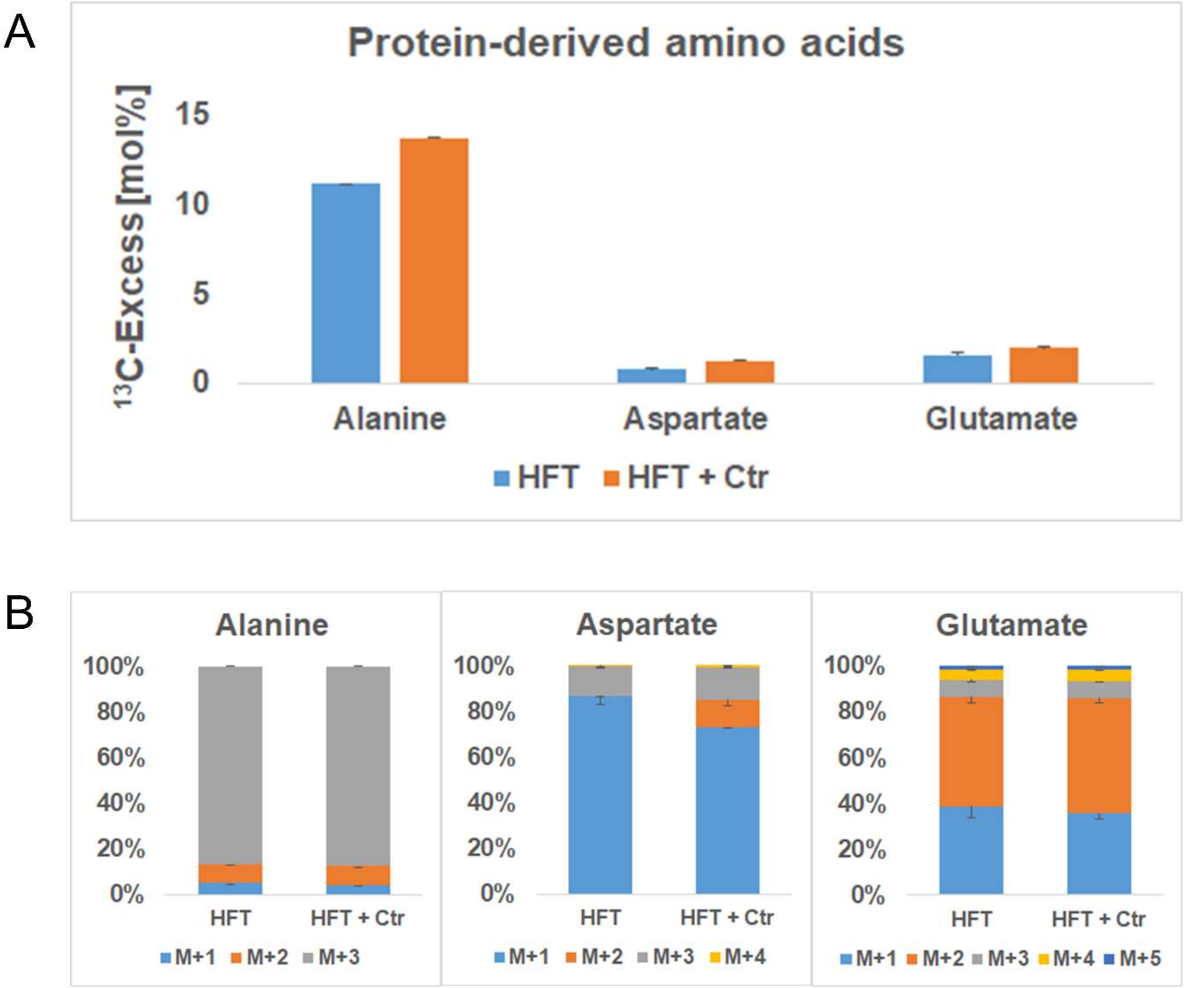

Figure S2: ^{13}C-Excess in mol% (A) and isotopologue profiles (B) of protein-derived amino acids from uninfected HFT cells and with *C. trachomatis* infected HFT cells. M+X represents the isotopologue profiles with X ^{13}C-atoms incorporated into the protein-derived amino acids. Error bars show the standard deviations from one biological replicate (R2) with three technical replicates.

HFT cells - Biological Replicate 2 (R2): Incorporation of ^{13}C into TCA intermediates

A

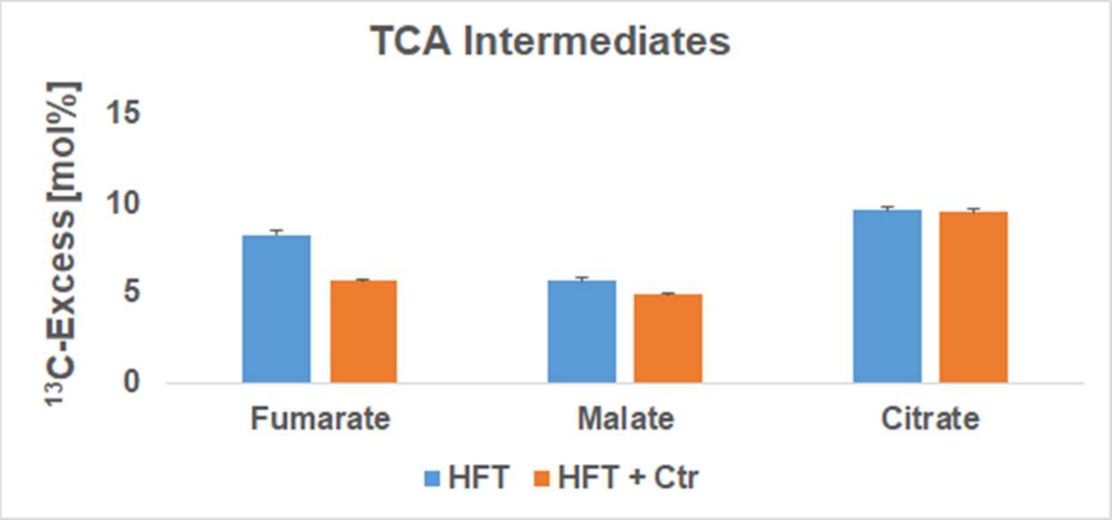

B

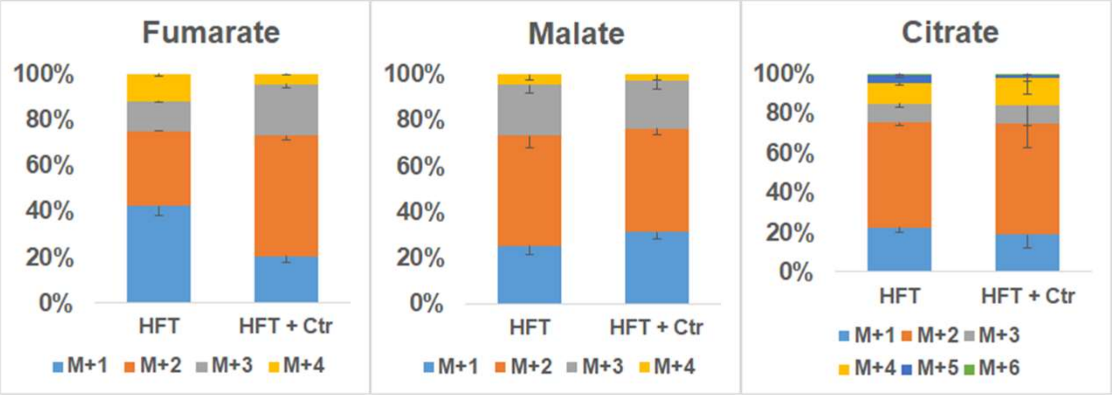

Figure S3: ^{13}C-Excess in mol% (A) and isotopologue profiles (B) of TCA intermediates from uninfected HFT cells and with *C. trachomatis* infected HFT cells. M+X represents the isotopologue profiles with X ^{13}C-atoms incorporated into the TCA intermediates. Error bars show the standard deviations from one biological replicate (R2) with three technical replicates.

HFT cells - Biological Replicate 2 (R2): Incorporation of ^{13}C into fatty acids

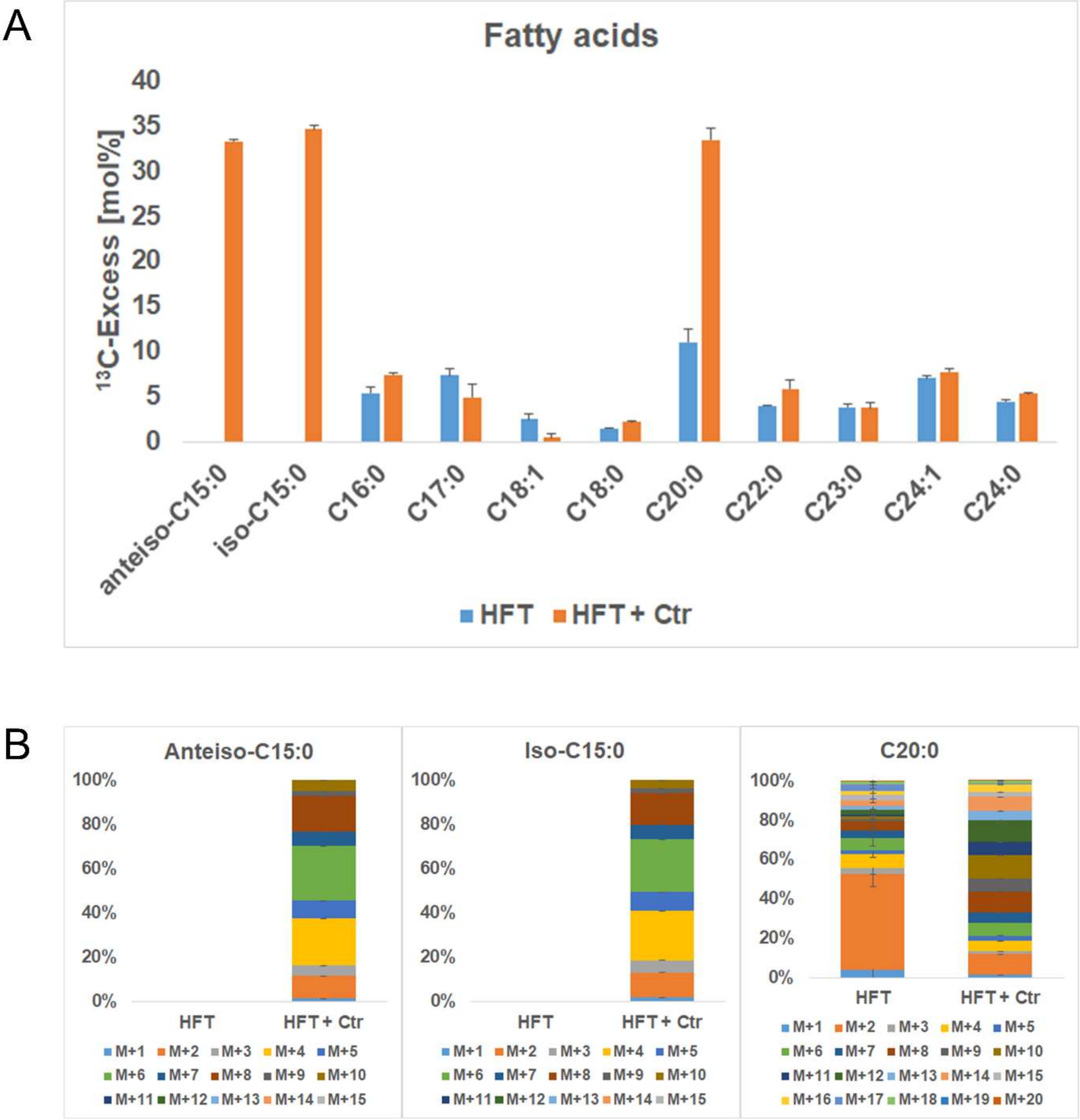

Figure S4: ^{13}C-Excess in mol% (A) and isotopologue profiles (B) of fatty acids from uninfected HFT cells and with *C. trachomatis* infected HFT cells. M+X represents the isotopologue profiles with X ^{13}C-atoms incorporated into the fatty acids. Error bars show the standard deviations from one biological replicate (R2) with three technical replicates.

HFT cells - Biological Replicate 3 (R3): Incorporation of ^{13}C into protein-derived amino acids

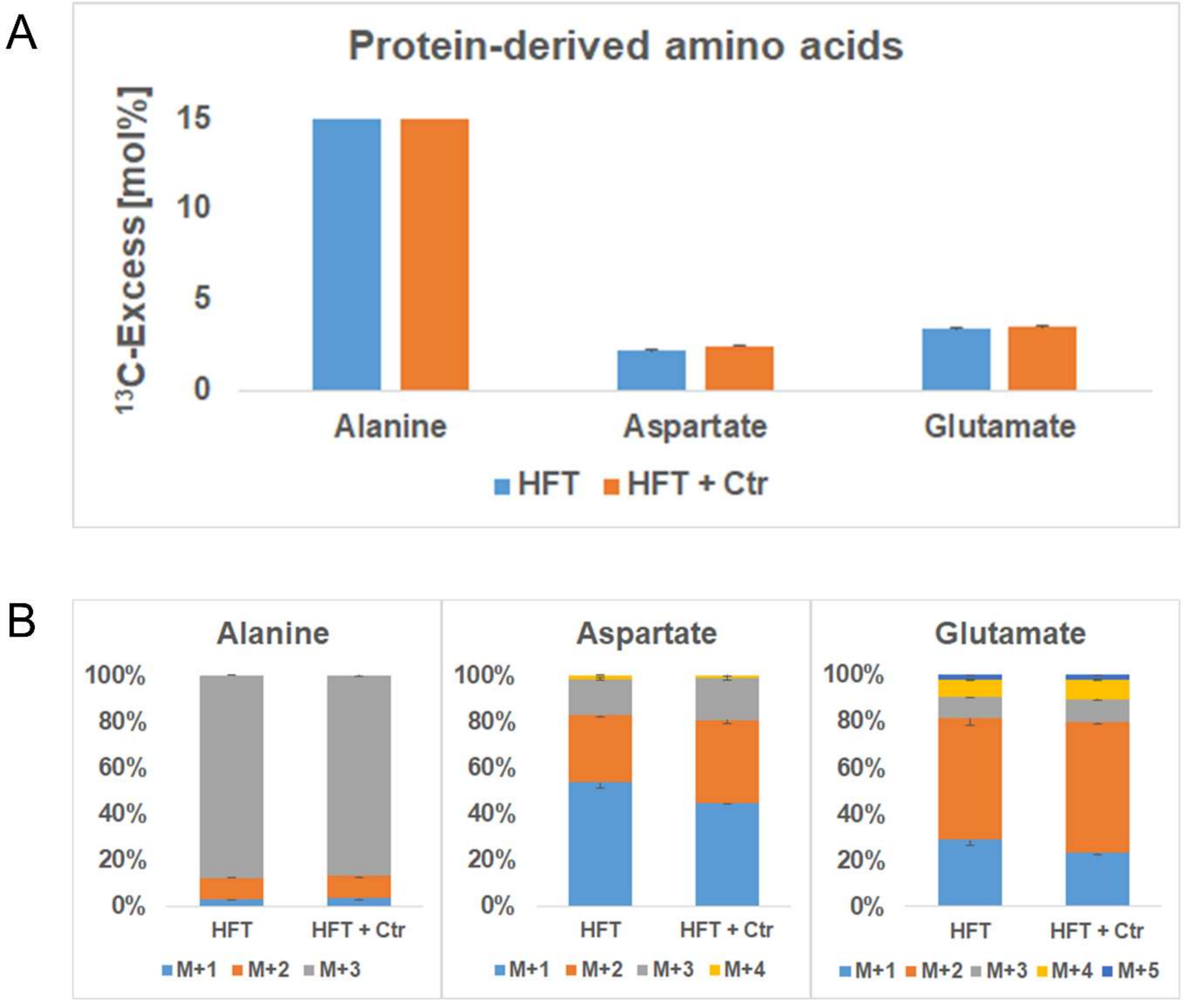

Figure S5: ^{13}C-Excess in mol% (A) and isotopologue profiles (B) of protein-derived amino acids from uninfected HFT cells and with *C. trachomatis* infected HFT cells. M+X represents the isotopologue profiles with X ^{13}C-atoms incorporated into the protein-derived amino acids. Error bars show the standard deviations from one biological replicate (R3) with three technical replicates.

HFT cells - Biological Replicate 3 (R3): Incorporation of ^{13}C into TCA intermediates

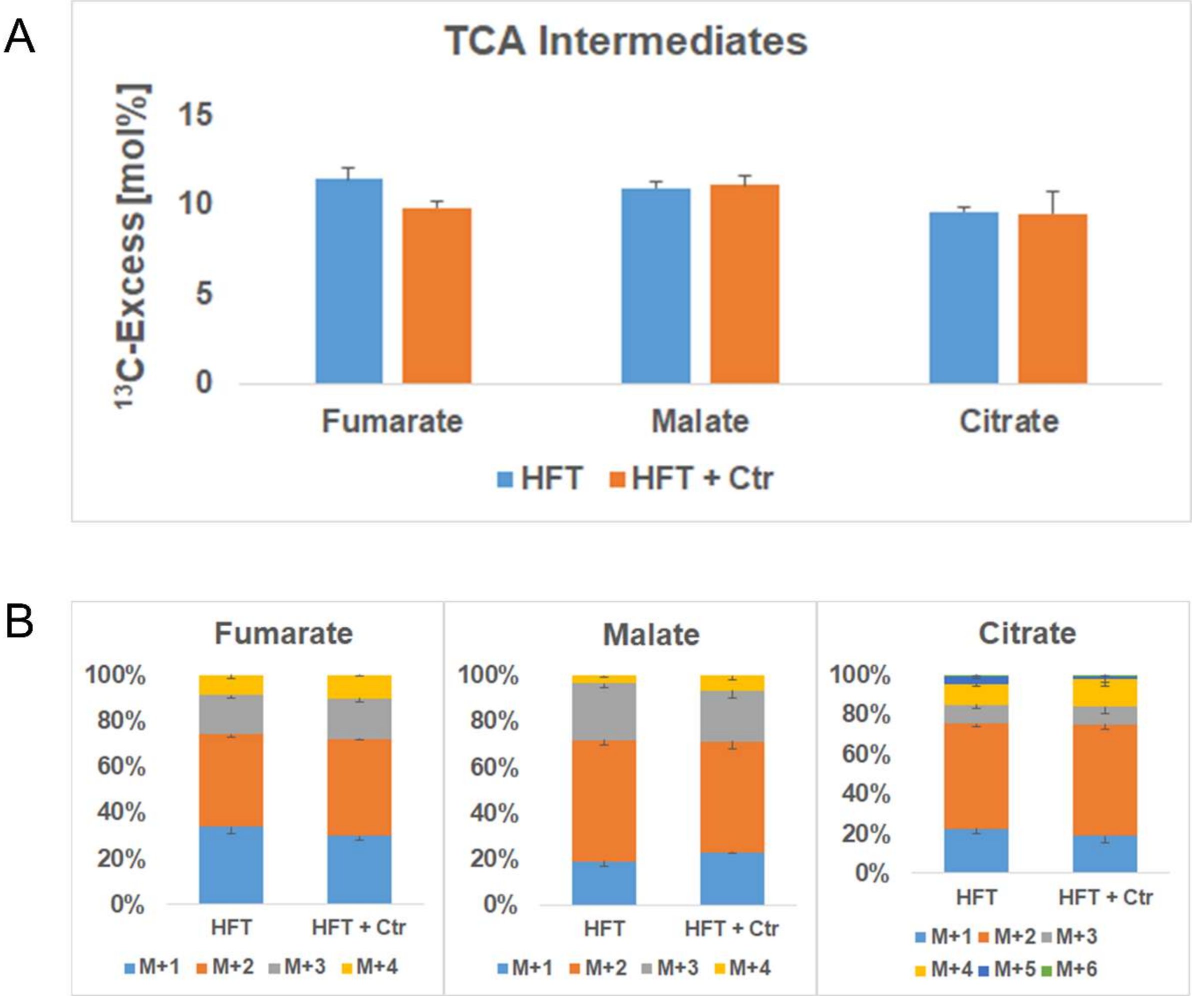

Figure S6: ^{13}C-Excess in mol% (A) and isotopologue profiles (B) of TCA intermediates from uninfected HFT cells and with *C. trachomatis* infected HFT cells. M+X represents the isotopologue profiles with X ^{13}C-atoms incorporated into the TCA intermediates. Error bars show the standard deviations from one biological replicate (R3) with three technical replicates.

HFT cells - Biological Replicate 3 (R3): Incorporation of ^{13}C into fatty acids

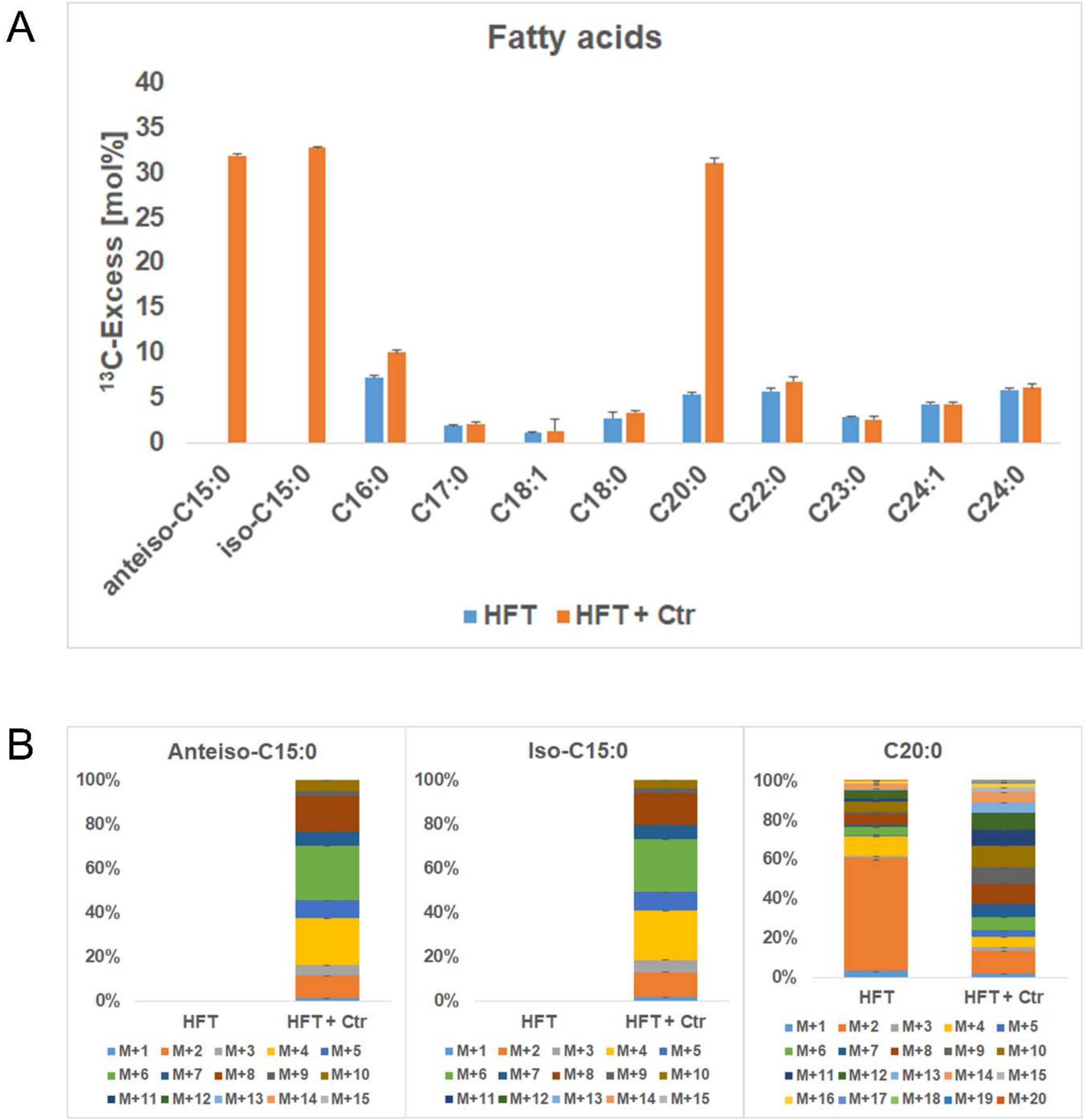

Figure S7: ^{13}C-Excess in mol% (A) and isotopologue profiles (B) of fatty acids from uninfected HFT cells and with *C. trachomatis* infected HFT cells. M+X represents the isotopologue profiles with X ^{13}C-atoms incorporated into the fatty acids. Error bars show the standard deviations from one biological replicate (R3) with three technical replicates.

Human M1 and M2 polarized macrophages - Biological Replicate 2 (R2): Incorporation of ^{13}C into protein-derived amino acids

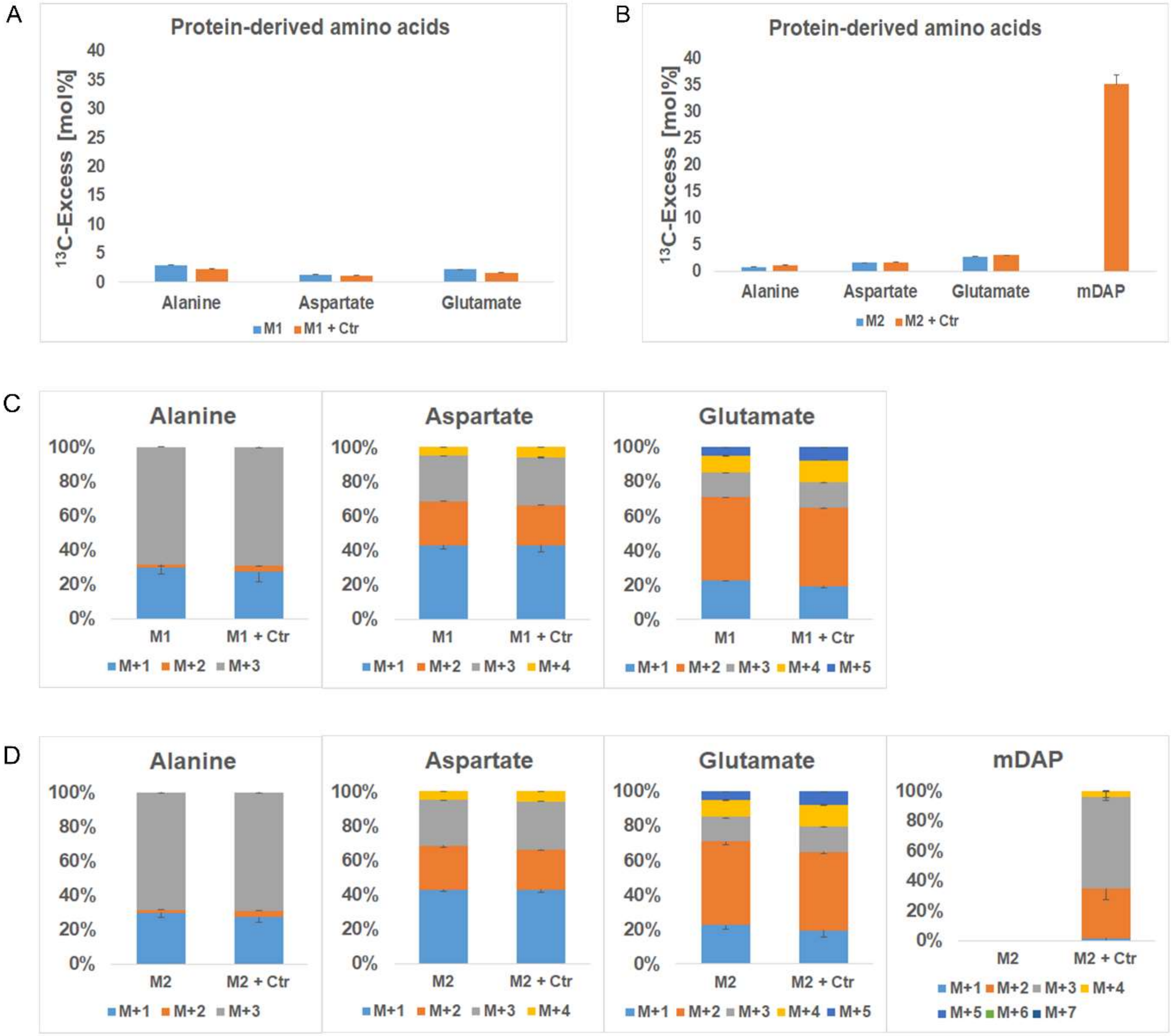

Figure S8: ^{13}C-Excess in mol% of protein-derived amino acids and mDAP from uninfected and infected M1 phenotype (A) and M2 phenotype (B) as well as the isotopologue profiles of protein-derived amino acids and mDAP from uninfected and infected M1 phenotype (C) and M2 phenotype (D). M+X represents the isotopologue profiles with X ^{13}C-atoms incorporated into the amino acids. Error bars show the standard deviations from one biological replicate (R2) with three technical replicates.

Human M1 and M2 polarized macrophages - Biological Replicate 2 (R2): Incorporation of ^{13}C into TCA intermediates

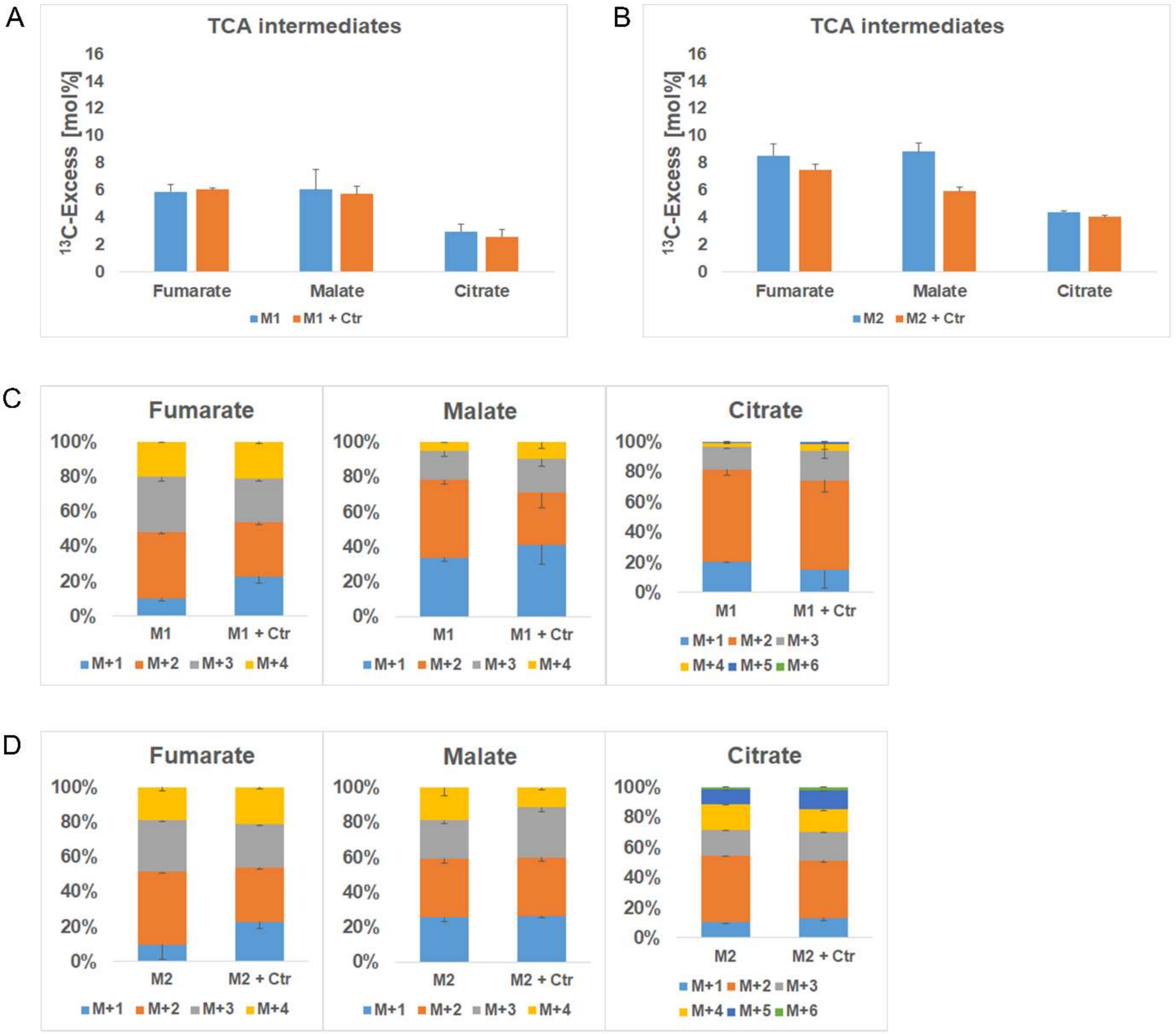

Figure S9: ^{13}C-Excess in mol% of TCA intermediates from uninfected and infected M1 phenotype (A) and M2 phenotype (B) as well as the isotopologue profiles of TCA intermediates from uninfected and infected M1 phenotype (C) and M2 phenotype (D). M+X represents the isotopologue profiles with X ^{13}C-atoms incorporated into the TCA intermediates. Error bars show the standard deviations from one biological replicate (R2) with three technical replicates.

Human M1 and M2 polarized macrophages - Biological Replicate 2 (R2): Incorporation of ^{13}C into fatty acids

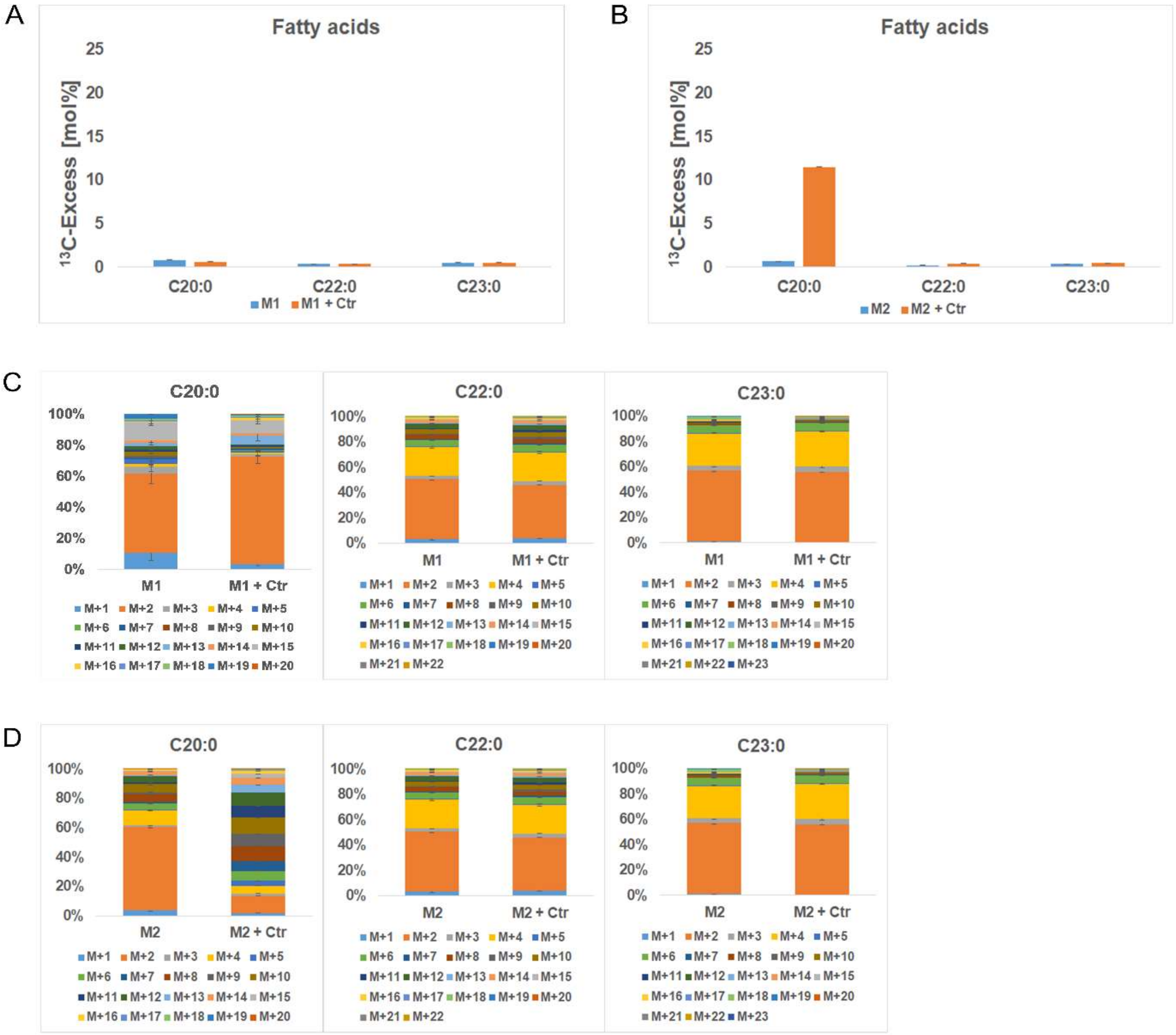

Figure S10: ^{13}C-Excess in mol% of fatty acids from uninfected and infected M1 phenotype (A) and M2 phenotype (B) as well as the isotopologue profiles of fatty acids of uninfected and infected M1 phenotype (C) and M2 phenotype (D). M+X represents the isotopologue profiles with X ^{13}C-atoms incorporated into the fatty acids. Error bars show the standard deviations from one biological replicate (R2) with three technical replicates.

Table S1. ^{13}C-Excess values in mol% of protein-derived amino acids, TCA intermediates and fatty acids from uninfected and with *C. trachomatis* infected HFT cells based on a labelling experiment with [U-^{13}C$_6$]glucose. Mean value (MV) and standard deviation (sd) of three biological replicates (R1, R2, R3) with three technical replicates. n.d. not detected.

	Uninfected human fallopian tube cells				**Infected human fallopian tube cells**			
metabolite	**R1 ^{13}C-Excess (± sd)**	**R2 ^{13}C-Excess (± sd)**	**R3 ^{13}C-Excess (± sd)**	**MV ^{13}C-Excess (± sd)**	**R1 ^{13}C-Excess (± sd)**	**R2 ^{13}C-Excess (± sd)**	**R3 ^{13}C-Excess (± sd)**	**MV ^{13}C-Excess (± sd)**
Alanine	9.56% (± 0.05%)	11.20% (± 0.01%)	20.13 (± 0.04%)	13.63% (± 5.69%)	11.17% (± 0.05%)	13.80% (± 0.07%)	21.65% (± 0.05%)	15.54% (± 5.45%)
Aspartate	0.80 (± 0.03%)	0.82% (± 0.02%)	2.19% (± 0.05%)	1.27% (± 0.80%)	1.38% (± 0.12%)	1.28% (± 0.05%)	2.47% (± 0.05%)	1.71% (± 0.66%)
Glutamate	1.02% (± 0.04%)	1.65% (± 0.09%)	3.40% (± 0.11%)	2.02% (± 1.24%)	1.18% (± 0.07%)	2.02% (± 0.06%)	3.50% (± 0.03%)	2.23% (± 1.18%)
Fumarate	3.16% (± 0.10%)	8.26% (± 0.29%)	11.48% (± 0.61%)	7.63% (± 4.21%)	3.55% (± 0.21%)	5.70% (± 0.06%)	9.87% (± 0.33%)	6.37% (± 3.22%)
Malate	2.74% (± 0.22%)	5.69% (± 0.16%)	10.95% (± 0.38%)	6.46% (± 4.17%)	3.14% (± 0.04%)	4.96% (± 0.08%)	11.13% (± 0.56%)	6.41% (± 4.19%)
Citrate	4.80% (± 0.50%)	9.66% (± 0.19%)	11.20% (± 0.79%)	8.55% (± 3.38%)	9.17% (± 0.10%)	9.56% (± 0.82%)	12.78% (± 1.02%)	10.50% (± 2.08%)
Anteiso-C15:0	n.d.	n.d.	n.d.	- - -	34.85% (± 0.13%)	33.19% (± 0.21%)	31.88% (± 0.12%)	33.31% (± 1.50%)
Iso-C15:0	n.d.	n.d.	n.d.	- - -	34.55% (± 0.14%)	34.61% (± 0.44%)	32.73% (± 0.11%)	33.96% (± 1.09%)
C16:0	2.39% (± 0.24%)	5.37% (± 0.61%)	7.15% (± 0.28%)	4.97% (± 2.43%)	7.16% (± 0.32%)	7.40% (± 0.26%)	10.0% (± 0.26%)	8.19% (± 1.60%)
C17:0	1.31% (± 0.98%)	7.37% (± 0.76%)	1.88% (± 0.15%)	3.52% (± 3.41%)	0.93% (± 0.33%)	4.89% (± 0.97%)	2.07% (± 0.25%)	2.63% (± 2.10%)
C18:1	0.78% (± 0.20%)	2.47% (± 0.64%)	1.08% (± 0.03%)	1.44% (± 0.95%)	0.46% (± 0.09%)	0.43% (± 0.43%)	1.34% (± 0.99%)	0.74% (± 0.72%)
C18:0	0.70% (± 0.03%)	1.47% (± 0.05%)	2.73% (± 0.57%)	1.63% (± 1.05%)	2.47% (± 0.13%)	2.19% (± 0.14%)	3.36% (± 0.23%)	2.67% (± 0.63%)
C20:0	2.58% (± 0.49%)	11.05% (± 1.06%)	5.30% (± 0.22%)	6.31% (± 4.36%)	34.55% (± 1.04%)	33.44% (± 1.02%)	31.0% (± 0.58%)	33.00% (± 2.02%)
C22:0	2.80% (± 0.16%)	3.95% (± 0.04%)	5.68% (± 0.38%)	4.10% (± 1.46%)	5.28% (± 0.35%)	5.88% (± 0.97%)	6.79% (± 0.47%)	5.98% (± 0.97%)
C23:0	2.59% (± 0.59%)	3.79% (± 0.38%)	2.85% (± 0.08%)	3.08% (± 0.72%)	2.24% (± 0.05%)	3.75% (± 0.61%)	2.54% (± 0.29%)	2.84% (± 0.86%)
C24:1	5.25% (± 0.84%)	6.99% (± 0.38%)	4.30% (± 0.19%)	5.51% (± 1.44%)	4.10% (± 0.27%)	7.71% (± 0.42%)	4.28% (± 0.15%)	5.36% (± 2.05%)
C24:0	3.96% (± 0.12%)	4.47% (± 0.19%)	5.88% (± 0.20%)	4.74% (± 1.05%)	5.06% (± 0.15%)	5.26% (± 0.12%)	6.04% (± 0.41%)	5.45% (± 0.57%)

Table S2: ^{13}C-Excess values in mol% of protein-derived amino acids, TCA intermediates and fatty acids from uninfected and with *C. trachomatis* infected human M1 macrophages based on a labelling experiment with [U-$^{13}C_6$]glucose. Mean value (MV) and standard deviation (sd) of two biological replicates (R1, R2) with three technical replicates. n.d. not detected.

	Uninfected M1 macrophages			**Infected M1 macrophages**		
metabolite	**R1 ^{13}C-Excess (± sd)**	**R2 ^{13}C-Excess (± sd)**	**MV ^{13}C-Excess (± sd)**	**R1 ^{13}C-Excess (± sd)**	**R2 ^{13}C-Excess (± sd)**	**MV ^{13}C-Excess (± sd)**
Alanine	3.15% (± 0.07%)	2.93% (± 0.02%)	3.04% (± 0.16%)	3.28% (± 0.07%)	2.20% (± 0.04%)	2.74% (± 0.77%)
Aspartate	1.86% (± 0.13%)	1.29% (± 0.04%)	1.58% (± 0.41%)	1.89% (± 0.01%)	1.10% (± 0.07%)	1.50% (± 0.56%)
Glutamate	3.91% (± 0.05%)	2.16% (± 0.01%)	3.04% (± 1.24%)	3.74% (± 0.02%)	1.62% (± 0.03%)	2.68% (± 1.50%)
mDAP	n.d.	n.d.	- - -	n.d.	n.d.	- - -
Fumarate	5.87% (± 0.54%)	9.23% (± 0.37%)	7.55% (± 2.42%)	6.03% (± 0.11%)	7.79% (± 0.55%)	6.91% (± 1.29%)
Malate	6.03% (± 1.02%)	4.11% (± 0.37%)	5.07% (± 1.53%)	5.71% (± 0.59%)	3.70% (± 0.22%)	4.71% (± 1.48%)
Citrate	2.98% (± 0.49%)	1.11% (± 0.08%)	2.05% (± 1.35%)	2.57% (± 0.56%)	1.14% (± 0.07%)	1.86% (± 1.06%)
C20:0	4.35% (± 0.54%)	0.81% (± 0.15%)	2.58% (± 2.53%)	1.94% (± 0.16%)	0.59% (± 0.16%)	1.27% (± 0.97%)
C22:0	3.04% (± 1.05%)	0.34% (± 0.05%)	1.69% (± 1.99%)	2.92% (± 0.08%)	0.35% (± 0.10%)	1.64% (± 1.82%)
C23:0	4.98% (± 0.91%)	0.52% (± 0.14%)	2.75% (± 3.20%)	5.38% (± 0.80%)	0.51% (± 0.11%)	2.95% (± 3.47%)

Table S3: ^{13}C-Excess values in mol% of protein-derived amino acids, TCA intermediates and fatty acids from uninfected and with *C. trachomatis* infected human M2 macrophages based on a labelling experiment with [U-$^{13}C_6$]glucose. Mean value (MV) and standard deviation (sd) of two biological replicates (R1, R2) with three technical replicates. n.d. not detected.

	Uninfected M2 macrophages			**Infected M2 macrophages**		
metabolite	**R1 ^{13}C-Excess (± sd)**	**R2 ^{13}C-Excess (± sd)**	**MV ^{13}C-Excess (± sd)**	**R1 ^{13}C-Excess (± sd)**	**R2 ^{13}C-Excess (± sd)**	**MV ^{13}C-Excess (± sd)**
Alanine	1.48% (± 0.03%)	0.79% (± 0.02%)	1.14% (± 0.49%)	2.27% (± 0.01%)	1.05% (± 0.04%)	1.66% (± 0.86%)
Aspartate	3.02% (± 0.13%)	1.55% (± 0.02%)	2.29% (± 1.04%)	4.60% (± 0.20%)	1.64% (± 0.07%)	3.12% (± 2.10%)
Glutamate	5.86% (± 0.10%)	2.76% (± 0.02%)	4.31% (± 2.19%)	7.94% (± 0.03%)	2.97% (± 0.01%)	5.46% (± 3.51%)
mDAP	n.d.	n.d.	- - -	32.64% (± 0.93%)	35.01% (± 0.78%)	33.83% (± 1.88%)
Fumarate	11.41% (± 0.39%)	8.55% (± 0.84%)	9.98% (± 2.11%)	8.64% (± 0.25%)	7.51% (± 0.41%)	8.08% (± 0.86%)
Malate	14.77% (± 0.61%)	8.84% (± 0.63%)	11.81% (± 4.24%)	8.06% (± 0.18%)	5.90% (± 0.33%)	6.98% (± 1.55%)
Citrate	13.68% (± 0.52%)	4.40% (± 0.10%)	9.04% (± 6.57%)	7.10% (± 0.35%)	4.05% (± 0.09%)	5.58% (± 2.17%)
C20:0	4.14% (± 0.51%)	0.64% (± 0.16%)	2.39% (± 2.50%)	14.71% (± 0.35%)	11.51% (± 0.19%)	13.11% (± 2.28%)
C22:0	2.61% (± 0.18%)	0.49% (± 0.02%)	1.40% (± 1.71%)	2.75% (± 1.17%)	0.37% (± 0.01%)	1.56% (± 1.78%)
C23:0	5.22% (± 0.18%)	0.49% (± 0.24%)	2.86% (± 3.35%)	4.61% (± 1.48%)	0.44% (± 0.24%)	2.53% (± 3.07%)

10. Reprint permissions

10.1 Reprint permission to “Fast Identification of Food Thickeners by Nontargeted NMR-Spectroscopy”

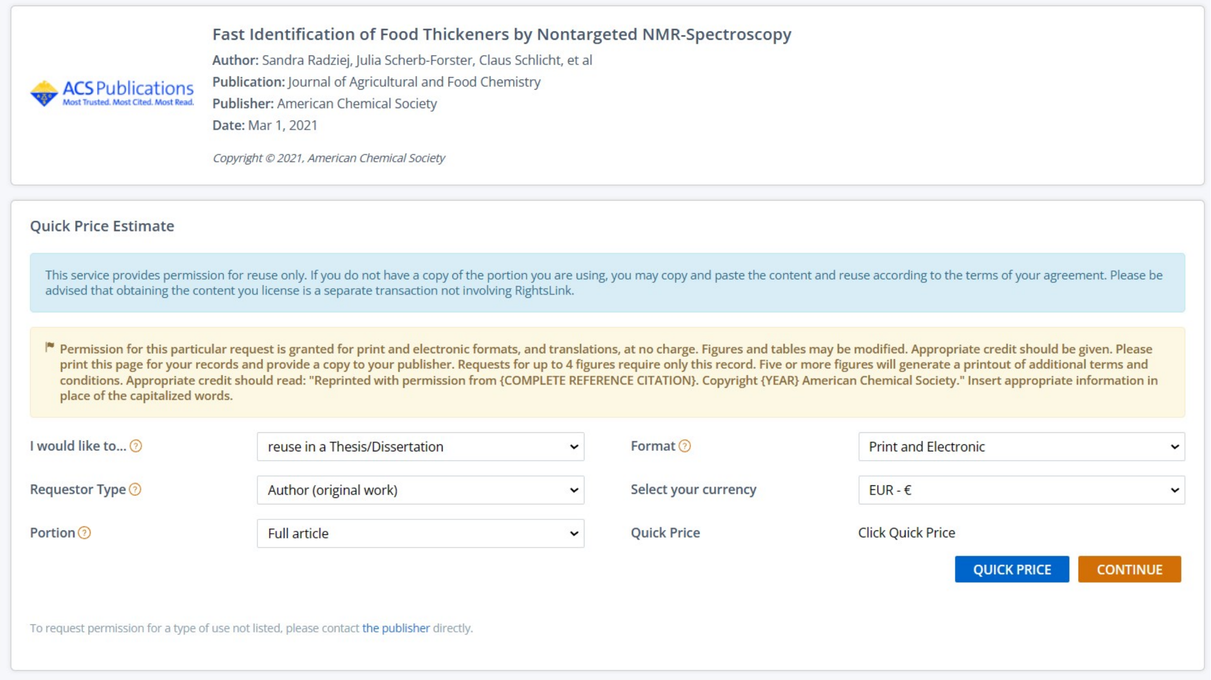

Fast Identification of Food Thickeners by Nontargeted NMR-Spectroscopy

Author: Sandra Radziej, Julia Scherb-Forster, Claus Schlicht, et al
Publication: Journal of Agricultural and Food Chemistry
Publisher: American Chemical Society
Date: Mar 1, 2021

Copyright © 2021, American Chemical Society

Quick Price Estimate

This service provides permission for reuse only. If you do not have a copy of the portion you are using, you may copy and paste the content and reuse according to the terms of your agreement. Please be advised that obtaining the content you license is a separate transaction not involving RightsLink.

Permission for this particular request is granted for print and electronic formats, and translations, at no charge. Figures and tables may be modified. Appropriate credit should be given. Please print this page for your records and provide a copy to your publisher. Requests for up to 4 figures require only this record. Five or more figures will generate a printout of additional terms and conditions. Appropriate credit should read: "Reprinted with permission from {COMPLETE REFERENCE CITATION}. Copyright {YEAR} American Chemical Society." Insert appropriate information in place of the capitalized words.

I would like to...	reuse in a Thesis/Dissertation	Format	Print and Electronic
Requestor Type	Author (original work)	Select your currency	EUR - €
Portion	Full article	Quick Price	Click Quick Price

To request permission for a type of use not listed, please contact the publisher directly.

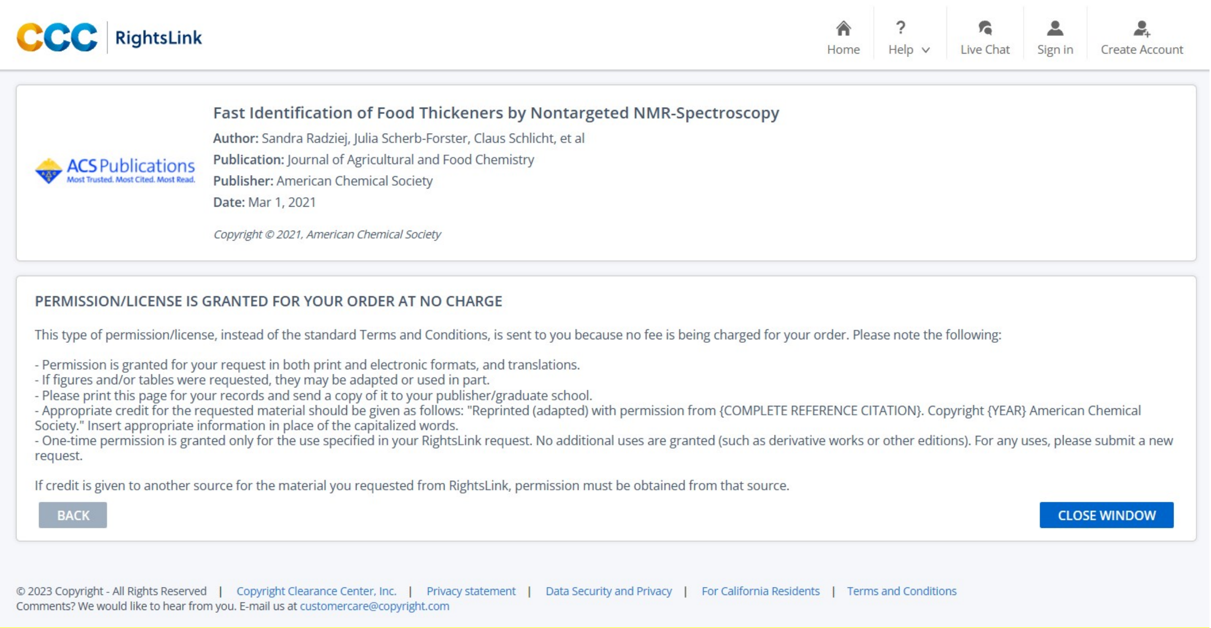

Fast Identification of Food Thickeners by Nontargeted NMR-Spectroscopy

Author: Sandra Radziej, Julia Scherb-Forster, Claus Schlicht, et al
Publication: Journal of Agricultural and Food Chemistry
Publisher: American Chemical Society
Date: Mar 1, 2021

Copyright © 2021, American Chemical Society

PERMISSION/LICENSE IS GRANTED FOR YOUR ORDER AT NO CHARGE

This type of permission/license, instead of the standard Terms and Conditions, is sent to you because no fee is being charged for your order. Please note the following:

- Permission is granted for your request in both print and electronic formats, and translations.
- If figures and/or tables were requested, they may be adapted or used in part.
- Please print this page for your records and send a copy of it to your publisher/graduate school.
- Appropriate credit for the requested material should be given as follows: "Reprinted (adapted) with permission from {COMPLETE REFERENCE CITATION}. Copyright {YEAR} American Chemical Society." Insert appropriate information in place of the capitalized words.
- One-time permission is granted only for the use specified in your RightsLink request. No additional uses are granted (such as derivative works or other editions). For any uses, please submit a new request.

If credit is given to another source for the material you requested from RightsLink, permission must be obtained from that source.

10.2 Reprint permission to “NMR-based identification of thickeners in membrane-filtered food premixtures”

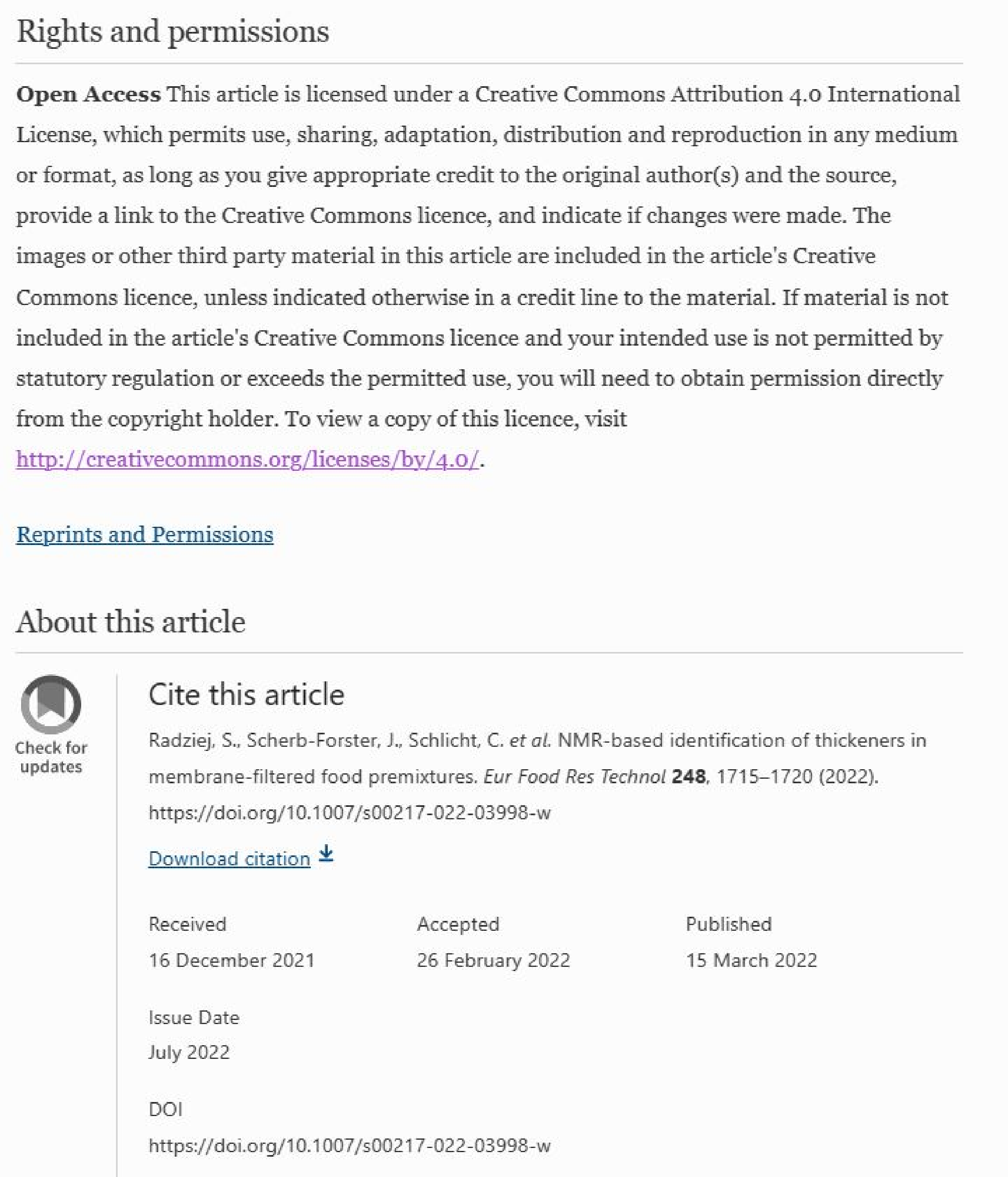

Rights and permissions

Open Access This article is licensed under a Creative Commons Attribution 4.0 International License, which permits use, sharing, adaptation, distribution and reproduction in any medium or format, as long as you give appropriate credit to the original author(s) and the source, provide a link to the Creative Commons licence, and indicate if changes were made. The images or other third party material in this article are included in the article's Creative Commons licence, unless indicated otherwise in a credit line to the material. If material is not included in the article's Creative Commons licence and your intended use is not permitted by statutory regulation or exceeds the permitted use, you will need to obtain permission directly from the copyright holder. To view a copy of this licence, visit http://creativecommons.org/licenses/by/4.0/.

Reprints and Permissions

About this article

Cite this article

Radziej, S., Scherb-Forster, J., Schlicht, C. *et al.* NMR-based identification of thickeners in membrane-filtered food premixtures. *Eur Food Res Technol* **248**, 1715–1720 (2022). https://doi.org/10.1007/s00217-022-03998-w

Download citation

Received	Accepted	Published
16 December 2021	26 February 2022	15 March 2022

Issue Date
July 2022

DOI
https://doi.org/10.1007/s00217-022-03998-w

11. List of Publications

Radziej, S.; Scherb-Forster, J.; Schlicht, C. and Eisenreich, W. Fast Identification of Food Thickeners by Nontargeted NMR-Spectroscopy. *J Agric Food Chem*, **2021**, 69 (12), 3761 – 3775.

DOI: https://doi.org/10.1021/acs.jafc.0c07760

Radziej, S.; Scherb-Forster, J.; Schlicht, C. and Eisenreich, W. NMR-based identification of thickeners in membrane-filtered food premixtures. *Eur Food Res Technol*, **2022**, 248, 1715 – 1720.

DOI: https://doi.org/10.1007/s00217-022-03998-w

Steiner, T.; Zachary, M.; Bauer, S.; Müller, MJ.; Krischke, M.; **Radziej, S**.; Klepsch, M.; Huettel, B.; Eisenreich, W.; Rudel, T. and Beier, D. Central Role of Sibling Small RNAs NgncR_162 and NgncR_163 in Main Metabolic Pathways of *Neisseria gonorrhoeae*. *mBio*, **2023**, e0309322

DOI: https://doi.org/10.1128/mbio.03093-22

Radziej, S., Moldovan, A.; Rudel, T. and Eisenreich, W. Dual Isotopologue Profiling of Bacterial Pathogens and their Host Cells: Metabolic Adaptation of Human Macrophages and Fallopian Tube Cells to Intracellular *Chlamydia trachomatis*

Manuscript in Preparation for *The Journal of Biological Chemistry*

Fuchs, T.; **Radziej, S**., Großmann, P., Kränzlein, M., Bauer, M.; Rickert, C.; Fahmy, A.; Paper, M.; Lorenzen, J.; Masri, M.; Haack, M.; Huber, C.; Garbe, D.; Mehlmer, N.; Rieger, B.; Lieleg, O.; Becker, T.; Jelke, M.; Eisenreich, W and Brueck TB. Sustainable production, characterization and application of a new exopolysaccharide secreted by *Chlorella sorokiniana*.

Manuscript in Preparation for *Carbohydrate Polymers*

Hauke, M.; Metz, F.; Rapp, J.; Faass, L.; Bats, S.H.; **Radziej, S**.; Link, H.; Eisenreich, W. and Josenhans, C. Multiple mechanisms how *Helicobacter pylori* modulates heptose metabolite biosynthesis and heptose-dependent host cell activation.

Manuscript in Revision for *Microbiology Spectrum* [1]

---

[1]: *see notation on the next page*

Notation to *[1]:*

After submission of the presented Ph.D work, the manuscript was accepted for publication and published online.

New citation:

Hauke, M.; Metz, F.; Rapp, J.; Faass, L.; Bats, S.H.; **Radziej, S**.; Link, H.; Eisenreich, W. and Josenhans, C. *Helicobacter pylori* Modulates Heptose Metabolite Biosynthesis and Heptose-Dependent Innate Immune Host Cell Activation by Multiple Mechanisms. *Microbiol Spectr*, **2023**,11(3):e0313222.

DOI: https://doi.org/10.1128/spectrum.03132-22